Mechanisms for Exercise, High-Fat Diet, and Muscle Fiber-Type Effects on Insulin-Stimulated Glucose Uptake in Skeletal Muscle

by

Mark Pataky

A dissertation submitted in partial fulfillment
of the requirements for the degree of
Doctor of Philosophy
(Kinesiology)
in The University of Michigan
2019

Doctoral Committee:

Professor Gregory D. Cartee, Chair
Assistant Professor Dave Bridges
Professor Jeffrey F. Horowitz
Associate Professor Christopher L. Mendias

Mark Pataky

patakymw@umich.edu

ORCID iD: 0000-0003-3273-7886

© Mark Pataky 2019

This dissertation is dedicated to my parents,

Snook and Nancy Pataky.

ACKNOWLEDGEMENTS

It seems like I've been in Ann Arbor for more than 4 years. I've spent countless hours in the lab running western blots, sectioning muscles for histochemical analysis, and fiber typing nearly 12,000 fibers (which amounts to over 1,000 SDS-PAGE gels). However, the reason that I feel as though I been in Ann Arbor for decades is that I've learned so much since moving here a short 4 years ago. When I started working in the Muscle Biology Lab in June of 2015 I had very little wet lab experience, I had never worked with rats, and I was lost during ~90% of our weekly lab meetings. Frankly, I was lucky to have the opportunity to join Greg Cartee's lab, but I had a long way to go. I'm certain that I could not have chosen a better advisor to learn from. Without Greg's patience, thoughtfulness, and exceptional guidance my time as a Ph.D. student would have been far more difficult and far less enjoyable. He has set me up for a successful career and will be someone that I take advice from for years to come. Thank you, Greg, for all that you have done for me as a scientist and person.

Others that deserve quite a bit of credit for my progress to this point in my career include multiple people from the Muscle Biology Lab. For the last 4 years I've used Ed Arias as a walking (and smiling) lab encyclopedia. It will seem strange sitting at my desk a few months from now at Mayo without Ed sitting to my right telling me about his newest anti-aging supplements. Additionally, Carmen Yu, Haiyan Wang, and Amy Zheng have helped me out so much and I am thankful for all of their support. Though no other Ph.D. student was in the Cartee lab while I was here, there was one Master's student, Michelle Nie, to suffer through some classes with and I truly enjoyed working with her as well. If it were not for 5 exceptional undergrads (Manak Singh, Jalal Almallouhi, Sydney Van Acker, Rhea Dhingra, and Marina Freeburg) then the final study of my dissertation would have been impossible. I am so grateful to them and know that they all have bright futures ahead.

My committee members have been extremely insightful and are a great group of scientists to look up to. Jeff Horowitz, Chris Mendias and Dave Bridges are exceptional scientists and fantastic mentors. I have taken great advice from each of them and it has helped shaped the scientist that I am today. I am honored to have each of them on my committee and hope to continue to be in touch with each of them throughout my career.

There are countless people at the University of Michigan that I have interacted with that I want to thank. First, Alison Ludzki is one of my favorite people in the world. I'm lucky to have met her and am glad to call her my friend. Other people who have either helped with my dissertation, provided great scientific discussions, or were just great people to spend time with include: Doug Van Pelt, Lisa Pitchford, Jon Gumucio, Ben Ryan, Mike Schleh, Tiwa Tjibewa, Edwin Miranda, Ryan Perkins, Tori Meyers, Chris Ahn, Pete Bodary, Andy Ludlow, Jake Haus, Charlene Ruloff, and anyone else that I have left out. I am thankful to each of them for all that they have done for me and have truly enjoyed the Michigan Kinesiology community.

Before I came to Michigan I spent 2 years at James Madison University, one of my favorite places on earth. The people that I met there showed me how to make science fun. There is no doubt in my mind that Mike Saunders and Nick Luden are THE best Master's advisors in the world. If they can't get someone excited about exercise science then that person should find a different career. I am so thankful to have found them in Harrisonburg. I am also incredibly lucky to have met Alec McKenzie, Andrew D'Lugos, Jess Ehrbar, Paul Roberson, Taylor Wenos, and Gabe Giersch. These people are some of my best friends and have made a huge impact on the direction of my scientific career. I am so grateful for all of their love and support.

The most important person that I met at JMU was Leanne Clifford (now Pataky). I could not have completed this dissertation without her love and support. I'm so proud to call her my wife and am thankful to have her by my side. She must be the happiest person I have ever met, and that joy rubs off on everyone around her (including me). I'm not sure what my life would look like without her, but it certainly would be a heck of a lot worse.

The love that Leanne's family has given me is more than I could have ever asked for and has helped me in so many ways throughout my time at Michigan. Bill and Robin are two of my favorite people and I am lucky to have gained two new parents that are as fun as they are. In

addition, Claude, Carol, Uncle John, Tina, Scott, Reed, and Billy have given me so much love and I am thankful to have married into such a great family.

My family is equally as amazing and supportive. My grandma has given me so much love and I am so happy that we have her back in the Midwest with us! I've got three older siblings that I am in awe of. How many people finish a Ph.D. at the University of Michigan and can confidently say that they are the dumbest of their siblings? Kim is an amazing scientist and mother. Andy is an incredible dad, role model, and one of the funniest people I know. Ann gets along with everyone and is now a brilliant scientist turned marketer. Those three continue to set the bar so high for the baby in the family, and I am very thankful for that. My family in Columbus (Aunt Bev, Uncle Lanny, Emily, and Clayton) are so supportive as well and are another group of people that I look up to. They are some of the happiest people I know and I enjoy every minute that I spend with them. I just hope that they can get used to me rooting for "the team up north". Go Blue!

Finally, I want to thank my mom and dad. They have given me everything I have ever needed or wanted. They are the most amazing parents a kid could ask for. When I was about 5 or 6 years-old I remember "lifting weights out" with my dad in our basement and then having chicken at dinner. My parents told me that I needed to eat all of my chicken because it would help my muscles grow. I then flexed my bicep, ate a bite of chicken, and flexed again. They told me that it was getting bigger. This was my first lesson in exercise science and nutrition. My parents were fantastic role models that taught me I could have anything I ever wanted, with one caveat: just work hard enough to get it. I may not have worked hard at everything (like high school Spanish or cleaning my room), but I eventually learned another important lesson they worked so hard to teach me: "Nothing is worth doing half way". Over the last four years I have used their lessons and have worked incredibly hard on this dissertation. I'm very proud of what I have accomplished and am a lucky person to have had the parents that provided me with amazing guidance, motivation, love, and support to help me along the way. This dissertation is dedicated to them.

TABLE OF CONTENTS

LIST OF FIGURES

Figure

LIST OF TABLES

Table

LIST OF APPENDICES

ABSTRACT

Insulin resistance of skeletal muscle, a tissue which accounts for up to 85% of insulin-mediated glucose disposal, is a primary and essential precursor that leads to type 2 diabetes. A single bout of exercise can subsequently enhance insulin-stimulated glucose uptake (ISGU) in insulin-resistant skeletal muscle. Although much work has been performed in healthy muscle, the mechanisms which lead to increased post-exercise insulin sensitivity in insulin-resistant muscle are far less understood. Therefore, the main objective of this dissertation was to provide insights into the mechanisms for enhanced post-exercise ISGU in muscle from insulin-resistant rats. Further complicating our understanding of post-exercise insulin sensitivity is the fact that skeletal muscle is a heterogeneous tissue composed of multiple fiber types with varied metabolic properties. Therefore, research in this thesis exploited the metabolic heterogeneity of different fiber types to investigate potential mechanisms for enhanced post-exercise ISGU in insulin-resistant muscle at a cellular level. Study 1 revealed that a 2-week high-fat diet (HFD), which causes whole muscle insulin resistance, results in fiber type-specific decrements in ISGU. Study 2 uncovered that acute exercise by HFD-fed rats results in increased ISGU of all type II fiber types (including IIB, IIBX, IIX, IIAX, and IIA), but ISGU was unaltered post-exercise in type I fibers, the only fiber type to maintain normal insulin sensitivity on a HFD. The striking fiber type-specific results of both a HFD and of acute exercise on ISGU revealed a need to better understand mechanisms for enhanced post-exercise ISGU at a cellular level. Studies 3 and 4 assessed key post-exercise signaling events in whole muscle and different fiber types, respectively, from HFD-fed rats. The results from insulin-resistant whole muscle tissue support the concept that increased γ3-AMPK activity is an important post-exercise event which eventually leads to enhanced insulin-stimulated AS160 phosphorylation. Further, the results revealed that fiber type-specific insulin-stimulated AS160 phosphorylation was site-specific. The fiber type-specific AS160 phosphorylation in Study 4 roughly corresponded with the observed fiber type-specific ISGU in Study 2. Therefore, these results support the idea, at least in some

fiber types from insulin-resistant muscle, that AS160 plays a key role in mediating enhanced post-exercise ISGU. Further studies are warranted to assess the direct effect of site-specific AS160 phosphorylation and γ3-AMPK activity on post-exercise ISGU. A better understanding of the mechanisms for enhanced ISGU following exercise in insulin-resistant skeletal muscle will facilitate the development and implementation of novel therapies and interventions to mitigate the deleterious effects of insulin resistance.

CHAPTER I

Introduction

Insulin resistance is a primary and essential defect in the progression to type 2 diabetes, which affects approximately 400 million people worldwide [1]. Insulin resistance is linked to numerous negative health outcomes including atherogenesis, hypertension, stroke, cognitive dysfunction, and some forms of cancer [2-4]. Skeletal muscle accounts for up to 85% of insulin-mediated glucose disposal, making it an extremely important target for combatting type 2 diabetes and insulin resistance [5]. Because glucose transport into the muscle is a rate limiting step for glucose disposal, it is important to more clearly understand the mechanisms which govern this process.

Exercise can enhance skeletal muscle glucose uptake independent of insulin [6]. Interestingly, after the insulin-independent effect of exercise has worn off (around 1-3hr post-exercise) insulin-stimulated glucose uptake is enhanced by exercise [7]. A single bout of exercise can have a powerful and long-lasting effect on insulin sensitivity, subsequently enhancing insulin-stimulated glucose uptake in muscle for up to 48hr after exercise [8, 9]. When rats are fed a high-fat diet insulin-stimulated glucose uptake is impaired, but exercise can still improve insulin-stimulated glucose uptake in these animals [10]. However, exercise does not completely recover insulin-stimulated glucose uptake in high-fat fed rats to the level attained in chow-fed rats after the same exercise protocol, and the mechanisms for this phenomenon are unknown.

The distal insulin signaling protein, AS160 (Akt substrate of 160 kDa; also known as TBC1D4), has been shown to be phosphorylated on multiple residues (Ser588, Thr642, Ser704, Ser318, Ser341, Ser751) in insulin-stimulated skeletal muscle several hours after exercise, when insulin-stimulated glucose uptake is also elevated [10-16]. In an unphosphorylated state AS160 acts as a brake, restraining GLUT4 vesicles within the interior of the cell. Leinhard et al. discovered that mutations of S588A, T642A, or both S588A and T642A on AS160 resulted in an inhibitory effect of insulin to stimulate GLUT4 translocation in adipocytes that was not further

inhibited by additional mutations preventing phosphorylation on other AS160 phosphomotifs (S318A, S341A, S570A, or S751A) [17]. Once phosphorylated on Ser588 and/or Thr642 the inhibitory effect of AS160 is released and GLUT4 vesicles can move to and become incorporated with the plasma membrane, subsequently increasing glucose uptake. These two AS160 phosphomotifs (Ser588 and Thr642), which are phosphorylated by Akt, have been proposed to be important for the improved insulin sensitivity observed post-exercise in insulin-sensitive and insulin-resistant individuals. However, it was reported that an identical exercise protocol had a greater effect in muscle from insulin-sensitive compared to insulin-resistant individuals for AS160 phosphorylation on these sites [10]. Recently, a phosphomotif on AS160 that is activated by AMPK, Ser704, has been identified as a potential contributor to enhanced insulin sensitivity post-exercise [14, 18], but there is limited information regarding how this site responds to exercise in insulin-resistant individuals.

AMPK is a heterotrimeric complex composed of a catalytic α subunit (α1 or α2 isoform) and two regulatory subunits (β1 or β2 isoform; and γ1, γ2, or γ3 isoform). The activation of γ3-AMPK has been shown to be increased in muscle by exercise in humans [19, 20] and rats [21] or by electrically stimulated contractions in mice [20, 22]. Additionally, γ1-AMPK can be weakly activated by prolonged exercise, but even during prolonged exercise a larger increase in γ3-AMPK activity is observed [23]. Prior incubation of isolated muscles from wild-type mice with 5-aminoimidazole-4-carboxamide ribonucleotide (AICAR) resulted in enhanced insulin-stimulated glucose uptake, but this AICAR-effect on insulin sensitivity was absent in muscles from γ3-AMPK knockout mice [24]. Moreover, electrically stimulated *in situ* contractile activity which enhances insulin-stimulated pAS160^{Ser704} in WT mice did not increase insulin-stimulated pAS160^{Ser704} in γ3-AMPK knockout mice [22]. These findings suggest γ3-AMPK activation and pAS160^{Ser704} may be critical steps for enhancing insulin-stimulated glucose uptake after AICAR or contraction in insulin-sensitive animals. However, neither prior AICAR treatment nor *in situ* contractions completely recapitulate *in vivo* exercise, and no published study has evaluated γ3-AMPK activity after exercise in insulin-resistant rats. Given our current understanding and recent findings, a more thorough investigation of the insulin signaling events which occur after exercise in insulin-resistant individuals is necessary to more clearly understand the complexities of insulin resistance.

Skeletal muscle is a heterogeneous tissue composed of multiple fiber types which have varied metabolic and contractile properties [25]. It has recently been discovered that in insulin-sensitive rats not all fiber types exhibit enhanced insulin-stimulated glucose uptake after a given exercise protocol [26]. However, neither the effect of high-fat diet in sedentary rats nor the effect of exercise in rats fed a high-fat diet on insulin-stimulated glucose uptake of different fiber types has been evaluated. It seems possible that insulin-stimulated glucose uptake is altered in select fiber types after exercise in high-fat fed rats. Fiber-type specific insulin signaling responses to high-fat diet and exercise, specifically on various phosphosites of AS160, may play a large role in fiber type specific insulin sensitivity, but insulin signaling has not yet been measured in different fiber types from insulin-resistant muscle of sedentary or acutely exercised rats. Additionally, whole muscle glycogen and intramuscular triglyceride (IMTG) levels have been proposed to be related to insulin sensitivity [27-30]. However, glycogen and IMTGs have not been measured in a fiber type-selective manner in muscles of animals for which fiber type-specific insulin sensitivity is also known.

The research in this dissertation focuses on the following goals: 1) Identify fiber type-specific differences for insulin-stimulated glucose uptake, glycogen content, and IMTG abundance and localization in insulin-resistant rats that are sedentary or exercised, 2) Probe key signaling events (pAS160^{Thr642}, pAS160^{Ser588}, pAS160^{Ser704}, and AMPK-γ1 and AMPK-γ3 activity) that have been proposed to influence the effect of exercise on insulin-stimulated glucose uptake in whole muscle from insulin-sensitive and insulin-resistant rats, and 3) Evaluate key signaling events (pAS160^{Thr642}, pAS160^{Ser588}, pAS160^{Ser704}) that have been implicated in the effect of exercise on insulin sensitivity in single fibers from insulin-resistant rats.

Study 1: *High-Fat Diet-Induced Insulin Resistance in Single Skeletal Muscle Fibers is Fiber Type Selective*

Insulin resistance can be induced by feeding rodents a high-fat diet for a period of weeks to months. After only two to four weeks of a high-fat diet, insulin resistance is detectable in whole muscle [10, 31-33]. However, for a complete understanding of insulin resistance measurements must be made at a cellular level because muscle tissue includes multiple fiber types with different metabolic properties [25]. Type I, IIA, IIX, and IIB are the major myosin

heavy chain (MHC) isoforms expressed in adult rat skeletal muscle, and MHC expression is the gold standard for determining fiber type [34]. The conventional approach to assess fiber type differences in glucose uptake uses whole muscle tissue or a region of muscle tissue that is enriched in a certain fiber type. Relatively few studies had considered a possible relationship between fiber type and high-fat diet-induced insulin resistance. Some, but not all, of these studies suggested that high-fat diet can differentially influence insulin-stimulated glucose uptake in muscles composed of different fiber type proportions [33, 35-38]. No studies had determined insulin-stimulated glucose uptake in single muscle fibers of known fiber type from high-fat fed rats. Therefore, the first aim of Study 1 was to evaluate insulin-stimulated glucose uptake in different fiber types from high-fat and low-fat fed rats. Because some groups have demonstrated altered fiber type composition after four or more weeks of high-fat feeding it seemed possible that a 2-week high-fat diet could also alter fiber type proportion. If fiber type-specific insulin resistance were observed following a 2-week high fat diet, then the fiber type proportion of whole muscle would be extremely important. Therefore, the second aim of Study 1 was to determine the effect of 2-weeks of high-fat feeding on fiber type composition of the rat epitrochlearis muscle. Finally, insulin-stimulated glucose uptake of skeletal muscles relies on the expression of the GLUT4 glucose transporter protein. It has previously been observed that GLUT4 protein expression in whole muscle tissue is not altered by a brief high-fat diet, but it seemed possible that high-fat diet could induce fiber type specific alterations in GLUT4 protein expression. Therefore, the third aim of Study 1 was to measure changes in GLUT4 protein abundance induced by a 2-week high-fat diet in different muscle fiber types.

Study 2: *Skeletal Muscle Fiber Type-selective Effects of Acute Exercise on Insulin-stimulated Glucose Uptake in Insulin-Resistant, High Fat-fed Rats*

The ability of exercise to improve insulin sensitivity of whole skeletal muscle is well established [7, 8, 27, 39-43]. Additionally, increased skeletal muscle insulin-stimulated glucose uptake after exercise has been observed during insulin resistance [9, 44, 45]. It has recently been discovered that insulin-stimulated glucose uptake after exercise is significantly enhanced in all fiber types except for type IIX fibers from insulin-sensitive rats [26]. However, the effect of exercise on insulin-stimulated glucose uptake during insulin resistance had never been evaluated

in different fiber types. The groups of rats that were studied in these experiments are: 1) low-fat diet (LFD) sedentary, 2) high-fat diet (HFD) sedentary, 3) HFD immediately post-exercise (IPEX), and 4) HFD three hours post-exercise (3hPEX). The first aim of Study 2 was to identify if there are fiber type-selective differences for insulin-stimulated glucose uptake after acute exercise in rats fed a 2-week high-fat diet. If some fiber types did not display enhanced insulin sensitivity after exercise then it would be important to determine which of the fiber types were recruited during the exercise protocol. Therefore, the second aim of Study 2 was to measure insulin-independent glucose uptake and glycogen concentration in each fiber type from high-fat fed rats that are sedentary or IPEX to identify epitrochlearis fiber type-specific recruitment by the exercise protocol. Because lipid accumulation has been suggested as a potential contributor to insulin resistance in skeletal muscle [29, 30, 46], the third aim of Study 2 was to measure the abundance, size, and subcellular localization of lipid droplets in all fiber types from sedentary low-fat fed, sedentary high-fat fed and exercised high-fat fed rats. The fourth and final aim of Study 2 was to compare the abundance of GLUT4 protein content in single fibers from high-fat fed exercised rats, along with low- and high-fat fed sedentary rats, to determine if acute exercise or high-fat diet alters the expression of this critical protein for enhancing glucose uptake.

Study 3: *Exercise Effects on γ3-AMPK Activity, Phosphorylation of Akt2 and AS160, and Insulin-stimulated Glucose Uptake in Insulin-Resistant Rat Skeletal Muscle*

Exercise is a powerful and long-lasting (1-48 hrs) stimulus to improve insulin-stimulated glucose uptake into skeletal muscle in healthy (insulin-sensitive) subjects [27, 39, 42]. Skeletal muscle insulin sensitivity can also be improved in insulin-resistant subjects following exercise [10, 44, 47]. Castorena et al. demonstrated that insulin sensitivity is enhanced after exercise in insulin-resistant rats, but is not elevated to attain the same level observed in insulin-sensitive rats after exercise [10]. In insulin-sensitive subjects many groups have attributed the enhanced insulin sensitivity after exercise to increased AS160 phosphorylation on multiple sites (Ser588, Thr642, Ser704) [13-15, 48]. Castorena et al. found that exercise enhances insulin-stimulated $pAS160^{Ser588}$ in insulin-sensitive rats to a greater extent than in insulin-resistant rats. It is possible that different mechanisms may exist which enhance insulin sensitivity after exercise in insulin-sensitive versus insulin-resistant muscle. Evidence that $pAS160^{Ser588}$ and $pAS160^{Thr642}$

are potential mediators for the effect of exercise on insulin sensitivity in insulin-sensitive muscle are abundant [10, 12, 15, 49], but less evidence exists for insulin-resistant muscle. Subsequent to the Castorena et al. study there have been some reports which have provided evidence that pAS160^{Ser704}, an AMPK phosphomotif, may potentially play an important role in the effect of either prior muscle contraction or prior treatment with AMPK activating compound AICAR on insulin-stimulated glucose uptake in mouse skeletal muscle [18, 48]. Therefore, the first aim of this study was to investigate the effect of exercise during diet-induced insulin resistance on AS160 phosphorylation sites (Ser588, Thr642, Ser704). Because pAS160^{Ser704} is an AMPK phosphosite it was also important to measure the level of muscle AMPK activity following exercise. AMPK is a heterotrimeric protein complex composed of α, β, and γ subunits each of which have multiple isoforms (α1, α2, β1, β2, γ1, γ2, γ3) [50]. Activation of the γ3-isoform of AMPK seems to be important in mediating the effect of AICAR or electrically stimulated muscle contractions on insulin sensitivity [24]. Additionally, γ1-containing AMPK activity has been shown to be increased after prolonged exercise, but to a lesser extent than γ3-containing AMPK [23]. These potentially critical signaling steps had not been evaluated during insulin-resistant conditions following *in vivo* exercise. Therefore, the second aim of this study was to investigate the post-exercise effect on γ1- and γ3-AMPK activity in muscles from insulin-resistant rats fed a high-fat diet, compared to sedentary high-fat and low-fat diet-fed controls. Earlier research reported that post-exercise increases in insulin-stimulated pAS160 or glucose uptake occur independent of Akt phosphorylation, but these studies did not include the evaluation of Akt2 phosphorylation, the Akt isoform implicated in insulin-stimulated AS160 phosphorylation [51] and insulin-stimulated glucose uptake [52, 53]. Accordingly, the third aim of this study was to determine if exercise enhanced insulin-stimulated pAkt2^{Thr309} or pAkt2^{Ser474} in insulin-resistant muscle.

Study 4: *Fiber Type-specific Effects of Acute Exercise on Insulin-stimulated AS160 Phosphorylation in Insulin-Resistant Rat Skeletal Muscle*

Diet and/or exercise have the potential to cause fiber type-specific differences in insulin-stimulated glucose uptake (Study 1 and 2). Therefore, impairments in insulin signaling after high-fat feeding or improvements in insulin signaling after exercise in the whole muscle may not

reflect what is occurring at the fiber type level. One study has measured fiber type-specific insulin signaling in human skeletal muscle [54], but this publication did not evaluate insulin signaling after exercise, nor did it differentiate between different type II isoforms in muscle fibers. Because this earlier study was performed in humans, it was also unable to evaluate insulin signaling in fibers from which fiber type-specific insulin-stimulated glucose uptake was also known. Our laboratory group has recently identified fiber type-specific insulin signaling differences (Akt and AS160 phosphorylation) in chow fed rats after exercise [55], a cohort which has been characterized for fiber type-specific insulin-stimulated glucose uptake [26]. Identifying insulin signaling differences that occur among fiber types after exercise in healthy subjects is exciting, but a more urgent need is to study insulin-resistant subjects after exercise. The fiber type-specific effect of exercise appears to be different when rats are fed a normal chow diet [26] versus a 2-week high-fat diet (Study 2), which has been shown to induce insulin resistance [10]. Insulin signaling events in different fiber types following exercise of insulin-resistant subjects had never been measured. Therefore the first aim of Study 4 was to evaluate fiber-type-specific effects of exercise (both immediately post-exercise and 3 hours post-exercise with and without insulin) on the phosphorylation of key signaling proteins (AMPK, Akt, and AS160) that have been implicated in the regulation of exercise effects on skeletal muscle glucose uptake. Because glycogen accumulation has been implicated in the reversal of post-exercise insulin sensitivity, our second aim was to determine fiber type-specific glycogen content in epitrochlearis muscles from HFD-fed rats both immediately and 3-hours post-exercise compared to sedentary controls. Hexokinase II (HKII) abundance has been suggested to be important for insulin-stimulated glucose uptake by skeletal muscle [56]. Therefore, our final aim was to assess the abundance of HKII after acute exercise in different fiber types from insulin-resistant rat skeletal muscle.

REFERENCES

1. Nathan, D.M., *Diabetes: advances in diagnosis and treatment.* Jama, 2015. **314**(10): p. 1052-1062.
2. Facchini, F.S., N. Hua, F. Abbasi, and G.M. Reaven, *Insulin resistance as a predictor of age-related diseases.* The Journal of Clinical Endocrinology & Metabolism, 2001. **86**(8): p. 3574-3578.
3. Haffner, S.M., *Epidemiology of insulin resistance and its relation to coronary artery disease.* The American journal of cardiology, 1999. **84**(1): p. 11-14.
4. Kumari, M., E. Brunner, and R. Fuhrer, *Minireview: mechanisms by which the metabolic syndrome and diabetes impair memory.* The Journals of Gerontology Series A: Biological Sciences and Medical Sciences, 2000. **55**(5): p. B228-B232.
5. DeFronzo, R.A., E. Jacot, E. Jequier, E. Maeder, J. Wahren, and J.P. Felber, *The effect of insulin on the disposal of intravenous glucose. Results from indirect calorimetry and hepatic and femoral venous catheterization.* Diabetes, 1981. **30**(12): p. 1000-7.
6. Garetto, L.P., E.A. Richter, M.N. Goodman, and N.B. Ruderman, *Enhanced muscle glucose metabolism after exercise in the rat: the two phases.* American Journal of Physiology-Endocrinology And Metabolism, 1984. **246**(6): p. E471-E475.
7. Wallberg-Henriksson, H., S. Constable, D. Young, and J. Holloszy, *Glucose transport into rat skeletal muscle: interaction between exercise and insulin.* Journal of applied physiology, 1988. **65**(2): p. 909-913.
8. Cartee, G.D., D.A. Young, M.D. Sleeper, J. Zierath, H. Wallberg-Henriksson, and J.O. Holloszy, *Prolonged increase in insulin-stimulated glucose transport in muscle after exercise.* Am J Physiol, 1989. **256**(4 Pt 1): p. E494-9.
9. Betts, J.J., W.M. Sherman, M.J. Reed, and J.P. Gao, *Duration of improved muscle glucose uptake after acute exercise in obese Zucker rats.* Obesity, 1993. **1**(4): p. 295-302.
10. Castorena, C.M., E.B. Arias, N. Sharma, and G.D. Cartee, *Postexercise improvement in insulin-stimulated glucose uptake occurs concomitant with greater AS160 phosphorylation in muscle from normal and insulin-resistant rats.* Diabetes, 2014. **63**(7): p. 2297-308.
11. Arias, E.B., J. Kim, K. Funai, and G.D. Cartee, *Prior exercise increases phosphorylation of Akt substrate of 160 kDa (AS160) in rat skeletal muscle.* American Journal of Physiology-Endocrinology and Metabolism, 2007. **292**(4): p. E1191-E1200.
12. Funai, K., G.G. Schweitzer, N. Sharma, M. Kanzaki, and G.D. Cartee, *Increased AS160 phosphorylation, but not TBC1D1 phosphorylation, with increased postexercise insulin sensitivity in rat skeletal muscle.* American Journal of Physiology-Endocrinology and Metabolism, 2009. **297**(1): p. E242-E251.
13. Funai, K., G.G. Schweitzer, C.M. Castorena, M. Kanzaki, and G.D. Cartee, *In vivo exercise followed by in vitro contraction additively elevates subsequent insulin-stimulated glucose transport by rat skeletal muscle.* American Journal of Physiology-Endocrinology and Metabolism, 2010. **298**(5): p. E999-E1010.
14. Pehmøller, C., N. Brandt, J.B. Birk, L.D. Høeg, K.A. Sjøberg, L.J. Goodyear, B. Kiens, E.A. Richter, and J.F. Wojtaszewski, *Exercise alleviates lipid-induced insulin resistance in human skeletal muscle–signaling interaction at the level of TBC1 domain family member 4.* Diabetes, 2012. **61**(11): p. 2743-2752.

15. Schweitzer, G.G., E.B. Arias, and G.D. Cartee, *Sustained postexercise increases in AS160 Thr 642 and Ser 588 phosphorylation in skeletal muscle without sustained increases in kinase phosphorylation.* Journal of applied physiology, 2012. **113**(12): p. 1852-1861.
16. Iwabe, M., E. Kawamoto, K. Koshinaka, and K. Kawanaka, *Increased postexercise insulin sensitivity is accompanied by increased AS160 phosphorylation in slow-twitch soleus muscle.* Physiological reports, 2014. **2**(12): p. e12162.
17. Sano, H., S. Kane, E. Sano, C.P. Mîinea, J.M. Asara, W.S. Lane, C.W. Garner, and G.E. Lienhard, *Insulin-stimulated phosphorylation of a Rab GTPase-activating protein regulates GLUT4 translocation.* Journal of Biological Chemistry, 2003. **278**(17): p. 14599-14602.
18. Sjøberg, K.A., C. Frøsig, R. Kjøbsted, L. Sylow, M. Kleinert, A.C. Betik, C.S. Shaw, B. Kiens, J.F. Wojtaszewski, and S. Rattigan, *Exercise increases human skeletal muscle insulin sensitivity via coordinated increases in microvascular perfusion and molecular signaling.* Diabetes, 2017. **66**(6): p. 1501-1510.
19. Kjøbsted, R., A.J. Pedersen, J.R. Hingst, R. Sabaratnam, J.B. Birk, J.M. Kristensen, K. Højlund, and J.F. Wojtaszewski, *Intact regulation of the AMPK signaling network in response to exercise and insulin in skeletal muscle of male patients with type 2 diabetes: illumination of AMPK activation in recovery from exercise.* Diabetes, 2016. **65**(5): p. 1219-1230.
20. Treebak, J.T., C. Pehmøller, J.M. Kristensen, R. Kjøbsted, J.B. Birk, P. Schjerling, E.A. Richter, L.J. Goodyear, and J.F. Wojtaszewski, *Acute exercise and physiological insulin induce distinct phosphorylation signatures on TBC1D1 and TBC1D4 proteins in human skeletal muscle.* The Journal of physiology, 2014. **592**(2): p. 351-375.
21. Wang, H., E.B. Arias, M.W. Pataky, L.J. Goodyear, and G.D. Cartee, *Postexercise improvement in glucose uptake occurs concomitant with greater γ3-AMPK activation and AS160 phosphorylation in rat skeletal muscle.* American Journal of Physiology-Endocrinology and Metabolism, 2018.
22. Kjøbsted, R., N. Munk-Hansen, J.B. Birk, M. Foretz, B. Viollet, M. Björnholm, J.R. Zierath, J.T. Treebak, and J.F. Wojtaszewski, *Enhanced muscle insulin sensitivity after contraction/exercise is mediated by AMPK.* Diabetes, 2017. **66**(3): p. 598-612.
23. Treebak, J.T., J.B. Birk, A.J. Rose, B. Kiens, E.A. Richter, and J.F. Wojtaszewski, *AS160 phosphorylation is associated with activation of α2β2γ1-but not α2β2γ3-AMPK trimeric complex in skeletal muscle during exercise in humans.* American Journal of Physiology-Endocrinology and Metabolism, 2007. **292**(3): p. E715-E722.
24. Kjøbsted, R., J.T. Treebak, J. Fentz, L. Lantier, B. Viollet, J.B. Birk, P. Schjerling, M. Björnholm, J.R. Zierath, and J.F. Wojtaszewski, *Prior AICAR stimulation increases insulin sensitivity in mouse skeletal muscle in an AMPK-dependent manner.* Diabetes, 2015. **64**(6): p. 2042-2055.
25. Pette, D. and R.S. Staron, *Cellular and molecular diversities of mammalian skeletal muscle fibers.* Rev Physiol Biochem Pharmacol, 1990. **116**: p. 1-76.
26. Cartee, G.D., E.B. Arias, S.Y. Carmen, and M.W. Pataky, *Novel single skeletal muscle fiber analysis reveals a fiber type-selective effect of acute exercise on glucose uptake.* American Journal of Physiology-Endocrinology and Metabolism, 2016. **311**(5): p. E818-E824.

27. Cartee, G. and J. Holloszy, *Exercise increases susceptibility of muscle glucose transport to activation by various stimuli.* American Journal of Physiology-Endocrinology And Metabolism, 1990. **258**(2): p. E390-E393.
28. Jazet, I., G. Schaart, A. Gastaldelli, E. Ferrannini, M. Hesselink, P. Schrauwen, J. Romijn, J. Maassen, H. Pijl, and D. Ouwens, *Loss of 50% of excess weight using a very low energy diet improves insulin-stimulated glucose disposal and skeletal muscle insulin signalling in obese insulin-treated type 2 diabetic patients.* Diabetologia, 2008. **51**(2): p. 309-319.
29. Nakagawa, Y., M. Hattori, K. Harada, R. Shirase, M. Bando, and G. Okano, *Age-related changes in intramyocellular lipid in humans by in vivo 1H-MR spectroscopy.* Gerontology, 2007. **53**(4): p. 218-223.
30. Storlien, L.H., A.B. Jenkins, D.J. Chisholm, W.S. Pascoe, S. Khouri, and E.W. Kraegen, *Influence of dietary fat composition on development of insulin resistance in rats: relationship to muscle triglyceride and ω-3 fatty acids in muscle phospholipid.* Diabetes, 1991. **40**(2): p. 280-289.
31. Turner, N., G.M. Kowalski, S.J. Leslie, S. Risis, C. Yang, R.S. Lee-Young, J.R. Babb, P.J. Meikle, G.I. Lancaster, D.C. Henstridge, P.J. White, E.W. Kraegen, A. Marette, G.J. Cooney, M.A. Febbraio, and C.R. Bruce, *Distinct patterns of tissue-specific lipid accumulation during the induction of insulin resistance in mice by high-fat feeding.* Diabetologia, 2013. **56**(7): p. 1638-48.
32. Chisholm, K.W. and K. O'Dea, *Effect of short-term consumption of a high fat diet on glucose tolerance and insulin sensitivity in the rat.* Journal of nutritional science and vitaminology, 1987. **33**(5): p. 377-390.
33. Han, D.-H., P.A. Hansen, H.H. Host, and J.O. Holloszy, *Insulin resistance of muscle glucose transport in rats fed a high-fat diet: a reevaluation.* Diabetes, 1997. **46**(11): p. 1761-1767.
34. Pandorf, C.E., T. Garland, W. Aoi, C. Handschin, L. Gorza, P.M. Garcia-Roves, S.W. Copp, C.M. Tipton, V.J. Caiozzo, and F. Haddad, *A Rationale for SDS-PAGE of MHC Isoforms as a Gold Standard for Determining Contractile Phenotype.* Journal of Applied Physiology, 2010. **108**(1): p. 222-225.
35. Cresser, J., A. Bonen, A. Chabowski, L.E. Stefanyk, R. Gulli, I. Ritchie, and D.J. Dyck, *Oral administration of a PPAR-δ agonist to rodents worsens, not improves, maximal insulin-stimulated glucose transport in skeletal muscle of different fibers.* American Journal of Physiology-Regulatory, Integrative and Comparative Physiology, 2010. **299**(2): p. R470-R479.
36. Kraegen, E., D. James, L. Storlien, K. Burleigh, and D. Chisholm, *In vivo insulin resistance in individual peripheral tissues of the high fat fed rat: assessment by euglycaemic clamp plus deoxyglucose administration.* Diabetologia, 1986. **29**(3): p. 192-198.
37. Storlien, L.H., A.W. Thorburn, G.A. Smythe, A.B. Jenkins, D.J. Chisholm, and E.W. Kraegen, *Effect of d-fenfluramine on basal glucose turnover and fat-feeding-induced insulin resistance in rats.* Diabetes, 1989. **38**(4): p. 499-503.
38. Han, D.-H., S.H. Kim, K. Higashida, S.-R. Jung, K.S. Polonsky, S. Klein, and J.O. Holloszy, *Ginsenoside Re rapidly reverses insulin resistance in muscles of high-fat diet fed rats.* Metabolism, 2012. **61**(11): p. 1615-1621.

39. Richter, E.A., L.P. Garetto, M.N. Goodman, and N.B. Ruderman, *Muscle glucose metabolism following exercise in the rat: increased sensitivity to insulin.* Journal of Clinical Investigation, 1982. **69**(4): p. 785.
40. Bonen, A., M. Tan, and W. Watson-Wright, *Effects of exercise on insulin binding and glucose metabolism in muscle.* Canadian journal of physiology and pharmacology, 1984. **62**(12): p. 1500-1504.
41. Richter, E.A., L.P. Garetto, M.N. Goodman, and N.B. Ruderman, *Enhanced muscle glucose metabolism after exercise: modulation by local factors.* American Journal of Physiology-Endocrinology And Metabolism, 1984. **246**(6): p. E476-E482.
42. Richter, E.A., K. Mikines, H. Galbo, and B. Kiens, *Effect of exercise on insulin action in human skeletal muscle.* Journal of applied physiology, 1989. **66**(2): p. 876-885.
43. Gulve, E.A., G.D. Cartee, J.R. Zierath, V. Corpus, and J. Holloszy, *Reversal of enhanced muscle glucose transport after exercise: roles of insulin and glucose.* American Journal of Physiology-Endocrinology And Metabolism, 1990. **259**(5): p. E685-E691.
44. Tanaka, S., T. Hayashi, T. Toyoda, T. Hamada, Y. Shimizu, M. Hirata, K. Ebihara, H. Masuzaki, K. Hosoda, and T. Fushiki, *High-fat diet impairs the effects of a single bout of endurance exercise on glucose transport and insulin sensitivity in rat skeletal muscle.* Metabolism, 2007. **56**(12): p. 1719-1728.
45. Sharoff, C.G., T.A. Hagobian, S.K. Malin, S.R. Chipkin, H. Yu, M.F. Hirshman, L.J. Goodyear, and B. Braun, *Combining short-term metformin treatment and one bout of exercise does not increase insulin action in insulin-resistant individuals.* American Journal of Physiology-Endocrinology and Metabolism, 2010. **298**(4): p. E815-E823.
46. Lara-Castro, C., B.R. Newcomer, J. Rowell, P. Wallace, S.M. Shaughnessy, A.J. Munoz, A.M. Shiflett, D.Y. Rigsby, J.C. Lawrence, and D.E. Bohning, *Effects of short-term very low-calorie diet on intramyocellular lipid and insulin sensitivity in nondiabetic and type 2 diabetic subjects.* Metabolism, 2008. **57**(1): p. 1-8.
47. Ropelle, E.R., J.R. Pauli, P.O. Prada, C.T. De Souza, P.K. Picardi, M.C. Faria, D.E. Cintra, M.F.d.A. Fernandes, M.B. Flores, and L.A. Velloso, *Reversal of diet-induced insulin resistance with a single bout of exercise in the rat: the role of PTP1B and IRS-1 serine phosphorylation.* The Journal of physiology, 2006. **577**(3): p. 997-1007.
48. Vendelbo, M.H., A.B. Møller, J.T. Treebak, L.C. Gormsen, L.J. Goodyear, J.F. Wojtaszewski, J.O.L. Jørgensen, N. Møller, and N. Jessen, *Sustained AS160 and TBC1D1 phosphorylations in human skeletal muscle 30 min after a single bout of exercise.* Journal of applied physiology, 2014. **117**(3): p. 289-296.
49. Arias, E.B., H. Wang, and G.D. Cartee, *Akt substrate of 160 kDa dephosphorylation rate is reduced in insulin-stimulated rat skeletal muscle after acute exercise.* Physiological research, 2017.
50. Hardie, D.G., J.W. Scott, D.A. Pan, and E.R. Hudson, *Management of cellular energy by the AMP-activated protein kinase system.* FEBS letters, 2003. **546**(1): p. 113-120.
51. Kramer, H.F., C.A. Witczak, N. Fujii, N. Jessen, E.B. Taylor, D.E. Arnolds, K. Sakamoto, M.F. Hirshman, and L.J. Goodyear, *Distinct signals regulate AS160 phosphorylation in response to insulin, AICAR, and contraction in mouse skeletal muscle.* Diabetes, 2006. **55**(7): p. 2067-2076.
52. Cho, H., J. Mu, J.K. Kim, J.L. Thorvaldsen, Q. Chu, E.B. Crenshaw, K.H. Kaestner, M.S. Bartolomei, G.I. Shulman, and M.J. Birnbaum, *Insulin resistance and a diabetes mellitus-*

like syndrome in mice lacking the protein kinase Akt2 (PKBβ). Science, 2001. **292**(5522): p. 1728-1731.
53. McCurdy, C.E. and G.D. Cartee, *Akt2 is essential for the full effect of calorie restriction on insulin-stimulated glucose uptake in skeletal muscle.* Diabetes, 2005. **54**(5): p. 1349-1356.
54. Albers, P.H., A.J. Pedersen, J.B. Birk, D.E. Kristensen, B.F. Vind, O. Baba, J. Nøhr, K. Højlund, and J.F. Wojtaszewski, *Human Muscle Fiber Type–Specific Insulin Signaling: Impact of Obesity and Type 2 Diabetes.* Diabetes, 2015. **64**(2): p. 485-497.
55. Wang, H., E.B. Arias, K. Oki, M.W. Pataky, J.A. Almallouhi, and G.D. Cartee, *Fiber Type-selective Exercise Effects on AS160 Phosphorylation.* American Journal of Physiology-Endocrinology and Metabolism, 2019.
56. Fueger, P.T., H.S. Hess, D.P. Bracy, R.R. Pencek, K.A. Posey, M.J. Charron, and D.H. Wasserman, *Regulation of insulin-stimulated muscle glucose uptake in the conscious mouse: role of glucose transport is dependent on glucose phosphorylation capacity.* Endocrinology, 2004. **145**(11): p. 4912-4916.

CHAPTER II

Review of Literature

Importance of Skeletal Muscle Glucose Transport

The prevalence of type 2 diabetes has more than doubled in recent decades and affects more than 30 million Americans (~9.4% of the population), with another 86 million Americans at high risk for future diabetes [1]. This increasing prevalence in type 2 diabetes is evident across age, gender, race, and ethnicity [2]. The widespread economic burden of type 2 diabetes related illnesses in the United States has now reached more than $133 billion annually and is expected to nearly triple in the next 15-20 years [3]. This value is estimated to be greater than $300 billion when considering the cost of undiagnosed diabetes [1]. Insulin resistance, defined as a subnormal response to a physiological dose of insulin, is a precursor to the development of type 2 diabetes. Even for people who do not have type 2 diabetes, insulin resistance is associated with poor health and increased risk for mortality [4]. Skeletal muscle insulin resistance is a primary and essential defect in the progression to type 2 diabetes, and skeletal muscle accounts for approximately 85% of insulin-stimulated glucose disposal [5]. The large role that skeletal muscle plays in glucose disposal makes it a preeminent target to combat insulin resistance and type 2 diabetes.

In skeletal muscle, glucose transport into the cell is a rate limiting step for glucose disposal [6, 7]. Because glucose cannot freely pass through the skeletal muscle plasma membrane, glucose transporter proteins (GLUTs) must translocate to the sarcolemma and T-tubules to bring glucose into the cell. GLUT4 is the major GLUT expressed in skeletal muscle and is predominantly responsible for insulin-stimulated glucose disposal [8, 9]. However, GLUT4 does not constitutively reside at the cell surface and must be stimulated to move from intracellular storage vesicles to the plasma membrane. Both insulin and muscle contraction/exercise can independently stimulate GLUT4 to move to the plasma membrane in skeletal muscle [10]. This process is generically referred to as GLUT4 translocation. Once

GLUT4 is incorporated into the plasma membrane of skeletal muscle cells, then glucose uptake can proceed via facilitated diffusion.

Not only do insulin and exercise independently increase skeletal muscle glucose uptake, but a single exercise session can subsequently enhance skeletal muscle insulin sensitivity [11-15]. This phenomenon is evident approximately 1-3 hours after the exercise bout, when the insulin-independent effect of exercise on glucose uptake has worn off [16], and can last up to 48 hours [17, 18]. The effect of exercise on insulin sensitivity may contribute to improved health in individuals who are not insulin-resistant, but a more urgent public health concern is to understand the influence of exercise on insulin sensitivity in insulin-resistant individuals. Insulin-resistant humans and rodents have subnormal GLUT4 cell surface membrane translocation and glucose uptake in response to insulin in skeletal muscle [19]. Therefore, the enhancement of insulin-stimulated glucose uptake is a very important benefit of exercise for insulin-resistant subjects. The processes that govern this important health benefit of exercise have been extensively investigated, but they are still not completely understood.

Insulin Signaling Pathway and Insulin-Stimulated Glucose Transport

The insulin signaling pathway regulates glucose uptake into skeletal muscle and adipose cells. The signaling processes that lead to insulin-stimulated glucose uptake result in the translocation of GLUT4 from an intracellular location to the cell surface membranes [20-22], bringing glucose into the cell. Following the ingestion of carbohydrates, increased glucose in the blood leads to enhanced insulin secretion from the pancreas [23]. High levels of insulin in the blood will result in the rapid binding of insulin to the insulin receptor (IR), a tyrosine kinase protein, on the surface of cells. The insulin receptor is a transmembrane receptor which is composed of two extracellular α subunits and two transmembrane β subunits that are linked by disulfide bonds. When insulin binds to the α subunits on the exterior of the muscle or adipose cell there is a resultant conformational change of the β subunits of the IR (moving these subunits closer together) and tyrosine autophosphorylation of the β subunit [24]. The tyrosine phosphorylation of the β subunits of the IR activates the IR, leading to the phosphorylation of its downstream protein substrates within the interior of the cell.

Insulin receptor substrate (IRS) proteins are the important substrates of the IR involved in the metabolic actions of insulin. IRS-1 and IRS-2 belong to the IRS family of proteins, and have a phosphotyrosine binding (PTB) domain [25]. Although both IRS-1 and IRS-2 relay insulin signaling, GLUT4 translocation and glucose uptake are primarily regulated by IRS-1 in muscle [26]. When the IR is phosphorylated on Tyr^{960}, the PTB domain of IRS-1 is recruited to the location of the IR and specifically binds to this tyrosine residue of the IR. This binding of the IR with IRS-1 results in the tyrosine phosphorylation of IRS-1 on multiple tyrosine residues by the insulin receptor tyrosine kinase (IRTK). This results in further downstream actions that eventually lead to the translocation of GLUT4 protein to the cell surface membranes. In some insulin-resistant conditions, the downstream actions of IRS-1 can be impaired. When IRS-1 is phosphorylated on specific serine or threonine residues, IR-mediated tyrosine phosphorylation of IRS-1 can be inhibited [27]. Serine phosphorylation of IRS-1 is seen in multiple insulin-resistant conditions and is implicated as one of the major locations for the mechanistic effects of insulin resistance [28-30].

IRS-1 is an adaptor protein that acts as a docking protein for the regulatory region of phosphatidylinositol 3-kinase (PI 3-kinase) [31]. Once PI 3-kinase associates with IRS-1 the active site of PI 3-kinase is able to move in close proximity to the cell membrane. The association of the activation site of PI 3-kinase with the membrane results in the phosphorylation of the plasma membrane lipid phosphatidylinositol-4,5 -biphosphate [$PI(4,5)P_2$]. When $PI(4,5)P_2$ is phosphorylated by PI 3-kinase it is converted into its active form, phosphatidylinositol-3,4,5 -triphosphate [$PI(3,4,5)P_3$][32]. Upon generation of $PI(3,4,5)P_3$, this membrane lipid moves along the cell surface membrane until it reaches PIP_3-dependent protein kinase (PDK-1). $PI(3,4,5)P_3$ then binds to and activates PDK-1, which results in the phosphorylation of protein kinase B (PKB; also known as Akt). Along with the activation of Akt, it is important to note that insulin-stimulated PI 3-kinase signaling also plays an important role in the activation of a protein called Rac1 in muscle [33]. Rac1 signaling stimulates the cyclic branching of actin filaments which the GLUT4 vesicles use as scaffolding for translocation to the cell surface membranes [34]. Rac1 signaling downstream of PI 3-kinase is completely independent of Akt signaling, but both are important for insulin-mediated glucose uptake [35].

Akt is a serine/threonine kinase that can be activated by phosphorylation on the Ser473 (in the hydrophobic motif) and Thr308 (within the catalytic domain) sites [36]. When activated, PDK-1 is the protein kinase that is primarily responsible for the phosphorylation of Akt on Thr308 [37]. Phosphorylation of Akt at Ser473 has been attributed to the activation of multiple kinases [38], but strong evidence implicates mTORC2 as a major regulator of Akt on Ser473 [39]. When Akt is activated it phosphorylates the Rab GAP Akt substrate of 160kDa (AS160; also known as TBC1D4). However, Akt's actions are not limited to this protein, as it has many downstream targets including GSK3, PRAS40, FOXO1/3A, TSC2, eNOS, and others [40]. AS160 is the Akt substrate most clearly linked to insulin-stimulated glucose transport [41]. Other Akt substrates that have been linked to insulin-stimulated glucose uptake include myosin 5A, CDP138 and tropomodulin 3 in adipocytes, but they have not been assessed in skeletal muscle [42-44].

A critical functional feature of AS160 is that it includes a GTPase activating domain for Rab proteins. Rab proteins are small G proteins which coordinate the formation, transport, and tethering of vesicles to a targeted location [45]. AS160's GTPase activating domain regulates Rab-mediated coordination of GLUT4 vesicle transport (specifically Rab8A, Rab13, and Rab28 have been implicated as important in skeletal muscle) to the cell surface membranes [34, 46-48]. In the absence of insulin stimulation, unphosphorylated AS160 favors Rab binding to GDP through increasing GTP hydrolysis by the GTPase-activating protein (GAP) domain of AS160. GDP-bound Rab inhibits GLUT4 vesicle exocytosis. AS160 can be phosphorylated on at least 6 sites by Akt, but two of those sites appear to be the most influential for GLUT4 translocation, Ser588 and Thr642. Sano et al. discovered that inhibiting phosphorylation on $AS160^{Thr642}$ by mutating Thr to Ala resulted in decreased insulin-stimulated GLUT4 translocation in adipocytes [49]. Similarly, Chen et al. developed a T649A knockin mouse (T649 corresponds to human T642) which displayed insulin-resistance and impaired insulin-stimulated GLUT4 translocation to the cell surface membranes [50]. Mutation of only Ser588 to Ala on AS160 caused reduced insulin-stimulated GLUT4 translocation in adipocytes, and combined T642A and S588A double mutation resulted in further inhibition of insulin-stimulated GLUT4 translocation in adipocytes [49]. However, no further inhibition of insulin-stimulated GLUT4 translocation resulted from mutation on six Akt phosphomotifs on AS160 (S318A, S341A, S588A, T642A, S570A, S751A) in adipocytes [49]. Phosphorylation of AS160 on Thr642 and/or Ser588 apparently results in the

movement of GLUT4 to the cell surface membrane by inactivating the GAP activity of AS160 towards Rab proteins. Inactivating the GAP activity towards these Rab proteins results in an increase in the active GTP bound Rab, and GLUT4 exocytosis can proceed. Put simply, AS160 serves as a brake on GLUT4 translocation, and phosphorylation by Akt causes AS160 to release the brake, allowing GLUT4 translocation to proceed [51].

Once GLUT4 vesicles have been localized to the cell surface membranes by Rab proteins they must fuse with the surface membranes for the GLUT4 protein to transport glucose into the cell. Soluble NSF attachment protein receptor (SNARE) proteins mediate the fusion of GLUT4 vesicles with the surface membranes [52]. Two SNARE proteins from the surface membranes (syntaxin4 and SNAP23) and one SNARE protein from the incoming GLUT4 vesicle (VAMP2) form a ternary complex that fuses these membranes, incorporating the GLUT4 proteins with the surface membranes [52]. Multiple SNARE proteins have been implicated in GLUT4 fusion with the surface membranes, but it appears that VAMP2 is the primary vesicle SNARE in skeletal muscle (but not in adipocytes) [53]. However, some have suggested that VAMP7 is an important vesicle SNARE for recycling vesicles [9]. Once the GLUT4 proteins are incorporated into the cell surface membranes they can then facilitate glucose's entry into the cell.

Mechanisms for Exercise Mediated Glucose Transport

A single bout of exercise can enhance glucose uptake into the muscle cell in the absence of insulin. This "insulin-like" effect of exercise occurs during and immediately after the exercise bout, and it is typically either mostly or entirely reversed by 1-3 hours post-exercise. Exercise can increase GLUT4 translocation independent of insulin [54], but the mechanisms which regulate GLUT4 translocation to cell surface membranes are not entirely resolved. The insulin-independent increase in glucose uptake after exercise has been considered to be due to multiple signaling events, including, but possibly not limited to, increased intracellular calcium concentrations [55, 56], enhanced AMP-activated protein kinase (AMPK) activation [57], mechanical tension-related events [58, 59], nitric oxide signaling [60, 61], and reactive oxygen species [62, 63]. It is important to note that these events occur independent of the insulin signaling pathway. Once most or all of the insulin independent effect of exercise has worn off, enhanced insulin-stimulated glucose uptake can be detected after exercise.

In the sequence of events for muscle contraction, membrane depolarization is followed by the release of calcium from the sarcoplasmic reticulum into the cytosol of muscle fibers. Calcium binds to troponin and initiates myosin binding to actin, resulting in a "power stroke" (muscle contraction). Increased calcium levels during muscle contraction can activate the calcium-sensitive serine/threonine kinase calcium/calmodulin activated protein kinase II (CaMKII) and CaMK kinase α (CaMKKα), which have been suggested to play a role in enhanced glucose uptake [64, 65]. The increased insulin-independent glucose uptake initiated by increased calcium, CaMKII activity, and CaMKKα activity observed after exercise appears to occur independent of AMPK activation [64, 66, 67]. However, the downstream calcium-related mechanisms/signaling to enhance glucose uptake remain controversial and incompletely understood.

AMPK is often described as a key sensor of cellular energy status, which is activated when AMP levels rise and ATP levels fall [68, 69]. Because ATP levels are not markedly reduced during normal exercise, with only modest decrements detected even during extremely high intensity exercise, it is the increase in AMP/ATP ratio that influences AMPK activation [70]. Exercise requires large amounts of ATP for fuel, and the hydrolysis of ATP to ADP during exercise followed by the conversion of ADP to AMP by the adenylate kinase reaction generates a high AMP/ATP ratio, allosterically activating AMPK [71-74]. Multiple groups have shown that exercise increases AMPK activity in skeletal muscle [71, 73, 75, 76], and *in vivo* exercise which activates AMPK has also been shown to increase skeletal muscle glucose uptake [77-79]. It has also been demonstrated that AMPK activation by muscle contractions or AICAR stimulation can increase glucose uptake [57, 80].

AMPK is a heterotrimeric protein complex composed of α, β, and γ subunits each of which have multiple isoforms (α1, α2, β1, β2, γ1, γ2, γ3) [81]. The α-subunit displays the calalytic activity, the β- subunit functions as a scaffold to hold the α and γ subunits together, and the γ-subunit is associated with binding of AMP [82, 83]. In human skeletal muscle only three heterotrimer isoforms of AMPK have been identified (α2β2γ1, α2β2γ3, and α1β2γ1) [84], whereas two additional heterotrimeric isoforms have been reported in mouse skeletal muscle (α2β1γ1, α1β1γ1) (Figure 2.1) [85]. When AMP levels are elevated by exercise, increased AMP binding to the γ-subunit of AMPK occurs, promoting phosphorylation of Thr^{172} on the catalytic

α-subunit, resulting in increased AMPK activity [68]. The activation of different isoforms of AMPK is dependent on exercise intensity and duration. It appears that γ3-containing complexes are highly activated during high intensity/short duration exercise, whereas γ1-containing complexes are unaltered [86]. In humans, exercise of moderate to low intensity of longer duration activates α2β2γ1 and α1β2γ1 isoforms of AMPK [86], but prolonged low intensity exercise will also increase γ3-containing AMPK [87]. When the γ3 isoform of AMPK is knocked out in mice, AICAR-stimulated skeletal muscle glucose uptake is completely inhibited [88], suggesting that the γ3 subunit is essential for the effect of AMPK on muscle glucose uptake.

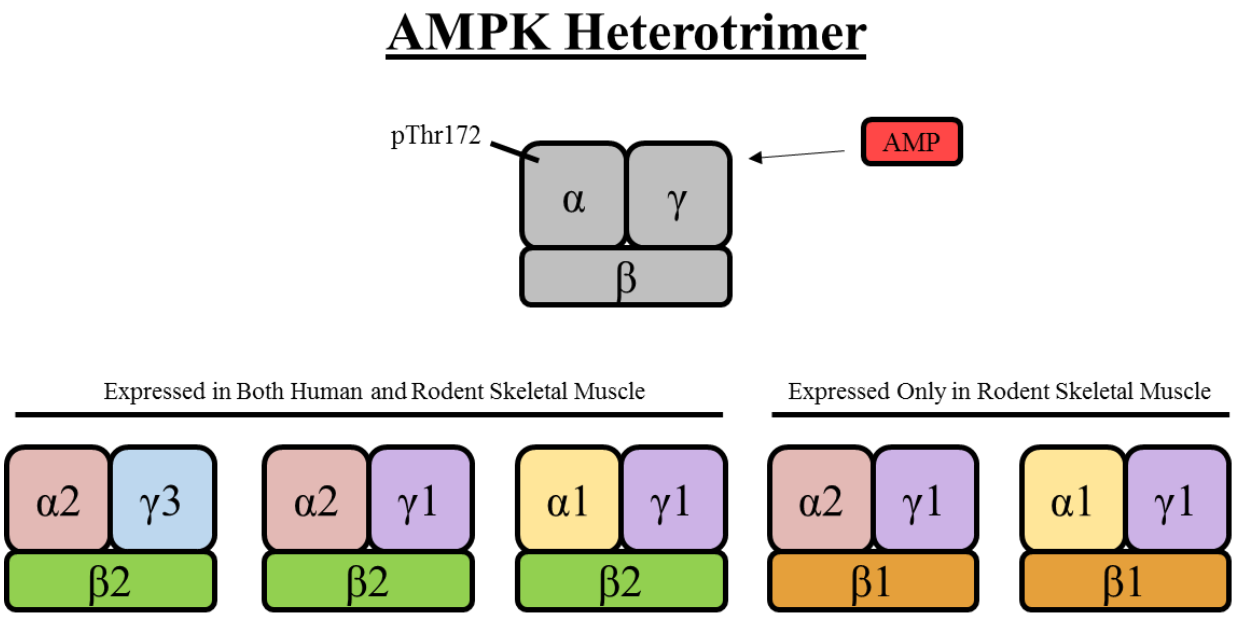

Figure 2.1

AMPK heterotrimeric combinations in human and rodent skeletal muscle. AMPK is a heterotrimeric protein complex composed of a catalytic α subunit, and two regulatory subunits (β and γ). There are multiple isoforms of each subunit (α1 and α2; β1 and β2; γ1, γ2, and γ3). In human skeletal muscle three heterotrimeric combinations have been detected, whereas two additional heterotrimeric combinations have been detected in rodent skeletal muscle. AMPK is activated by the binding of AMP or ADP to the Bateman domain of the γ subunit, resulting in a conformational change and phosphorylation of Thr172 on the α subunit.

AMPK is believed to act, at least in part, through downstream targets TBC1D1 and/or TBC1D4 (AS160) to enhance GLUT4 translocation, resulting in glucose uptake in muscle [89-91]. AICAR or contraction have been shown to increase phosphorylation of AS160 and TBC1D1 independently from Akt signaling [92-94], and in mice AMPK can phosphorylate AS160 on Ser711 (equivalent to Ser704 in humans) [95]. A recent finding showed that contraction-induced

phosphorylation of AS160^{Ser704} is dependent on the γ3 isoform of AMPK [96]. However, when muscles were incubated with Compound C (an AMPK inhibitor) AS160 phosphorylation (measured with the PAS antibody which is not entirely selective to a single phosphosite) remained elevated after contractions, while the TBC1D1 phosphorylation and glucose uptake were inhibited [94]. These results suggests that phosphorylation of TBC1D1, and perhaps not AS160, may be important for the effect of AMPK on exercise-induced, insulin-independent glucose uptake.

Mechanical tension during muscle contraction may provide a potent stimulus to increase glucose uptake. In fact, mechanical stress passively imposed on skeletal muscle has been shown to enhance glucose uptake, independent of insulin [59]. Some researchers have found that by stretching muscles *ex vivo*, glucose uptake in skeletal muscle is increased [97]. Mechanical stress may be sensed by cell surface membrane proteins that relay this mechanical stimulus to downstream signaling proteins. The Rho family GTPase, Rac1, is activated by passive stretch, and pharmacological inhibition of Rac1 significantly decreases stretch-induced glucose uptake [97]. However, since inhibiting Rac1 only partially reduces glucose uptake by passive-stretching, it remains possible that other mechanical stress-related signaling events exist that have yet to be discovered.

Nitric oxide and reactive oxygen species are both elevated by muscle contraction [98, 99]. Although both have been implicated to enhance glucose uptake after exercise [60-63], the data are conflicting. Inhibiting nitric oxide synthase (NOS) decreased glucose transport in some [60], but not all studies [100, 101]. Additionally, some have speculated that the production of reactive oxygen species during exercise is important for exercise-mediated glucose uptake, but this has not been proven *in vivo*.

In summary, the intracellular signaling processes which lead to enhanced glucose transport after exercise are quite complex. Substantial evidence points towards calcium- and AMPK-related signaling, and mechanical stress as playing important roles to mediate this effect. Future studies will be required to further discern the mechanisms by which distal signaling steps act to enhance glucose uptake into skeletal muscle in response to exercise.

Enhanced Insulin-Stimulated Glucose Transport following Acute Exercise

Increased skeletal muscle insulin-stimulated glucose uptake following acute exercise was first clearly demonstrated in 1982 by Richter et al. in perfused rat hindlimb preparations and in rat soleus and gastrocnemius muscles across a range of insulin concentrations [11]. Multiple groups have subsequently reported enhanced insulin-stimulated glucose uptake after acute exercise or muscle contractions in normal mouse, rat, and human skeletal muscle (See Table 2.1), and the effect of exercise on insulin sensitivity is detectable approximately 1-3 hours after the completion of exercise. In fact, Wallberg-Henriksson et al. demonstrated that the effects of insulin and exercise on skeletal muscle glucose uptake are additive in the first hour of recovery following exercise, but the effects of insulin and exercise become greater than additive between 1-3 hours after the cessation of exercise, once the insulin-independent effect of exercise on glucose uptake has largely worn off [16]. Some, but not all, of the experiments that have reported enhanced insulin-stimulated glucose uptake after exercise used supraphysiologic insulin doses, and should therefore be interpreted with caution. This review will emphasize experiments which have used submaximally effective, and thus more physiologically relevant, insulin doses.

Several groups have reported that the enhanced insulin sensitivity in the muscle or whole body, which begins approximately 3 hours post-exercise, appears to have a persistent effect lasting anywhere from 12-48 hours post-exercise [17, 18, 102-105]. Cartee et al. were able to provide insights about this phenomenon by restricting the carbohydrate access (fasting or feeding lard) of rats following exercise and measuring insulin sensitivity hours later [17]. This study identified a relationship between persistent post-exercise muscle glycogen depletion and repletion on enhanced insulin sensitivity, where muscles which remained glycogen depleted after exercise were more insulin-sensitive than those which super-compensated glycogen content above normal levels by carbohydrate feeding. A similar result was reported by Funai et al. who detected decreased glycogen and enhanced insulin sensitivity from 3-27 hours post-exercise in fasted rats, but found increased glycogen and a lack of enhanced insulin sensitivity by 3 hours post-exercise in rats fed carbohydrates [106]. Kim et al. studied rat skeletal muscle subjected to multiple *in situ* contraction protocols that differed on the basis of train duration, train rate, pulse frequency, number of 5-min bouts, or pulse duration [107]. They found that muscle glycogen was decreased following several of the *in situ* muscle contraction protocols that also increased

insulin-stimulated glucose uptake, but muscle glycogen was also decreased after several other protocols which failed to enhance insulin-stimulated glucose uptake [107]. These results suggested that muscle glycogen depletion may be necessary but not sufficient for the post-contraction increase in insulin-stimulated glucose uptake. However, Fisher et al. saw enhanced insulin-stimulated glucose uptake in muscle after AICAR incubation without a decrease in glycogen content [108], suggesting glycogen depletion may not be necessary for this effect. Kjøbsted et al. found that following prior *in situ* contractions, insulin-stimulated glucose uptake was not enhanced in muscle from AMPKα1α2 muscle-specific double-knockout mice, despite a significant decrease in glycogen content [96], suggesting glycogen depletion is not required for this effect. However, it is possible that the mechanisms for increased insulin-stimulated glucose uptake are not identical following exercise and prior AICAR treatment or *in situ* contractions.

The exercise-induced enhancement of skeletal muscle insulin sensitivity has been well described, but the mechanisms for this effect are not completely understood. It is apparent that the improved insulin-stimulated glucose uptake several hours following acute exercise is a result of increased GLUT4 glucose transporter protein at the cell surface in skeletal muscle of normal rats [10]. Multiple studies have reported unaltered GLUT4 abundance post-exercise concomitant with increased insulin-stimulated glucose uptake [10, 77, 106, 109], but one study found greater GLUT4 protein in human muscle 3 hours post-exercise [110]. Apparently no one has studied fiber type-selective changes in GLUT4 abundance after acute exercise when insulin sensitivity is enhanced, and it seems possible that exercise could rapidly alter GLUT4 content in a fiber type specific manner. Regardless, it is unclear exactly what factors mediate the ability of a prior exercise stimulus to subsequently enhance insulin-stimulated translocation of GLUT4 to the sarcolemma and increase glucose uptake. It was proposed that local rather than systemic factors mediate the effect of exercise on insulin sensitivity when it was first demonstrated that stimulating a single rat hindlimb to contract resulted in enhanced insulin-stimulated glucose uptake only in the stimulated limb [111]. In humans, one-legged knee extensor exercise increases insulin-stimulated glucose uptake of the vastus lateralis in the exercised leg, but not in the sedentary leg [12]. Additionally, cycling exercise has shown to increase insulin-stimulated glucose uptake of the leg, but not the forearm, providing further evidence for local factors influencing this effect [112]. Finally, insulin-stimulated glucose uptake was unaltered 3h following swim exercise in rat EDQP, a forearm muscle presumably not recruited by swim

exercise [113]. Together, these results suggest that local, rather than systemic, factors are primarily responsible for the majority of enhanced insulin-stimulated glucose uptake in muscle post-exercise.

Although the exercise effects on insulin sensitivity are limited to the contracting skeletal muscle there is some evidence that there may be a serum factor which is required during muscle contraction for this effect to occur. Muscles incubated with serum during contractions enhance insulin-stimulated glucose uptake to a similar magnitude to exercised muscles, but muscles incubated without serum do not [108, 114]. It is important to note that the serum was from a non-exercised human or rat (i.e., the effect was not attributable to an exercise-induced increase in the putative serum factor). It is also significant to recognize that these experiments used *ex vivo* contractions by isolated muscle preparations, and the mechanisms may be distinct from the effects of *in vivo* exercise. Regardless of the uncertainty about the physiological relevance of the serum factor, there is evidence that the effect of exercise on insulin sensitivity is limited to the stimulated or exercised muscle. Therefore, in the early 1990's many researchers aimed to discover a local mechanism for the effect of exercise on insulin sensitivity.

Cartee and Holloszy demonstrated that exposure of isolated muscles to insulin mimetics, vanadate and H_2O_2, which act distal to insulin binding to the insulin receptor, increase skeletal muscle glucose transport following *in vivo* exercise [115]. This finding indicated that exercise elicits its enhancement of insulin sensitivity somewhere distal to insulin binding to the insulin receptor. Additionally, proximal insulin signaling such as IRTK activation [109, 116, 117], IRS1 phosphorylation [10, 116], and IRS1-associated PI3-kinase activity [108, 116, 117] were not increased post-exercise compared to sedentary control values, indicating that amplification of these signaling events does not mediate enhanced post-exercise insulin sensitivity. Further downstream of PI3-kinase, exercise does not enhance insulin's effect on Akt Ser473 phosphorylation in most [77-79, 108, 109, 117-124], but not all studies [125, 126]. Similarly, insulin-stimulated phosphorylation of Akt on Thr308 after exercise is unaltered in many [77, 118, 119, 121-124, 127, 128], but not all studies [78, 79, 106, 125, 126]. However, there are three isoforms of Akt (Akt1, Akt2, and Akt3), and the aforementioned studies have not included evaluation of post-exercise insulin-stimulated Akt2 phosphorylation, the Akt isoform implicated in insulin-stimulated AS160 phosphorylation [93] and insulin-stimulated glucose uptake [129,

130]. Probably more indicative of the role of Akt in mediating enhanced insulin sensitivity post-exercise is Akt activity, which has shown to be unaltered [77, 106]. To summarize, substantial evidence indicates that exercise can increase insulin sensitivity without altering proximal insulin signaling in muscles from normal individuals stimulated with a physiologic insulin dose.

In 2003 Gustav Leinhard's group demonstrated in adipocytes that insulin-stimulated site-selective phosphorylation of AS160 was required for increased GLUT4 translocation [49]. An antibody was subsequently developed that was designed to recognize Akt phosphomotifs, known as the phospho Akt substrate (PAS) antibody [41]. At the time the PAS antibody was the only antibody available for the detection of AS160 phosphorylation, but the PAS antibody may not equally bind to all Akt phosphomotifs on AS160 [131]. An S588A mutation on AS160 did not decrease PAS signal, but a T642A mutation of AS160 resulted in a large decrease in signal, indicating a preference of the PAS antibody for pAS160^{Thr642} over pAS160^{Ser588} [132]. The Cartee laboratory then demonstrated that insulin, contraction, or AICAR result in increased PAS signal [92, 133]. In 2007 Arias et al. were the first to show that insulin-stimulated phosphorylation of AS160 (also using the PAS antibody) was increased ~4 hours after exercise in exercised muscle [78]. Arias et al. also demonstrated an insulin-independent effect of exercise on AS160 phosphorylation by anti-PAS that occurred immediately after exercise and lasted 4-hours post-exercise [78]. Additionally, Funai et al. found that the phosphorylation of AS160 and insulin sensitivity remained elevated for 3-27 hours after exercise unless feeding occurred [106]. Schweitzer et al. studied the four kinases known to phosphorylate AS160 (Akt, AMPK, RSK, and SGK1) and found evidence for activation of only AMPK immediately post-exercise [79]. Because the effect of exercise on pAS160 at 4-hours post-exercise occurred in the absence of increased phosphorylation of these four kinases of AS160, the authors speculated that the persistent phosphorylation of AS160 was due to a residual effect of increased pAMPK and/or effects of other kinases or phosphatases that regulate AS160 which occurred immediately after exercise. Since these initial findings, multiple reports have shown a positive relationship between greater insulin-stimulated glucose uptake and enhanced insulin-stimulated phosphorylation of AS160 on multiple sites after exercise [77, 79, 106, 121, 122, 125, 127, 134]. The two insulin-stimulated AS160 phosphorylation sites that are most often reported to increase by exercise are Thr642 and Ser588. Using the same exercise protocol that will be used for the experiments in this dissertation multiple reports have demonstrated enhanced insulin-stimulated pAS160^{Ser588}

and pAS160^{Thr642} in epitrochlearis muscle post-exercise [77, 79, 106]. Funai et al. showed persistently enhanced insulin-stimulated pAS160^{Thr642} and glucose uptake of the epitrochlearis muscle for 3-27 hours post-swim exercise, but carbohydrate feeding reversed the effect of exercise for pAS160^{Thr642} and glucose uptake, demonstrating a consistent relationship between insulin-stimulated glucose uptake and pAS160^{Thr642} [106]. Using this swim protocol, Schweitzer et al. demonstrated enhanced pAS160^{Thr642} and pAS160^{Ser588} at 3 hours post-exercise in epitrochlearis muscle concomitant with increased insulin-stimulated glucose uptake [79]. In Leinhard's seminal finding, mutation of these two sites eliminated the majority of GLUT4 translocation in adipocytes [49]. Kramer et al. provided further evidence in skeletal muscle for the critical role of site specific phosphorylation of AS160 by showing decreased insulin-stimulated glucose uptake in mouse skeletal muscles electroporated with the 4P mutant of AS160, which included mutations to prevent phosphorylation on Ser588, Thr642, Ser318, and Ser751 [135].

Recently, another phosphosite of AS160, Ser704, has been identified as a potential contributor to the enhanced insulin sensitivity after exercise. AS160^{Ser704} is of particular interest because it is an AMPK phosphosite that is phosphorylated immediately following exercise in skeletal muscle [95]. Two reports have shown enhanced insulin-stimulated pAS160^{Ser704} after exercise in humans concomitant with increased insulin-stimulated glucose uptake [121, 136], and one of these studies also showed enhanced pAS160^{Thr642} and pAS160^{Ser588} [121]. *In situ* contraction of mouse EDL muscle can also lead to subsequently enhanced insulin-stimulated pAS160^{Ser704}, pAS160^{Thr642}, and glucose uptake [96]. Mutation AS160 Ser704 to Ala704 in mice reduced the insulin-stimulated increase in pAS160^{Thr642} [88], suggesting that phosphorylation of Ser704 contributes to enhanced phosphorylation on Thr642, a phosphosite critical for insulin-stimulated GLUT4 translocation after exercise. However, these researchers did not report the influence of the S704A mutation on pAS160^{Ser588}, another important residue on AS160 for insulin-stimulated GLUT4 translocation.

A potentially critical precursor to site-specific pAS160 after exercise is γ3-AMPK activation. Kjøbsted et al. found that AICAR (an AMPK activator and exercise mimetic) resulted in enhanced γ3-AMPK activation, pAS160^{Ser704}, pAS160^{Thr642}, and insulin-stimulated glucose uptake in wild type mouse muscle, but not in γ3-AMPK knockouts [88]. A caveat to these

findings was that the role of γ3-AMPK activity on pAS160 had not been assessed during *in vivo* exercise. Wang et al. were the first to show that γ3-AMPK activity, insulin-stimulated pAS160, and insulin-stimulated glucose uptake were all concomitantly enhanced following *in vivo* exercise [113]. Overall, multiple groups have identified that the effects of exercise on site-specific phosphorylation of AS160 is potentially a crucial step for the improvement in insulin-stimulated glucose uptake seen following exercise, but the exact mechanisms behind this effect are not completely clear.

Because both AS160 and TBC1D1 share many key features including a Rab GTPase-activating domain, the activation of TBC1D1 has also been proposed as a potential mediator of enhanced insulin sensitivity following exercise. PAS-TBC1D1 was also shown to increase immediately after contractions [94, 137]. However, multiple studies have shown that this effect is lost by 3-4 hours post-exercise, when insulin-independent effect of exercise is largely reversed [106, 121-123, 127]. Moreover, mutation of TBC1D1 so that it cannot be phosphorylated does not affect skeletal muscle insulin-stimulated glucose uptake [138]. In TBC1D1-null rats insulin-stimulated GLUT4 translocation was unaltered compared to wild type controls [139]. Therefore, it seems that AS160 phosphorylation, and not TBC1D1 phosphorylation, is implicated as a potential event in the process leading to greater insulin-stimulated glucose uptake after exercise.

In summary, it is well established that exercise enhances insulin-stimulated glucose uptake into skeletal muscle. Enhancement of proximal insulin signaling steps does not appear to be required for this major health benefit of exercise. However, the phosphorylation of AS160 has been reported to track with enhanced insulin-stimulated glucose uptake after exercise under many conditions and is currently a leading mechanistic candidate for this effect. Further work needs to be performed to understand how AS160 may influence glucose uptake and how AS160 is influenced by exercise.

High-Fat Diet-Induced Insulin Resistance

High-fat diets often lead to increased caloric intake, resulting in gains in body mass and fat mass, along with insulin resistance in rodents [77, 140-142]. Brief high-fat diets (≤ 2 to 4 weeks) have been shown to produce insulin resistance preceding large changes in body mass,

body composition and some of the other negative outcomes often thought to produce insulin resistance (See Table 2.2). Extensive research has aimed to elucidate the complexities of high-fat diet-induced insulin resistance, but the exact molecular mechanisms that link defective lipid metabolism and impaired insulin action remain unclear. High-fat diets provide an abundant supply of fatty acids. Fatty acid availability, ectopic lipid deposition (accumulation of lipids in non-adipose tissue), fatty acid metabolites (DAGs, ceramides), and skeletal muscle lipid droplet (LD) size and subcellular location have been associated with insulin resistance. However, the specific mechanisms which influence high-fat diet-induced insulin resistance are not completely clear.

A relatively weak correlation has been reported between plasma fatty acid concentrations and insulin resistance [143]. Under some conditions, intramyocellular triglycerides (IMTGs) are reported to be a better predictor of insulin resistance than circulating fatty acids [144]. A positive association has been reported between elevated IMTG content and insulin resistance in animal models of high-fat feeding [145]. In obese humans, improving insulin sensitivity by markedly reducing caloric intake was accompanied by reduced IMTG content [146, 147]. Additionally, insulin resistance during aging can be accompanied by increased IMTG content [148]. Although there appears to be an inverse association between IMTG content and insulin sensitivity in various circumstances [149-151], there have been some studies which have been able to dissociate this relationship. Both endurance trained athletes and type 2 diabetics display elevated IMTG content, but endurance training enhances insulin sensitivity and type 2 diabetics are extremely insulin-resistant [152]. Additionally, when diabetic Zucker rats were treated with either fenofibrate (PPAR-α agonist which caused increased IMTG) or rosiglitazone (PPAR-γ agonist which caused decreased IMTG) they improved insulin sensitivity, showing an obvious discordance between IMTG content and insulin sensitivity [153].

It has been suggested that the inconsistent association between IMTGs and insulin sensitivity may be due to particular lipid metabolites, rather than triglycerides, which provide the greatest negative influence on muscle insulin sensitivity. Liu et al. showed in mice that overexpressing diacylglycerol acyltransferase (DGAT) in skeletal muscle, which partitions fatty acid substrates towards triglyceride synthesis and decreases diacylglycerol (DAG) and ceramide content, improved insulin sensitivity despite increased IMTG content [154]. Additionally, DAGs

and ceramides can be increased in muscle during insulin-resistant conditions [155], and DAGs can act as signaling intermediates that activate members of the protein kinase C (PKC) family [150]. It has been proposed that once accumulated in the muscle, DAGs are embedded in the membrane where they recruit PKC-θ, stabilizing it in its active form [156]. Active PKC-θ increases pIRS-1^{Ser}, inhibiting insulin signaling [157]. Further evidence supporting the role of PKC-θ in insulin resistance shows that knocking out PKC-θ in mice maintains insulin sensitivity during lipid infusion [158].

Ceramides, on the other hand, are believed to impair insulin signaling by decreasing activation of Akt [159-161]. It has been shown that ceramides impair the phosphorylation of Akt, but not the upstream kinase PDK1, through the activation of PKCζ [162, 163]. Additionally, ceramides have been shown to stimulate the dephosphorylation of Akt through protein phosphatase 2A (PP2A) [163]. However, much of the work linking ceramides to insulin resistance has been done *in vitro*, and more work must be done to functionally understand how ceramides influence insulin resistance.

The subcellular location of lipids within skeletal muscle cells has recently been implicated as a potential factor influencing insulin resistance. IMTGs are stored in lipid droplets (LDs) within the muscle fiber, and several groups have provided evidence suggesting that subsarcolemmal lipid droplets, but not intermyofibrillar lipid droplets, are associated with insulin resistance [164-167]. Sarcolemmal DAG also appears to be negatively related to insulin sensitivity [168]. Localization near the cell surface membranes may provide lipids and lipid species the opportunity to disrupt crucial insulin signaling processes that also occur in the same location, but the specific mechanisms are unclear. Lipid droplet size has also been associated with insulin sensitivity, where larger lipid droplets have been proposed to confer insulin resistance [169]. Some reports have not been able to detect changes in lipid droplet size when insulin sensitivity is altered [170, 171]. However, these studies measured lipid droplets across the entire cross sectional area of each muscle fiber. Nielsen and colleagues discovered that subsarcolemmal LD size was negatively associated with insulin sensitivity, and that type II fibers had larger subsarcolemmal LDs compared to type I fibers [172]. The authors speculated that the high surface area to volume ratio of small lipid droplets was advantageous for rapid mobilization and turnover. The interesting findings related to lipid droplet size and location in these studies

introduce an additional layer of complexity in deciphering the causes of high-fat diet induced insulin resistance.

Acute Exercise Effects on Insulin Sensitivity in Insulin-Resistant Individuals

Similar to what has been shown in insulin-sensitive subjects, exercise can improve insulin sensitivity in insulin-resistant rodents [77, 120, 142, 173, 174] and humans [103, 121, 175-177]. A surprisingly small number of studies have examined the effects of acute exercise on insulin signaling in insulin-resistant subjects. Because high-fat diet-induced insulin resistance is linked to impaired insulin receptor, IRS-1, and PI3-kinase signaling in the sedentary condition [178, 179], it is not unreasonable to expect that improvements in insulin sensitivity by exercise may be due to improvements in these proximal insulin signaling steps. In fact, exercise has been shown to improve proximal insulin signaling during high-fat diet induced insulin resistance in some [173, 180], but not all [77, 120, 121] studies. Ropelle et al. showed that when skeletal muscle insulin resistance was induced in rats by 3 month high-fat feeding that pIR, pIRS1, pIRS2, pAkt, and IRS-associated PI3-kinase were all impaired, and then slightly improved by acute exercise [173]. Pauli et al. then used the same model of 3 month high-fat diet induced insulin resistance and showed that exercise enhanced insulin-stimulated pIR, pIRS1, IRS1associated PI3-kinase, and $pAkt^{Ser473}$ for up to 16 hours following exercise [180]. A major caveat to both of these studies is that insulin signaling was determined after rats were injected with a large bolus of insulin that would result in highly variable and supraphysiologic insulin concentrations. Additionally, acute exercise following shorter term high-fat diets (2-4 weeks) can improve subsequent insulin-stimulated glucose uptake without altering several important proximal insulin signaling steps (pIR, IRS1-associated PI3-kinase, $pAkt^{Ser473}$, $pAkt^{Thr308}$, and Akt activity) [77, 120].

In insulin-sensitive subjects it has been repeatedly demonstrated that exercise enhances downstream insulin signaling such as AS160 phosphorylation [78, 122, 127, 134], with no effect on proximal signaling [10, 108, 109, 116, 117]. Recently, evidence has been reported that in insulin-resistant rats after a high-fat diet, obese humans or humans made insulin-resistant by a lipid infusion the insulin-stimulated phosphorylation of AS160 is greater after exercise [77, 121, 122, 176]. It is important to understand AS160's role in enhancing insulin-stimulated glucose

uptake after exercise in insulin-sensitive subjects, but a more urgent public health concern is to identify how exercise affects insulin-resistant subjects. Surprisingly, there are still very few studies that have examined the effect of exercise on AS160 phosphorylation during insulin resistance.

Heterogeneity of Skeletal Muscle

Skeletal muscle is a heterogeneous tissue composed of multiple fiber types with different metabolic and contractile properties (See Table 2.3). Muscle fibers can be classified by their myosin heavy chain (MHC) isoform expression, and MHC is used as a gold standard for determining fiber type [181]. Four major MHCs are expressed in adult rodent skeletal muscle (MHC type I, IIA, IIX, and IIB) and three are expressed in human skeletal muscle (MHC type I, IIA, and IIX) [182]. Muscle fibers that express more than one MHC isoform are known as hybrid fibers and typically possess intermediate metabolic or contractile properties of the two MHC isoforms that they express [183]. It is also important to note that there are differences in the characteristics of fiber types between species. For example, the fiber type which has been reported to have the highest oxidative capacity in humans is type I [184], but in rats it is type IIA which possesses the greatest oxidative capacity [185]. Regardless, identifying fiber type differences within a given species is important because molecular differences at the cellular level are impossible to discern using whole tissue analysis.

Conventionally, fiber type comparisons for glucose uptake were made by evaluating differences of whole muscles or regions of whole muscles which are mostly composed of a given fiber type, which can vary greatly [186]. For example, insulin-independent glucose uptake after exercise in rat skeletal muscle was greatest in the soleus muscle (~90% type I, ~10% type IIA), followed by the red gastrocnemius (~20% types I and IIA, ~30% types IIX and IIB), and the lowest glucose uptake was observed in the white gastrocnemius (~0-5% types I and IIA, ~20% type IIX, ~75% type IIB) and EDL (~5-10% types I and IIA, ~25% IIX, ~55% type IIB) [187]. However, major complications arise when attempting to evaluate differences in different fiber types by using whole muscle tissues *in vivo* following exercise: 1) recruitment of different muscles during a given mode of exercise is not uniform, 2) vascularization can be very different in various muscles, affecting glucose delivery, and 3) no whole muscle is entirely composed of a

single fiber type. One approach to address or attenuate some of these issues is by stimulating muscle to contract *in situ* or *ex vivo*, but results have been variable [111, 188-196], and electrically stimulated contraction does not recapitulate all aspects of *in vivo* exercise.

Some groups have measured the effect of *in vivo* exercise on insulin-stimulated glucose uptake in various muscles [11, 112, 197, 198], but there was no consistent pattern of fiber type specific insulin-stimulated glucose uptake or obvious, specific explanation for the lack of uniform results across studies. Comparing insulin-stimulated glucose uptake at the whole muscle level is imperfect because: 1) No whole muscle is entirely composed of a single fiber type, 2) hybrid fibers cannot be evaluated, 3) No whole muscle in rat has been identified that is mostly composed of type IIX fibers, and 4) whole muscles contain multiple cell types (neural, vascular, connective, and adipose) which can contribute to glucose uptake. Moreover, there is evidence that exercise training [199], metabolic disease [200-202], and old age [203, 204] can alter fiber type proportion, and this may be important for health. It would be valuable to identify differences in single fibers for insulin-stimulated glucose uptake to more clearly understand insulin resistance at a cellular level.

MacKrell and Cartee developed and validated the first and currently only method for measuring glucose uptake and MHC isoform in the same muscle fiber [205]. This method requires incubation of whole rat epitrochlearis muscle in [^{3}H]-2-deoxyglucose, followed by collagenase incubation for enzymatic digestion of extracellular collagen, and finally the isolation of individual fibers using fine forceps under a dissecting microscope. Once each fiber is isolated they are placed in individual tubes and processed to measure glucose uptake (by scintillation counting) and MHC expression (by SDS PAGE). Using this method our laboratory has demonstrated that insulin-stimulated glucose uptake is greater in the type I and IIA fibers (which are roughly equal to each other) compared to type IIX, IIBX, and IIB fibers [205-207]. Insulin-stimulated glucose uptake is decreased in all fiber types from obese Zucker rats compared to lean Zucker rats [205]. Additionally, insulin-stimulated glucose uptake is increased in all fiber types from calorically restricted rats compared to ad libitum fed rats [208]. Surprisingly, when insulin-sensitive rats were exercised for two hours, subsequent insulin-stimulated glucose uptake was enhanced 3.5 hours following exercise in all fiber types except for type IIX fibers [207]. As noted previously, a more important public health concern is to determine the effect of exercise on

insulin-stimulated glucose uptake in insulin-resistant subjects. Therefore, it will be important to identify fiber type-specific differences in insulin-stimulated glucose uptake after exercise in rats that have developed insulin resistance by high-fat feeding.

Importance of Identifying Fiber Type-Specific Differences in Insulin Signaling

Humans can have markedly different muscle fiber type proportions [209, 210]. It has been reported that insulin-resistant humans compared to humans with normal insulin sensitivity possess a greater proportion of type II fibers [201, 202]. It could be that a shift in fiber type proportion occurs during insulin resistance or that a certain fiber type predisposes people to a greater risk for insulin resistance. Of course, environmental factors such as diet and physical activity level may play a role in this relationship as well. Although fiber type characteristics are not identical in human and rat skeletal muscles, there are many similar features between the species, so careful research on fiber type-selective differences has potential implications for understanding exercise effects on insulin sensitivity in humans [209]. The complexities of the relationship between fiber type and insulin resistance is currently incompletely understood, but a useful step to more clearly understand insulin resistance is to identify the fiber types which become insulin-resistant by high-fat feeding or that do not become insulin-sensitive after exercise. After determining which fibers have divergent sensitivity to insulin during these conditions, we can then attempt to identify what occurs at a molecular level within these fibers to cause such a phenotype.

Although it is unclear why some fiber types may differ in their susceptibility to the deleterious effects of a high-fat diet or be more susceptible to the beneficial effects of exercise, it seems possible that different fiber types can have divergent exercise- or insulin-related signaling during these conditions. Recently, Albers et al. discovered that insulin-stimulated Akt phosphorylation on Thr308 and Ser473 was lower in both type I and type II human muscle fibers from type 2 diabetic patients compared to lean or non-diabetic obese subjects [211]. They did not observe a decrease in insulin-stimulated AS160 phosphorylation on any of the residues that were analyzed (Ser588, Thr642, Ser704, Ser318) in either fiber type. However, the effect of exercise was not evaluated in this study and the effect of exercise on these AS160 residues may be crucial for insulin-stimulated glucose uptake. Kristensen et al. discovered that $pAMPK^{Thr172}$ was

increased by exercise in both type I and type II fiber types, but type II fibers (combined IIA and IIX in this experiment) displayed a larger increase than type I fibers following high intensity interval cycling exercise [212]. They also showed that the increase in pAS160^{Ser704}, an AMPK phosphosite, was greater in type II versus type I fibers immediately following either continuous or interval cycling. However, the insulin-stimulated effect of exercise was not evaluated in this study.

Neither of the aforementioned studies differentiated between type IIA and type IIX fibers, nor did they assess hybrid fibers or determine fiber type-selective glucose uptake [211, 212]. The fiber type-specific effects of exercise on both insulin signaling and glucose uptake have only been reported together in a non-insulin-resistant rat model [207, 213]. It was reported that post-exercise fiber type-specific insulin-stimulated glucose uptake corresponded to insulin-stimulated AS160 phosphorylation [213]. It will be important to determine differences in insulin signaling of different fiber types from insulin-resistant rats from which fiber type-specific insulin-stimulated glucose uptake can be determined. Further, identifying signaling differences following exercise in insulin-resistant rats will provide mechanistic insight into the effects of exercise on insulin-stimulated glucose uptake during insulin resistance. Such findings could provide the foundation for research which will lead to the development of therapies to treat insulin resistance.

Research Models Used

Feeding rodents a high-fat diet induces insulin resistance [77, 141, 142, 214, 215], increases serum free fatty acids [141, 216-218], increases fat mass [77, 141, 214, 219], and increases muscle lipid deposition [142, 216]. The induction of skeletal muscle insulin resistance in rodents by a high-fat diet can occur within 2-4 weeks [77, 220, 221]. All of the studies in this dissertation employ 2-week high-fat feeding of Wistar rats. The composition of dietary fat that was used for these studies (60% in high-fat diet vs 13% in low-fat diet) has been widely used to induce insulin resistance in rodents. A benefit to studying rats following short-term high-fat feeding is that skeletal muscle insulin resistance often occurs before the onset of many other negative health outcomes that are often associated with insulin resistance such as large increases in body mass [77, 221]. It is useful to better understand the early stages of insulin resistance for

the development of therapies that will prevent insulin resistance. However, a limitation to studying short-term high-fat feeding was that we did not elucidate the additional differences observed in skeletal muscle after chronic diet-induced insulin resistance. Besides diet-induced insulin resistance, other approaches have been used to induce insulin resistance such as streptozotocin (STZ) [222], dexamethasone [223], zymosan [224], and immobilization [225]. Rodent genetic models of insulin resistance such as Zucker rats [226], Goto Kakizaki (GK) rats [227], OLETF rats [228], and New Zealand Obese (NZO) mice [229] have also been used to study insulin resistance. However, diet-induced insulin resistance is more relevant to insulin resistance experienced by humans.

All experiments used the rat epitrochlearis muscle for various measures related to insulin sensitivity. The epitrochlearis muscle has been frequently used to measure insulin-stimulated glucose uptake by multiple researchers [15-17, 230, 231], providing an extensive foundation of information regarding the responses of this muscle to various stimuli. Because it is only ~25 fibers thick, the epitrochlearis is well suited for *ex vivo* incubation experiments in which a relatively thin diffusion distance is required for nutrients to reach all muscle fibers. Additionally, it has been shown that glycogen content is depleted and insulin independent glucose uptake immediately following exercise is increased in the epitrochlearis muscle following swim exercise, indicating that this muscle is recruited during swim exercise [77, 106, 207]. The fiber type profile of the epitrochlearis muscle [186] is similar to the overall fiber type proportion of the rat hindlimb [185], making it a relatively representative muscle. The epitrochlearis is also the only muscle that has been used to measure glucose uptake and fiber type in individual muscle fibers [205-208, 232]. The epitrochlearis has also been widely used for isolated muscle incubation experiments which measure glucose uptake and signaling. Isolating the epitrochlearis and incubating *ex vivo* versus measuring glucose uptake and signaling *in vivo* eliminates multiple confounding variables such as systemic hormone secretion and muscle tissue vascularization that can highly influence glucose uptake and signaling. This approach also allows very precise control of insulin concentration. The selected concentration of insulin that was used for all experiments is 100μU/ml because of the extensive literature that has used this submaximally effective dose to assess insulin signaling and glucose uptake in insulin-resistant skeletal muscle after exercise. Although it would also be interesting to measure the effects of hormone secretion and vascular differences on glucose uptake in skeletal muscle *in vivo*, this project focused on the

intrinsic properties in the skeletal muscle that influence insulin-stimulated glucose uptake post-exercise. Because of multiple beneficial characteristics of the epitrochlearis, this muscle is appropriate for the experiments of this dissertation.

A variety of protocols have been used to exercise or mimic exercise in rats. Swim exercise was selected for the experiments in this dissertation due to extensive evidence that has shown elevated post-exercise glucose uptake and pAS160 in the epitrochlearis muscle [77-79, 106]. It has been demonstrated that all fiber types of the rat epitrochlearis muscle are recruited during swim exercise [207]. Forced treadmill and wheel running are also commonly used to exercise rodents [233, 234], but the effects of these modes of exercise on glucose uptake and AS160 phosphorylation in the epitrochlearis muscle are unknown. Electrical stimulation has been used to increase insulin-independent glucose transport [114, 127, 235]. However, *in vitro* contractions do not fully replicate *in vivo* exercise. Exposure to AICAR has also been used as an exercise mimetic because both exercise and AICAR activate AMPK [108], but it is unclear if AMPK is the only upstream kinase that acts on AS160. Therefore, swim exercise using a protocol that had been previously used for analysis of whole muscle signaling and glucose uptake in chow-fed and high-fat-fed rats and single fiber glucose uptake in chow-fed rats was used to examine insulin-stimulated glucose uptake and signaling processes for the projects of this dissertation.

Gaps Filled in the Literature

In Study 1, epitrochlearis muscles from rats fed a high-fat or low-fat (chow) diet for 2-weeks were isolated for the measurement of whole muscle and single fiber glucose uptake. Insulin can cause greater glucose uptake in some fiber types than others [205-207] and insulin-stimulated glucose uptake can be altered within a given fiber type during certain conditions [207]. Because Castorena et al. demonstrated modest insulin resistance after only 2-weeks of high-fat feeding in rat whole epitrochlearis muscle [77], I measured fiber type-specific insulin-stimulated glucose uptake from rats fed either a high- or low-fat diet. The results from this study revealed previously unknown differences among fiber types for insulin-stimulated glucose uptake during insulin resistance. Some fiber types became more insulin-resistant than others after 2 weeks of high-fat feeding. Therefore, insulin resistance of the whole muscle may be highly

influenced by fiber type proportion. Some studies that compared rodents consuming a high-fat diet for four or more weeks with healthy controls consuming a low-fat diet identified differences between the diet groups in their muscle fiber type composition [236-239]. The abundance of MHC isoforms in the whole epitrochlearis muscles from high- and low-fat fed rats from this study were also measured to determine if 2-week high-fat feeding induced a change in fiber type proportion. Although GLUT4 abundance is unaltered by 2-week high-fat feeding in whole epitrochlearis muscle [77], it seemed possible that the high-fat diet might induce changes in the GLUT4 content at the single fiber level. Therefore, the GLUT4 abundance was evaluated in different fiber types in low- and high-fat fed rats.

Study 2 evaluated fiber type-specific insulin-stimulated glucose uptake following exercise by high-fat fed rats compared to low- and high-fat fed sedentary controls. Enhanced insulin-stimulated glucose uptake of whole muscles from rats made insulin-resistant by consuming a 2-week high-fat diet has been previously reported following exercise [77]. Exercise can increase insulin sensitivity in insulin-resistant individuals, but it does not completely recover insulin-stimulated glucose uptake to levels observed in insulin-sensitive individuals after the same exercise protocol. One possible explanation for this outcome is that insulin-stimulated glucose uptake may be equally enhanced in all fiber types following exercise in insulin-resistant individuals, but not to the level seen in insulin-sensitive fibers. However, even in insulin-sensitive rats, not all fiber types improve insulin-stimulated glucose uptake after exercise [207]. Therefore, it seemed possible that some fiber types would not improve insulin-stimulated glucose uptake following exercise in insulin-resistant rats, and that this putative lack of an effect in some fiber types may contribute to the lower insulin-stimulated glucose uptake compared to insulin-sensitive individuals after exercise. In Study 2 insulin-stimulated glucose uptake was determined in epitrochlearis muscle fibers from exercised high-fat fed rats and low- and high-fat fed sedentary rats. To evaluate if all fiber types were recruited during the exercise protocol, fiber type specific insulin-independent glucose uptake was measured immediately following exercise. As a secondary measure to assess fiber type recruitment, fiber type-specific glycogen content was also determined immediately following exercise. Because ectopic lipid accumulation has been implicated in insulin resistance [145, 147, 148], fiber type-specific lipid droplet abundance, size, and subcellular localization in exercised high-fat fed rats versus sedentary low- and high-fat fed controls was compared to determine if lipid droplet abundance, size, or location are

associated with fiber type specific insulin sensitivity. Finally, fiber type-specific GLUT4 abundance was measured to determine if the abundance of this protein is altered by diet or exercise after a 2-week high-fat diet.

In Study 3, important signaling events that have been associated with enhanced insulin sensitivity after exercise were measured using whole epitrochlearis muscles from insulin-resistant rats post-exercise compared to sedentary low- and high-fat fed controls. Castorena et al. demonstrated that insulin sensitivity is enhanced after exercise in insulin-resistant rats, but is not completely elevated to the level observed in insulin-sensitive rats after exercise [77]. In the same study it was shown that exercise enhanced insulin-stimulated pAS160^{Ser588} in insulin-sensitive rats to a greater extent than in insulin-resistant rats. It is possible that different mechanisms may exist which enhance insulin sensitivity after exercise in insulin-sensitive versus insulin-resistant muscle. Evidence that pAS160^{Ser588} and pAS160^{Thr642} are potential mediators for the effect of exercise on insulin sensitivity in insulin-sensitive muscle has been reported in several earlier studies [77, 79, 106, 240], but less evidence exists for insulin-resistant muscle. Recently, an AMPK phosphosite of AS160, Ser704, was shown to increase after exercise [95]. pAS160^{Ser704} has also been demonstrated to track well with enhanced insulin-sensitivity post-exercise [121, 136], but pAS160^{Ser704} has yet to be measured in muscle from insulin-resistant animals after exercise. It is possible that the effect of exercise on insulin sensitivity is influenced by greater phosphorylation of AS160^{Ser704} in insulin-resistant muscle. Accordingly, I evaluated changes in pAS160^{Ser704} in muscle from exercised rats that had been fed a high-fat diet for two weeks compared to sedentary low- and high-fat fed controls. Because pAS160^{Ser704} is an AMPK phosphosite it was also important to measure the level of muscle AMPK activity following exercise in these animals. AMPK is a heterotrimeric protein complex composed of α, β, and γ subunits each of which have multiple isoforms (α1, α2, β1, β2, γ1, γ2, γ3) [81]. γ3-AMPK is activated in muscle by exercise in humans [241, 242] or by electrically stimulated contractions in mice [96, 242]. In skeletal muscle γ1-AMPK is also expressed (γ2-heterotrimer containing AMPK activity has not been detected in skeletal muscle) and γ1-containing AMPK isoforms are weakly activated during prolonged low intensity exercise. However, even during prolonged, low intensity exercise a larger relative increase in activation of γ3- versus γ1-containing AMPK is observed [87]. Recently published data from our laboratory has shown that γ3-AMPK activity, insulin-stimulated pAS160^{Ser704}, and insulin-stimulated glucose uptake are elevated 3 hours post-

exercise in insulin-sensitive rats [113]. Therefore, I measured γ1- and γ3-AMPK activity and insulin-stimulated pAS160^{Ser704} after exercise in insulin-resistant rats to identify potential signaling differences during insulin resistance. Although earlier research has reported that acute exercise typically leads to subsequently elevated insulin-stimulated glucose uptake independent of increasing Akt phosphorylation above sedentary control values [77, 78, 121, 122, 136], these studies have not included the evaluation of Akt2 phosphorylation, the Akt isoform implicated in insulin-stimulated AS160 phosphorylation [93] and insulin-stimulated glucose uptake [129, 130]. Therefore, I measured insulin-stimulated pAkt2^{Thr309} and pAkt2^{Ser474} after exercise in insulin-resistant rats after exercise.

Study 4 used a recently developed technique [211, 243] to evaluate the phosphorylation of insulin signaling proteins in different fiber types from sedentary and acutely exercised high-fat fed rats. Studies 1 and 2 from this dissertation characterized the capacity of different muscle fiber types from 2-week high-fat fed rats to uptake glucose in response to insulin either following exercise or during sedentary conditions. To gain further insights into the possible mechanism for the effects of diet and/or exercise on fiber type-selective glucose uptake, I assessed possible exercise effects during a high-fat diet on key proximal (pAkt^{Thr308} and pAkt^{Ser473}) and distal (pAS160^{Ser588}, pAS160^{Thr642}, and pAS160^{Ser704}) insulin signaling proteins in different fiber types from rat epitrochlearis muscle. I also probed for possible fiber type-specific differences in signaling events that are implicated in mediating the exercise-induced enhancement in insulin signaling (pAMPK^{Thr172} and pAS160^{Ser704}) from 2-week high-fat fed rats. In addition, because HKII is an enzyme that can potentially influence the rate of glucose metabolism, I determined the fiber type-specific abundance of HKII following exercise in high-fat fed rats. Lastly, I measured fiber type-specific glycogen content both IPEX and 3hPEX to determine if fiber type differences in insulin-stimulated glucose uptake might be related to fiber type-specific glycogen replenishment after exercise.

Table 2.1: Skeletal Muscle Insulin-Stimulated Glucose Uptake after Acute Exercise or Contraction

Reference [citation number]	**Richter et al. 1982 [11]**	**Richter et al. 1984 [111]**	**Garetto et al. 1984 [197]**	**Richter et al. 1985 [198]**
Journal	J. Clin. Invest.	Am. J. Physiol. Endocrinol. Metab.	Am. J. Physiol. Endocrinol. Metab.	Diabetes
Sex, Species & Strain	Male Sprague-Dawley Rats	Male Sprague-Dawley Rats	Male Sprague-Dawley Rats	Male Wistar Rats (STZ-induced diabetes or control)
Exercise or Contraction Protocol	Treadmill: 45min at 18m/min	Sciatic nerve stimulation: 2 x 5min	Treadmill: 5 x 10min at 36m/min	Treadmill: 45min at 19m/min/ Also estim
Muscles Used	Soleus, Red & White Gastroc	Soleus, Red & White Gastroc	Soleus, Red & White Gastroc	Soleus, Red & White Gastroc
Measurement Technique	Perfused Hindlimb	Perfused Hindlimb	Perfused Hindlimb	Perfused Hindlimb
Insulin Concentration or Infusion Rate	10, 30, 75, 500, 20k, & 40k µU/ml	75 and 20k µU/ml	75 and 20k µU/ml	100 and 20k µU/ml
Insulin-stimulated Glucose Uptake	↑ for perfused hindlimb up to 4hr PEX	↑ in soleus and RG at 2hr post-stimulation, but not in WG.	↑ for perfused hindlimb up at 2.5hr PEX	↑ for perfused hindlimb up ~1hr PEX in normal and STZ-treated rats
Insulin Signaling Post-Exercise	--	--	--	--
Main Findings	First study to show enhanced skeletal muscle insulin sensitivity post-exercise	Demonstrated that estim-mediated insulin sensitivity is due to local factors	Enhanced post-exercise GU is composed of two phases: 1) IPEX 2) after glycogen compensation	Increased insulin-sensitivity PEX does not require insulin to be present during exercise.
Additional Information	Effect of exercise on insulin sensitivity only occurred in deglycogenated muscles	The unstimulated hindlimb was an internal control in these experiments	~1hr PEX insulin-stimulated glucose incorporation into glycogen is ↑ in Sol, RG, but not WG	~1hr PEX insulin-stimulated glucose incorporation into glycogen is ↑ in Sol, RG, but not WG

Table 2.1: Continued

Reference [citation number]	Davis et al. 1986 [15]	Zorzano et al. 1986 [14]	Wallberg-Henriksson et al. 1988 [16]	Richter et al. 1989 [12]
Journal	Am. J. Physiol. Endocrinol. Metab.	Am. J. Physiol. Endocrinol. Metab.	J. Appl. Physiol.	J. Appl. Physiol.
Sex, Species & Strain	Female Sprague-Dawley Rats	Male Sprague-Dawley Rats	Male Wistar Rats	Male Humans
Exercise or Contraction Protocol	Untrained and trained (2hr/day, 5days/wk, 4wks) rats were sedentary or performed 2h acute swim exercise	Treadmill: 5 x 10min at 36m/min	4 x 30min swim, last 3 bouts weights tied to tail	One-legged knee extensor exercise: 60min at 75% max leg work capacity
Muscles Used	Epitrochlearis	Soleus, Red & White Gastroc	Epitrochlearis	Vastus Lateralis
Measurement Technique	Muscle Incubation	Perfused Hindlimb	Muscle Incubation	Insulin Clamp, muscle blood flow and a-v glucose difference
Insulin Concentration or Infusion Rate	Range: 0.01-100 µU/ml	75 and 20k µU/ml	20, 60, 120, 180, 500, and 20k µU/ml	0.3, 0.7, and 5.0 mU/kg/min
Insulin-stimulated Glucose Uptake	↑ 2-3hr PEX across range of concentrations in trained and untrained rats	↑ 2.5hr PEX	↑ across a range of concentrations at 3hr PEX	↑ across a range of concentrations 4hPEX in exercised leg only
Insulin Signaling Post-Exercise	--	--	--	--
Main Findings	Skeletal muscle insulin-stimulated glucose uptake is also enhanced in trained rats, despite high resting glycogen.	Uptake of glucose and AIB in skeletal muscle is improved after exercise	Insulin and exercise had additive effects at 30min and 60min PEX, but was more than additive at 3hr PEX	First study to show that exercise enhances insulin sensitivity in muscle in humans
Additional Information	Trained started with higher glycogen content, and also had higher starting insulin sensitivity	Additive at 30min PEX, but later ↑ GU is solely due to increase in insulin responsiveness	Insulin-independent glucose uptake gradually wears off PEX and was nearly back to normal by 3hPEX	Local contraction induced increases in insulin sensitivity play important role in post-exercise recovery

Table 2.1: Continued

Reference [citation number]	Cartee et al. 1989 [244]	Gulve et al. 1990 [230]	Cartee & Holloszy 1990 [115]	Annuzzi et al. 1991 [112]
Journal	Am. J. Physiol. Endocrinol. Metab.	Am. J. Physiol. Endocrinol. Metab.	Am. J. Physiol. Endocrinol. Metab.	Eur. J. Clin. Invest.
Sex, Species & Strain	Male Sprague-Dawley Rats	Male Wistar Rats	Male Wistar Rats	Male Humans
Exercise or Contraction Protocol	4 x 30min swim, last 3 bouts weights tied to tail	4 x 30min and one 60min swim bouts, last 3 bouts weights tied to tail	4 x 30min swim, last 3 bouts weights tied to tail. Or 10min *in vitro* contractions	3hrs combined cycling and running at 50% VO_2max
Muscles Used	Epitrochlearis	Epitrochlearis	Epitrochlearis	Forearm and Leg
Measurement Technique	Muscle Incubation	Muscle Incubation	Muscle Incubation	Insulin Clamp, muscle blood flow and a-v glucose difference
Insulin Concentration or Infusion Rate	60, 500, 1k, and 20k µU/ml	7.5, 30, and 2k µU/ml	30 µU/ml	2 mU/kg/min
Insulin-stimulated Glucose Uptake	↑ 3hPEX in fat and chow fed. ↑ 18h PEX in fasted and fat fed. ↑ 48hPEX in fat fed.	↑3hPEX for all submaximal concentrations after exercise	↑ 3.5hPEX vs rested controls. *In vitro* contractions (no serum) do not enhance ISGU.	↑ 24hPEX in the leg only, not in the forearm.
Insulin Signaling Post-Exercise	--	--	none measured, evidence for post-IR mechanisms	--
Main Findings	CHO feeding (not caloric intake) reverses insulin sensitivity post-exercise.	Shows that incubation of muscle in high glucose during recovery decreased insulin-stimulated glucose uptake 3hPEX	Shows that vanadate or H_2O_2 (insulin mimetics acting distal to the insulin receptor) enhance insulin-stimulated glucose uptake 18hPEX.	Indicates that leg exercise does not increase insulin-stimulated glucose uptake in the forearm.
Additional Information	Muscle glycogen content was decreased in most conditions where insulin sensitivity was still elevated, but recovered or super-compensated where it was not.	Maintenance of insulin sensitivity after exercise does not require humoral factors normally present *in vivo*	Contractions without serum did not ↑ insulin sensitivity. A serum factor during contractions is likely needed to enhance insulin sensitivity PEX	Further evidence for local effect of exercise

Table 2.1: Continued

Reference [citation number]	Gao et al. 1994 [114]	Nolte et al. 1994 [231]	Asp et al. 1996 [245]	Asp & Richter 1996 [246]
Journal	Am. J. Physiol. Endocrinol. Metab.	J. Appl. Physiol.	J. Physiol.	J. Appl. Physiol.
Sex, Species & Strain	Male Wistar Rats	Male Wistar Rats	Male Humans	Male Wistar Rats
Exercise or Contraction Protocol	4 x 30min swim w/ weights, *in vitro* or *in situ* contractions	One 30min bout + 6 x 15min with tail weights swimming	40min of eccentric contractions	4 x 10 eccentric contractions with 1min rest between each set of 4
Muscles Used	Epitrochlearis	Epitrochlearis	Vastus Lateralis	Soleus, Red & White Gastroc
Measurement Technique	Muscle Incubation	Muscle Incubation	Insulin Clamp	Perfused Hindlinb
Insulin Concentration or Infusion Rate	30 µU/ml	30 µU/ml	0.8 and 13 mU/kg/min	200 and 20k µU/ml
Insulin-stimulated Glucose Uptake	↑ 3.5hPEX but not 3.5h after *in vitro* contractions when contracted 15 post excision. Slightly ↑ by *in vitro* contractions when contracted right after excision	↑ 2.5hPEX from saline or propranolol injected rats	Unchanged 48h post-eccentric contractions with physiologic insulin. ↓ 48h after eccentric contractions with max insulin.	↓ 48h after eccentric exercise in WG with 200 µU/ml insulin, but unchanged in RG or soleus.
Insulin Signaling Post-Exercise	--	--	--	--
Main Findings	ISGU is enhanced following *in situ* contractions in serum. Humoral factor must be present during contractions	Propranolol ↓ the exercise-mediated decrease in muscle glycogen, but insulin-stimulated glucose uptake was still enhanced	Eccentric contractions do not enhance insulin-stimulated glucose uptake in human skeletal muscle	Insulin-stimulated glucose uptake is decreased or remains unchanged in rat skeletal muscle 48 h after eccentric exercise.
Additional Information	Serum factor needed is >10kDa	--	GLUT4 content in skeletal muscle decreased 48h after eccentric contractions	Attributed changes in ISGU after eccentric contractions to diff GLUT4 content in various muscles, as measured in a separate study

Table 2.1: Continued

Reference [citation number]	Perseghin et al. 1996 [247]	Wojtaszewski et al. 1997 [116]	Hansen et al. 1998 [10]	Wojtaszewski et al. 2000 [109]
Journal	N Engl. J Med.	Diabetes	J. Appl. Physiol.	Diabetes
Sex, Species & Strain	Male and Female Humans	Male Humans	Male Wistar Rats	Male Humans
Exercise or Contraction Protocol	45min stair climbing at 65% VO_2 max	One-legged knee extensor exercise: 60min at 75% max leg work capacity	4 x 30min swim, last 3 bouts weights tied to tail	One-legged knee extensor exercise: 60min at 75-90% max leg work capacity
Muscles Used	Gastrocnemius	Vastus Lateralis	Epitrochlearis	Vastus Lateralis
Measurement Technique	Insulin Clamp and NMR	Insulin Clamp, muscle blood flow and a-v glucose difference	Muscle Incubation	Insulin Clamp, muscle blood flow and a-v glucose difference
Insulin Concentration or Infusion Rate	6 pmol/kg/min	1.5 mU/kg/min	30 µU/ml	1.5 mU/kg/min
Insulin-stimulated Glucose Uptake	↑ 48hPEX in normal and insulin- resistant offspring of patients with diabetes	↑ 3hPEX in the exercised limb	↑ 3hPEX	↑ 4hPEX in the exercised limb
Insulin Signaling Post-Exercise	--	Unaltered ITRK activity or pIRS-1. ↓ IRS-1 associated PI3-K activity.	Unaltered pIR or pIRS-1	Unaltered IRTK activity or $pAkt^{Ser473}$
Main Findings	Acute exercise ↑ muscle insulin-stimulated glucose uptake in healthy and insulin-resistant subjects.	Enhanced insulin-stimulated glucose uptake post-exercise is not due to increased proximal insulin signaling	Insulin-stimulated cell surface GLUT4 is increased in the exercised muscle compared to sedentary	Post-exercise improvement in muscle insulin sensitivity is not due to steps before or including Akt
Additional Information	--	--	Magnitude of increased ISGU and CS GLUT4 are similar.	Insulin-stimulated GSK3 activity and pGSK3 S21 were also unchanged after exercise

Table 2.1: Continued

Reference [citation number]	Fisher et al. 2002 [108]	Dumke et at. 2002 [235]	Thong et al. 2002 [117]	Kim et al. 2004 [107]
Journal	Am. J. Physiol. Endocrinol. Metab.	J. Appl. Physiol.	Diabetes	J. Appl. Physiol.
Sex, Species & Strain	Male Wistar Rats	Male Wistar Rats	Male Humans	Male Wistar Rats
Exercise or Contraction Protocol	2hr swimming, 1hr AICAR, or 80 min hypoxia	*In vitro* contraction 10 min	One-legged knee extensor exercise: 60min at 75-100% peak leg work capacity	Multiple contraction protocols (train rate, train duration, pulse frequency, pulse duration, number of bouts)
Muscles Used	Epitrochlearis	Epitrochlearis	Vastus Lateralis	Epitrochlearis
Measurement Technique	Muscle Incubation	Muscle Incubation	Insulin Clamp, muscle blood flow and a-v glucose difference	Muscle Incubation
Insulin Concentration or Infusion Rate	30 µU/ml	30 µU/ml	1.5mU/kg/min	60 µU/ml
Insulin-stimulated Glucose Uptake	Exercise, AICAR, and hypoxia each ↑ ISGU 3hPEX	↑ in muscles that did contractions in normal serum, but not kallikrein deficient	Caffeine ↓ muscle ISGU. Exercise ↑ ISGU in both placebo and caffeine groups	↑ or unchanged depending on the contraction protocol
Insulin Signaling Post-Exercise	PI3-K activity and $pAkt^{Ser473}$ are unchanged by exercise or AICAR	--	Unaltered IRTK activation, IRS-1 associated PI3-K activity, or $pAkt^{Ser473}$	--
Main Findings	AICAR, hypoxia and exercise each increase AMPK activity and enhanced ISGU. Not due to protein synthesis (cyclohexamide)	Suggests that kallikrein is essential for muscle insulin sensitivity after contractions	Caffeine decreases ISGU in muscle, but enhanced ISGU after exercise is still observed when caffeine is ingested	↑ AMPK activity or ↓ glycogen may be necessary but not sufficient for improved muscle ISGU post-contraction
Additional Information	Stimulating muscles to contract in serum vs KHB enhanced ISGU 3h post-contractions	Bradykinin was insufficient for post-contraction-enhanced insulin sensitivity	--	--

Table 2.1: Continued

Reference [citation number]	Hamada et al. 2006 [118]	Arias et al. 2007 [78]	Treebak et al. 2009 [134]	Funai et al. 2009 [106]
Journal	J. Appl. Physiol.	Am. J. Physiol. Endocrinol. Metab.	Diabetologia	Am. J. Physiol. Endocrinol. Metab.
Sex, Species & Strain	Male C57B1/6 Mice	Male Wistar Rats	Male Human	Male Wistar Rats
Exercise or Contraction Protocol	Treadmill: 60min at 15-25 m/min	4 x 30min swim	One-legged knee extensor exercise: 60min at 80-100% peak leg work capacity	4 x 30min swim
Muscles Used	Epitrochlearis, EDL, Soleus	Epitrochlearis	Vastus Lateralis	Epitrochlearis
Measurement Technique	Muscle Incubation	Muscle Incubation	Insulin Clamp, muscle blood flow and a-v glucose difference	Muscle Incubation
Insulin Concentration or Infusion Rate	60, 120, and 20k µU/ml	50 µU/ml	1.5 mU/kg/min	50 µU/ml
Insulin-stimulated Glucose Uptake	60µU/ml insulin ↑ GU 85min PEX in epi and soleus but not EDL (no Δ insulin with ex).	↑ 4hPEX	↑ 4hPEX	↑ 3h and 27hPEX when fasted. Unchanged 3hPEX when fed CHO.
Insulin Signaling Post-Exercise	Insulin-stimulated (60µU/ml) Akt^{Thr308} and ^{Ser473} are unaltered after exercise in epi, soleus, and EDL.	Unaltered pSerAkt. ↑ pThrAkt and PAS-AS160.	↑ AS160 Ser318, Ser341, Ser751, Ser588 (P=0.09). Unaltered PAS, Thr642 and Ser666.	↑ PAS-AS160, $pAS160^{Thr642}$, and $pAkt^{Thr308}$ 3 & 27h PEX when fasted. PAS-AS160, $pAS160^{Thr642}$, and $pAkt^{Thr308}$ not diff 3hPEX with CHO.
Main Findings	Exercise improves muscle ISGU in mouse skeletal muscle. No effect of exercise on insulin-stimulated pAkt.	First paper to show insulin-stimulated AS160 is ↑ in exercised muscle (IPEX & 4hPEX).	Role of AS160 to regulate PEX insulin sensitivity using phospho-specific antibodies	pAS160 may mediate improved PEX muscle insulin sensitivity, not TBC1D1
Additional Information	--	PAS-AS160 correlated with GU 4hPEX. Also, no Δ insulin PAS-AS160 PEX.	Also, no change with exercise in insulin-stimulated 14-3-3 binding capacity to AS160	Unaltered insulin-stimulated TBC1D1 after exercise in all rats

Table 2.1: Continued

Reference [citation number]	Funai et al. 2009 [94]	Schweitzer et al. 2012 [79]	Xiao et al. 2013 [125]	Iwabe et al. 2014 [122]
Journal	Am. J. Physiol. Endocrinol. Metab.	J. Appl. Physiol.	Age	Physiol. Rep.
Sex, Species & Strain	Male Wistar Rats	Male Wistar Rats	Male FBN Rats	Male Wistar Rats
Exercise or Contraction Protocol	1 or 2hr swim, 5 or 10min *in vitro* contraction, 2hr swim + 10min *in vitro* contraction	4 x 30min swim	9 x 10min bouts of swimming	Treadmill: 3hr at 9m/min, 15% incline
Muscles Used	Epitrochlearis	Epitrochlearis	Epitrochlearis and Soleus	Soleus
Measurement Technique	Muscle Incubation	Muscle Incubation	Muscle Incubation	Muscle Incubation
Insulin Concentration or Infusion Rate	50 µU/ml	50 µU/ml	100, 200, and 5k µU/ml	50 and 10k µU/ml
Insulin-stimulated Glucose Uptake	↑ equally 3hPEX by 1 or 2hr swim. ↑ equally 3hPES by 5 or 10min e-stim. Additive effect of exercise and e-stim	↑ 3hPEX	↑ 3hPEX in epi and soleus for 100 and 200 µU/ml, but only in epi for 5k µU/ml	↑ 2hPEX with 50 µU/ml
Insulin Signaling Post-Exercise	Signaling unaltered after e-stim. Increased insuin-stimulated PAS-AS160 and $pAS160^{Thr642}$ 3hPEX.	↑ $pAS160^{Thr642}$ and $pAS160^{Ser588}$ IPEX and 3hPEX with insulin stimulation. $pAkt^{Thr308}$ unaltered IPEX, but ↑ with insulin 3hPEX.	pIR and $pAS160^{Ser588}$ unchanged. $pAkt^{Thr308}$, $pAkt^{Ser473}$, and $pAS160^{Thr642}$ ↑ with 100 µU/ml in epi but not soleus.	↑ $pAS160^{Ser588}$ and $pAS160^{Thr642}$ 2hPEX with insulin. $pAkt^{Ser473}$ and $pAkt^{Thr308}$ were unaltered.
Main Findings	Exercise plus *in vitro* contractions additively improve muscle insulin sensitivity.	Shows that Ser588 and Thr642 are sustained during exercise recovery, when ISGU is enhanced.	Shows that exercise can increase muscle insulin sensitivity in old rats.	Shows that exercise improves insulin sensitivity and pAS160 in slow twitch soleus muscle.
Additional Information	E-stim does not additively improve pAS160. Different mechanisms?	--	--	pTBC1D1 unaltered by exercise with insulin.

Table 2.1: Continued

Reference [citation number]	Castorena et al. 2014 [77]	Sharma et al. 2015 [126]	Wang et al. 2015 [124]	Sylow et al. 2016 [248]
Journal	Diabetes	Am. J. Physiol. Endocrinol. Metab.	J. Gerontol. A. Biol. Sci. Med. Sci.	Endocrinology
Sex, Species & Strain	Male Wistar Rats	Male FBN Rats	Male FBN Rats	Female WT and Rac1 inducible KO mice
Exercise or Contraction Protocol	4 x 30min swim	9 x 10min bouts of swimming	9 x 10min bouts of swimming	Treadmill: 30min at 18m/min, 15% incline
Muscles Used	Epitrochlearis	Epitrochlearis	Soleus	Soleus
Measurement Technique	Muscle Incubation	Muscle Incubation	Muscle Incubation	Muscle Incubation
Insulin Concentration or Infusion Rate	100 μU/ml	0.6nM (~100 μU/ml)	0.6nm (~100 μU/ml)	100 μU/ml
Insulin-stimulated Glucose Uptake	↑ 3hPEX	↑3hPEX	Unchanged, but caloric restriction ↑ ISGU w/ exercise vs ad libitum group.	↑2.5hPEX in WT and Rac1KO soleus
Insulin Signaling Post-Exercise	↑ $pAS160^{Ser588}$ in LFD and HFD groups. Post-ex insulin-stimulated $pAS160^{Thr642}$ in LFD > HFD. Unaltered pIR, IRS-1-PI3K, Akt Thr308 and Ser473, or Akt activity.	↑ $pAkt^{Ser473}$ and $pAkt^{Thr308}$. Unaltered $pAS160^{Ser588}$ and $pAS160^{Thr642}$.	Unchanged pAkt, pAS160 in ad libitum group after exercise. However, caloric restriction ↑ pAkt after exercise with insulin.	--
Main Findings	↑pAS160 may also be responsible for enhanced ISGU post-exercise in insulin-resistant animals.	Suggests that old rats improve insulin sensitivity after exercise through effects on Akt.	Exercise does not increase insulin sensitivity of pAS160 in soleus from old rats	Rac1 is dispensable for the insulin sensitizing effect of exercise.
Additional Information	--	Combining CR and exercise potentiate the enhancement in insulin sensitivity	--	--

Table 2.1: Continued

Reference [citation number]	Arias at al. 2017 [78]	Sjoberg et al. 2017 [136]	Kjobsted et al. 2017 [96]	
Journal	Physiol. Res.	Diabetes	Diabetes	
Sex, Species & Strain	Male Wistar Rats	Male Humans	WT & AMPKα1α2 muscle KO mice	
Exercise or Contraction Protocol	4 x 30min swim	One-legged knee extensor exercise: 60min at 80-100% peak leg work capacity	10min e-stim	
Muscles Used	Epitrochlearis	Vastus lateralis	EDL and Soleus	
Measurement Technique	Muscle Incubation	Insulin Clamp, muscle blood flow and a-v glucose difference	Muscle Incubation	
Insulin Concentration or Infusion Rate	0.6nM (~100 µU/ml)	1.4 mU/kg/min	100 or 10k µU/ml	
Insulin-stimulated Glucose Uptake	↑ 3hPEX	↑ 4hPEX	↑ in EDL from WT, but not KO mice with 100 µU/ml. No e-stim effect in soleus.	
Insulin Signaling Post-Exercise	↑ $pAS160^{Thr642}$ and $pAS160^{Ser588}$ at 3hPEX. Also, ↓ dephosphorylation of $pAS160^{Thr642}$ and $pAS160^{Ser588}$ in the ~30-50min after exercise.	pAkt unchanged on both sites. $pAS160^{Ser704}$ and $pAS160^{Ser318}$ ↑ (main effect) with exercise. pAS160 Ser588 and Thr642 were unchanged.	Akt unchanged. EDL AS160 Thr642 and Ser704 increased in WT but not KO. AS160 Ser317 and Ser588 unchanged.	
Main Findings	AS160 dephosphorylation is ↓ PEX, which may influence the enhanced insulin-stimulated pAS160 3hPEX.	Acute exercise increases insulin sensitivity by microvascular perfusion and AS160 signaling.	AMPK activity is important for the effect of exercise on insulin sensitivity and pAS160	
Additional Information	--	--	γ3-AMPK is required for the effect of contraction on $AS160^{Ser704}$	

Table 2.2: Skeletal Muscle Insulin-Stimulated Glucose Uptake after Short-Term High-Fat Diet

Reference [citation number]	Grundleger and Thenen 1982 [249]	Storlein et al. 1986 [250]	Kraegen et al. 1986 [251]	Chisholm and O'Dea 1987 [220]
Journal	Diabetes	Endocrinol. Metab.	Diabetologia	J. Nutr. Sci. Vitaminol.
Sex, Species & Strain	Male and Female lean Zucker Rats	Male Wistar Rats	Male Wistar Rats	Male Sprague-Dawley Rats
HFD Composition	67% fat, 12% carb	59% fat, 20% carb	60% fat, 20% carb	66% fat, 12% carb
LFD Composition	12% fat, 67% carb	10% fat, 69% carb	12% fat, 65% carb	12% fat, 66% carb
Isocaloric?	No (ad libitum)	Yes	No (ad libitum)	No (ad libitum)
Diet Duration	10 days	24 days	22 days	14 days
Morphological Changes with HFD	No change in body mass, fat mass not measured	No change in body mass, greater total fat mass	No difference in body mass (trend). Epididymal and interscapular fat mass ↑ in HFD	No change in body mass, fat mass not measured
Muscles Used	Soleus	Soleus, White Gastroc, Red Gastroc, and EDL	Soleus, White Gastroc, Red Gastroc, and EDL	Soleus strips
Measurement Technique	Muscle Incubation	Insulin Clamp	Insulin Clamp	Muscle incubation
Insulin Concentration or Infusion Rate	0.16-33.5nM	4.1mU/kg/min	4.1 and 33 mU/kg/min	50-1k µU/ml
Insulin-stimulated Glucose Uptake	↓ in HFD group across range of insulin concentrations	ISGU ↓ in soleus on HFD. Main effect of diet in RG. No effect of insulin or diet in EDL or WG.	ISGU ↓ in Soleus, WG and RG with 4.1 insulin. No change in EDL.	No change in ISGU across range of insulin concentrations (trend for decrease at all conc.)
Insulin Signaling	↓ insulin binding and receptor number in HFD soleus. No change in receptor affinity.	--	--	No change in insulin binding in soleus with HFD (trend for decrease at all conc.)
Additional Information	↓ insulin receptors didn't account for insulin resistance. Post-receptor mechanism as well	--	Later studied other muscles and saw ↓ ISGU in plantaris and Red Quadriceps	--
Main Findings	Receptor and post-receptor influence on skeletal muscle insulin-resistance with a short-term HFD.	Considerable Heterogeneity in different muscles for ISGU with a HFD.	Emphasized that largest changes are in oxidative muscle tissues.	HFD was high in poly-unsaturated fats, which the authors speculated may be cause for null results.

Table 2.2: Continued

Reference [citation number]	Zierath et al. 1997 [179]	Han et al. 1997 [252]	Oakes et al. 1997 [142]	Wilkes et al. 1998 [253]
Journal	Diabetes	Diabetes	Diabetes	Am. J. Physiol. Endocrinol. Metab.
Sex, Species & Strain	Male and Female FVB mice	Male Wistar Rats	Male Wistar Rats	Male Sprague-Dawley Rats
HFD Composition	55% fat, 24% carb	50% fat, 27% carb	59% fat, 20% carb	59% fat, 20% carb
LFD Composition	17% fat, 57% carb	12% fat, 59% carb	16% fat, 58% carb	10% fat, 70% carb
Isocaloric?	No (ad libitum)	No (ad libitum)	Yes	Yes
Diet Duration	21 days	28 days	21 days	21 days
Morphological Changes with HFD	No change in body mass, greater gonadal fat mass	No change in body mass, greater total fat mass	No change in body mass, fat mass not measured	No change in body mass, mixed HFD (saturated) ↑ fat mass vs HFD-Saff (safflower oil)
Muscles Used	EDL and Soleus	Epitrochlearis and Soleus	Red and White Gastroc, and Soleus	Oxidative: sol, Red-G, Red-TA Mixed: EDL, plant Glycolytic: W-Gastroc, W-TA
Measurement Technique	Muscle Incubation	Muscle Incubation	Estimated by Insulin Clamp	Perfused Hindlimb
Insulin Concentration or Infusion Rate	2k µU/ml	60 and 2k µU/ml	1.8nmol/kg/min	40nM
Insulin-stimulated Glucose Uptake	↓ ISGU in both male and female soleus with a HFD, but not in EDL	↓ with 60 and 2k insulin in the epitrochlearis and soleus	↓ in soleus, RG and WG	↓ in all muscle types with both HFDs
Insulin Signaling	↓ insulin-stimulated PI3-K activity and cell surface GLUT4 with HFD	--	--	--
Additional Information	Magnitude of decrease in IGSU and CS GLUT4 was very similar	GLUT4 abundance is unaltered by HFD in soleus or epi. 8wk-HFD ↑ body mass.	--	--
Main Findings	Deficit in PI3-K signaling is impaired in HFD, leading to ↓ CS GLUT4 and ↓ ISGU	Effect of HFD in ISGU not due to ↓ GLUT4 content.	Elevated lipid oxidation may oppose ISGU in muscle	Multiple types of HFD induce insulin resistance

Table 2.2: Continued

Reference [citation number]	Kim et al. 2000 [254]	Tremblay et al. 2001 [255]	Tanaka et al. 2007 [120]	Turner et al. 2013 [221]
Journal	Am. J. Physiol. Regul. Integr. Comp. Physiol.	Diabetes	Metab. Clin. Exp.	Diabetologia
Sex, Species & Strain	Male Wistar Rats	Male Wistar Rats	Male Wistar Rats	Male C57B1/6 mice
HFD Composition	50% fat, 27% carb	65% fat, 20% carb	60% fat, 20% carb	42-45% fat
LFD Composition	12% fat, 59% carb	5% fat, 57% carb	12% fat	5-8% fat
Isocaloric?	No (ad libitum)	No (ad libitum)	Not specified	No (ad libitum)
Diet Duration	14 and 28 days	28 days	28 days	3days - 12 weeks
Morphological Changes with HFD	No change in body mass, greater total fat mass	Not reported	Increased body mass and abdominal fat	Body mass did not ↑ until 3-5 wk. Fat mass ↑ by 3-7 d.
Muscles Used	Epitrochlearis and Soleus strips	Soleus, Tibialis, Gastroc, Quads	Soleus	Quads, Tibialis Anterior, Soleus
Measurement Technique	Muscle Incubation	Insulin Clamp	Muscle Incubation	Insulin Clamp
Insulin Concentration or Infusion Rate	2k µU/ml	8 U/kg injection	0.9nmol/L	4mU/kg/min
Insulin-stimulated Glucose Uptake	↓ ISGU in epi and soleus with both 4wk corn and fish oil based HFD, but corn oil greater ↓. No ↓ in ISGU after 2wk corn oil HFD in epi or soleus.	↓ in soleus and W gastroc, but trended to decrease in tibialis with HFD	↓ with HFD. Also, insulin-stimulated glucose uptake 2hPEX is ↓ with HFD	↓ by 3 weeks in all muscles with a HFD, but not at 1 week.
Insulin Signaling	--	↓ insulin-stimulated IRS-1 associated PI3-K, and pAkt. No change in pIR.	No difference in GLUT4 expression with HFD. No diff in $pAkt^{Ser473}$ in chow vs HFD	$pAkt^{Ser473}$ was unchanged by 1-3 weeks.
Additional Information	Highly correlated total visceral fat mass with ISGU in epitrochlearis.	PM and T-tubule GLUT4 content ↑ with insulin in the chow diet, but not in the HFD. Total GLUT4 content ↓.	IMTG content in both type I and type IIa fibers are ↑ with HFD (measured by oil red O).	Muscle TG and many DG species were changes at 3 weeks but not 1 week.
Main Findings	↑ Visceral fat is associated with insulin resistance	Identified PI3-k as first step in the insulin signaling pathway to be impaired by HFD.	HFD impairs acute HFD impairs acute exercise effect on insulin-stimulated GU	HFD muscle insulin resistance is associated with lipid species

Table 2.2: Continued

Reference [citation number]	Castorena et al. 2014 [77]	White et al. 2015 [256]		
Journal	Diabetes	Molecular Metabolism		
Sex, Species & Strain	Male Wistar rats	WT and STAT3 KO mice		
HFD Composition	60% fat, 20% carb	60% fat		
LFD Composition	14% fat, 58% carb	10% fat		
Isocaloric?	No (ab libitum)	No (ab libitum)		
Diet Duration	14 days	21 days		
Morphological Changes with HFD	No change in body mass, greater epididylmal fat mass	No change in body mass, greater % body fat		
Muscles Used	Epitrochlearis	Soleus and EDL		
Measurement Technique	Muscle Incubation	Muscle Incubation		
Insulin Concentration or Infusion Rate	100 µU/ml	60 µU/ml		
Insulin-stimulated Glucose Uptake	↓ with HFD	↓ with HFD in both WT and KO soleus and EDL		
Insulin Signaling	Unchanged pAMPK, pAkt, PAS160, pIR, or IRS-1 assoc. PI3-K	--		
Additional Information	Insulin-stimulated GU 3hPEX is impaired with a HFD. This is associated with pAS160.	--		
Main Findings	HFD ↓ insulin-stimulated glucose uptake 3hPEX and AS160 is a possible mediator	STAT3 does not underlie development of HFD-induced muscle insulin resistance		

Table 2.3: Fiber Type Comparisons (identified based on MHC in single myofibers, not including fiber type identified by other methods and not including tissue analysis)

	Fiber Type Comparisons	Reference citation number
Contractile Velocity (V_{max})	Rat I < IIA ~ IIX < IIB Human: I < I/IIA < IIA < IIAX < IIX	[257-261]
Stretch Activated Contractile Speed	Rat I < I/IIA < IIA < IIAX < IIX < IIBX < IIB Human: I < I/IIA < IIA < IIAX < IIX	[262-264]
Neural Activity	Identified in Rat and Rabbit fibers: Chronic, low frequency stimulation = slow twitch Phasic, high-frequency stimulation = fast twitch	[265-267]
Peak Power	Rat: I < IIA < IIX ~ IIB Human: I < I/IIA < IIA < IIAX < IIX	[257, 260, 261]
Cross Sectional Area	Usually, but not in all muscles Rat: I ≤ IIA < IIX < IIB Human: No consistently obvious differences Mouse: IIA ≤ I < IIX < IIB	[185, 268]
Mitochondrial Content	Rat: IIA > I > IIX > IIB Human: I > IIA > IIX Mouse: IIA > IIX > I > IIB	[269-272]
Capillary to Fiber Ratio	Rat: I > IIA > IIX > IIB Human: I > IIA > IIX	[271-273]
Glycolytic Enzyme Activity or Abundance	Human: I < IIA < IIX Rat: HKII not different between fiber types Mouse: I < IIA < IIX < IIB	[184, 208, 274]
Oxidative Enzyme Activity or Abundance	Human: I > IIA > IIX Rat: IIA ≥ I ~ IIX > IIB Mouse: IIA ≥ I ~ IIX > IIB	[184, 185, 208, 274]
Intramuscular Triglycerides	Human: I > IIA > IIX Rat: IIA > I > IIX ~ IIB	[120, 171, 271, 275, 276]
Glycogen	Human: I < IIA ~ IIX Rat: Unaware of any studies in rats	[211, 212, 277-280]
GLUT4 Abundance	Human: I > IIA ~ IIX Rat: IIA > IIAX > IIX ~ IIBX ~ IIB	[211, 232, 281]
Insulin-Stimulated Glucose Uptake	Human: Currently no method for measuring ISGU in human Rat: I ~ IIA > IIX ~ IIBX ≥ IIB	[205-207]
AMPK	Human: α1 and α2 isoforms - no difference in fiber types γ3 isoform - I < IIA < IIX Rat: Unaware of any studies in rats	[282]
Susceptibility to age-related atrophy	Human: II > I Rat: II > I	[203, 283, 284]
AS160 Abundance	Human: II > I (study did not distinguish between IIA and IIX) Rats: Unaware of any studies in rats	[211, 212]
TBC1D1 Abundance	Human: II > I (study did not distinguish between IIA and IIX) Rats: Unaware of any studies in rats	[211, 212]

REFERENCES

1. Dall, T.M., W. Yang, P. Halder, B. Pang, M. Massoudi, N. Wintfeld, A.P. Semilla, J. Franz, and P.F. Hogan, *The economic burden of elevated blood glucose levels in 2012: diagnosed and undiagnosed diabetes, gestational diabetes mellitus, and prediabetes.* Diabetes care, 2014. **37**(12): p. 3172-3179.
2. Geiss, L.S., J. Wang, Y.J. Cheng, T.J. Thompson, L. Barker, Y. Li, A.L. Albright, and E.W. Gregg, *Prevalence and incidence trends for diagnosed diabetes among adults aged 20 to 79 years, United States, 1980-2012.* Jama, 2014. **312**(12): p. 1218-1226.
3. Huang, E.S., A. Basu, M. O'grady, and J.C. Capretta, *Projecting the future diabetes population size and related costs for the US.* Diabetes Care, 2009. **32**(12): p. 2225-2229.
4. Facchini, F.S., N. Hua, F. Abbasi, and G.M. Reaven, *Insulin resistance as a predictor of age-related diseases.* The Journal of Clinical Endocrinology & Metabolism, 2001. **86**(8): p. 3574-3578.
5. DeFronzo, R.A., E. Jacot, E. Jequier, E. Maeder, J. Wahren, and J.P. Felber, *The effect of insulin on the disposal of intravenous glucose. Results from indirect calorimetry and hepatic and femoral venous catheterization.* Diabetes, 1981. **30**(12): p. 1000-7.
6. Ziel, F.H., N. Venkatesan, and M.B. Davidson, *Glucose transport is rate limiting for skeletal muscle glucose metabolism in normal and STZ-induced diabetic rats.* Diabetes, 1988. **37**(7): p. 885-890.
7. Ren, J.-M., B. Marshall, E. Gulve, J. Gao, D. Johnson, J. Holloszy, and M. Mueckler, *Evidence from transgenic mice that glucose transport is rate-limiting for glycogen deposition and glycolysis in skeletal muscle.* Journal of Biological Chemistry, 1993. **268**(22): p. 16113-16115.
8. Kern, M., J.A. Wells, J.M. Stephens, C.W. Elton, J.E. Friedman, E.B. Tapscott, P.H. Pekala, and G.L. Dohm, *Insulin responsiveness in skeletal muscle is determined by glucose transporter (Glut4) protein level.* Biochemical Journal, 1990. **270**(2): p. 397-400.
9. Jaldin-Fincati, J.R., M. Pavarotti, S. Frendo-Cumbo, P.J. Bilan, and A. Klip, *Update on GLUT4 Vesicle Traffic: A Cornerstone of Insulin Action.* Trends in Endocrinology & Metabolism, 2017.
10. Hansen, P.A., L.A. Nolte, M.M. Chen, and J.O. Holloszy, *Increased GLUT-4 translocation mediates enhanced insulin sensitivity of muscle glucose transport after exercise.* Journal of Applied Physiology, 1998. **85**(4): p. 1218-1222.
11. Richter, E.A., L.P. Garetto, M.N. Goodman, and N.B. Ruderman, *Muscle glucose metabolism following exercise in the rat: increased sensitivity to insulin.* Journal of Clinical Investigation, 1982. **69**(4): p. 785-793.
12. Richter, E.A., K. Mikines, H. Galbo, and B. Kiens, *Effect of exercise on insulin action in human skeletal muscle.* Journal of Applied Physiology, 1989. **66**(2): p. 876-885.
13. Bonen, A., M. Tan, and W. Watson-Wright, *Effects of exercise on insulin binding and glucose metabolism in muscle.* Canadian journal of physiology and pharmacology, 1984. **62**(12): p. 1500-1504.
14. Zorzano, A., T.W. Balon, M.N. Goodman, and N. Ruderman, *Additive effects of prior exercise and insulin on glucose and AIB uptake by rat muscle.* American Journal of Physiology-Endocrinology And Metabolism, 1986. **251**(1): p. E21-E26.
15. Davis, T.A., S. Klahr, E.D. Tegtmeyer, D.F. Osborne, T.L. Howard, and I.E. Karl, *Glucose metabolism in epitrochlearis muscle of acutely exercised and trained rats.*

American Journal of Physiology-Endocrinology And Metabolism, 1986. **250**(2): p. E137-E143.
16. Wallberg-Henriksson, H., S. Constable, D. Young, and J. Holloszy, *Glucose transport into rat skeletal muscle: interaction between exercise and insulin.* Journal of applied physiology, 1988. **65**(2): p. 909-913.
17. Cartee, G.D., D.A. Young, M.D. Sleeper, J. Zierath, H. Wallberg-Henriksson, and J.O. Holloszy, *Prolonged increase in insulin-stimulated glucose transport in muscle after exercise.* Am J Physiol, 1989. **256**(4 Pt 1): p. E494-9.
18. Mikines, K.J., B. Sonne, P. Farrell, B. Tronier, and H. Galbo, *Effect of physical exercise on sensitivity and responsiveness to insulin in humans.* American Journal of Physiology-Endocrinology And Metabolism, 1988. **254**(3): p. E248-E259.
19. Garvey, W.T., L. Maianu, J.-H. Zhu, G. Brechtel-Hook, P. Wallace, and A.D. Baron, *Evidence for defects in the trafficking and translocation of GLUT4 glucose transporters in skeletal muscle as a cause of human insulin resistance.* Journal of Clinical Investigation, 1998. **101**(11): p. 2377.
20. Karnieli, E., M. Zarnowski, P. Hissin, I. Simpson, L. Salans, and S. Cushman, *Insulin-stimulated translocation of glucose transport systems in the isolated rat adipose cell. Time course, reversal, insulin concentration dependency, and relationship to glucose transport activity.* Journal of Biological Chemistry, 1981. **256**(10): p. 4772-4777.
21. Klip, A., T. Ramlal, D.A. Young, and J.O. Holloszy, *Insulin-induced translocation of glucose transporters in rat hindlimb muscles.* FEBS letters, 1987. **224**(1): p. 224-230.
22. James, D.E., R. Brown, J. Navarro, and P.F. Pilch, *Insulin-regulatable tissues express a unique insulin-sensitive glucose transport protein.* 1988.
23. Cerasi, E. and R. Luft, *The plasma insulin response to glucose infusion in healthy subjects and in diabetes mellitus.* Acta endocrinologica, 1967. **55**(2): p. 278-304.
24. Lee, J., P.F. Pilch, S.E. Shoelson, and S.F. Scarlata, *Conformational changes of the insulin receptor upon insulin binding and activation as monitored by fluorescence spectroscopy.* Biochemistry, 1997. **36**(9): p. 2701-2708.
25. Sesti, G., M. Federici, M.L. Hribal, D. Lauro, P. Sbraccia, and R. Lauro, *Defects of the insulin receptor substrate (IRS) system in human metabolic disorders.* The FASEB Journal, 2001. **15**(12): p. 2099-2111.
26. Huang, C., A.C. Thirone, X. Huang, and A. Klip, *Differential contribution of insulin receptor substrates 1 versus 2 to insulin signaling and glucose uptake in l6 myotubes.* Journal of Biological Chemistry, 2005. **280**(19): p. 19426-19435.
27. Tanti, J.-F., T. Gremeaux, E. Van Obberghen, and Y. Le Marchand-Brustel, *Serine/threonine phosphorylation of insulin receptor substrate 1 modulates insulin receptor signaling.* Journal of Biological Chemistry, 1994. **269**(8): p. 6051-6057.
28. Bouzakri, K., M. Roques, P. Gual, S. Espinosa, F. Guebre-Egziabher, J.-P. Riou, M. Laville, Y. Le Marchand-Brustel, J.-F. Tanti, and H. Vidal, *Reduced activation of phosphatidylinositol-3 kinase and increased serine 636 phosphorylation of insulin receptor substrate-1 in primary culture of skeletal muscle cells from patients with type 2 diabetes.* Diabetes, 2003. **52**(6): p. 1319-1325.
29. Copps, K. and M. White, *Regulation of insulin sensitivity by serine/threonine phosphorylation of insulin receptor substrate proteins IRS1 and IRS2.* Diabetologia, 2012. **55**(10): p. 2565-2582.

30. Morino, K., K.F. Petersen, S. Dufour, D. Befroy, J. Frattini, N. Shatzkes, S. Neschen, M.F. White, S. Bilz, and S. Sono, *Reduced mitochondrial density and increased IRS-1 serine phosphorylation in muscle of insulin-resistant offspring of type 2 diabetic parents.* The Journal of clinical investigation, 2005. **115**(12): p. 3587-3593.
31. Esposito, D.L., Y. Li, A. Cama, and M.J. Quon, *Tyr612 and Tyr632 in Human Insulin Receptor Substrate-1 Are Important for Full Activation of Insulin-Stimulated Phosphatidylinositol 3-Kinase Activity and Translocation of GLUT4 in Adipose Cells 1.* Endocrinology, 2001. **142**(7): p. 2833-2840.
32. Rameh, L.E. and L.C. Cantley, *The role of phosphoinositide 3-kinase lipid products in cell function.* Journal of Biological Chemistry, 1999. **274**(13): p. 8347-8350.
33. JeBailey, L., A. Rudich, X. Huang, C.D. Ciano-Oliveira, A. Kapus, and A. Klip, *Skeletal muscle cells and adipocytes differ in their reliance on TC10 and Rac for insulin-induced actin remodeling.* Molecular endocrinology, 2004. **18**(2): p. 359-372.
34. Klip, A., Y. Sun, T.T. Chiu, and K.P. Foley, *Signal transduction meets vesicle traffic: the software and hardware of GLUT4 translocation.* American Journal of Physiology-Cell Physiology, 2014. **306**(10): p. C879-C886.
35. Sylow, L., M. Kleinert, C. Pehmøller, C. Prats, T.T. Chiu, A. Klip, E.A. Richter, and T.E. Jensen, *Akt and Rac1 signaling are jointly required for insulin-stimulated glucose uptake in skeletal muscle and downregulated in insulin resistance.* Cellular signalling, 2014. **26**(2): p. 323-331.
36. Alessi, D.R., M. Andjelkovic, B. Caudwell, P. Cron, N. Morrice, P. Cohen, and B. Hemmings, *Mechanism of activation of protein kinase B by insulin and IGF-1.* The EMBO journal, 1996. **15**(23): p. 6541.
37. Toker, A. and A.C. Newton, *Akt/protein kinase B is regulated by autophosphorylation at the hypothetical PDK-2 site.* Journal of Biological Chemistry, 2000. **275**(12): p. 8271-8274.
38. Toker, A. and S. Marmiroli, *Signaling specificity in the Akt pathway in biology and disease.* Advances in biological regulation, 2014. **55**: p. 28-38.
39. Sarbassov, D.D., D.A. Guertin, S.M. Ali, and D.M. Sabatini, *Phosphorylation and regulation of Akt/PKB by the rictor-mTOR complex.* Science, 2005. **307**(5712): p. 1098-1101.
40. Manning, B.D. and L.C. Cantley, *AKT/PKB signaling: navigating downstream.* Cell, 2007. **129**(7): p. 1261-1274.
41. Kane, S., H. Sano, S.C. Liu, J.M. Asara, W.S. Lane, C.C. Garner, and G.E. Lienhard, *A method to identify serine kinase substrates Akt phosphorylates a novel adipocyte protein with a Rab GTPase-activating protein (GAP) domain.* Journal of Biological Chemistry, 2002. **277**(25): p. 22115-22118.
42. Xie, X., Z. Gong, V. Mansuy-Aubert, Q.L. Zhou, S.A. Tatulian, D. Sehrt, F. Gnad, L.M. Brill, K. Motamedchaboki, and Y. Chen, *C2 domain-containing phosphoprotein CDP138 regulates GLUT4 insertion into the plasma membrane.* Cell metabolism, 2011. **14**(3): p. 378-389.
43. Lim, C.-Y., X. Bi, D. Wu, J.B. Kim, P.W. Gunning, W. Hong, and W. Han, *Tropomodulin3 is a novel Akt2 effector regulating insulin-stimulated GLUT4 exocytosis through cortical actin remodeling.* Nature communications, 2015. **6**: p. 5951.

44. Yoshizaki, T., T. Imamura, J.L. Babendure, J.-C. Lu, N. Sonoda, and J.M. Olefsky, *Myosin 5a is an insulin-stimulated Akt2 (protein kinase Bβ) substrate modulating GLUT4 vesicle translocation.* Molecular and cellular biology, 2007. **27**(14): p. 5172-5183.
45. Zerial, M. and H. McBride, *Rab proteins as membrane organizers.* Nature reviews Molecular cell biology, 2001. **2**(2): p. 107-117.
46. Sano, H., G.R. Peck, A.N. Kettenbach, S.A. Gerber, and G.E. Lienhard, *Insulin-stimulated GLUT4 protein translocation in adipocytes requires the Rab10 guanine nucleotide exchange factor Dennd4C.* Journal of Biological Chemistry, 2011. **286**(19): p. 16541-16545.
47. Sun, Y., P.J. Bilan, Z. Liu, and A. Klip, *Rab8A and Rab13 are activated by insulin and regulate GLUT4 translocation in muscle cells.* Proceedings of the National Academy of Sciences, 2010. **107**(46): p. 19909-19914.
48. Zhou, Z., F. Menzel, T. Benninghoff, A. Chadt, C. Du, G.D. Holman, and H. Al-Hasani, *Rab28 is a TBC1D1/TBC1D4 substrate involved in GLUT4 trafficking.* FEBS letters, 2017. **591**(1): p. 88-96.
49. Sano, H., S. Kane, E. Sano, C.P. Mîinea, J.M. Asara, W.S. Lane, C.W. Garner, and G.E. Lienhard, *Insulin-stimulated phosphorylation of a Rab GTPase-activating protein regulates GLUT4 translocation.* Journal of Biological Chemistry, 2003. **278**(17): p. 14599-14602.
50. Chen, S., D.H. Wasserman, C. MacKintosh, and K. Sakamoto, *Mice with AS160/TBC1D4-Thr649Ala knockin mutation are glucose intolerant with reduced insulin sensitivity and altered GLUT4 trafficking.* Cell Metabolism, 2011. **13**(1): p. 68-79.
51. Eguez, L., A. Lee, J.A. Chavez, C.P. Miinea, S. Kane, G.E. Lienhard, and T.E. McGraw, *Full intracellular retention of GLUT4 requires AS160 Rab GTPase activating protein.* Cell metabolism, 2005. **2**(4): p. 263-272.
52. Bryant, N.J. and G.W. Gould, *SNARE Proteins Underpin Insulin-Regulated GLUT4 Traffic.* Traffic, 2011. **12**(6): p. 657-664.
53. Kawaguchi, T., Y. Tamori, H. Kanda, M. Yoshikawa, S. Tateya, N. Nishino, and M. Kasuga, *The t-SNAREs syntaxin4 and SNAP23 but not v-SNARE VAMP2 are indispensable to tether GLUT4 vesicles at the plasma membrane in adipocyte.* Biochemical and biophysical research communications, 2010. **391**(3): p. 1336-1341.
54. Douen, A., T. Ramlal, S. Rastogi, P. Bilan, G. Cartee, M. Vranic, J. Holloszy, and A. Klip, *Exercise induces recruitment of the" insulin-responsive glucose transporter". Evidence for distinct intracellular insulin-and exercise-recruitable transporter pools in skeletal muscle.* Journal of Biological Chemistry, 1990. **265**(23): p. 13427-13430.
55. Holloszy, J.O., S.H. Constable, and D.A. Young, *Activation of glucose transport in muscle by exercise.* Diabetes/Metabolism Research and Reviews, 1986. **1**(4): p. 409-423.
56. Youn, J., E. Gulve, and J. Holloszy, *Calcium stimulates glucose transport in skeletal muscle by a pathway independent of contraction.* American Journal of Physiology-Cell Physiology, 1991. **260**(3): p. C555-C561.
57. Hayashi, T., M.F. Hirshman, E.J. Kurth, W.W. Winder, and L.J. Goodyear, *Evidence for 5' AMP-activated protein kinase mediation of the effect of muscle contraction on glucose transport.* Diabetes, 1998. **47**(8): p. 1369-1373.
58. Blair, D.R., K. Funai, G.G. Schweitzer, and G.D. Cartee, *A myosin II ATPase inhibitor reduces force production, glucose transport, and phosphorylation of AMPK and TBC1D1*

in electrically stimulated rat skeletal muscle. American Journal of Physiology-Endocrinology and Metabolism, 2009. **296**(5): p. E993-E1002.
59. Jensen, T.E., L. Sylow, A.J. Rose, A.B. Madsen, Y. Angin, S.J. Maarbjerg, and E.A. Richter, *Contraction-stimulated glucose transport in muscle is controlled by AMPK and mechanical stress but not sarcoplasmatic reticulum Ca2+ release.* Molecular metabolism, 2014. **3**(7): p. 742-753.
60. Kingwell, B.A., M. Formosa, M. Muhlmann, S.J. Bradley, and G.K. McConell, *Nitric oxide synthase inhibition reduces glucose uptake during exercise in individuals with type 2 diabetes more than in control subjects.* Diabetes, 2002. **51**(8): p. 2572-2580.
61. Bradley, S.J., B.A. Kingwell, and G.K. McConell, *Nitric oxide synthase inhibition reduces leg glucose uptake but not blood flow during dynamic exercise in humans.* Diabetes, 1999. **48**(9): p. 1815-1821.
62. Sandström, M.E., S.J. Zhang, J. Bruton, J.P. Silva, M.B. Reid, H. Westerblad, and A. Katz, *Role of reactive oxygen species in contraction-mediated glucose transport in mouse skeletal muscle.* The Journal of physiology, 2006. **575**(1): p. 251-262.
63. Chambers, M.A., J.S. Moylan, J.D. Smith, L.J. Goodyear, and M.B. Reid, *Stretch-stimulated glucose uptake in skeletal muscle is mediated by reactive oxygen species and p38 MAP-kinase.* The Journal of physiology, 2009. **587**(13): p. 3363-3373.
64. Wright, D.C., K.A. Hucker, J.O. Holloszy, and D.H. Han, *Ca2+ and AMPK both mediate stimulation of glucose transport by muscle contractions.* Diabetes, 2004. **53**(2): p. 330-335.
65. Witczak, C.A., N. Jessen, D.M. Warro, T. Toyoda, N. Fujii, M.E. Anderson, M.F. Hirshman, and L.J. Goodyear, *CaMKII regulates contraction-but not insulin-induced glucose uptake in mouse skeletal muscle.* American Journal of Physiology-Endocrinology and Metabolism, 2010. **298**(6): p. E1150-E1160.
66. Jensen, T.E., A.J. Rose, S.B. Jorgensen, N. Brandt, P. Schjerling, J.F. Wojtaszewski, and E.A. Richter, *Possible CaMKK-dependent regulation of AMPK phosphorylation and glucose uptake at the onset of mild tetanic skeletal muscle contraction.* Am J Physiol Endocrinol Metab, 2007. **292**(5): p. E1308-17.
67. Witczak, C.A., N. Fujii, M.F. Hirshman, and L.J. Goodyear, *Ca2+/calmodulin-dependent protein kinase kinase-α regulates skeletal muscle glucose uptake independent of AMP-activated protein kinase and Akt activation.* Diabetes, 2007. **56**(5): p. 1403-1409.
68. Richter, E.A. and N.B. Ruderman, *AMPK and the biochemistry of exercise: implications for human health and disease.* Biochemical Journal, 2009. **418**(2): p. 261-275.
69. Hardie, D.G., *AMP-activated/SNF1 protein kinases: conserved guardians of cellular energy.* Nature reviews Molecular cell biology, 2007. **8**(10): p. 774-785.
70. Hardie, D.G., I.P. Salt, and S.P. Davies, *Analysis of the role of the AMP-activated protein kinase in the response to cellular stress.* Stress Response: Methods and Protocols, 2000: p. 63-74.
71. Wojtaszewski, J.F., P. Nielsen, B.F. Hansen, E.A. Richter, and B. Kiens, *Isoform-specific and exercise intensity-dependent activation of 5'-AMP-activated protein kinase in human skeletal muscle.* J Physiol, 2000. **528 Pt 1**: p. 221-6.
72. Chen, Z.-P., T.J. Stephens, S. Murthy, B.J. Canny, M. Hargreaves, L.A. Witters, B.E. Kemp, and G.K. McConell, *Effect of exercise intensity on skeletal muscle AMPK signaling in humans.* Diabetes, 2003. **52**(9): p. 2205-2212.

73. Fujii, N., T. Hayashi, M.F. Hirshman, J.T. Smith, S.A. Habinowski, L. Kaijser, J. Mu, O. Ljungqvist, M.J. Birnbaum, and L.A. Witters, *Exercise induces isoform-specific increase in 5′ AMP-activated protein kinase activity in human skeletal muscle.* Biochemical and biophysical research communications, 2000. **273**(3): p. 1150-1155.
74. Suter, M., U. Riek, R. Tuerk, U. Schlattner, T. Wallimann, and D. Neumann, *Dissecting the role of 5′-AMP for allosteric stimulation, activation, and deactivation of AMP-activated protein kinase.* Journal of Biological Chemistry, 2006. **281**(43): p. 32207-32216.
75. Winder, W. and D. Hardie, *Inactivation of acetyl-CoA carboxylase and activation of AMP-activated protein kinase in muscle during exercise.* American Journal of Physiology-Endocrinology And Metabolism, 1996. **270**(2): p. E299-E304.
76. Chen, Z.-P., G.K. McConell, B.J. Michell, R.J. Snow, B.J. Canny, and B.E. Kemp, *AMPK signaling in contracting human skeletal muscle: acetyl-CoA carboxylase and NO synthase phosphorylation.* American Journal of Physiology-Endocrinology And Metabolism, 2000. **279**(5): p. E1202-E1206.
77. Castorena, C.M., E.B. Arias, N. Sharma, and G.D. Cartee, *Postexercise improvement in insulin-stimulated glucose uptake occurs concomitant with greater AS160 phosphorylation in muscle from normal and insulin-resistant rats.* Diabetes, 2014. **63**(7): p. 2297-308.
78. Arias, E.B., J. Kim, K. Funai, and G.D. Cartee, *Prior exercise increases phosphorylation of Akt substrate of 160 kDa (AS160) in rat skeletal muscle.* American Journal of Physiology-Endocrinology and Metabolism, 2007. **292**(4): p. E1191-E1200.
79. Schweitzer, G.G., E.B. Arias, and G.D. Cartee, *Sustained postexercise increases in AS160 Thr 642 and Ser 588 phosphorylation in skeletal muscle without sustained increases in kinase phosphorylation.* Journal of Applied Physiology, 2012. **113**(12): p. 1852-1861.
80. Merrill, G., E. Kurth, D. Hardie, and W. Winder, *AICA riboside increases AMP-activated protein kinase, fatty acid oxidation, and glucose uptake in rat muscle.* American Journal of Physiology-Endocrinology And Metabolism, 1997. **273**(6): p. E1107-E1112.
81. Hardie, D.G., J.W. Scott, D.A. Pan, and E.R. Hudson, *Management of cellular energy by the AMP-activated protein kinase system.* FEBS letters, 2003. **546**(1): p. 113-120.
82. Cheung, P.C., S.P. Davies, D.G. Hardie, and D. Carling, *Characterization of AMP-activated protein kinase γ-subunit isoforms and their role in AMP binding.* Biochemical Journal, 2000. **346**(3): p. 659-669.
83. Hardie, D.G., F.A. Ross, and S.A. Hawley, *AMPK: a nutrient and energy sensor that maintains energy homeostasis.* Nature reviews Molecular cell biology, 2012. **13**(4): p. 251-262.
84. Wojtaszewski, J.F., J.B. Birk, C. Frøsig, M. Holten, H. Pilegaard, and F. Dela, *5′ AMP activated protein kinase expression in human skeletal muscle: effects of strength training and type 2 diabetes.* The Journal of physiology, 2005. **564**(2): p. 563-573.
85. Treebak, J.T., J.B. Birk, B.F. Hansen, G.S. Olsen, and J.F. Wojtaszewski, *A-769662 activates AMPK β1-containing complexes but induces glucose uptake through a PI3-kinase-dependent pathway in mouse skeletal muscle.* American Journal of Physiology-Cell Physiology, 2009. **297**(4): p. C1041-C1052.

86. Kjøbsted, R., J.R. Hingst, J. Fentz, M. Foretz, M.-N. Sanz, C. Pehmøller, M. Shum, A. Marette, R. Mounier, and J.T. Treebak, *AMPK in skeletal muscle function and metabolism.* The FASEB Journal, 2017: p. fj. 201700442R.
87. Treebak, J.T., J.B. Birk, A.J. Rose, B. Kiens, E.A. Richter, and J.F. Wojtaszewski, *AS160 phosphorylation is associated with activation of α2β2γ1-but not α2β2γ3-AMPK trimeric complex in skeletal muscle during exercise in humans.* American Journal of Physiology-Endocrinology and Metabolism, 2007. **292**(3): p. E715-E722.
88. Kjøbsted, R., J.T. Treebak, J. Fentz, L. Lantier, B. Viollet, J.B. Birk, P. Schjerling, M. Björnholm, J.R. Zierath, and J.F. Wojtaszewski, *Prior AICAR stimulation increases insulin sensitivity in mouse skeletal muscle in an AMPK-dependent manner.* Diabetes, 2015. **64**(6): p. 2042-2055.
89. Chen, S., J. Murphy, R. Toth, D.G. Campbell, N.A. Morrice, and C. Mackintosh, *Complementary regulation of TBC1D1 and AS160 by growth factors, insulin and AMPK activators.* Biochemical Journal, 2008. **409**(2): p. 449-459.
90. Pehmøller, C., J.T. Treebak, J.B. Birk, S. Chen, C. MacKintosh, D.G. Hardie, E.A. Richter, and J.F. Wojtaszewski, *Genetic disruption of AMPK signaling abolishes both contraction-and insulin-stimulated TBC1D1 phosphorylation and 14-3-3 binding in mouse skeletal muscle.* American Journal of Physiology-Endocrinology and Metabolism, 2009. **297**(3): p. E665-E675.
91. Cartee, G.D., *Roles of TBC1D1 and TBC1D4 in insulin-and exercise-stimulated glucose transport of skeletal muscle.* Diabetologia, 2015. **58**(1): p. 19-30.
92. Bruss, M.D., E.B. Arias, G.E. Lienhard, and G.D. Cartee, *Increased phosphorylation of Akt substrate of 160 kDa (AS160) in rat skeletal muscle in response to insulin or contractile activity.* Diabetes, 2005. **54**(1): p. 41-50.
93. Kramer, H.F., C.A. Witczak, N. Fujii, N. Jessen, E.B. Taylor, D.E. Arnolds, K. Sakamoto, M.F. Hirshman, and L.J. Goodyear, *Distinct signals regulate AS160 phosphorylation in response to insulin, AICAR, and contraction in mouse skeletal muscle.* Diabetes, 2006. **55**(7): p. 2067-2076.
94. Funai, K. and G.D. Cartee, *Inhibition of contraction-stimulated AMP-activated protein kinase inhibits contraction-stimulated increases in PAS-TBC1D1 and glucose transport without altering PAS-AS160 in rat skeletal muscle.* Diabetes, 2009. **58**(5): p. 1096-104.
95. Treebak, J.T., E.B. Taylor, C.A. Witczak, D. An, T. Toyoda, H.-J. Koh, J. Xie, E.P. Feener, J.F. Wojtaszewski, and M.F. Hirshman, *Identification of a novel phosphorylation site on TBC1D4 regulated by AMP-activated protein kinase in skeletal muscle.* American Journal of Physiology-Cell Physiology, 2010. **298**(2): p. C377-C385.
96. Kjøbsted, R., N. Munk-Hansen, J.B. Birk, M. Foretz, B. Viollet, M. Björnholm, J.R. Zierath, J.T. Treebak, and J.F. Wojtaszewski, *Enhanced muscle insulin sensitivity after contraction/exercise is mediated by AMPK.* Diabetes, 2017. **66**(3): p. 598-612.
97. Sylow, L., L.L. Møller, M. Kleinert, E.A. Richter, and T.E. Jensen, *Stretch-stimulated glucose transport in skeletal muscle is regulated by Rac1.* The Journal of physiology, 2015. **593**(3): p. 645-656.
98. Roberts, C.K., R.J. Barnard, A. Jasman, and T.W. Balon, *Acute exercise increases nitric oxide synthase activity in skeletal muscle.* American Journal of Physiology-Endocrinology And Metabolism, 1999. **277**(2): p. E390-E394.

99. Patwell, D.M., A. McArdle, J.E. Morgan, T.A. Patridge, and M.J. Jackson, *Release of reactive oxygen and nitrogen species from contracting skeletal muscle cells.* Free Radical Biology and Medicine, 2004. **37**(7): p. 1064-1072.
100. Heinonen, I., B. Saltin, J. Kemppainen, P. Nuutila, J. Knuuti, K. Kalliokoski, and Y. Hellsten, *Effect of nitric oxide synthase inhibition on the exchange of glucose and fatty acids in human skeletal muscle.* Nutrition & metabolism, 2013. **10**(1): p. 43.
101. Hong, Y.H., A.C. Betik, D. Premilovac, R.M. Dwyer, M.A. Keske, S. Rattigan, and G.K. McConell, *No effect of NOS inhibition on skeletal muscle glucose uptake during in situ hindlimb contraction in healthy and diabetic Sprague-Dawley rats.* American Journal of Physiology-Regulatory, Integrative and Comparative Physiology, 2015. **308**(10): p. R862-R871.
102. Bogardus, C., P. Thuillez, E. Ravussin, B. Vasquez, M. Narimiga, and S. Azhar, *Effect of muscle glycogen depletion on in vivo insulin action in man.* Journal of Clinical Investigation, 1983. **72**(5): p. 1605.
103. Devlin, J. and E. Horton, *Effects of prior high-intensity exercise on glucose metabolism in normal and insulin-resistant men.* Diabetes, 1985. **34**(10): p. 973-979.
104. Devlin, J.T., M. Hirshman, E.D. Horton, and E.S. Horton, *Enhanced peripheral and splanchnic insulin sensitivity in NIDDM men after single bout of exercise.* Diabetes, 1987. **36**(4): p. 434-439.
105. Betts, J.J., W.M. Sherman, M.J. Reed, and J.P. Gao, *Duration of improved muscle glucose uptake after acute exercise in obese Zucker rats.* Obesity, 1993. **1**(4): p. 295-302.
106. Funai, K., G.G. Schweitzer, N. Sharma, M. Kanzaki, and G.D. Cartee, *Increased AS160 phosphorylation, but not TBC1D1 phosphorylation, with increased postexercise insulin sensitivity in rat skeletal muscle.* American Journal of Physiology-Endocrinology and Metabolism, 2009. **297**(1): p. E242-E251.
107. Kim, J., R.S. Solis, E.B. Arias, and G.D. Cartee, *Postcontraction insulin sensitivity: relationship with contraction protocol, glycogen concentration, and 5' AMP-activated protein kinase phosphorylation.* Journal of Applied Physiology, 2004. **96**(2): p. 575-583.
108. Fisher, J.S., J. Gao, D.-H. Han, J.O. Holloszy, and L.A. Nolte, *Activation of AMP kinase enhances sensitivity of muscle glucose transport to insulin.* American Journal of Physiology-Endocrinology And Metabolism, 2002. **282**(1): p. E18-E23.
109. Wojtaszewski, J.F., B.F. Hansen, B. Kiens, J. Markuns, L. Goodyear, and E. Richter, *Insulin signaling and insulin sensitivity after exercise in human skeletal muscle.* Diabetes, 2000. **49**(3): p. 325-331.
110. Kraniou, G.N., D. Cameron-Smith, and M. Hargreaves, *Acute exercise and GLUT4 expression in human skeletal muscle: influence of exercise intensity.* Journal of applied physiology, 2006. **101**(3): p. 934-937.
111. Richter, E.A., L.P. Garetto, M.N. Goodman, and N.B. Ruderman, *Enhanced muscle glucose metabolism after exercise: modulation by local factors.* American Journal of Physiology-Endocrinology And Metabolism, 1984. **246**(6): p. E476-E482.
112. Annuzzi, G., G. Riccardi, B. Capaldo, and L. KAUSER, *Increased insulin-stimulated glucose uptake by exercised human muscles one day after prolonged physical exercise.* European journal of clinical investigation, 1991. **21**(1): p. 6-12.
113. Wang, H., E.B. Arias, M.W. Pataky, L.J. Goodyear, and G.D. Cartee, *Postexercise improvement in glucose uptake occurs concomitant with greater γ3-AMPK activation and*

AS160 phosphorylation in rat skeletal muscle. American Journal of Physiology-Endocrinology and Metabolism, 2018. **315**: p. E859-E871.
114. Gao, J., E. Gulve, and J. Holloszy, *Contraction-induced increase in muscle insulin sensitivity: requirement for a serum factor.* American Journal of Physiology-Endocrinology And Metabolism, 1994. **266**(2): p. E186-E192.
115. Cartee, G. and J. Holloszy, *Exercise increases susceptibility of muscle glucose transport to activation by various stimuli.* American Journal of Physiology-Endocrinology And Metabolism, 1990. **258**(2): p. E390-E393.
116. Wojtaszewski, J.F., B.F. Hansen, B. Kiens, and E.A. Richter, *Insulin signaling in human skeletal muscle: time course and effect of exercise.* Diabetes, 1997. **46**(11): p. 1775-1781.
117. Thong, F.S., W. Derave, B. Kiens, T.E. Graham, B. Ursø, J.F. Wojtaszewski, B.F. Hansen, and E.A. Richter, *Caffeine-induced impairment of insulin action but not insulin signaling in human skeletal muscle is reduced by exercise.* Diabetes, 2002. **51**(3): p. 583-590.
118. Hamada, T., E.B. Arias, and G.D. Cartee, *Increased submaximal insulin-stimulated glucose uptake in mouse skeletal muscle after treadmill exercise.* Journal of Applied Physiology, 2006. **101**(5): p. 1368-1376.
119. Frøsig, C., M.P. Sajan, S.J. Maarbjerg, N. Brandt, C. Roepstorff, J.F. Wojtaszewski, B. Kiens, R.V. Farese, and E.A. Richter, *Exercise improves phosphatidylinositol-3, 4, 5-trisphosphate responsiveness of atypical protein kinase C and interacts with insulin signalling to peptide elongation in human skeletal muscle.* The Journal of Physiology, 2007. **582**(3): p. 1289-1301.
120. Tanaka, S., T. Hayashi, T. Toyoda, T. Hamada, Y. Shimizu, M. Hirata, K. Ebihara, H. Masuzaki, K. Hosoda, and T. Fushiki, *High-fat diet impairs the effects of a single bout of endurance exercise on glucose transport and insulin sensitivity in rat skeletal muscle.* Metabolism, 2007. **56**(12): p. 1719-1728.
121. Pehmøller, C., N. Brandt, J.B. Birk, L.D. Høeg, K.A. Sjøberg, L.J. Goodyear, B. Kiens, E.A. Richter, and J.F. Wojtaszewski, *Exercise alleviates lipid-induced insulin resistance in human skeletal muscle–signaling interaction at the level of TBC1 domain family member 4.* Diabetes, 2012. **61**(11): p. 2743-2752.
122. Iwabe, M., E. Kawamoto, K. Koshinaka, and K. Kawanaka, *Increased postexercise insulin sensitivity is accompanied by increased AS160 phosphorylation in slow-twitch soleus muscle.* Physiological Reports, 2014. **2**(12): p. e12162.
123. Vendelbo, M.H., A.B. Møller, J.T. Treebak, L.C. Gormsen, L.J. Goodyear, J.F. Wojtaszewski, J.O.L. Jørgensen, N. Møller, and N. Jessen, *Sustained AS160 and TBC1D1 phosphorylations in human skeletal muscle 30 min after a single bout of exercise.* Journal of Applied Physiology, 2014. **117**(3): p. 289-296.
124. Wang, H., N. Sharma, E.B. Arias, and G.D. Cartee, *Insulin signaling and glucose uptake in the soleus muscle of 30-month-old rats after calorie restriction with or without acute exercise.* Journals of Gerontology Series A: Biomedical Sciences and Medical Sciences, 2015. **71**(3): p. 323-332.
125. Xiao, Y., N. Sharma, E.B. Arias, C.M. Castorena, and G.D. Cartee, *A persistent increase in insulin-stimulated glucose uptake by both fast-twitch and slow-twitch skeletal muscles after a single exercise session by old rats.* Age, 2013. **35**(3): p. 573-582.
126. Sharma, N., H. Wang, E.B. Arias, C.M. Castorena, and G.D. Cartee, *Mechanisms for independent and combined effects of calorie restriction and acute exercise on insulin-*

stimulated glucose uptake by skeletal muscle of old rats. American Journal of Physiology-Endocrinology and Metabolism, 2015. **308**(7): p. E603-E612.
127. Funai, K., G.G. Schweitzer, C.M. Castorena, M. Kanzaki, and G.D. Cartee, *In vivo exercise followed by in vitro contraction additively elevates subsequent insulin-stimulated glucose transport by rat skeletal muscle.* American Journal of Physiology-Endocrinology and Metabolism, 2010. **298**(5): p. E999-E1010.
128. Schweitzer, G.G., C.M. Castorena, T. Hamada, K. Funai, E.B. Arias, and G.D. Cartee, *The B2 receptor of bradykinin is not essential for the post-exercise increase in glucose uptake by insulin-stimulated mouse skeletal muscle.* Physiological research/Academia Scientiarum Bohemoslovaca, 2011. **60**(3): p. 511.
129. McCurdy, C.E. and G.D. Cartee, *Akt2 is essential for the full effect of calorie restriction on insulin-stimulated glucose uptake in skeletal muscle.* Diabetes, 2005. **54**(5): p. 1349-1356.
130. Cho, H., J. Mu, J.K. Kim, J.L. Thorvaldsen, Q. Chu, E.B. Crenshaw, K.H. Kaestner, M.S. Bartolomei, G.I. Shulman, and M.J. Birnbaum, *Insulin resistance and a diabetes mellitus-like syndrome in mice lacking the protein kinase Akt2 (PKBβ).* Science, 2001. **292**(5522): p. 1728-1731.
131. Cartee, G.D. and J.F. Wojtaszewski, *Role of Akt substrate of 160 kDa in insulin-stimulated and contraction-stimulated glucose transport.* Applied Physiology, Nutrition, and Metabolism, 2007. **32**(3): p. 557-566.
132. Ramm, G., M. Larance, M. Guilhaus, and D.E. James, *A role for 14-3-3 in insulin-stimulated GLUT4 translocation through its interaction with the RabGAP AS160.* Journal of Biological Chemistry, 2006. **281**(39): p. 29174-29180.
133. Arias, E.B., J. Kim, and G.D. Cartee, *Prolonged incubation in PUGNAc results in increased protein O-Linked glycosylation and insulin resistance in rat skeletal muscle.* Diabetes, 2004. **53**(4): p. 921-930.
134. Treebak, J.T., C. Frøsig, C. Pehmøller, S. Chen, S.J. Maarbjerg, N. Brandt, C. MacKintosh, J. Zierath, D. Hardie, and B. Kiens, *Potential role of TBC1D4 in enhanced post-exercise insulin action in human skeletal muscle.* Diabetologia, 2009. **52**(5): p. 891-900.
135. Kramer, H.F., C.A. Witczak, E.B. Taylor, N. Fujii, M.F. Hirshman, and L.J. Goodyear, *AS160 regulates insulin-and contraction-stimulated glucose uptake in mouse skeletal muscle.* Journal of Biological Chemistry, 2006. **281**(42): p. 31478-31485.
136. Sjøberg, K.A., C. Frøsig, R. Kjøbsted, L. Sylow, M. Kleinert, A.C. Betik, C.S. Shaw, B. Kiens, J.F. Wojtaszewski, and S. Rattigan, *Exercise increases human skeletal muscle insulin sensitivity via coordinated increases in microvascular perfusion and molecular signaling.* Diabetes, 2017. **66**(6): p. 1501-1510.
137. Taylor, E.B., D. An, H.F. Kramer, H. Yu, N.L. Fujii, K.S. Roeckl, N. Bowles, M.F. Hirshman, J. Xie, and E.P. Feener, *Discovery of TBC1D1 as an insulin-, AICAR-, and contraction-stimulated signaling nexus in mouse skeletal muscle.* Journal of Biological Chemistry, 2008. **283**(15): p. 9787-9796.
138. An, D., T. Toyoda, E.B. Taylor, H. Yu, N. Fujii, M.F. Hirshman, and L.J. Goodyear, *TBC1D1 regulates insulin-and contraction-induced glucose transport in mouse skeletal muscle.* Diabetes, 2010. **59**(6): p. 1358-1365.
139. Whitfield, J., S. Paglialunga, B.K. Smith, P.M. Miotto, G. Simnett, H.L. Robson, S.S. Jain, E.A. Herbst, E.M. Desjardins, and D.J. Dyck, *Ablating the protein TBC1D1 impairs*

contraction-induced sarcolemmal glucose transporter 4 redistribution but not insulin-mediated responses in rats. Journal of Biological Chemistry, 2017. **292**(40): p. 16653-16664.
140. Kraegen, E.W., P.W. Clark, A.B. Jenkins, E.A. Daley, D.J. Chisholm, and L.H. Storlien, *Development of muscle insulin resistance after liver insulin resistance in high-fat-fed rats.* Diabetes, 1991. **40**(11): p. 1397-403.
141. Hancock, C.R., D.-H. Han, M. Chen, S. Terada, T. Yasuda, D.C. Wright, and J.O. Holloszy, *High-fat diets cause insulin resistance despite an increase in muscle mitochondria.* Proceedings of the National Academy of Sciences, 2008. **105**(22): p. 7815-7820.
142. Oakes, N.D., G.J. Cooney, S. Camilleri, D.J. Chisholm, and E.W. Kraegen, *Mechanisms of liver and muscle insulin resistance induced by chronic high-fat feeding.* Diabetes, 1997. **46**(11): p. 1768-74.
143. Perseghin, G., S. Ghosh, K. Gerow, and G.I. Shulman, *Metabolic defects in lean nondiabetic offspring of NIDDM parents: a cross-sectional study.* Diabetes, 1997. **46**(6): p. 1001-1009.
144. Krssak, M., K.F. Petersen, A. Dresner, L. DiPietro, S. Vogel, D. Rothman, G. Shulman, and M. Roden, *Intramyocellular lipid concentrations are correlated with insulin sensitivity in humans: a 1H NMR spectroscopy study.* Diabetologia, 1999. **42**(1): p. 113-116.
145. Storlien, L.H., A.B. Jenkins, D.J. Chisholm, W.S. Pascoe, S. Khouri, and E.W. Kraegen, *Influence of dietary fat composition on development of insulin resistance in rats: relationship to muscle triglyceride and ω-3 fatty acids in muscle phospholipid.* Diabetes, 1991. **40**(2): p. 280-289.
146. Jazet, I., G. Schaart, A. Gastaldelli, E. Ferrannini, M. Hesselink, P. Schrauwen, J. Romijn, J. Maassen, H. Pijl, and D. Ouwens, *Loss of 50% of excess weight using a very low energy diet improves insulin-stimulated glucose disposal and skeletal muscle insulin signalling in obese insulin-treated type 2 diabetic patients.* Diabetologia, 2008. **51**(2): p. 309-319.
147. Lara-Castro, C., B.R. Newcomer, J. Rowell, P. Wallace, S.M. Shaughnessy, A.J. Munoz, A.M. Shiflett, D.Y. Rigsby, J.C. Lawrence, and D.E. Bohning, *Effects of short-term very low-calorie diet on intramyocellular lipid and insulin sensitivity in nondiabetic and type 2 diabetic subjects.* Metabolism, 2008. **57**(1): p. 1-8.
148. Nakagawa, Y., M. Hattori, K. Harada, R. Shirase, M. Bando, and G. Okano, *Age-related changes in intramyocellular lipid in humans by in vivo 1H-MR spectroscopy.* Gerontology, 2007. **53**(4): p. 218-223.
149. Kraegen, E.W. and G.J. Cooney, *Free fatty acids and skeletal muscle insulin resistance.* Current opinion in lipidology, 2008. **19**(3): p. 235-241.
150. Samuel, V.T. and G.I. Shulman, *Mechanisms for insulin resistance: common threads and missing links.* Cell, 2012. **148**(5): p. 852-871.
151. Coen, P.M. and B.H. Goodpaster, *Role of intramyocelluar lipids in human health.* Trends in Endocrinology & Metabolism, 2012. **23**(8): p. 391-398.
152. Goodpaster, B.H., J. He, S. Watkins, and D.E. Kelley, *Skeletal muscle lipid content and insulin resistance: evidence for a paradox in endurance-trained athletes.* The Journal of Clinical Endocrinology & Metabolism, 2001. **86**(12): p. 5755-5761.

153. Nadeau, K., L. Ehlers, L. Aguirre, J. Reusch, and B. Draznin, *Discordance between intramuscular triglyceride and insulin sensitivity in skeletal muscle of Zucker diabetic rats after treatment with fenofibrate and rosiglitazone.* Diabetes, Obesity and Metabolism, 2007. **9**(5): p. 714-723.
154. Liu, L., Y. Zhang, N. Chen, X. Shi, B. Tsang, and Y.-H. Yu, *Upregulation of myocellular DGAT1 augments triglyceride synthesis in skeletal muscle and protects against fat-induced insulin resistance.* Journal of Clinical Investigation, 2007. **117**(6): p. 1679.
155. Turinsky, J., D.M. O'Sullivan, and B.P. Bayly, *1, 2-Diacylglycerol and ceramide levels in insulin-resistant tissues of the rat in vivo.* Journal of Biological Chemistry, 1990. **265**(28): p. 16880-16885.
156. Samuel, V.T., K.F. Petersen, and G.I. Shulman, *Lipid-induced insulin resistance: unravelling the mechanism.* The Lancet, 2010. **375**(9733): p. 2267-2277.
157. Yu, C., Y. Chen, G.W. Cline, D. Zhang, H. Zong, Y. Wang, R. Bergeron, J.K. Kim, S.W. Cushman, and G.J. Cooney, *Mechanism by which fatty acids inhibit insulin activation of insulin receptor substrate-1 (IRS-1)-associated phosphatidylinositol 3-kinase activity in muscle.* Journal of Biological Chemistry, 2002. **277**(52): p. 50230-50236.
158. Kim, J.K., J.J. Fillmore, M.J. Sunshine, B. Albrecht, T. Higashimori, D.-W. Kim, Z.-X. Liu, T.J. Soos, G.W. Cline, and W.R. O'Brien, *PKC-θ knockout mice are protected from fat-induced insulin resistance.* Journal of Clinical Investigation, 2004. **114**(6): p. 823.
159. Holland, W.L., T.A. Knotts, J.A. Chavez, L.P. Wang, K.L. Hoehn, and S.A. Summers, *Lipid mediators of insulin resistance.* Nutrition reviews, 2007. **65**(s1).
160. Summers, S.A. and B.H. Goodpaster, *CrossTalk proposal: Intramyocellular ceramide accumulation does modulate insulin resistance.* The Journal of physiology, 2016. **594**(12): p. 3167-3170.
161. Chaurasia, B. and S.A. Summers, *Ceramides - Lipotoxic Inducers of Metabolic Disorders.* Trends Endocrinol Metab, 2015. **26**(10): p. 538-50.
162. Hajduch, E., S. Turban, X. Le Liepvre, S. Le Lay, C. Lipina, N. Dimopoulos, I. Dugail, and H.S. Hundal, *Targeting of PKCζ and PKB to caveolin-enriched microdomains represents a crucial step underpinning the disruption in PKB-directed signalling by ceramide.* Biochemical Journal, 2008. **410**(2): p. 369-379.
163. Stratford, S., K.L. Hoehn, F. Liu, and S.A. Summers, *Regulation of insulin action by ceramide dual mechanisms linking ceramide accumulation to the inhibition of Akt/protein kinase B.* Journal of Biological Chemistry, 2004. **279**(35): p. 36608-36615.
164. Chee, C., C.E. Shannon, A. Burns, A.L. Selby, D. Wilkinson, K. Smith, P.L. Greenhaff, and F.B. Stephens, *Relative contribution of intramyocellular lipid to whole-body fat oxidation is reduced with age but subsarcolemmal lipid accumulation and insulin resistance are only associated with overweight individuals.* Diabetes, 2016. **65**(4): p. 840-850.
165. Crane, J.D., M.C. Devries, A. Safdar, M.J. Hamadeh, and M.A. Tarnopolsky, *The effect of aging on human skeletal muscle mitochondrial and intramyocellular lipid ultrastructure.* Journals of Gerontology Series A: Biomedical Sciences and Medical Sciences, 2009. **65**(2): p. 119-128.
166. Li, Y., S. Lee, T. Langleite, F. Norheim, S. Pourteymour, J. Jensen, H.K. Stadheim, T.H. Storås, S. Davanger, and H.L. Gulseth, *Subsarcolemmal lipid droplet responses to a combined endurance and strength exercise intervention.* Physiological reports, 2014. **2**(11): p. e12187.

167. Nielsen, J., M. Mogensen, B.F. Vind, K. Sahlin, K. Højlund, H.D. Schrøder, and N. Ørtenblad, *Increased subsarcolemmal lipids in type 2 diabetes: effect of training on localization of lipids, mitochondria, and glycogen in sedentary human skeletal muscle.* American Journal of Physiology-Endocrinology and Metabolism, 2010. **298**(3): p. E706-E713.
168. Bergman, B., D. Hunerdosse, A. Kerege, M. Playdon, and L. Perreault, *Localisation and composition of skeletal muscle diacylglycerol predicts insulin resistance in humans.* Diabetologia, 2012. **55**(4): p. 1140-1150.
169. He, J., B.H. Goodpaster, and D.E. Kelley, *Effects of weight loss and physical activity on muscle lipid content and droplet size.* Obesity, 2004. **12**(5): p. 761-769.
170. Van Loon, L.J., R. Koopman, R. Manders, W. van der Weegen, G.P. van Kranenburg, and H.A. Keizer, *Intramyocellular lipid content in type 2 diabetes patients compared with overweight sedentary men and highly trained endurance athletes.* American Journal of Physiology-Endocrinology And Metabolism, 2004. **287**(3): p. E558-E565.
171. Malenfant, P., D. Joanisse, R. Theriault, B. Goodpaster, D. Kelley, and J. Simoneau, *Fat content in individual muscle fibers of lean and obese subjects.* International journal of obesity, 2001. **25**(9): p. 1316.
172. Nielsen, J., A.E. Christensen, B. Nellemann, and B. Christensen, *Lipid droplet size and location in human skeletal muscle fibers are associated with insulin sensitivity.* American Journal of Physiology-Endocrinology and Metabolism, 2017: p. ajpendo. 00062.2017.
173. Ropelle, E.R., J.R. Pauli, P.O. Prada, C.T. De Souza, P.K. Picardi, M.C. Faria, D.E. Cintra, M.F.d.A. Fernandes, M.B. Flores, and L.A. Velloso, *Reversal of diet-induced insulin resistance with a single bout of exercise in the rat: the role of PTP1B and IRS-1 serine phosphorylation.* The Journal of Physiology, 2006. **577**(3): p. 997-1007.
174. Gao, J., W. Sherman, S. McCune, and K. Osei, *Effects of acute running exercise on whole body insulin action in obese male SHHF/Mcc-facp rats.* Journal of Applied Physiology, 1994. **77**(2): p. 534-541.
175. Sharoff, C.G., T.A. Hagobian, S.K. Malin, S.R. Chipkin, H. Yu, M.F. Hirshman, L.J. Goodyear, and B. Braun, *Combining short-term metformin treatment and one bout of exercise does not increase insulin action in insulin-resistant individuals.* American Journal of Physiology-Endocrinology and Metabolism, 2010. **298**(4): p. E815-E823.
176. Levinger, I., G. Jerums, N.K. Stepto, L. Parker, F.R. Serpiello, G.K. McConell, M. Anderson, D.L. Hare, E. Byrnes, and P.R. Ebeling, *The effect of acute exercise on undercarboxylated osteocalcin and insulin sensitivity in obese men.* Journal of Bone and Mineral Research, 2014. **29**(12): p. 2571-2576.
177. Schenk, S. and J.F. Horowitz, *Acute exercise increases triglyceride synthesis in skeletal muscle and prevents fatty acid–induced insulin resistance.* The Journal of clinical investigation, 2007. **117**(6): p. 1690-1698.
178. Björnholm, M., Y. Kawano, M. Lehtihet, and J.R. Zierath, *Insulin receptor substrate-1 phosphorylation and phosphatidylinositol 3-kinase activity in skeletal muscle from NIDDM subjects after in vivo insulin stimulation.* Diabetes, 1997. **46**(3): p. 524-527.
179. Zierath, J.R., K.L. Houseknecht, L. Gnudi, and B.B. Kahn, *High-fat feeding impairs insulin-stimulated GLUT4 recruitment via an early insulin-signaling defect.* Diabetes, 1997. **46**(2): p. 215-223.
180. Pauli, J.R., E.R. Ropelle, D.E. Cintra, M.A. Carvalho-Filho, J.C. Moraes, C.T. De Souza, L.A. Velloso, J.B. Carvalheira, and M.J. Saad, *Acute physical exercise reverses*

S-nitrosation of the insulin receptor, insulin receptor substrate 1 and protein kinase B/Akt in diet-induced obese Wistar rats. The Journal of physiology, 2008. **586**(2): p. 659-671.
181. Pandorf, C.E., T. Garland, W. Aoi, C. Handschin, L. Gorza, P.M. Garcia-Roves, S.W. Copp, C.M. Tipton, V.J. Caiozzo, and F. Haddad, *A Rationale for SDS-PAGE of MHC Isoforms as a Gold Standard for Determining Contractile Phenotype.* Journal of Applied Physiology, 2010. **108**(1): p. 222-225.
182. Pette, D. and R.S. Staron, *Cellular and molecular diversities of mammalian skeletal muscle fibers.* Rev Physiol Biochem Pharmacol, 1990. **116**: p. 1-76.
183. Pette, D. and R.S. Staron, *Myosin isoforms, muscle fiber types, and transitions.* Microsc Res Tech, 2000. **50**(6): p. 500-9.
184. He, J., S. Watkins, and D.E. Kelley, *Skeletal muscle lipid content and oxidative enzyme activity in relation to muscle fiber type in type 2 diabetes and obesity.* Diabetes, 2001. **50**(4): p. 817-823.
185. Delp, M.D. and C. Duan, *Composition and size of type I, IIA, IID/X, and IIB fibers and citrate synthase activity of rat muscle.* Journal of applied physiology, 1996. **80**(1): p. 261-270.
186. Castorena, C.M., J.G. Mackrell, J.S. Bogan, M. Kanzaki, and G.D. Cartee, *Clustering of GLUT4, TUG, and RUVBL2 protein levels correlate with myosin heavy chain isoform pattern in skeletal muscles, but AS160 and TBC1D1 levels do not.* J Appl Physiol (1985), 2011. **111**(4): p. 1106-17.
187. James, D.E., E.W. Kraegen, and D.J. Chisholm, *Muscle glucose metabolism in exercising rats: comparison with insulin stimulation.* American Journal of Physiology-Endocrinology And Metabolism, 1985. **248**(5): p. E575-E580.
188. Brozinick, J., G. Etgen, B. Yaspelkis, and J. Ivy, *Contraction-activated glucose uptake is normal in insulin-resistant muscle of the obese Zucker rat.* Journal of Applied Physiology, 1992. **73**(1): p. 382-387.
189. Derave, W., S. Lund, G.D. Holman, J. Wojtaszewski, O. Pedersen, and E.A. Richter, *Contraction-stimulated muscle glucose transport and GLUT-4 surface content are dependent on glycogen content.* American Journal of Physiology-Endocrinology And Metabolism, 1999. **277**(6): p. E1103-E1110.
190. Han, X., T. Ploug, and H. Galbo, *Effect of diet on insulin-and contraction-mediated glucose transport and uptake in rat muscle.* American Journal of Physiology-Regulatory, Integrative and Comparative Physiology, 1995. **269**(3): p. R544-R551.
191. Johannsson, E., J. Jensen, K. Gundersen, H. Dahl, and A. Bonen, *Effect of electrical stimulation patterns on glucose transport in rat muscles.* American Journal of Physiology-Regulatory, Integrative and Comparative Physiology, 1996. **271**(2): p. R426-R431.
192. Ploug, T., H. Galbo, and E.A. Richter, *Increased muscle glucose uptake during contractions: no need for insulin.* Am J Physiol, 1984. **247**(6 Pt 1): p. E726-31.
193. Rattigan, S., K. Dora, A. Tong, and M.G. Clark, *Perfused skeletal muscle contraction and metabolism improved by angiotensin II-mediated vasoconstriction.* American Journal of Physiology-Endocrinology And Metabolism, 1996. **271**(1): p. E96-E103.
194. Wojtaszewski, J.F., J. Lynge, A.B. Jakobsen, L.J. Goodyear, and E.A. Richter, *Differential regulation of MAP kinase by contraction and insulin in skeletal muscle:*

metabolic implications. American Journal of Physiology-Endocrinology And Metabolism, 1999. **277**(4): p. E724-E732.
195. Henriksen, E.J., R.E. Bourey, K.J. Rodnick, L. Koranyi, M.A. Permutt, and J.O. Holloszy, *Glucose transporter protein content and glucose transport capacity in rat skeletal muscles.* Am J Physiol, 1990. **259**(4 Pt 1): p. E593-8.
196. Ai, H., J. Ihlemann, Y. Hellsten, H.P. Lauritzen, D.G. Hardie, H. Galbo, and T. Ploug, *Effect of fiber type and nutritional state on AICAR-and contraction-stimulated glucose transport in rat muscle.* American Journal of Physiology-Endocrinology and Metabolism, 2002. **282**(6): p. E1291-E1300.
197. Garetto, L.P., E.A. Richter, M.N. Goodman, and N.B. Ruderman, *Enhanced muscle glucose metabolism after exercise in the rat: the two phases.* American Journal of Physiology-Endocrinology And Metabolism, 1984. **246**(6): p. E471-E475.
198. Richter, E.A., T. Ploug, and H. Galbo, *Increased muscle glucose uptake after exercise: no need for insulin during exercise.* Diabetes, 1985. **34**(10): p. 1041-1048.
199. Simoneau, J.-A., G. Lortie, M. Boulay, M. Marcotte, M.-C. Thibault, and C. Bouchard, *Human skeletal muscle fiber type alteration with high-intensity intermittent training.* European journal of applied physiology and occupational physiology, 1985. **54**(3): p. 250-253.
200. Lillioja, S., A.A. Young, C.L. Culter, J.L. Ivy, W. Abbott, J.K. Zawadzki, H. Yki-Järvinen, L. Christin, T.W. Secomb, and C. Bogardus, *Skeletal muscle capillary density and fiber type are possible determinants of in vivo insulin resistance in man.* Journal of Clinical Investigation, 1987. **80**(2): p. 415.
201. Stuart, C.A., M.P. McCurry, A. Marino, M.A. South, M.E. Howell, A.S. Layne, M.W. Ramsey, and M.H. Stone, *Slow-twitch fiber proportion in skeletal muscle correlates with insulin responsiveness.* J Clin Endocrinol Metab, 2013. **98**(5): p. 2027-36.
202. Gaster, M., P. Staehr, H. Beck-Nielsen, H.D. Schroder, and A. Handberg, *GLUT4 is reduced in slow muscle fibers of type 2 diabetic patients: is insulin resistance in type 2 diabetes a slow, type 1 fiber disease?* Diabetes, 2001. **50**(6): p. 1324-9.
203. Nilwik, R., T. Snijders, M. Leenders, B.B. Groen, J. van Kranenburg, L.B. Verdijk, and L.J. van Loon, *The decline in skeletal muscle mass with aging is mainly attributed to a reduction in type II muscle fiber size.* Experimental gerontology, 2013. **48**(5): p. 492-498.
204. Korhonen, M.T., A. Cristea, M. Alén, K. Häkkinen, S. Sipilä, A. Mero, J.T. Viitasalo, L. Larsson, and H. Suominen, *Aging, muscle fiber type, and contractile function in sprint-trained athletes.* Journal of Applied Physiology, 2006. **101**(3): p. 906-917.
205. Mackrell, J.G. and G.D. Cartee, *A novel method to measure glucose uptake and myosin heavy chain isoform expression of single fibers from rat skeletal muscle.* Diabetes, 2012. **61**(5): p. 995-1003.
206. Mackrell, J.G., E.B. Arias, and G.D. Cartee, *Fiber type-specific differences in glucose uptake by single fibers from skeletal muscles of 9- and 25-month-old rats.* J Gerontol A Biol Sci Med Sci, 2012. **67**(12): p. 1286-94.
207. Cartee, G.D., E.B. Arias, S.Y. Carmen, and M.W. Pataky, *Novel single skeletal muscle fiber analysis reveals a fiber type-selective effect of acute exercise on glucose uptake.* American Journal of Physiology-Endocrinology and Metabolism, 2016. **311**(5): p. E818-E824.
208. Wang, H., E.B. Arias, C.S. Yu, A.R. Verkerke, and G.D. Cartee, *Effects of Calorie Restriction and Fiber Type on Glucose Uptake and Abundance of Electron Transport*

Chain and Oxidative Phosphorylation Proteins in Single Fibers from Old RatsCalorie restriction effects on single fiber glucose uptake. The Journals of Gerontology: Series A, 2017.
209. Schiaffino, S. and C. Reggiani, *Fiber types in mammalian skeletal muscles.* Physiological reviews, 2011. **91**(4): p. 1447-1531.
210. Simoneau, J.A. and C. Bouchard, *Human variation in skeletal muscle fiber-type proportion and enzyme activities.* Am J Physiol, 1989. **257**(4 Pt 1): p. E567-72.
211. Albers, P.H., A.J. Pedersen, J.B. Birk, D.E. Kristensen, B.F. Vind, O. Baba, J. Nøhr, K. Højlund, and J.F. Wojtaszewski, *Human Muscle Fiber Type–Specific Insulin Signaling: Impact of Obesity and Type 2 Diabetes.* Diabetes, 2015. **64**(2): p. 485-497.
212. Kristensen, D.E., P.H. Albers, C. Prats, O. Baba, J.B. Birk, and J.F. Wojtaszewski, *Human muscle fibre type-specific regulation of AMPK and downstream targets by exercise.* The Journal of Physiology, 2015. **593**(8): p. 2053-2069.
213. Wang, H., E.B. Arias, K. Oki, M.W. Pataky, J.A. Almallouhi, and G.D. Cartee, *Fiber Type-selective Exercise Effects on AS160 Phosphorylation.* American Journal of Physiology-Endocrinology and Metabolism, 2019. **316**: p. E837-E851.
214. Storlien, L., D. James, K. Burleigh, D. Chisholm, and E. Kraegen, *Fat feeding causes widespread in vivo insulin resistance, decreased energy expenditure, and obesity in rats.* American Journal of Physiology-Endocrinology And Metabolism, 1986. **251**(5): p. E576-E583.
215. Wang, J., S. Obici, K. Morgan, N. Barzilai, Z. Feng, and L. Rossetti, *Overfeeding rapidly induces leptin and insulin resistance.* Diabetes, 2001. **50**(12): p. 2786-2791.
216. Ochiai, M. and T. Matsuo, *Effects of short-term dietary change from high-carbohydrate diet to high-fat diet on storage, utilization, and fatty acid composition of rat muscle triglyceride during swimming exercise.* Journal of clinical biochemistry and nutrition, 2009. **44**(2): p. 168-177.
217. Wilson, C.R., M.K. Tran, K.L. Salazar, M.E. Young, and H. Taegtmeyer, *Western diet, but not high fat diet, causes derangements of fatty acid metabolism and contractile dysfunction in the heart of Wistar rats.* Biochemical Journal, 2007. **406**(3): p. 457-467.
218. Buettner, R., J. Schölmerich, and L.C. Bollheimer, *High-fat diets: modeling the metabolic disorders of human obesity in rodents.* Obesity, 2007. **15**(4): p. 798-808.
219. Song, S., S. Andrikopoulos, C. Filippis, A.W. Thorburn, D. Khan, and J. Proietto, *Mechanism of fat-induced hepatic gluconeogenesis: effect of metformin.* American Journal of Physiology-Endocrinology And Metabolism, 2001. **281**(2): p. E275-E282.
220. Chisholm, K.W. and K. O'Dea, *Effect of short-term consumption of a high fat diet on glucose tolerance and insulin sensitivity in the rat.* Journal of nutritional science and vitaminology, 1987. **33**(5): p. 377-390.
221. Turner, N., G.M. Kowalski, S.J. Leslie, S. Risis, C. Yang, R.S. Lee-Young, J.R. Babb, P.J. Meikle, G.I. Lancaster, D.C. Henstridge, P.J. White, E.W. Kraegen, A. Marette, G.J. Cooney, M.A. Febbraio, and C.R. Bruce, *Distinct patterns of tissue-specific lipid accumulation during the induction of insulin resistance in mice by high-fat feeding.* Diabetologia, 2013. **56**(7): p. 1638-48.
222. Ding, S.-y., Z.-f. Shen, Y.-t. Chen, S.-j. Sun, Q. Liu, and M.-z. Xie, *Pioglitazone can ameliorate insulin resistance in low-dose streptozotocin and high sucrose-fat diet induced obese rats.* Acta Pharmacologica Sinica, 2005. **26**(5): p. 575-580.

223. Severino, C., P. Brizzi, A. Solinas, G. Secchi, M. Maioli, and G. Tonolo, *Low-dose dexamethasone in the rat: a model to study insulin resistance.* American Journal of Physiology-Endocrinology and Metabolism, 2002. **283**(2): p. E367-E373.
224. Petit, F., G.J. Bagby, and C.H. Lang, *Tumor necrosis factor mediates zymosan-induced increase in glucose flux and insulin resistance.* American Journal of Physiology-Endocrinology and Metabolism, 1995. **268**(2): p. E219-E228.
225. Hirose, M., M. Kaneki, H. Sugita, S. Yasuhara, and J.J. Martyn, *Immobilization depresses insulin signaling in skeletal muscle.* American Journal of Physiology-Endocrinology And Metabolism, 2000. **279**(6): p. E1235-E1241.
226. Oana, F., H. Takeda, K. Hayakawa, A. Matsuzawa, S. Akahane, M. Isaji, and M. Akahane, *Physiological difference between obese (fa/fa) Zucker rats and lean Zucker rats concerning adiponectin.* Metabolism, 2005. **54**(8): p. 995-1001.
227. Galli, J., L.-S. Li, A. Glaser, C.-G. Östenson, H. Jiao, H. Fakhrai-Rad, H.J. Jacob, E.S. Lander, and H. Luthman, *Genetic analysis of non-insulin dependent diabetes mellitus in the GK rat.* Nature genetics, 1996. **12**(1): p. 31-37.
228. Ishida, K., A. Mizuno, Z. Min, T. Sano, and K. Shima, *Which is the primary etiologic event in Otsuka Long-Evans Tokushima Fatty rats, a model of spontaneous non—insulin-dependent diabetes mellitus, insulin resistance, or impaired insulin secretion?* Metabolism, 1995. **44**(7): p. 940-945.
229. Veroni, M.C., J. Proietto, and R.G. Larkins, *Evolution of insulin resistance in New Zealand obese mice.* Diabetes, 1991. **40**(11): p. 1480-1487.
230. Gulve, E.A., G.D. Cartee, J.R. Zierath, V. Corpus, and J. Holloszy, *Reversal of enhanced muscle glucose transport after exercise: roles of insulin and glucose.* American Journal of Physiology-Endocrinology And Metabolism, 1990. **259**(5): p. E685-E691.
231. Nolte, L., E. Gulve, and J. Holloszy, *Epinephrine-induced in vivo muscle glycogen depletion enhances insulin sensitivity of glucose transport.* Journal of Applied Physiology, 1994. **76**(5): p. 2054-2058.
232. Castorena, C.M., E.B. Arias, N. Sharma, J.S. Bogan, and G.D. Cartee, *Fiber type effects on contraction-stimulated glucose uptake and GLUT4 abundance in single fibers from rat skeletal muscle.* American Journal of Physiology-Endocrinology and Metabolism, 2015. **308**(3): p. E223-E230.
233. Brown, D.A., M.S. Johnson, C.J. Armstrong, J.M. Lynch, N.M. Caruso, L.B. Ehlers, M. Fleshner, R.L. Spencer, and R.L. Moore, *Short-term treadmill running in the rat: what kind of stressor is it?* Journal of applied physiology, 2007. **103**(6): p. 1979-1985.
234. Iversen, I.H., *Techniques for establishing schedules with wheel running as reinforcement in rats.* Journal of the experimental analysis of behavior, 1993. **60**(1): p. 219-238.
235. Dumke, C., J. Kim, E. Arias, and G. Cartee, *Role of kallikrein-kininogen system in insulin-stimulated glucose transport after muscle contractions.* Journal of Applied Physiology, 2002. **92**(2): p. 657-664.
236. Liao, B. and Y. Xu, *Exercise improves skeletal muscle insulin resistance without reduced basal mTOR/S6K1 signaling in rats fed a high-fat diet.* European journal of applied physiology, 2011. **111**(11): p. 2743-2752.
237. de Wilde, J., R. Mohren, S. van den Berg, M. Boekschoten, K. Willems-Van Dijk, P. De Groot, M. Müller, E. Mariman, and E. Smit, *Short-term high fat-feeding results in morphological and metabolic adaptations in the skeletal muscle of C57BL/6J mice.* Physiological genomics, 2008. **32**(3): p. 360-369.

238. Moreno, M., E. Silvestri, R. De Matteis, P. de Lange, A. Lombardi, D. Glinni, R. Senese, F. Cioffi, A.M. Salzano, and A. Scaloni, *3, 5-Diiodo-L-thyronine prevents high-fat-diet-induced insulin resistance in rat skeletal muscle through metabolic and structural adaptations.* The FASEB Journal, 2011. **25**(10): p. 3312-3324.
239. Mrad, J.A., F. Yakubu, D. Lin, J.C. Peters, J. Atkinson, and J. Hill, *Skeletal muscle composition in dietary obesity-susceptible and dietary obesity-resistant rats.* American Journal of Physiology-Regulatory, Integrative and Comparative Physiology, 1992. **262**(4): p. R684-R688.
240. Arias, E.B., H. Wang, and G.D. Cartee, *Akt substrate of 160 kDa dephosphorylation rate is reduced in insulin-stimulated rat skeletal muscle after acute exercise.* Physiological research, 2018. **67**(1): p. 143-147.
241. Kjøbsted, R., A.J. Pedersen, J.R. Hingst, R. Sabaratnam, J.B. Birk, J.M. Kristensen, K. Højlund, and J.F. Wojtaszewski, *Intact regulation of the AMPK signaling network in response to exercise and insulin in skeletal muscle of male patients with type 2 diabetes: illumination of AMPK activation in recovery from exercise.* Diabetes, 2016. **65**(5): p. 1219-1230.
242. Treebak, J.T., C. Pehmøller, J.M. Kristensen, R. Kjøbsted, J.B. Birk, P. Schjerling, E.A. Richter, L.J. Goodyear, and J.F. Wojtaszewski, *Acute exercise and physiological insulin induce distinct phosphorylation signatures on TBC1D1 and TBC1D4 proteins in human skeletal muscle.* The Journal of Physiology, 2014. **592**(2): p. 351-375.
243. Murphy, R.M., *Enhanced technique to measure proteins in single segments of human skeletal muscle fibers: fiber-type dependence of AMPK-α 1 and-β 1.* Journal of Applied Physiology, 2011. **110**(3): p. 820-825.
244. Cartee, G.D., D.A. Young, M.D. Sleeper, J. Zierath, H. Wallberg-Henriksson, and J. Holloszy, *Prolonged increase in insulin-stimulated glucose transport in muscle after exercise.* American Journal of Physiology-Endocrinology And Metabolism, 1989. **256**(4): p. E494-E499.
245. Asp, S., J.R. Daugaard, S. Kristiansen, B. Kiens, and E. Richter, *Eccentric exercise decreases maximal insulin action in humans: muscle and systemic effects.* The Journal of physiology, 1996. **494**(3): p. 891-898.
246. Asp, S. and E.A. Richter, *Decreased insulin action on muscle glucose transport after eccentric contractions in rats.* Journal of Applied Physiology, 1996. **81**(5): p. 1924-1928.
247. Perseghin, G., T.B. Price, K.F. Petersen, M. Roden, G.W. Cline, K. Gerow, D.L. Rothman, and G.I. Shulman, *Increased glucose transport–phosphorylation and muscle glycogen synthesis after exercise training in insulin-resistant subjects.* New England Journal of Medicine, 1996. **335**(18): p. 1357-1362.
248. Sylow, L., L.L. Møller, G. D'hulst, P. Schjerling, T.E. Jensen, and E.A. Richter, *Rac1 in muscle is dispensable for improved insulin action after exercise in mice.* Endocrinology, 2016. **157**(8): p. 3009-3015.
249. Grundleger, M.L. and S.W. Thenen, *Decreased insulin binding, glucose transport, and glucose metabolism in soleus muscle of rats fed a high fat diet.* Diabetes, 1982. **31**(3): p. 232-237.
250. Storlien, L.H., D.E. James, K.M. Burleigh, D.J. Chisholm, and E.W. Kraegen, *Fat feeding causes widespread in vivo insulin resistance, decreased energy expenditure, and obesity in rats.* Am J Physiol, 1986. **251**(5 Pt 1): p. E576-83.

251. Kraegen, E., D. James, L. Storlien, K. Burleigh, and D. Chisholm, *In vivo insulin resistance in individual peripheral tissues of the high fat fed rat: assessment by euglycaemic clamp plus deoxyglucose administration.* Diabetologia, 1986. **29**(3): p. 192-198.
252. Han, D.-H., P.A. Hansen, H.H. Host, and J.O. Holloszy, *Insulin resistance of muscle glucose transport in rats fed a high-fat diet: a reevaluation.* Diabetes, 1997. **46**(11): p. 1761-1767.
253. Wilkes, J.J., A. Bonen, and R.C. Bell, *A modified high-fat diet induces insulin resistance in rat skeletal muscle but not adipocytes.* American Journal of Physiology-Endocrinology And Metabolism, 1998. **275**(4): p. E679-E686.
254. Kim, J.-Y., L.A. Nolte, P.A. Hansen, D.-H. Han, K. Ferguson, P.A. Thompson, and J.O. Holloszy, *High-fat diet-induced muscle insulin resistance: relationship to visceral fat mass.* American Journal of Physiology-Regulatory, Integrative and Comparative Physiology, 2000. **279**(6): p. R2057-R2065.
255. Tremblay, F., C. Lavigne, H. Jacques, and A. Marette, *Defective insulin-induced GLUT4 translocation in skeletal muscle of high fat–fed rats is associated with alterations in both Akt/protein kinase B and atypical protein kinase C (ζ/λ) activities.* Diabetes, 2001. **50**(8): p. 1901-1910.
256. White, A.T., S.A. LaBarge, C.E. McCurdy, and S. Schenk, *Knockout of STAT3 in skeletal muscle does not prevent high-fat diet-induced insulin resistance.* Molecular metabolism, 2015. **4**(8): p. 569-575.
257. Bottinelli, R., S. Schiaffino, and C. Reggiani, *Force-velocity relations and myosin heavy chain isoform compositions of skinned fibres from rat skeletal muscle.* The Journal of Physiology, 1991. **437**(1): p. 655-672.
258. Larsson, L. and R. Moss, *Maximum velocity of shortening in relation to myosin isoform composition in single fibres from human skeletal muscles.* The Journal of physiology, 1993. **472**(1): p. 595-614.
259. Harridge, S., R. Bottinelli, M. Canepari, M. Pellegrino, C. Reggiani, M. Esbjörnsson, and B. Saltin, *Whole-muscle and single-fibre contractile properties and myosin heavy chain isoforms in humans.* Pflügers Archiv, 1996. **432**(5): p. 913-920.
260. Widrick, J.J., S.W. Trappe, D.L. Costill, and R.H. Fitts, *Force-velocity and force-power properties of single muscle fibers from elite master runners and sedentary men.* American Journal of Physiology-Cell Physiology, 1996. **271**(2): p. C676-C683.
261. Bottinelli, R., M. Canepari, M. Pellegrino, and C. Reggiani, *Force-velocity properties of human skeletal muscle fibres: myosin heavy chain isoform and temperature dependence.* The Journal of physiology, 1996. **495**(2): p. 573-586.
262. Galler, S., T.L. Schmitt, and D. Pette, *Stretch activation, unloaded shortening velocity, and myosin heavy chain isoforms of rat skeletal muscle fibres.* The Journal of physiology, 1994. **478**(3): p. 513-521.
263. Galler, S., K. Hilber, and D. Pette, *Force responses following stepwise length changes of rat skeletal muscle fibre types.* The Journal of physiology, 1996. **493**(1): p. 219-227.
264. Hilber, K., S. Galler, B. Gohlsch, and D. Pette, *Kinetic properties of myosin heavy chain isoforms in single fibers from human skeletal muscle.* FEBS letters, 1999. **455**(3): p. 267-270.

265. Conjard, A., H. Peuker, and D. Pette, *Energy state and myosin heavy chain isoforms in single fibres of normal and transforming rabbit muscles.* Pflügers Archiv, 1998. **436**(6): p. 962-969.
266. Gorza, L., K. Gundersen, T. Lømo, S. Schiaffino, and R. Westgaard, *Slow-to-fast transformation of denervated soleus muscles by chronic high-frequency stimulation in the rat.* The Journal of physiology, 1988. **402**(1): p. 627-649.
267. Hämäläinen, N. and D. Pette, *Slow-to-fast transitions in myosin expression of rat soleus muscle by phasic high-frequency stimulation.* FEBS letters, 1996. **399**(3): p. 220-222.
268. Bloemberg, D. and J. Quadrilatero, *Rapid determination of myosin heavy chain expression in rat, mouse, and human skeletal muscle using multicolor immunofluorescence analysis.* PloS one, 2012. **7**(4): p. e35273.
269. Howald, H., H. Hoppeler, H. Claassen, O. Mathieu, and R. Straub, *Influences of endurance training on the ultrastructural composition of the different muscle fiber types in humans.* Pflügers Archiv, 1985. **403**(4): p. 369-376.
270. Gerrits, M.F., S. Ghosh, N. Kavaslar, B. Hill, A. Tour, E.L. Seifert, B. Beauchamp, S. Gorman, J. Stuart, and R. Dent, *Distinct skeletal muscle fiber characteristics and gene expression in diet-sensitive versus diet-resistant obesity.* Journal of lipid research, 2010. **51**(8): p. 2394-2404.
271. Gouspillou, G., N. Sgarioto, B. Norris, S. Barbat-Artigas, M. Aubertin-Leheudre, J.A. Morais, Y. Burelle, T. Taivassalo, and R.T. Hepple, *The relationship between muscle fiber type-specific PGC-1α content and mitochondrial content varies between rodent models and humans.* PloS one, 2014. **9**(8): p. e103044.
272. Ingjer, F., *Capillary supply and mitochondrial content of different skeletal muscle fiber types in untrained and endurance-trained men. A histochemical and ultrastructural study.* European Journal of Applied Physiology and Occupational Physiology, 1979. **40**(3): p. 197-209.
273. Waters, R.E., S. Rotevatn, P. Li, B.H. Annex, and Z. Yan, *Voluntary running induces fiber type-specific angiogenesis in mouse skeletal muscle.* American Journal of Physiology-Cell Physiology, 2004. **287**(5): p. C1342-C1348.
274. Hallauer, P.L. and K.E. Hastings, *Coregulation of fast contractile protein transgene and glycolytic enzyme expression in mouse skeletal muscle.* American Journal of Physiology-Cell Physiology, 2002. **282**(1): p. C113-C124.
275. Shepherd, S.O., M. Cocks, K. Tipton, A.M. Ranasinghe, T.A. Barker, J.G. Burniston, A.J. Wagenmakers, and C.S. Shaw, *Preferential utilization of perilipin 2-associated intramuscular triglycerides during 1 h of moderate-intensity endurance-type exercise.* Experimental physiology, 2012. **97**(8): p. 970-980.
276. Kawada, S. and N. Ishii, *Changes in skeletal muscle size, fibre-type composition and capillary supply after chronic venous occlusion in rats.* Acta physiologica, 2008. **192**(4): p. 541-549.
277. Vøllestad, M.K., O. Vaage, and L. Hermansen, *Muscle glycogen depletion patterns in type I and subgroups of type II fibres during prolonged severe exercise in man.* Acta Physiologica, 1984. **122**(4): p. 433-441.
278. Greenhaff, P., K. Söderlund, J.-M. Ren, and E. Hultman, *Energy metabolism in single human muscle fibres during intermittent contraction with occluded circulation.* The Journal of Physiology, 1993. **460**(1): p. 443-453.

279. De Bock, K., W. Derave, M. Ramaekers, E.A. Richter, and P. Hespel, *Fiber type-specific muscle glycogen sparing due to carbohydrate intake before and during exercise.* Journal of Applied Physiology, 2007. **102**(1): p. 183-188.
280. Prats, C., A. Gomez-Cabello, P. Nordby, J.L. Andersen, J.W. Helge, F. Dela, O. Baba, and T. Ploug, *An optimized histochemical method to assess skeletal muscle glycogen and lipid stores reveals two metabolically distinct populations of type I muscle fibers.* PLoS One, 2013. **8**(10): p. e77774.
281. Daugaard, J.R., J.N. Nielsen, S. Kristiansen, J.L. Andersen, M. Hargreaves, and E.A. Richter, *Fiber type-specific expression of GLUT4 in human skeletal muscle: influence of exercise training.* Diabetes, 2000. **49**(7): p. 1092-1095.
282. Lee-Young, R.S., B.J. Canny, D.E. Myers, and G.K. McConell, *AMPK activation is fiber type specific in human skeletal muscle: effects of exercise and short-term exercise training.* Journal of applied physiology, 2009. **107**(1): p. 283-289.
283. Lushaj, E.B., J.K. Johnson, D. McKenzie, and J.M. Aiken, *Sarcopenia accelerates at advanced ages in Fisher 344× Brown Norway rats.* The Journals of Gerontology Series A: Biological Sciences and Medical Sciences, 2008. **63**(9): p. 921-927.
284. Kramer, I.F., T. Snijders, J.S. Smeets, M. Leenders, J. van Kranenburg, M. den Hoed, L.B. Verdijk, M. Poeze, and L.J. van Loon, *Extensive Type II muscle fiber atrophy in elderly female hip fracture patients.* Journals of Gerontology Series A: Biomedical Sciences and Medical Sciences, 2017. **72**(10): p. 1369-1375.

CHAPTER III

Study 1

High-Fat Diet-Induced Insulin Resistance in Single Skeletal Muscle Fibers is Fiber Type Selective

ABSTRACT

Skeletal muscle is the major site for insulin-stimulated glucose disposal, and muscle insulin resistance confers many negative health outcomes. Muscle is composed of multiple fiber types, and conventional analysis of whole muscles cannot elucidate fiber type differences at the cellular level. Previous research demonstrated that a brief (two weeks) high fat diet (HFD) caused insulin resistance in rat skeletal muscle. The primary aim of this study was to determine in rat skeletal muscle the influence of a brief (two weeks) HFD on glucose uptake (GU) ± insulin in single fibers that were also characterized for fiber type. Epitrochlearis muscles were incubated with [^{3}H]-2-deoxyglucose (2DG) ±100µU/ml insulin. Fiber type (myosin heavy chain expression) and 2DG accumulation were measured in whole muscles and single fibers. Although fiber type composition of whole muscles did not differ between diet groups, GU of insulin-stimulated whole muscles from LFD rats significantly exceeded HFD values ($P<0.005$). For HFD versus LFD rats, GU of insulin-stimulated single fibers was significantly ($P<0.05$) lower for IIA, IIAX, IIBX, IIB, and approached significance for IIX ($P=0.100$), but not type I ($P=0.776$) fibers. These results revealed HFD-induced insulin resistance was attributable to fiber type selective insulin resistance and independent of altered fiber type composition.

INTRODUCTION

Skeletal muscle is the major site for insulin-stimulated glucose disposal [1], and skeletal muscle insulin resistance is a primary and essential event in the progression to type 2 diabetes [2]. Even in the absence of type 2 diabetes, insulin resistance confers negative health outcomes

[3]. It is important to understand the processes responsible for insulin resistance of skeletal muscle to develop interventions that effectively combat this health-related functional deficit.

Insulin resistance, concomitant with substantial weight gain and obesity, can be induced by feeding rodents a high fat diet (HFD) for a period of many weeks to months [4-7]. However, insulin resistance is detectable in rodents after only one to three weeks of a HFD, prior to major increases in body mass or body fat [8, 9]. To gain insights about this rapid HFD-induced insulin resistance in skeletal muscle, we studied rats eating a two week HFD protocol that was previously reported to produce skeletal muscle insulin resistance [9].

Fully understanding insulin resistance in skeletal muscle at the cellular level is challenging because this tissue includes multiple muscle fiber types that vary greatly in their metabolic properties [10]. The gold standard for muscle fiber type classification is based on myosin heavy chain (MHC) isoform expression, and type I, IIA, IIX, and IIB are the major MHC isoforms expressed in adult rat skeletal muscle [11]. The usual approach for assessing fiber type differences involves using muscle tissue (either whole muscles or muscle regions) that is enriched with a particular fiber type. Relatively few studies have considered a possible relationship between muscle fiber type and HFD-induced insulin resistance. The results of some, but not all of these earlier studies suggest that HFD effects on insulin-stimulated glucose uptake can differ between muscles with different fiber type composition [12-16].

There are significant caveats in delineating fiber type differences based on conventional whole muscle analysis, including that: 1) no muscle is entirely composed of a single fiber type, 2) to our knowledge no rat muscle is primarily composed to type IIX fibers, 3) it is impossible to adequately evaluate fibers that express multiple MHC isoforms (known as hybrid fibers) using conventional whole muscle analysis, and 4) in addition to myocytes, muscle tissue contains many cell types, including vascular, adipose and neural cells. Because of these limitations, our laboratory has developed and validated a unique method for measuring both fiber type by MHC and glucose uptake in a single muscle fiber [17]. This approach has enabled the elucidation of fiber type-specific glucose uptake responses to various physiological conditions such as acute exercise, aging, and obesity [17-19].

This study's primary aim was to determine in rat skeletal muscle the influence of a short-term (2 weeks) HFD on glucose uptake ± insulin in single fibers that were also characterized for fiber type (types I, IIA, IIB, IIX, IIAX and IIBX). In addition, because some studies that compared rodents consuming a HFD for four or more weeks with healthy controls eating a low fat diet (LFD) have identified differences between the diet groups in their muscle fiber type composition [20-23], a secondary aim was to determine in rat skeletal muscle the influence of short-term HFD on the fiber type composition as assessed by MHC isoform expression.

Insulin-stimulated glucose uptake by skeletal muscle relies on the expression of the insulin regulated GLUT4 glucose transporter protein [24, 25]. Although we previously observed whole epitrochlearis muscle GLUT4 abundance was not altered by 2-weeks of HFD [9], it seemed possible that the HFD might induce fiber type-selective changes in GLUT4 abundance. Therefore, our third aim was to assess the HFD effect on GLUT4 abundance in single fibers of differing fiber types as a potential mechanism for HFD-induced insulin resistance.

There is extensive interest in the possibility of a mitochondrial role in skeletal muscle insulin resistance [26-29]. However, prior studies have not determined the influence of HFD on both insulin-stimulated glucose uptake and the abundance of mitochondrial proteins in a fiber type selective manner at the single fiber level. Accordingly, our fourth aim was to assess in single fibers that had been characterized for fiber type the HFD effect on the abundance of six mitochondrial proteins that are functionally important in the electron transport chain and oxidative phosphorylation.

METHODS

Materials. The reagents and apparatus for SDS-PAGE and nonfat dry milk (no. 170-6404) were from Bio-Rad (Hercules, CA). [^{3}H]-2-deoxyglucose (NET328001MC) and [^{14}C] mannitol (NEC314250UC) were from PerkinElmer (Waltham, MA). Tissue Protein Extraction Reagent, T-PER (PI78510), Bicinchoninic Acid Protein Assay Kit (PI23223), MemCode Reversible Protein Stain Kit (PI24585), and SimplyBlue™ SafeStain (LC6065) were from ThermoFisher (Pittsburgh, PA). Collagenase type 2 (305 U/mg) was from Worthington Biochemical (LS004177, Lakewood, NJ).). Anti-rabbit IgG horseradish peroxidase conjugate

(#7074) and anti-COXIV (#4850) were from Cell Signaling Technology (Danvers, MA). Anti-GLUT4 (#CBL243) was from EMD Millipore (Billerica, MA). Total Oxphos Antibody Cocktail (ab110413) was from Abcam (Cambridge, United Kingdom). The total OXPHOS Antibody Cocktail includes antibodies against five mitochondrial proteins involved in the electron transport chain and oxidative phosphorylation: NADH dehydrogenase (ubiquinone) 1β subcomplex subunit 8 (NDUFB8, part of Complex I); succinate dehydrogenase complex subunit 8 (SDHB, part of Complex II); ubiquinol-cytochrome-c reductase complex core protein 2 (UQCRC2, part of Complex III), Cytochrome c oxidase subunit I (MTCO1, part of Complex IV); and mitochondrial membrane ATP synthase (ATP5A, part of Complex V). Anti-mouse IgM (#sc-2973) horseradish peroxidase was from Santa Cruz Biotechnology (Santa Cruz, CA).

Animal treatment. Procedures for animal care were approved by the University of Michigan Committee on Use and Care of Animals. All methods were performed in accordance with the guidelines from the Guide for the Care and Use of Laboratory Animals of the National Institutes of Health, USA. Male Wistar rats (6-7 weeks old; Charles River Laboratories, Boston, MA) were individually housed and provided with standard rodent chow (Laboratory Diet no. 5L0D; LabDiet, St. Louis, MO) or high-fat chow (Laboratory Diet no. D12492; ResearchDiets, New Brunswick, NJ) and water *ad libitum* for two weeks until they were fasted the night before the experiment at ~1700. Caloric intake for each rat during the two week diet period was estimated based on the difference between the food provided on day one and the food remaining at ~1700 on the night prior to the experiment. On the day of the experiment rats were anesthetized (intraperitoneal sodium pentobarbital, 50 mg/kg weight) at ~1000, weighed, and their epitrochlearis muscles were dissected. Muscles from 10 rats in each diet group were used for measuring glucose uptake and MHC abundance in whole muscles, and muscles from 10 rats in each diet group were used for measuring glucose uptake and fiber type in single fibers. After muscle dissections, the epididymal fat pads were dissected and weighed.

Ex vivo incubations of muscles for single fiber and whole muscle glucose uptake. Dissected muscles used for single fiber glucose uptake were incubated in glass vials gassed (95% O_2, 5% CO_2) in a temperature controlled bath for a four-step process (35°C during steps 1, 2 and 4; and step 3 was on ice) throughout all of the incubation steps. For step 1 (20 min) paired muscles were placed in vials containing 2 ml of media 1 (Krebs Henseleit Buffer, KHB, supplemented with 0.1% bovine serum albumin, BSA, 2 mM sodium pyruvate and 6 mM

mannitol) with or without 100 µU/ml insulin. For step 2 (30 min), muscles were transferred to a vial containing 2 ml of media 2 [KHB supplemented with 0.1% BSA, 0.1 mM 2-DG (13.5 mCi/mmol [^{3}H]-2-DG), 2 mM sodium pyruvate and 6 mM mannitol) with or without 100 µU/ml insulin. For step 3, muscles underwent three washes (5 min/wash with shaking at 115 revolutions/min) in ice-cold wash media (Ca^{2+}-free KHB supplemented with 0.1% BSA and 8 mM glucose) to clear the extracellular space of [^{3}H]-2-DG. For step 4 (60 min), muscles were incubated in vials containing collagenase media (wash media supplemented with 8 mM glucose and 2.5% type 2 collagenase) for enzymatic digestion of muscle collagen. Collagenase-treated muscles are hereafter referred to as fiber bundles.

Muscles used for whole muscle glucose uptake were incubated in glass vials gassed (95% O_2, 5% CO_2) in a temperature controlled bath for a two-step process (35°C during both steps) throughout the incubation. These muscles were treated identically to muscles used for single fiber glucose uptake for incubation step 1. For incubation step 2 (30 min) these muscles were transferred to a vial containing 2 ml of media 3 [KHB supplemented with 0.1% BSA, 0.1 mM 2-DG (2.25 mCi/mmol [^{3}H]-2-DG), 2 mM sodium pyruvate and 6 mM mannitol (2 mCi/mmol [^{14}C] mannitol)] with or without 100 µU/ml insulin. After step 2, whole muscles were blotted, freeze clamped, and stored at -80°C until further processing.

Isolation and processing of single fibers for glucose uptake and MHC isoform identification. After incubation step 4, fiber bundles were removed from collagenase media, and rinsed with wash media at room temperature. Under a dissecting microscope (EZ4D; Leica, Buffalo Grove, IL), intact single fibers (~55 fibers per muscle) were gently teased away from the fiber bundle using forceps. After isolation, each fiber was imaged using a camera-enabled microscope with Leica Application Suite EZ software. After imaging, each fiber was transferred by pipette with 20 µl of wash media to a microcentrifuge tube. 30µl of lysis buffer (T-PER supplemented with 1% Triton X-100, 1 mM Na_3VO_4, 1 mM EDTA, 1 mM EGTA, 2.5 mM sodium pyrophosphate tetrabasic decahydrate, 1 mM β-glycerophosphate, 1 µg/ml leupeptin, and 1 mM phenylmethylsulfonyl fluoride) and 50µl of 2× Laemmli buffer were added to each isolated fiber tube. Tubes were then vortexed and a portion of each lysed fiber was aliquoted into a separate tube for immunoblotting of GLUT4, MTCO1, and COXIV protein abundance, which are affected by heating. These samples were stored at -20°C until used for immunoblotting. The

remainder of the lysed fiber sample was heated to 95–100°C for 10 min and was then stored at −20°C until glucose uptake and MHC isoform abundance were determined.

Single fiber glucose uptake. An aliquot (40 µl) from each lysed single fiber lysate was pipetted into a separate vial along with 8 ml of scintillation cocktail. The 2-[^{3}H]-DG disintegrations per min (dpm) in the aliquots from single fiber lysates together with the 2-[^{3}H]-DG in the media (dpm per picomole) were then used to calculate each fiber's accumulation of 2-[^{3}H]-DG expressed relative to fiber area (picomoles x mm^{-2}) that was determined based on images captured for each fiber as previously described [19].

Whole muscle glucose uptake. Frozen muscles used for GU were weighed and homogenized (Tissuelyser II homogenizer; Qiagen Inc., Valencia, CA) in ice-cold lysis buffer. Homogenates were then rotated at 4°C for 1 h before centrifugation at 15,000g for 10 min at 4°C. Aliquots (200 µl) of supernatant were added to vials containing 8 ml of scintillation cocktail. 2-[^{3}H]-DG and 2-[^{14}C]-mannitol disintegrations per min were measured by scintillation counter, and then 2-DG uptake was calculated as previously described [30].

MHC isoform identification. MHC isoforms in aliquots of single fiber lysates were separated and identified by SDS-PAGE essentially as previously described [19, 31]. MHC isoform expression was determined by comparing the migration of MHC protein band(s) from each fiber or whole muscle homogenate with a MHC isoform standard [6 µg protein of a 3:2 mixture of homogenized rat extensor digitorum longus (EDL) and soleus muscles, E+S] containing all four MHC isoforms: I, IIA, IIB, and IIX.

Immunoblotting. Total protein concentrations for whole muscle lysates were determined by bicinchoninic acid assay, and equal amounts of protein for each sample were separated via SDS-PAGE, and transferred to polyvinyl difluoride membranes. Aliquots of heated (95-100^{o}C) and non-heated single fiber lysates were separated by SDS-PAGE using 4–20% TGX gradient gels (#456-1096: Bio-Rad, Hercules, CA) or 10% gels, and then transferred to polyvinyl difluoride membranes. After electrotransfer, gels were stained in SimplyBlue™ SafeStain for 1 h at room temperature and then destained with deionized water for another 2 h. The SimplyBlue-stained MHC bands on the gels were quantified by densitometry (AlphaView; ProteinSimple, San Leandro, CA) and served as the loading controls for the subsequently immunoblotted proteins [32, 33]. Membranes were incubated with appropriate concentrations of primary and secondary antibodies, and subjected to enhanced chemiluminescence (Luminata Forte Western

HRP Substrate; #WBLUF0100; Millipore) to quantify protein bands by densitometry (FluoroChem E Imager, AlphaView software; ProteinSimple, San Leandro, CA). Individual values were normalized to the mean value of all samples on the membrane and divided by the corresponding MHC loading control value.

Statistics. All data are expressed as mean ± 95% confidence interval (95% CI), with two-tailed significance levels of $\alpha < 0.05$. Two-tailed *t*-tests were used to compare LFD and HFD groups for body weight, fat pad weight, caloric intake, fat mass to body mass ratio, MHC abundance (n=10 for each diet group), and whole muscle protein abundance (n=9-10 for each diet group). A two-way ANOVA was used to determine the effect of insulin and diet for whole muscle glucose uptake (n=10 per group). Because single fiber glucose uptake and protein abundance data was collected from multiple individual fibers per rat, we evaluated these data using mixed-effects linear regression models, incorporating fixed parameters evaluating the contributions of diet (LFD, HFD) and insulin (insulin, no insulin) and their interaction effects, a random Y-intercepts to account for multiple observations within each animal. The analyses were performed using StataIC 14.2 (College Station, TX).

RESULTS

Following the diet intervention, the HFD animals compared to the LFD animals had a significantly greater estimated 2-week caloric intake (1883 ± 122 vs. 1624 ± 85 kcals; $P < 0.005$), body mass (326 ± 17 vs. 302 ± 11 g; $P < 0.05$), epididymal fat mass (6780 ± 942 vs. 4310 ± 441 mg; $P<0.001$), and epididymal fat mass to body mass ratio (20 ± 2 vs. 14 ± 1 mg/g; $P<0.001$).

For whole muscles, the LFD and HFD groups were not significantly different for the relative abundance of any of the MHC isoforms (Table 1 and Supplementary Figure 3.1). For whole muscles there was a significant ($P<0.010$, n=10 per group) interaction between diet and insulin for glucose uptake (Figure 3.1). Post-hoc analysis indicated that insulin-independent glucose uptake was not significantly different between LFD and HFD groups, but glucose uptake of insulin-stimulated muscles was greater ($P<0.01$) for LFD compared to HFD animals. Additionally, glucose uptake with insulin exceeded ($P<0.01$) values with no insulin in each diet group.

MHC isoform of each single fiber was identified by SDS PAGE with subsequent protein staining, and six distinct fiber types were identified: type I, IIA, IIAX, IIX, IIBX, and IIB (Supplementary Figures 3.2 and 3.3). For single fibers in the LFD group, the total number of fibers (no insulin/insulin) isolated for each fiber type were: type I (18/28), type IIA (129/175), type IIAX (32/46), type IIX (142/102), type IIBX (73/49), and type IIB (114/116). The number of muscles (no insulin/insulin) from which the LFD fibers were isolated were: type I (3/7), type IIA (10/10), type IIAX (8/9), type IIX (10/9), type IIBX (10/10), type IIB (10/10). In the HFD group, the total number of fibers (no insulin/insulin) isolated for each fiber type were: type I (10/12), type IIA (153/187), type IIAX (32/18), type IIX (127/139), type IIBX (67/80), and type IIB (123/100). The number of muscles (no insulin/insulin) from which the HFD fibers were isolated were: type I (3/4), type IIA (8/10), type IIAX (6/5), type IIX (10/10), type IIBX (9/10), type IIB (10/10).

All fiber types (I, IIA, IIAX, IIX, IIBX, and IIB) showed a significantly higher glucose uptake in the insulin treated muscles versus non-insulin-treated muscles ($P<0.001$) (Figure 3.2). We also observed a significant main effect of diet ($P<0.05$) on glucose uptake in the type IIBX fibers, with higher uptake in the LFD relative to HFD. We observed an insulin by diet interaction effect on glucose uptake in type IIA ($P<0.05$), IIAX ($P<0.001$), and IIB fibers ($P<0.01$), showing greater effects of diet within the insulin treated muscle relative to the non-insulin treated muscles. Additionally, values for type IIX fibers approached significance for a main effect of diet ($P=0.075$) and an insulin and diet interaction ($P=0.100$) for glucose uptake.

For whole muscles from LFD versus HFD rats, no significant differences were detected for GLUT4 or any of the six mitochondrial proteins that were analyzed (NDUFB8, SDHB, UQCRC2, MTCO1, ATP5A, and COXIV) (Supplementary Figures 3.4 and 3.5). For single fibers, GLUT4 abundance was significantly decreased ($P<0.05$) only in type IIB fibers of HFD versus LFD rats, with no significant difference in the other fiber types (Figure 3.3). NDUFB8 and MTCO1 subunit protein abundance were significantly decreased ($P<0.05$) in type I fibers and significantly increased ($P<0.05$) in type IIX fibers from HFD compared to LFD rats (Figures 3.4 and 3.7). In type I fibers from HFD compared to LFD rats, there was a non-significant trend for reduced abundance of both SDHB ($P=0.054$; Figure 3.5) and COXIV ($P=0.054$; Figure 3.9) proteins. In type IIX fibers from HFD versus LFD rats, there was a non-significant trend for

greater abundance of SDHB (P=0.066), UQCRC2 (P=0.06; Figure 3.6) and COXIV (P=0.084; Figure 3.9). In type IIBX fibers from HFD compared to LFD rats, there was a non-significant trend for greater ATP5A abundance (P=0.064; Figure 3.8). Full length blots of from single fiber analysis are displayed in the supplemental information (Supplementary Figure 3.6).

DISCUSSION

Assessing the insulin-stimulated glucose uptake of single muscle fibers that were individually characterized for their MHC isoform expression revealed novel insights at the cellular level that would have been imperceptible using only conventional muscle tissue analysis. The most important new results included: 1) a physiologic insulin dose significantly increased glucose uptake above basal values for each of the six fiber types analyzed (I, IIA, IIAX, IIB, IIBX and IIB) in both the LFD and HFD groups; 2) significant HFD-related decrements in glucose uptake (based on either main effect of diet or diet x insulin interaction) were identified for type IIA, IIAX, IIBX, and IIB fiber types along with a non-significant trend for an HFD-related decrease in IIX fibers and no evidence for HFD-related decrements for type I fibers; 3) the HFD-induced insulin resistance in whole muscle was attributable to fiber type-selective insulin resistance without any evidence for an alteration in the fiber type composition as determined by MHC isoform expression; 4) GLUT4 protein abundance was lower in type IIB fibers from HFD versus LFD rats, but not in whole muscles or in any of the other fiber types; and 5) HFD versus LFD rats differed with regard to abundance of several mitochondrial proteins in type I fibers (NDUFB8 and MTCO1 were greater for LFD) and type IIX fibers (NDUFB8 and MTCO1 were greater for HFD), but no significant differences were identified in whole muscles or in any of the other fiber types.

Because glucose uptake and MHC expression were both determined at the whole muscle and single fiber levels, it is possible to compare the magnitude of the directly measured HFD-induced insulin resistance for whole muscle with an estimate of the magnitude of whole muscle insulin resistance that relies on glucose uptake measured in single fibers. The relative abundance of each MHC isoform in whole muscle (8% type I, 16% type IIA, 27% type IIX, and 49% type IIB) can be multiplied by the respective decrements in glucose uptake of HFD versus LFD (non-significant 4% lower value for type I and significant decrements of 12% for type IIA, 34% for

type IIX and 45% for type IIB). The sum of these isoform-selective values (33.5%) compares favorably to the 40% decrease that was directly measured in whole HFD versus LFD muscles. The similarity between these two values indicates that the single fiber results provide useful insights about whole muscle glucose uptake in addition to the insights at the cellular and fiber type-selective level that are uniquely revealed by single fiber analysis.

The current results identified fiber type-related differences in susceptibility to HFD-induced insulin resistance at the cellular level. Some [6, 16, 34], but not all [13, 14, 35] of the previous studies that evaluated muscle tissue glucose uptake using multiple muscles with differing fiber types have reported relatively greater insulin resistance for muscle enriched with type IIB fibers compared to muscles predominantly comprised of type I fibers. Careful scrutiny of the experimental designs and methods for the previously published whole muscle studies does not reveal a simple and obvious explanation for the differing results.

Multiple lines of evidence indicate that differences in muscle fiber type composition can influence insulin sensitivity. For example, whole body insulin sensitivity in humans was reported to be positively correlated to the percent of type I fibers in skeletal muscle [36]. In addition, insulin-stimulated glucose uptake is greater for rat skeletal muscle tissue enriched with type I and/or IIA fibers compared to muscles primarily comprised of type IIB fibers [37, 38]. Furthermore, insulin-stimulated glucose uptake single fibers expressing type I or IIA MHC exceeds the values for fibers expressing type IIB or IIX fibers [17-19]. Although a shift in fiber type composition would be predicted to influence insulin sensitivity, the HFD-induced insulin resistance in the whole epitrochlearis muscle in the current study was not accompanied by altered MHC isoform distribution. Rather, the current results demonstrate that the HFD-related insulin resistance in whole muscle was attributable to fiber type selective decrements in glucose uptake. It is notable that two earlier studies reporting fiber type changes in muscles of rodents eating a HFD found increased abundance of type I MHC rather than increased type IIB MHC [21, 22]. Taking together these studies with the current results, the available evidence does not support the idea that altered fiber type composition is a major cause for HFD-induced insulin resistance.

Single fiber glucose uptake has been previously reported in only one other insulin resistant model, the obese Zucker (OZ) rat [17]. OZ rats have a mutation in the leptin receptor leading to extreme hyperphagia, and their excessive body fat is already evident at 2 to 3 wk-old

[39]. Both the lean Zucker (LZ) and OZ rats in the earlier single fiber study were provided with ad libitum access to standard rats (i.e., LFD). Consistent with the typical obesity phenotype of OZ rats, it has been reported that ~8 wk-old OZ versus LZ rats have ~400% greater epididymal fat pad mass [40] which greatly exceeds the increases observed in the current study (36% greater epididymal fat pad mass for HFD versus LFD). Single fibers from epitrochlearis muscles of lean and LZ and OZ rats were stimulated using a supraphysiologic insulin dose (2000 μU/ml), and the relative magnitude of the genotype-related decrement (ranging from ~40 to 50%) in glucose uptake by insulin-stimulated fibers did not vary greatly among the four fiber types that were studied (IIA, IIB, IIX and IIB/X fibers) [17]. The substantially smaller change in glucose uptake of insulin-stimulated IIA fibers (16%) in the HFD rats from the current study compared to the ~40% decline in IIA fibers from OZ rats may be related to differences in the insulin resistance model and/or the insulin dose. Given the substantial differences between the OZ and brief HFD models with regard to their level of increased body fat and extent of insulin resistance for IIA fibers, it is striking that the relative decline in glucose uptake by IIB fibers from insulin-stimulated muscles after 2 wk of HFD (49%) was not less than the relative deficit in IIB fibers from OZ rats (41%). Insulin resistance is complex, so it should not be surprising that the extent of fiber type-related insulin resistance is not uniform across all insulin resistant conditions.

To gain insights into the potential mechanisms for the HFD-induced insulin resistance, we evaluated the GLUT4 content in whole muscles and single fibers. In the whole muscle, we confirmed our previous finding that a two-week HFD did not significantly alter total GLUT4 content of the epitrochlearis muscle [9]. The current study was apparently the first to determine the influence of HFD on both GLUT4 abundance and glucose uptake in single muscle fibers that had been characterized for fiber type. It seems reasonable to suspect that the lower abundance of GLUT4 protein found only in type IIB fibers contributed to the HFD-induced insulin resistance in type IIB fibers. However, the HFD-induced insulin resistance in other type II fiber types was not attributable to lower GLUT4 levels. Earlier research demonstrated a decline in insulin-stimulated GLUT4 localized in the cell surface membranes of whole epitrochlearis muscles from HFD compared to LFD rats [41]. We speculate that in the current study there was an HFD-induced decline in cell surface GLUT4 for each of the type II fiber types from insulin-stimulated muscles. Testing this idea will require the development of new methods that allow for the measurement of both cell surface GLUT4 and fiber type in the same fibers.

There is a great deal of interest, as well as controversy about the relationship between mitochondria and insulin sensitivity in skeletal muscle [26-29]. In whole skeletal muscles of rats consuming a HFD, the abundance of several mitochondrial proteins was previously reported to be unaltered after two weeks on the diet, but significant increases were evident for multiple mitochondrial proteins after four weeks [4]. The current study also found no detectable HFD effect on the abundance of six mitochondrial proteins in whole muscles after two weeks. However, single fiber analysis revealed compelling fiber type-selective HFD-effects on mitochondrial proteins that were obscured in whole muscle analysis. The lack of uniformity in the fiber type effects was evident even among the different type II fiber types that became insulin resistant, so these results do not point toward a simple relationship between changes in mitochondrial protein levels and induction of insulin resistance.

In conclusion, single fiber analysis revealed that the extent of HFD-induced insulin resistance can be profoundly variable for single muscle fibers expressing different MHC isoforms, even when the fibers are from the same muscles and rats. What might account for the strikingly fiber type-related difference in susceptibility to HFD-induced insulin resistance? In an earlier study [9] analyzing whole epitrochlearis muscles using the same dietary protocols and the same insulin concentration as the current study, we found that the insulin-stimulated muscles from LFD rats exceeded HFD values for phosphorylation of Akt substrate of 160 kDa (AS160, also known as TBC1D4) on Thr^{642} and Ser^{588}, two sites that are crucial for regulating insulin-stimulated GLUT4 translocation and glucose transport [42, 43]. Our working hypothesis is that fiber type-selective deficits in insulin-stimulation of AS160 on Thr^{642} and Ser^{588} underlies the fiber type-selective insulin resistance that we revealed in the current study. We further predict that these fiber type-selective deficits in AS160 phosphorylation are responsible for fiber type-selective deficits in insulin-stimulated GLUT4 translocation. What might account for the putative fiber type-selective HFD-induced deficits in AS160 phosphorylation? At the whole muscle level, the same two week HFD protocol did not result in significantly diminished insulin-stimulated Akt activation [9]. However, it is conceivable that fiber type selective deficits in Akt signaling were obscured by whole tissue analysis, so analysis at the single fiber level would be appropriate. It is clear that further metabolic analysis at the single fiber level will provide uniquely valuable insights regarding the mechanisms underlying skeletal muscle insulin resistance.

ACKNOWLEDGEMENTS

These experiments were supported by a grant from the National Institutes of Health (R01 DK71771). This study has been published; Pataky MW, Wang H, Yu CS, Arias EB, Ploutz-Snyder RJ, Zheng X, & Cartee GD. *Scientific reports* 7(1): 13642, 2017.

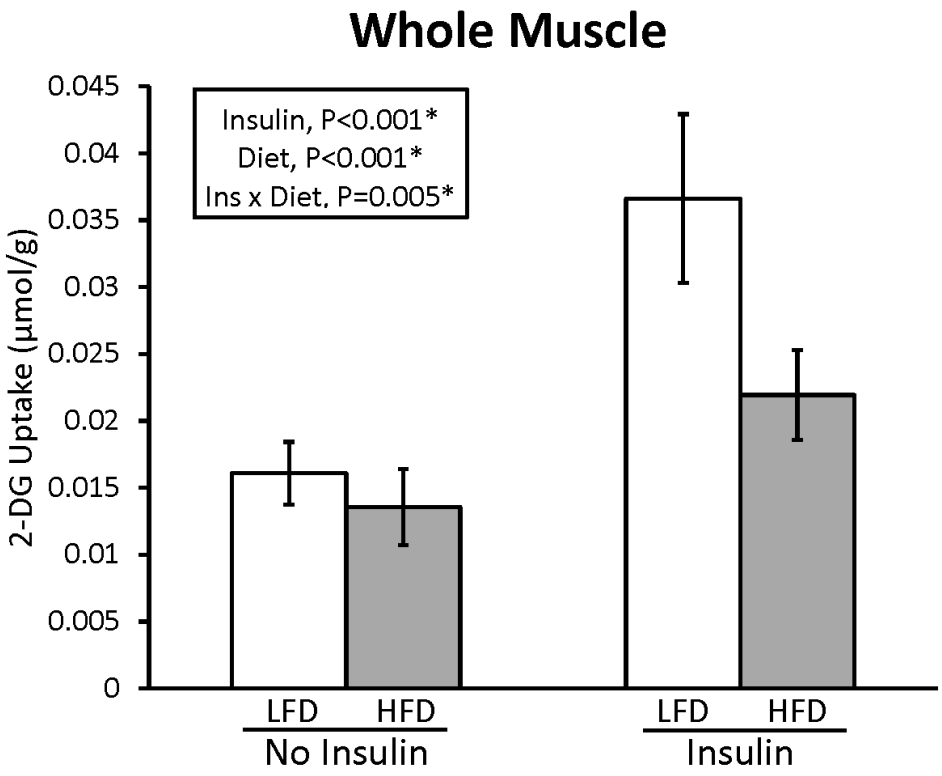

Figure 3.1

Effect of high fat diet (HFD) versus low fat diet (LFD) on 2-DG uptake in whole epitrochlearis muscles. P-values are displayed, and *P<0.05 was considered statistically significant. Values are means ±95% confidence interval.

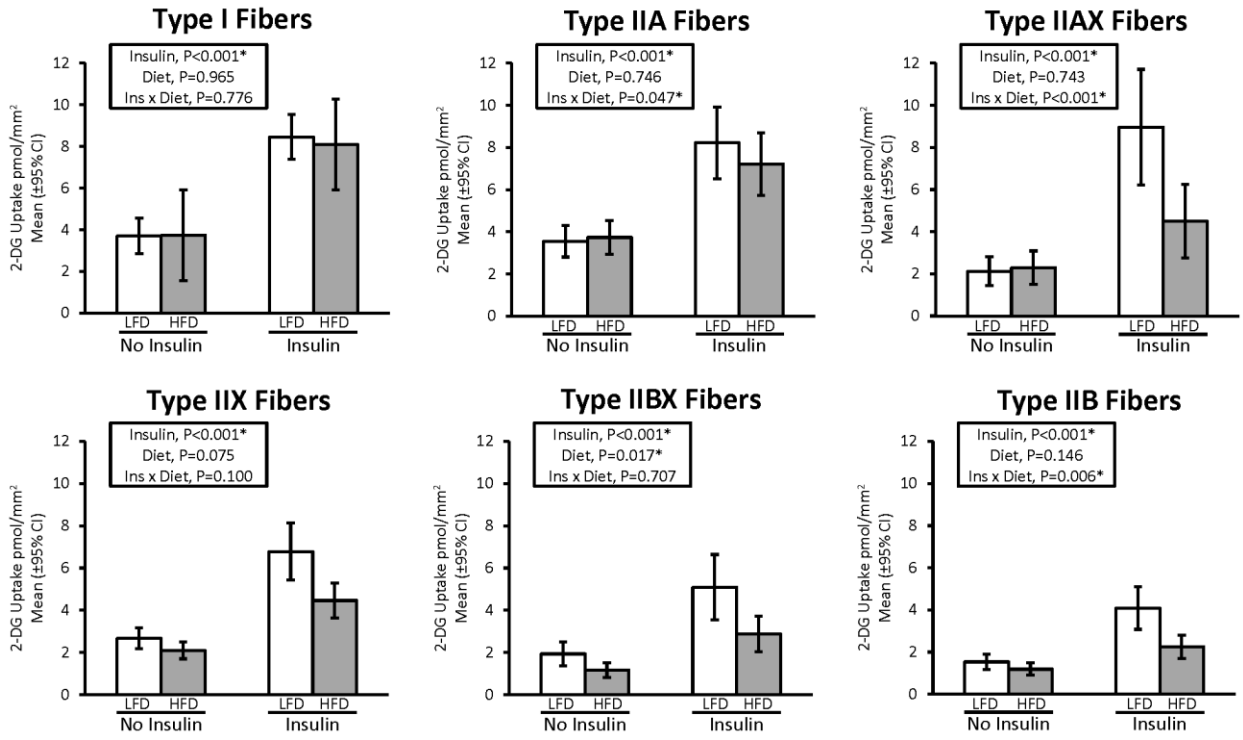

Figure 3.2

Effect of high fat diet (HFD) versus low fat diet (LFD) on 2-DG uptake in single fibers of each fiber type. P-values are displayed, and *P<0.05 was considered statistically significant. Values are means ±95% confidence interval.

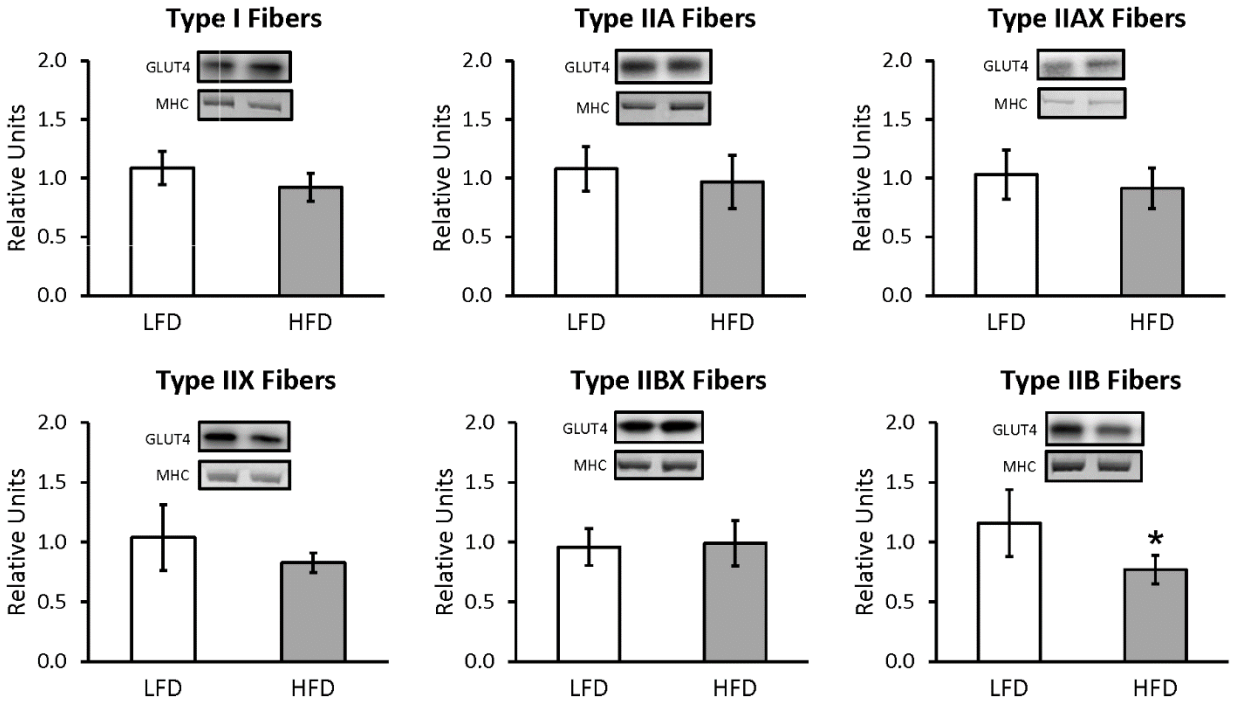

Figure 3.3

Effect of high fat diet (HFD) versus low fat diet (LFD) on the relative abundance of the glucose transporter protein, GLUT4, in single fibers of each fiber type. The loading control was myosin heavy chain (MHC). *Indicates a statistically significant difference between HFD and LFD ($P<0.05$). Values are means ±95% confidence interval.

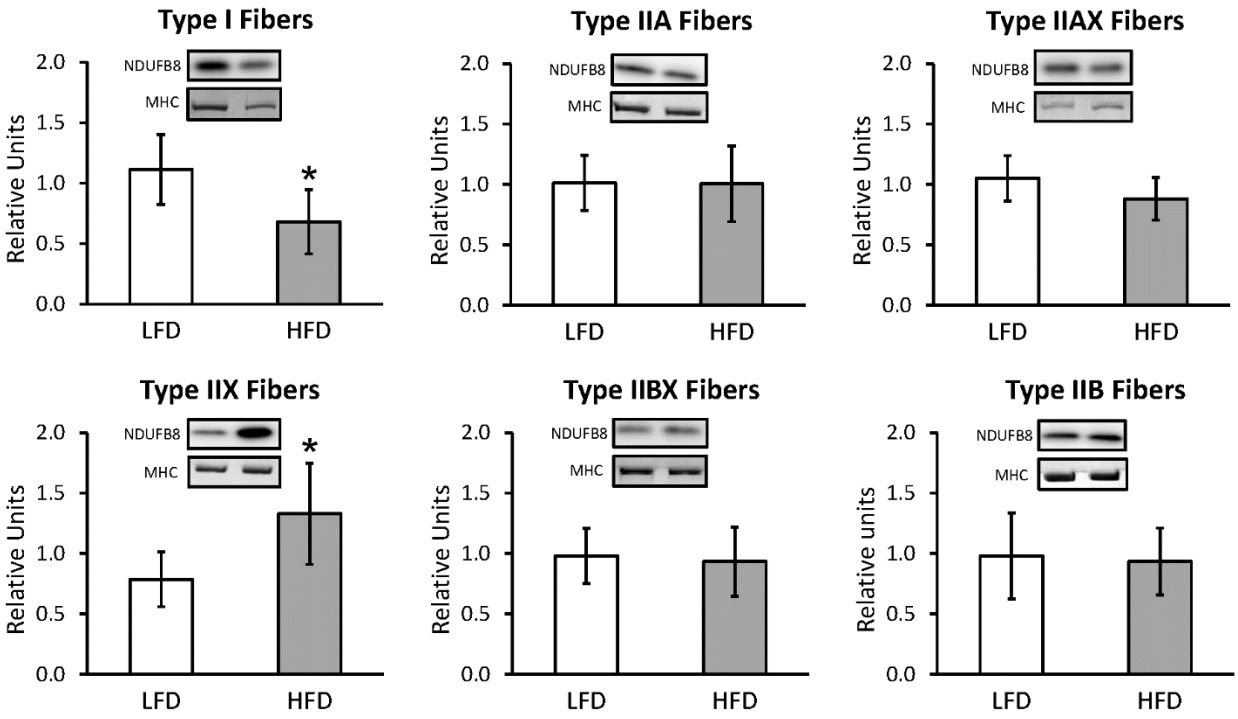

Figure 3.4

Effect of high fat diet (HFD) versus low fat diet (LFD) on the relative abundance of mitochondrial Complex I protein, NDUFB8, in single fibers of each fiber type. The loading control was myosin heavy chain (MHC). *Indicates a statistically significant difference between HFD and LFD ($P<0.05$). Values are means ±95% confidence interval.

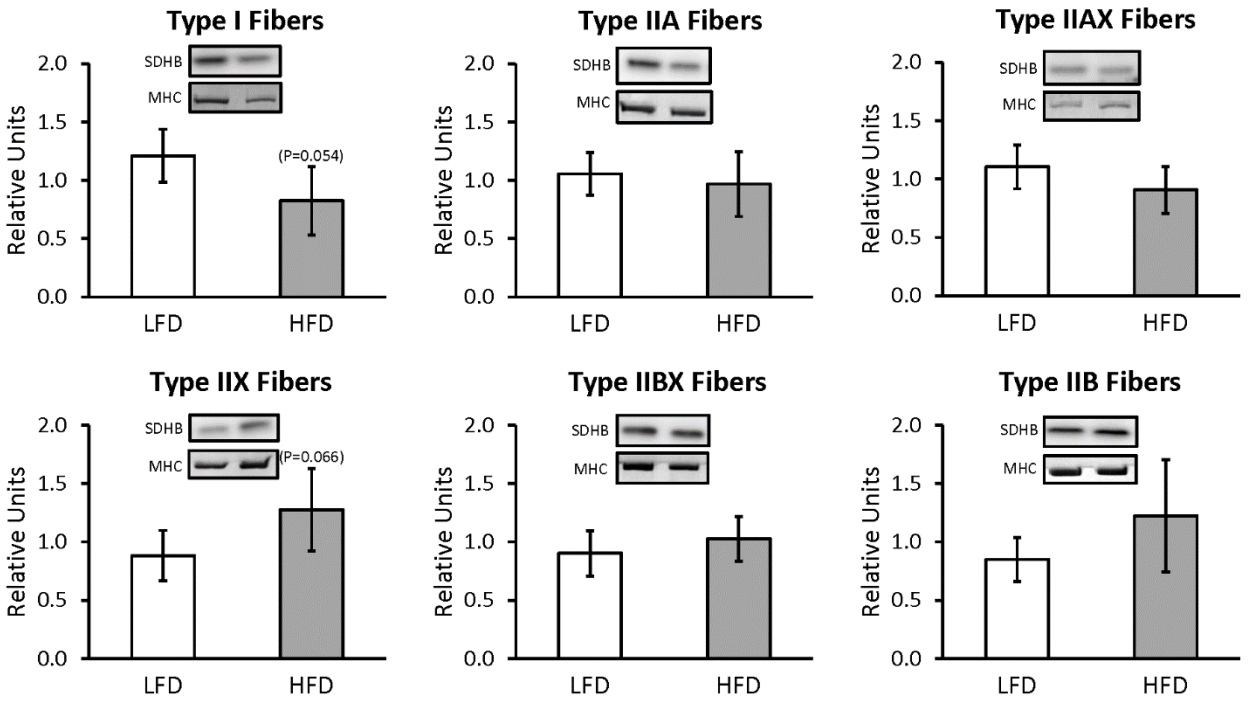

Figure 3.5

Effect of high fat diet (HFD) versus low fat diet (LFD) on the relative abundance of mitochondrial Complex II protein, SDHB, in single fibers of each fiber type. The loading control was myosin heavy chain (MHC). There was no significant difference between LFD and HFD for any fiber type. Values are means ±95% confidence interval.

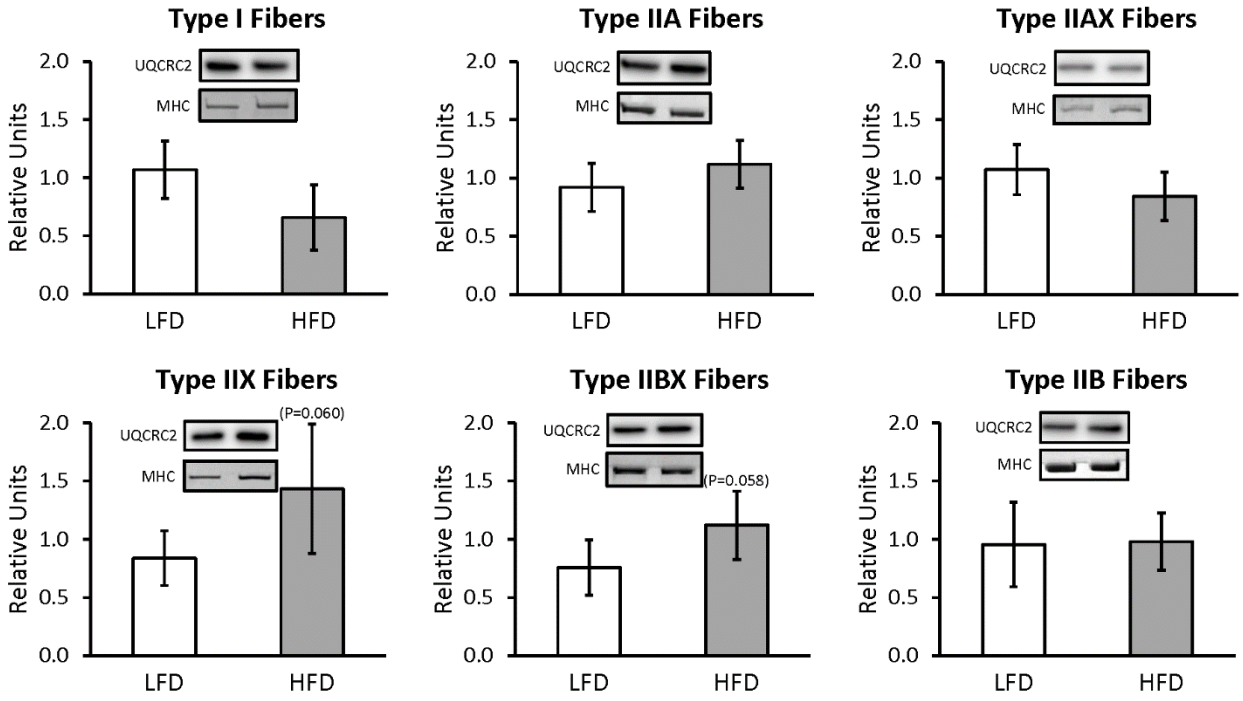

Figure 3.6

Effect of high fat diet (HFD) versus low fat diet (LFD) on the relative abundance of mitochondrial Complex III protein, UQCRC2, in single fibers of each fiber type. The loading control was myosin heavy chain (MHC). There were no significant differences between LFD and HFD for any fiber type. Values are means ±95% confidence interval.

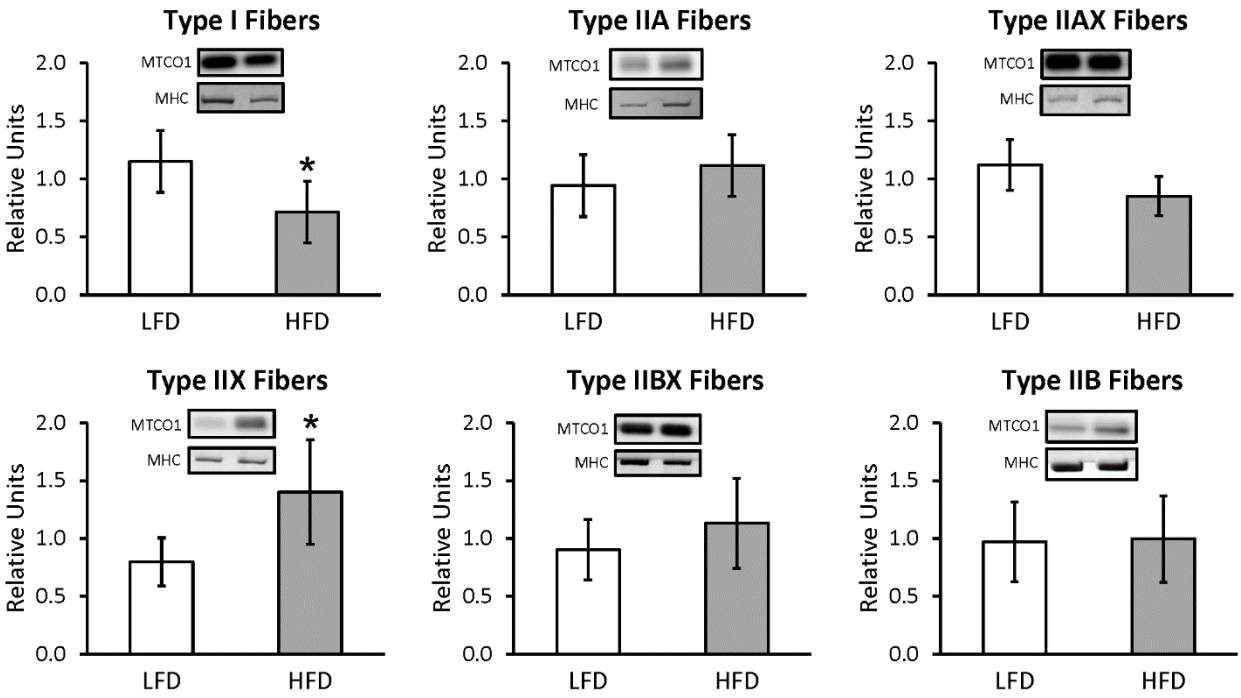

Figure 3.7

Effect of high fat diet (HFD) versus low fat diet (LFD) on the relative abundance of mitochondrial Complex IV protein, MTCO1, in single fibers of each fiber type. The loading control was myosin heavy chain (MHC). *Indicates a statistically significant difference between HFD and LFD at a level of $P<0.05$. Values are means ±95% confidence interval.

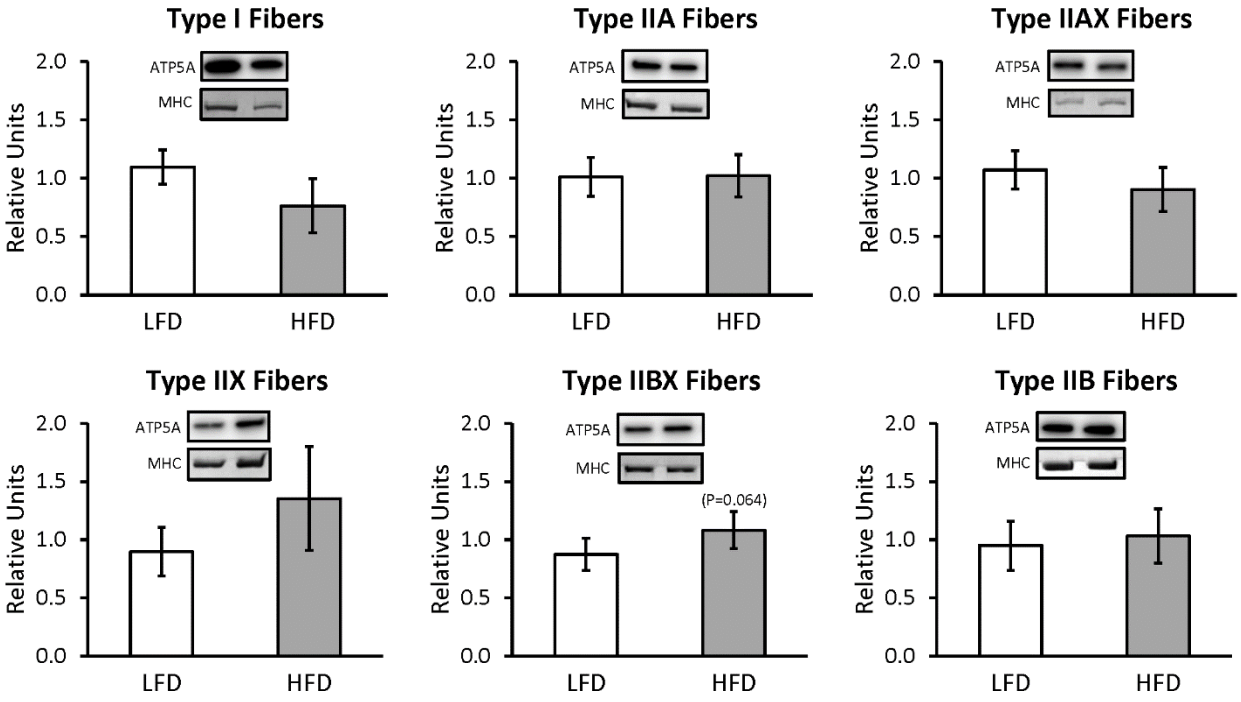

Figure 3.8

Effect of high fat diet (HFD) versus low fat diet (LFD) on the relative abundance of mitochondrial Complex V protein, ATP5A, in single fibers of each fiber type. The loading control was myosin heavy chain (MHC). There were no significant differences between LFD and HFD for any fiber type. Values are means ±95% confidence interval.

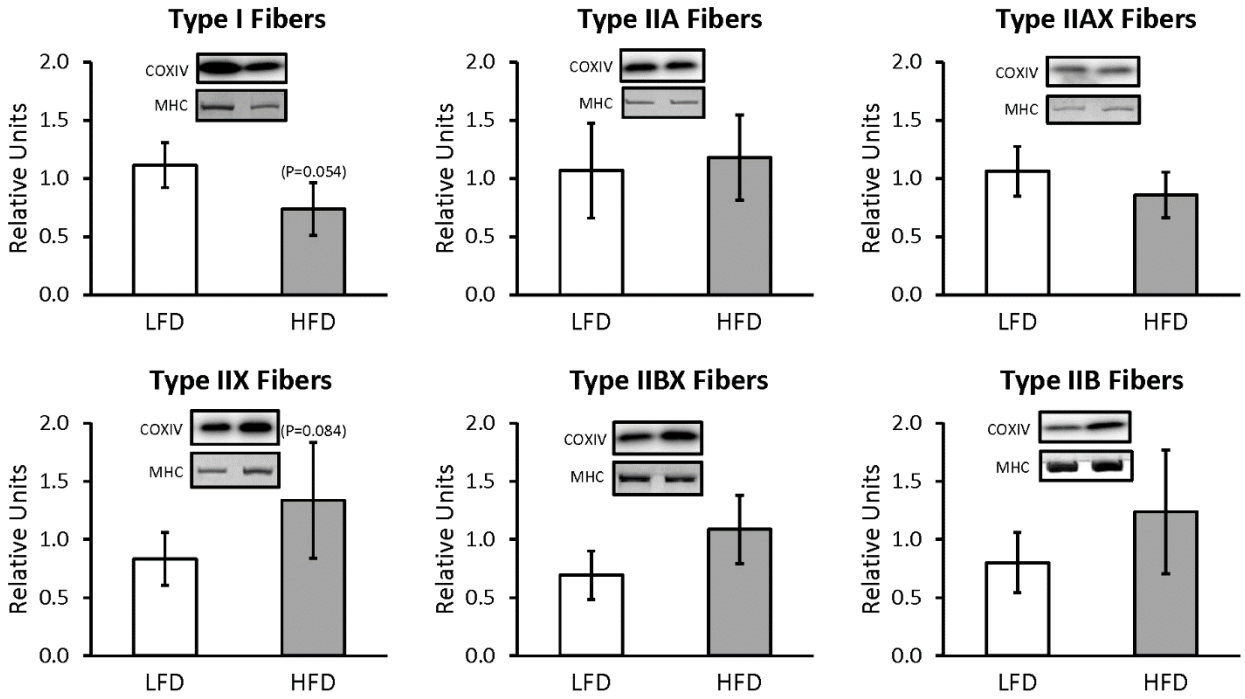

Figure 3.9

Effect of high fat diet (HFD) versus low fat diet (LFD) on the relative abundance of mitochondrial Complex IV protein, COXIV, in single fibers of each fiber type. The loading control was myosin heavy chain (MHC). There were no significant differences between LFD and HFD for any fiber type. Values are means ±95% confidence interval.

% MHC I		% MHC IIA		% MHC IIX		% MHC IIB	
LFD	HFD	LFD	HFD	LFD	HFD	LFD	HFD
8.6 ±1.8	7.5 ±1.7	16.8 ±2.3	15.0 ±2.1	27.1 ±3.6	26.2 ±3.3	47.4 ±5.5	51.3 ±4.2

Table 3.1

Relative myosin heavy chain isoform composition of whole epitrochlearis muscle. Myosin heavy chain (MHC) isoforms of whole epitrochlearis muscles from rats in the low fat diet (LFD) and high fat diet (HFD) groups were separated by SDS-PAGE, and the gels were stained with SimplyBlue™ SafeStain. Resulting bands were quantified by densitometry and expressed as relative values (%). Values are means ± 95% confidence interval.

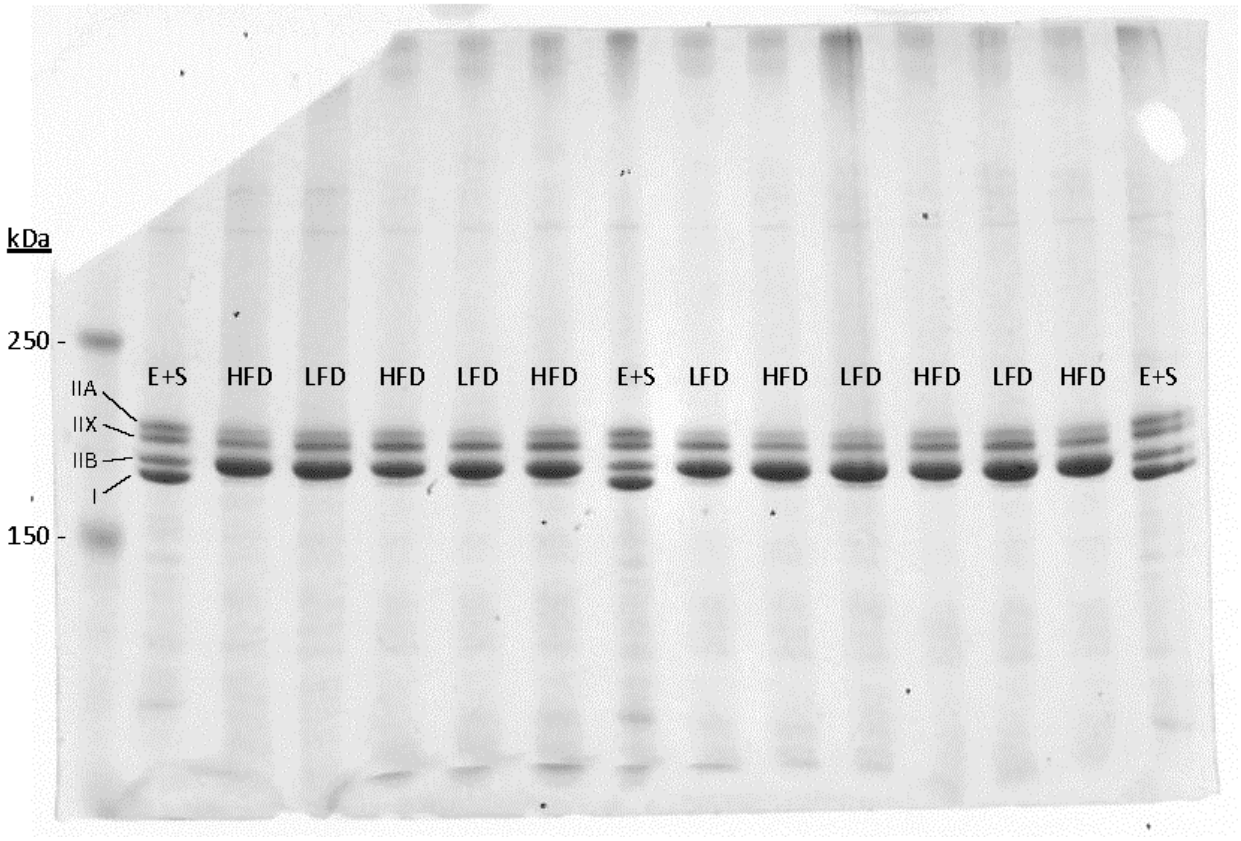

Supplementary Figure 3.S1

Uncropped representative SDS-PAGE gel of whole muscle lysates. Pooled rat extensor digitorum longus and soleus (E+S) standard was used to identify MHC isoform abundance in whole epitrochlearis muscle samples from LFD (low fat diet) and HFD (high fat diet) fed rats as is quantitatively reported in Figure 3.1.

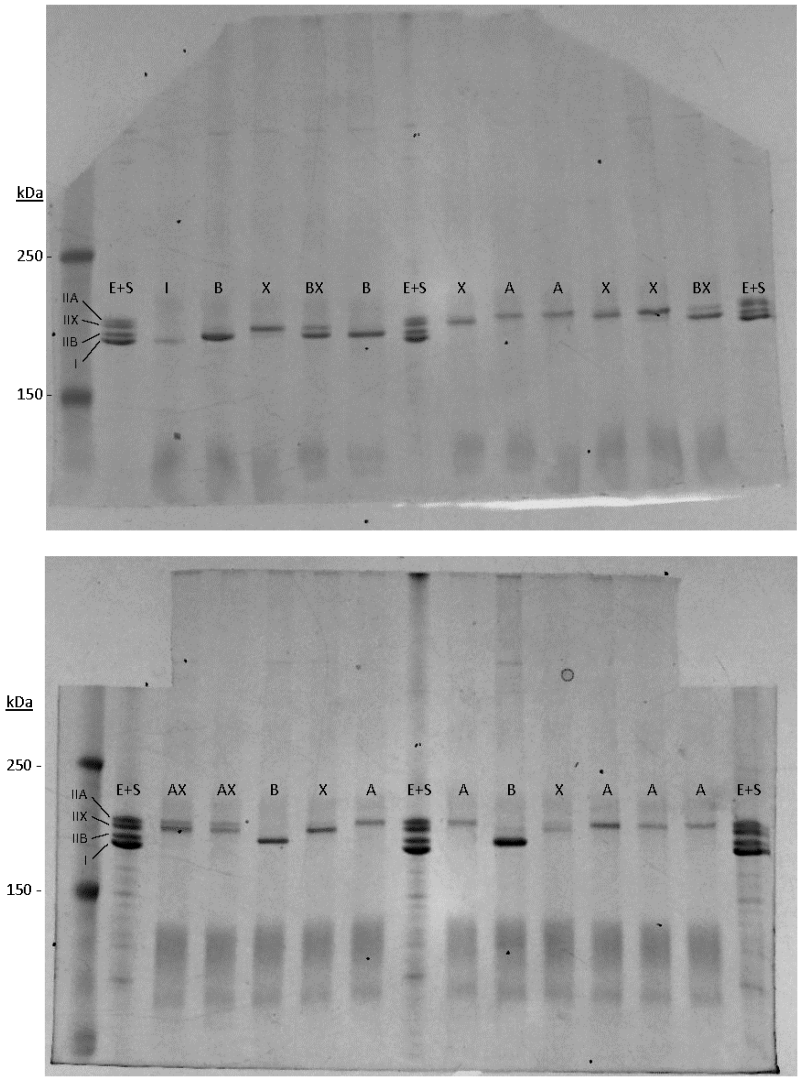

Supplementary Figure 3.S2 and 3.S3

Uncropped SDS-PAGE gels of single fiber lysates. Representative gels display MHC isoform separation in individual muscle fibers to identify fiber type. Pooled rat extensor digitorum longus and soleus (E+S) standard was used to identify MHC isoform expression.

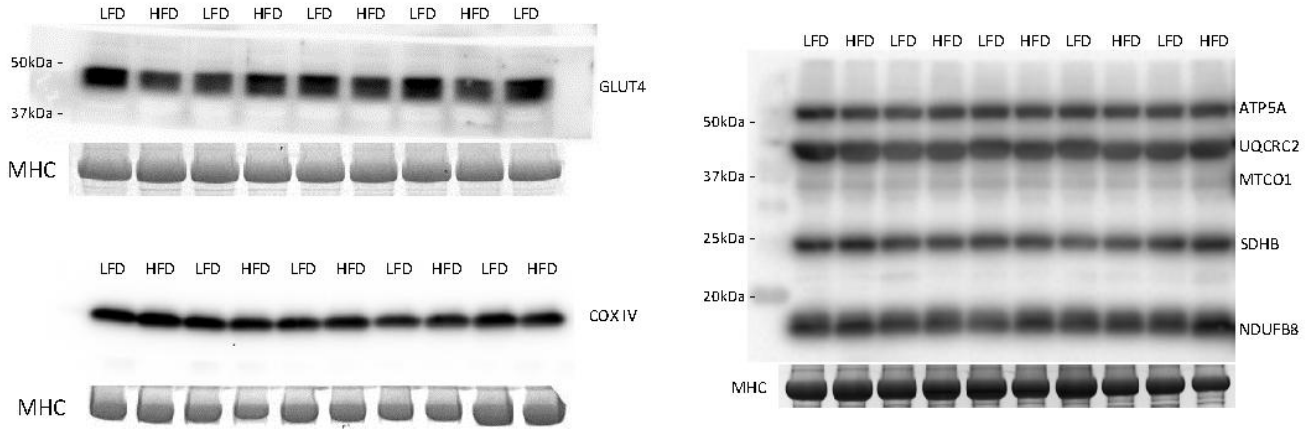

Supplementary Figure 3.S4

Immunoblots of GLUT4 and mitochondrial proteins from whole epitrochlearis muscles of LFD and HFD fed rats. Representative blots together with the corresponding image for MHC which was used as a loading control. There were no significant differences between LFD and HFD groups for the abundance of any of these proteins.

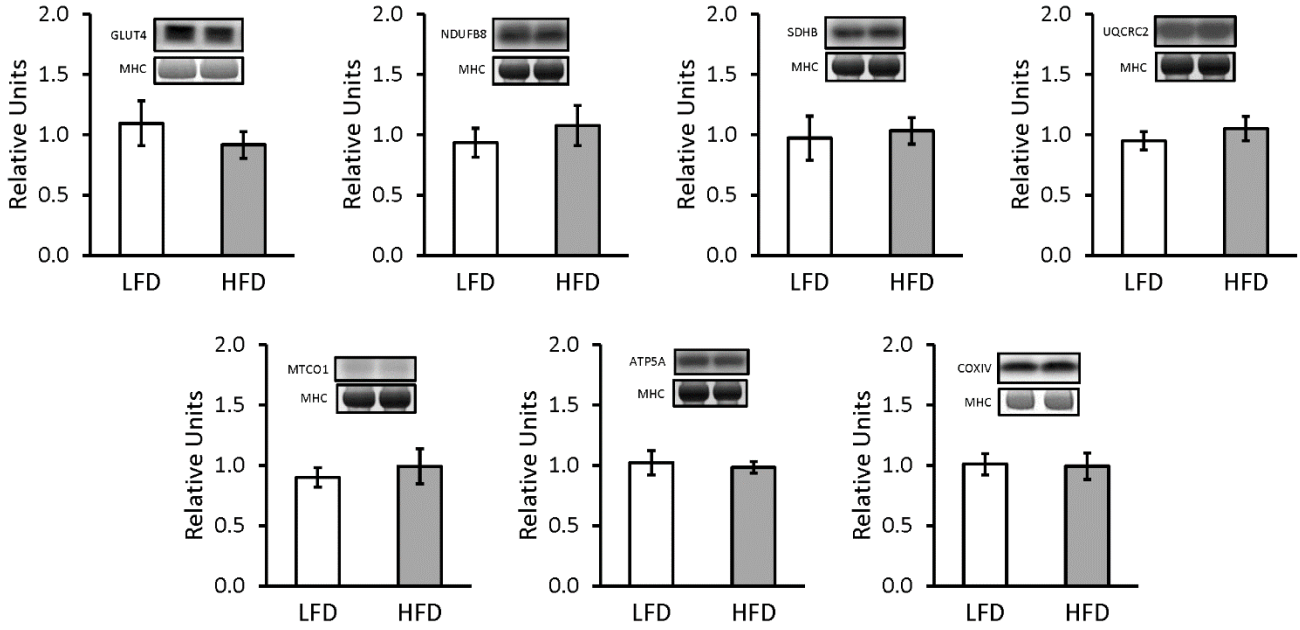

Supplementary Figure 3.S5

Quantification of whole muscle immunoblots of GLUT4 and mitochondrial proteins. Values are expressed relative to MHC loading control. There were no significant differences between LFD and HFD groups for the abundance of any of these proteins.

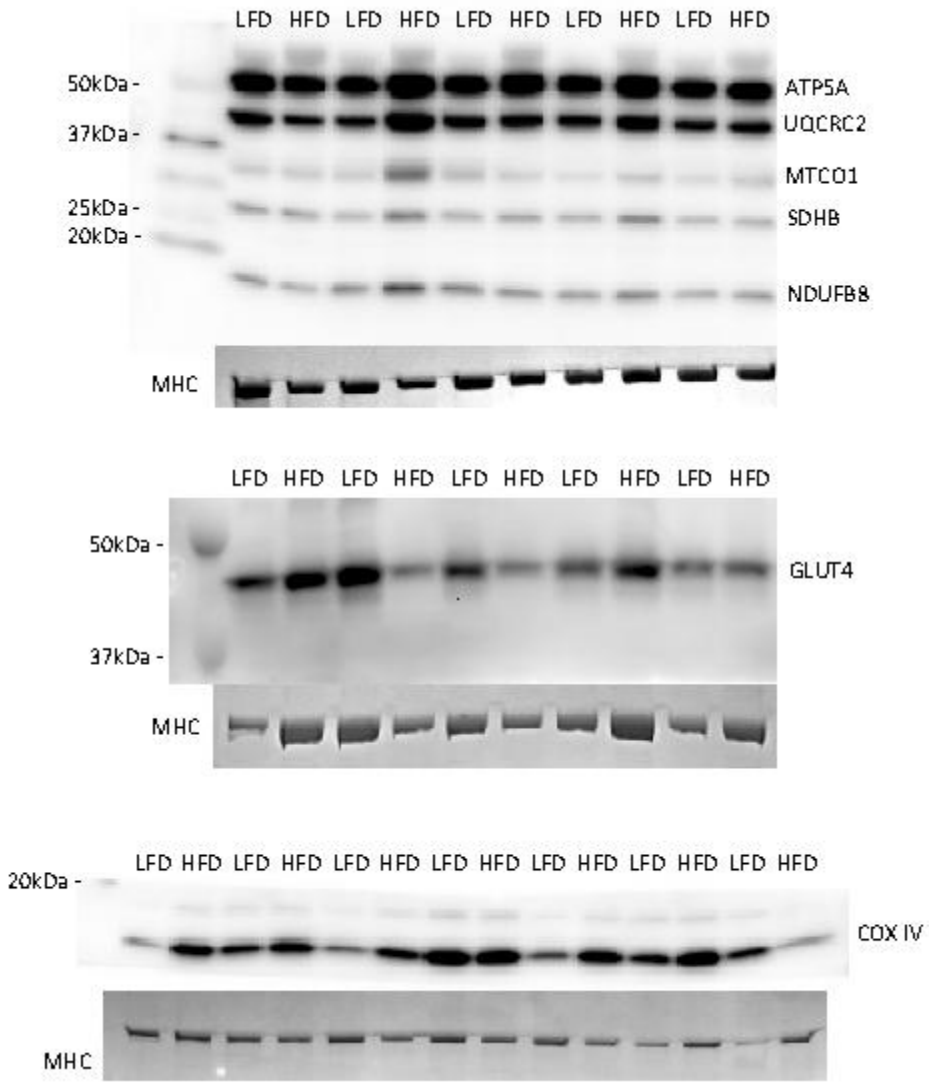

Supplementary Figure 3.S6

Immunoblots of GLUT4 and mitochondrial proteins from single muscle fibers of LFD and HFD fed rats. Representative blots together with the corresponding image for MHC which was used as a loading control.

REFERENCES

1. DeFronzo, R.A., E. Jacot, E. Jequier, E. Maeder, J. Wahren, and J.P. Felber, *The effect of insulin on the disposal of intravenous glucose. Results from indirect calorimetry and hepatic and femoral venous catheterization.* Diabetes, 1981. **30**(12): p. 1000-7.
2. DeFronzo, R.A. and D. Tripathy, *Skeletal muscle insulin resistance is the primary defect in type 2 diabetes.* Diabetes care, 2009. **32**(suppl 2): p. S157-S163.
3. Facchini, F.S., N. Hua, F. Abbasi, and G.M. Reaven, *Insulin resistance as a predictor of age-related diseases.* The Journal of Clinical Endocrinology & Metabolism, 2001. **86**(8): p. 3574-3578.
4. Hancock, C.R., D.-H. Han, M. Chen, S. Terada, T. Yasuda, D.C. Wright, and J.O. Holloszy, *High-fat diets cause insulin resistance despite an increase in muscle mitochondria.* Proceedings of the National Academy of Sciences, 2008. **105**(22): p. 7815-7820.
5. Kraegen, E.W., P.W. Clark, A.B. Jenkins, E.A. Daley, D.J. Chisholm, and L.H. Storlien, *Development of muscle insulin resistance after liver insulin resistance in high-fat-fed rats.* Diabetes, 1991. **40**(11): p. 1397-403.
6. Oakes, N.D., G.J. Cooney, S. Camilleri, D.J. Chisholm, and E.W. Kraegen, *Mechanisms of liver and muscle insulin resistance induced by chronic high-fat feeding.* Diabetes, 1997. **46**(11): p. 1768-74.
7. Storlien, L.H., D.E. James, K.M. Burleigh, D.J. Chisholm, and E.W. Kraegen, *Fat feeding causes widespread in vivo insulin resistance, decreased energy expenditure, and obesity in rats.* Am J Physiol, 1986. **251**(5 Pt 1): p. E576-83.
8. Turner, N., G.M. Kowalski, S.J. Leslie, S. Risis, C. Yang, R.S. Lee-Young, J.R. Babb, P.J. Meikle, G.I. Lancaster, D.C. Henstridge, P.J. White, E.W. Kraegen, A. Marette, G.J. Cooney, M.A. Febbraio, and C.R. Bruce, *Distinct patterns of tissue-specific lipid accumulation during the induction of insulin resistance in mice by high-fat feeding.* Diabetologia, 2013. **56**(7): p. 1638-48.
9. Castorena, C.M., E.B. Arias, N. Sharma, and G.D. Cartee, *Postexercise improvement in insulin-stimulated glucose uptake occurs concomitant with greater AS160 phosphorylation in muscle from normal and insulin-resistant rats.* Diabetes, 2014. **63**(7): p. 2297-308.
10. Pette, D. and R.S. Staron, *Cellular and molecular diversities of mammalian skeletal muscle fibers.* Rev Physiol Biochem Pharmacol, 1990. **116**: p. 1-76.
11. Pandorf, C.E., T. Garland, W. Aoi, C. Handschin, L. Gorza, P.M. Garcia-Roves, S.W. Copp, C.M. Tipton, V.J. Caiozzo, and F. Haddad, *A Rationale for SDS-PAGE of MHC Isoforms as a Gold Standard for Determining Contractile Phenotype.* Journal of Applied Physiology, 2010. **108**(1): p. 222-225.
12. Cresser, J., A. Bonen, A. Chabowski, L.E. Stefanyk, R. Gulli, I. Ritchie, and D.J. Dyck, *Oral administration of a PPAR-δ agonist to rodents worsens, not improves, maximal insulin-stimulated glucose transport in skeletal muscle of different fibers.* American Journal of Physiology-Regulatory, Integrative and Comparative Physiology, 2010. **299**(2): p. R470-R479.
13. Kraegen, E., D. James, L. Storlien, K. Burleigh, and D. Chisholm, *In vivo insulin resistance in individual peripheral tissues of the high fat fed rat: assessment by*

euglycaemic clamp plus deoxyglucose administration. Diabetologia, 1986. **29**(3): p. 192-198.
14. Han, D.-H., S.H. Kim, K. Higashida, S.-R. Jung, K.S. Polonsky, S. Klein, and J.O. Holloszy, *Ginsenoside Re rapidly reverses insulin resistance in muscles of high-fat diet fed rats.* Metabolism, 2012. **61**(11): p. 1615-1621.
15. Storlien, L.H., A.W. Thorburn, G.A. Smythe, A.B. Jenkins, D.J. Chisholm, and E.W. Kraegen, *Effect of d-fenfluramine on basal glucose turnover and fat-feeding-induced insulin resistance in rats.* Diabetes, 1989. **38**(4): p. 499-503.
16. Han, D.-H., P.A. Hansen, H.H. Host, and J.O. Holloszy, *Insulin resistance of muscle glucose transport in rats fed a high-fat diet: a reevaluation.* Diabetes, 1997. **46**(11): p. 1761-1767.
17. Mackrell, J.G. and G.D. Cartee, *A novel method to measure glucose uptake and myosin heavy chain isoform expression of single fibers from rat skeletal muscle.* Diabetes, 2012. **61**(5): p. 995-1003.
18. Mackrell, J.G., E.B. Arias, and G.D. Cartee, *Fiber type-specific differences in glucose uptake by single fibers from skeletal muscles of 9- and 25-month-old rats.* J Gerontol A Biol Sci Med Sci, 2012. **67**(12): p. 1286-94.
19. Cartee, G.D., E.B. Arias, S.Y. Carmen, and M.W. Pataky, *Novel single skeletal muscle fiber analysis reveals a fiber type-selective effect of acute exercise on glucose uptake.* American Journal of Physiology-Endocrinology and Metabolism, 2016. **311**(5): p. E818-E824.
20. Liao, B. and Y. Xu, *Exercise improves skeletal muscle insulin resistance without reduced basal mTOR/S6K1 signaling in rats fed a high-fat diet.* European journal of applied physiology, 2011. **111**(11): p. 2743-2752.
21. de Wilde, J., R. Mohren, S. van den Berg, M. Boekschoten, K. Willems-Van Dijk, P. De Groot, M. Müller, E. Mariman, and E. Smit, *Short-term high fat-feeding results in morphological and metabolic adaptations in the skeletal muscle of C57BL/6J mice.* Physiological genomics, 2008. **32**(3): p. 360-369.
22. Moreno, M., E. Silvestri, R. De Matteis, P. de Lange, A. Lombardi, D. Glinni, R. Senese, F. Cioffi, A.M. Salzano, and A. Scaloni, *3, 5-Diiodo-L-thyronine prevents high-fat-diet-induced insulin resistance in rat skeletal muscle through metabolic and structural adaptations.* The FASEB Journal, 2011. **25**(10): p. 3312-3324.
23. Mrad, J.A., F. Yakubu, D. Lin, J.C. Peters, J. Atkinson, and J. Hill, *Skeletal muscle composition in dietary obesity-susceptible and dietary obesity-resistant rats.* American Journal of Physiology-Regulatory, Integrative and Comparative Physiology, 1992. **262**(4): p. R684-R688.
24. Huang, S. and M.P. Czech, *The GLUT4 glucose transporter.* Cell metabolism, 2007. **5**(4): p. 237-252.
25. Lauritzen, H.P. and J.D. Schertzer, *Measuring GLUT4 translocation in mature muscle fibers.* American Journal of Physiology-Endocrinology and Metabolism, 2010. **299**(2): p. E169-E179.
26. Muoio, D.M., *Metabolic inflexibility: when mitochondrial indecision leads to metabolic gridlock.* Cell, 2014. **159**(6): p. 1253-1262.
27. Affourtit, C., *Mitochondrial involvement in skeletal muscle insulin resistance: A case of imbalanced bioenergetics.* Biochimica et Biophysica Acta (BBA)-Bioenergetics, 2016. **1857**(10): p. 1678-1693.

28. Koliaki, C. and M. Roden, *Alterations of mitochondrial function and insulin sensitivity in human obesity and diabetes mellitus.* Annual review of nutrition, 2016. **36**: p. 337-367.
29. Hesselink, M.K., V. Schrauwen-Hinderling, and P. Schrauwen, *Skeletal muscle mitochondria as a target to prevent or treat type 2 diabetes mellitus.* Nature Reviews Endocrinology, 2016. **12**(11): p. 633-645.
30. Cartee, G. and E. Bohn, *Growth hormone reduces glucose transport but not GLUT-1 or GLUT-4 in adult and old rats.* American Journal of Physiology-Endocrinology And Metabolism, 1995. **268**(5): p. E902-E909.
31. Castorena, C.M., E.B. Arias, N. Sharma, J.S. Bogan, and G.D. Cartee, *Fiber type effects on contraction-stimulated glucose uptake and GLUT4 abundance in single fibers from rat skeletal muscle.* American Journal of Physiology-Endocrinology and Metabolism, 2015. **308**(3): p. E223-E230.
32. Murphy, R.M., *Enhanced technique to measure proteins in single segments of human skeletal muscle fibers: fiber-type dependence of AMPK-α1 and-β1.* Journal of Applied Physiology, 2011. **110**(3): p. 820-825.
33. Murphy, R.M., E. Verburg, and G.D. Lamb, *Ca2+ activation of diffusible and bound pools of μ-calpain in rat skeletal muscle.* The Journal of physiology, 2006. **576**(2): p. 595-612.
34. Kim, J.-Y., L.A. Nolte, P.A. Hansen, D.-H. Han, K. Ferguson, P.A. Thompson, and J.O. Holloszy, *High-fat diet-induced muscle insulin resistance: relationship to visceral fat mass.* American Journal of Physiology-Regulatory, Integrative and Comparative Physiology, 2000. **279**(6): p. R2057-R2065.
35. Doh, K., J. Park, Y. Kim, and S. Park, *Effect of Leptin on Insulin Resistance of Muscle-Direct or Indirect?* Physiological research, 2006. **55**(4): p. 413.
36. Lillioja, S., A.A. Young, C.L. Culter, J.L. Ivy, W. Abbott, J.K. Zawadzki, H. Yki-Järvinen, L. Christin, T.W. Secomb, and C. Bogardus, *Skeletal muscle capillary density and fiber type are possible determinants of in vivo insulin resistance in man.* Journal of Clinical Investigation, 1987. **80**(2): p. 415.
37. Henriksen, E.J., R.E. Bourey, K.J. Rodnick, L. Koranyi, M.A. Permutt, and J.O. Holloszy, *Glucose transporter protein content and glucose transport capacity in rat skeletal muscles.* Am J Physiol, 1990. **259**(4 Pt 1): p. E593-8.
38. James, D.E., A.B. Jenkins, and E.W. Kraegen, *Heterogeneity of insulin action in individual muscles in vivo: euglycemic clamp studies in rats.* Am J Physiol, 1985. **248**(5 Pt 1): p. E567-74.
39. de Artinano, A.A. and M.M. Castro, *Experimental rat models to study the metabolic syndrome.* British Journal of Nutrition, 2009. **102**(09): p. 1246-1253.
40. Pouteau, E., S. Turner, O. Aprikian, M. Hellerstein, M. Moser, C. Darimont, L. Fay, and K. Mace, *Time course and dynamics of adipose tissue development in obese and lean Zucker rat pups.* International Journal of Obesity, 2008. **32**(4): p. 648-657.
41. Hansen, P.A., W. Wang, B.A. Marshall, J.O. Holloszy, and M. Mueckler, *Dissociation of GLUT4 translocation and insulin-stimulated glucose transport in transgenic mice overexpressing GLUT1 in skeletal muscle.* Journal of Biological Chemistry, 1998. **273**(29): p. 18173-18179.
42. Sano, H., S. Kane, E. Sano, C.P. Mîinea, J.M. Asara, W.S. Lane, C.W. Garner, and G.E. Lienhard, *Insulin-stimulated phosphorylation of a Rab GTPase-activating protein*

regulates GLUT4 translocation. Journal of Biological Chemistry, 2003. **278**(17): p. 14599-14602.
43. Cartee, G.D., *Roles of TBC1D1 and TBC1D4 in insulin-and exercise-stimulated glucose transport of skeletal muscle.* Diabetologia, 2015. **58**(1): p. 19-30.

CHAPTER IV

Study 2

Skeletal Muscle Fiber Type-selective Effects of Acute Exercise on Insulin-stimulated Glucose Uptake in Insulin-Resistant, High Fat-fed Rats

ABSTRACT

Insulin-stimulated glucose uptake (GU) by skeletal muscle is enhanced several hours after acute exercise in rats with normal or reduced insulin sensitivity. Skeletal muscle is composed of multiple fiber types, but exercise's effect on fiber type-specific insulin-stimulated GU in insulin-resistant muscle was previously unknown. Male rats were fed a high-fat diet (HFD; 2-weeks) and either sedentary (SED) or exercised (2h exercise). Other low-fat diet-fed (LFD) rats remained SED. Rats were studied immediately-post exercise (IPEX) or 3h post-exercise (3hPEX). Epitrochlearis muscles from IPEX rats were incubated in [^{3}H]-2-deoxyglucose (2-DG) without insulin. Epitrochlearis muscles from 3hPEX rats were incubated with 2-DG±100μU/ml insulin. After single fiber isolation, GU and fiber type were determined. Glycogen and lipid droplets (LDs) were assessed histochemically. GLUT4 abundance was determined by immunoblotting. In HFD-SED versus LFD-SED rats, insulin-stimulated GU was decreased in type IIB, IIX, IIAX, and IIBX fibers. Insulin-independent GU IPEX was increased and glycogen content was decreased in all fiber types (type I, IIA, IIB, IIX, IIAX, and IIBX). Exercise by HFD-fed rats enhanced insulin-stimulated GU in all fiber types except type I. Single fiber analyses enabled discovery of striking fiber type-specific differences in HFD and exercise effects on insulin-stimulated GU. The fiber type-specific differences in insulin-stimulated GU post-exercise in insulin resistant muscle were not attributable to a lack of fiber recruitment as indirectly evidenced by insulin-independent GU and glycogen IPEX, differences in multiple LD indices, or altered GLUT4 abundance, implicating fiber type-selective differences in the cellular processes responsible for post-exercise enhancement of insulin-mediated GLUT4 translocation.

INTRODUCTION

In 2015, an estimated 30.3 million individuals had diabetes in the U.S. and another 84.1 million had prediabetes [1]. Skeletal muscle insulin resistance is an essential defect leading to type 2 diabetes, and skeletal muscle is responsible for 60-80% of insulin-mediated glucose disposal [2, 3], making muscle a preeminent target to combat insulin resistance. Independent of diabetes, insulin resistance is linked to many prevalent and devastating pathologies, including atherogenesis, hypertension, cognitive dysfunction and some cancers [4-6]. Exercise by either humans or rodents leads to increased insulin-stimulated glucose uptake by skeletal muscle that is evident ~1-3h post-exercise and can persist up to 48h [7-16]. Both insulin-sensitive [7, 10, 17, 18] and insulin-resistant [14, 19-21] rats and humans can experience this exercise benefit. However, acute exercise does not completely bring glucose uptake of insulin resistant muscle to the level observed in healthy muscle after the same exercise protocol [19, 22]. The current study focuses on the enhanced insulin-stimulated glucose uptake by insulin resistant muscle after exercise because attenuating or eliminating muscle insulin resistance would be expected to have major implications for improving health.

By definition, glucose uptake is a cellular process, so it is essential to understand exercise effects on muscle glucose uptake at the cellular level. Moreover, because skeletal muscle is composed of multiple fiber types based on myosin heavy chain (MHC) expression (I, IIA, IIX, and IIB) with different metabolic properties [23], exercise may exert different fiber type-specific effects during insulin resistant versus insulin-sensitive conditions. Conventionally, researchers compare whole muscles or muscle portions with markedly different fiber type proportion to delineate fiber type differences. However, tissue analysis cannot reveal fiber type differences at the cellular level because several caveats. 1) No muscle is entirely composed of a single fiber type. 2) No rat muscle has been identified that is mostly type IIX fibers. 3) It is impossible to evaluate hybrid fibers (fibers which express more than one MHC) in whole muscles. The physiological relevance of evaluating hybrid fibers is undeniable given that although they can account for a substantial percentage of myofibers (>10-50%) in various species, including rats, mice and humans [24-27], almost nothing is known about their metabolic properties in response to *in vivo* exercise. 4) Muscle tissue contains cell types other than muscle fibers (vascular, neural, connective, and adipose cells) which contribute to measurements in tissues. We developed and

validated the only method that enables glucose uptake (based on [^{3}H]-2-deoxyglucose, [^{3}H]-2-DG, accumulation) and MHC measurement (using SDS polyacrylamide electrophoresis) in individual muscle fibers that are isolated by microdissection after collagenase treatment of the intact rat epitrochlearis muscle [28]. The specificity of glucose uptake by single fibers was established based on cytochalasin B's inhibition of [^{3}H]-2-DG accumulation.

Using this method, we recently reported that in rats with normal insulin sensitivity, acute exercise induced fiber type-specific effects on insulin-stimulated glucose uptake [29]. We discovered increased insulin-stimulated glucose uptake in all fiber types, except type IIX fibers, post-exercise. Subsequently, we found that a 2-week high-fat diet (HFD) induced a fiber type-selective decrease on insulin-stimulated glucose uptake [30]. There was no insulin resistance in type I fibers, slight insulin resistance in IIA fibers, and substantial insulin resistance in the other fibers (IIB, IIBX, IIX, and IIAX) [30]. In whole epitrochlearis muscles from HFD-fed rats, exercise elevated the insulin-stimulated glucose uptake rate to values that were equal to those found in muscles from unexercised rats on a control, low fat diet [19]. However, the exercise-effect on fiber type specific insulin-stimulated glucose uptake during insulin resistance has not been reported, and it is impossible to predict if this whole muscle outcome in insulin resistant muscle was attributable to a uniform effect in all fiber types or a fiber type-selective benefit. Therefore, our primary aim was to determine the exercise-effect on insulin-stimulated glucose uptake in different fiber types from insulin resistant rats. We evaluated fiber type-specific effects of a HFD and exercise (3h post-exercise, 3hPEX) on insulin-stimulated glucose uptake using muscles from rats that consumed a 2-week HFD and sedentary (HFD-SED and low-fat diet; LFD-SED) controls. This brief dietary intervention produces muscle insulin resistance prior to large changes in body mass, body composition, or other outcomes that may obscure the primary mechanisms responsible for muscle insulin resistance [31]. We also evaluated the effects of the exercise protocol on two separate indirect markers of fiber recruitment (insulin-independent glucose uptake and muscle glycogen immediately post-exercise, IPEX).

Intramyocellular lipid (IMCL) content correlates with insulin resistance under some circumstances [32], but this relationship can be disrupted (e.g., endurance exercise training can increase IMCL content and also improve insulin sensitivity [33]). Recent evidence suggested lipid droplet (LD) size and/or subcellular location may be more predictive of muscle insulin

resistance than total IMCL content [34-36]. However, previous studies have not evaluated LD size or location in different fiber types for which insulin-stimulated glucose uptake was also known. Therefore, another aim was to identify if LD size and/or location are related to insulin-stimulated glucose uptake in different fiber types from HFD-fed rats post-exercise, along with HFD-SED and LFD-SED controls.

Skeletal muscle insulin-stimulated glucose uptake depends on GLUT4 protein expression [37, 38]. We previously found unaltered GLUT4 abundance in whole muscles 3hPEX in rats [19]. However, increased muscle GLUT4 abundance was reported 3hPEX in humans [39]. It seemed possible that exercise might induce a fiber type-specific increase in GLUT4 abundance that would be obscured by tissue analysis. Therefore, our final aim was to assess possible differences in fiber type-specific GLUT4 abundance post-exercise from HFD-3hPEX, HFD-SED and LFD-SED rats.

METHODS

Materials. Reagents and apparatus for SDS-PAGE and nonfat-dry milk were from Bio-Rad (Hercules,CA). [^{3}H]-2-deoxyglucose and [^{14}C] mannitol were from PerkinElmer (Waltham,MA). Tissue Protein Extraction Reagent (T-PER), and SimplyBlue™ SafeStain were from ThermoFisher (Pittsburgh,PA). Collagenase type 2 (305U/mg) was from Worthington Biochemical (Lakewood,NJ). Periodic Acid-Schiff (PAS) kit and glycogen (type IX, bovine liver) were from Sigma Aldrich (St. Louis,MO). Antibodies and fluorescent probes are listed in Table 4.1.

Animal treatment and muscle preparation. Procedures for animal care were approved by the University of Michigan Committee on Use and Care of Animals. Male Wistar rats (6-7weeks-old; Charles River Laboratories, Boston,MA) were individually housed and randomly provided standard rodent chow (LFD: 14% kcal fat, 58% kcal carbohydrate; 5L0D, Lab Diet, St. Louis,MO) or HFD (60% kcal fat, 20% kcal carbohydrate; D12492, ResearchDiets, New Brunswick,NJ) for 2-weeks *ad libitum* until fasted at ~1700 on the night before the experiment. Caloric intake was estimated based on food provided on day-one and food remaining at ~1700 on the night before the experiment. Beginning at 0700 on the experimental-day, rats remained sedentary or swam in a barrel filled with water (35°C) for four 30-min bouts (5-min rest between

bouts) as previously described [19, 29, 40]. Some rats were anesthetized (intraperitoneal sodium pentobarbital, 50mg/kg weight) immediately post-exercise (IPEX and sedentary-controls), weighed, and epitrochlearis muscles were dissected and used either for immunohistochemical analyses or measuring single fiber insulin-independent glucose uptake. Other rats were anesthetized ~3h post-exercise (3hPEX and sedentary-controls), weighed, epitrochlearis muscles were dissected and used for measuring insulin-stimulated glucose uptake and fiber type in single fibers. Epididymal fat pads were dissected and weighed. Muscles used for immunohistochemical analyses were embedded in Tissue-Tek (Sakura, Torrance,CA), snap frozen in liquid nitrogen-cooled isopentane, and stored (-80°C) until analyzed.

Ex vivo muscle incubations. Dissected muscles used for single fiber glucose uptake were incubated in glass vials gassed (95% O_2, 5% CO_2) in a temperature-controlled bath for a four-step process (35°C during steps 1, 2 and 4; step 3 was on ice) essentially as previously described [29, 30]. For muscles from the IPEX experiment, in the first step, isolated muscles were placed for 10 min in vials containing 2 ml of media 1 [Krebs-Henseleit buffer (KHB) supplemented with 0.1% bovine serum albumin (BSA), 2 mM sodium pyruvate, and 6 mM mannitol]. In the second step, the muscles were incubated for 30 min in a vial containing 2 ml step 2 media [KHB supplemented with 0.1% BSA, 0.1 mM 2-DG (13.5 mCi/mmol 2-[^{3}H]DG), 2 mM sodium pyruvate, and 6 mM mannitol]. In the 3rd step, muscles were rinsed 3 times (5 min/rinse with shaking at 115 rpm) in ice cold rinse media (Ca^{2+}-free KHB along with 0.1% BSA and 8 mM glucose) to wash 2-[^{3}H]DG from the extracellular space. During the 4th step, muscles were incubated for 60 min in vials that included collagenase media (rinse media along with 8 mM glucose and 2.5% type 2 collagenase) to enzymatically digest muscle collagen. For the muscles from the 3hPEX experiment, during the 1st step, the media included KHB plus 2 mM sodium pyruvate and 6 mM mannitol with either 0 or 100 μU/ml insulin. During the second step, muscles were incubated for 60 min in media which was the same as the 1st step, but supplemented with 0.1 mM 2-deoxy-d-glucose and 13.5 mCi/mmol 2-[^{3}H]DG. The 3rd and 4th steps in the 3hPEX experiment were identical to the 3rd and 4th steps for the IPEX experiment.

Isolation and processing of single fibers. Under a dissecting microscope (EZ4D; Leica, Buffalo Grove,IL), intact single fibers (~55 fibers/muscle) were gently isolated using fine forceps [41]. After isolation, each fiber was imaged using a camera-enabled microscope with

Leica Application Suite EZ software. After imaging, fibers were transferred into individual tubes, processed for glucose uptake, MHC, and immunoblotting as previously described [30, 41].

Glucose uptake and MHC. Each lysed fiber was processed for glucose uptake and MHC isoform identification as previously described [29, 41].

Glycogen. External standards of known glycogen concentrations (2, 10, 25, 50, 100, and 150 mmol/L) were created as previously described [42]. PAS staining of 8μm sections of these external glycogen standards was performed on all slides to reliably compare staining of muscle sections on separate slides.

Muscles were serially sectioned at 8μm for PAS staining and MHC detection. Slides used for PAS staining were fixed in 10% formalin (1h; 4°C). Following fixation, slides were treated with 1% periodic acid (room temperature, 5min) and washed (deionized water, 1min) before Schiff's Reagent was applied (10min). Slides were then quickly washed (deionized water, ~5sec) and gently rinsed in tap water (10min) before being mounted with Dako mounting medium. The muscle sections used for MHC identification were processed using appropriate primary and secondary antibodies. Antibodies against MHCI, MHCIIa, and MHCIIb were used for the immunofluorescent detection of fiber type. MHCIIx was identified by the absence of signal amongst the other three MHC isoforms as previously described [43]. After exposure to secondary antibodies, slides were incubated in WGA-AF488 (10min), washed in PBS, and mounted (Dako mounting medium).

Lipid droplet (LD) analysis. Muscles were serially sectioned (8μm) and thaw-mounted on glass slides (one section from each treatment on each slide to minimize staining variability). One slide was used for MHC identification and processed as described above. The other slide was used for BODIPY staining. BODIPY is a lipophilic dye which is widely used to stain neutral lipid droplets [44-46]. The slides used for BODIPY staining were immediately fixed in 10% formalin (1h, room temperature). Slides were then washed (PBS), incubated in a 1:500 dilution of 2mg/ml BODIPY 493/503 (30min), and washed again (PBS). Finally, slides then were stained with WGA-AF555, washed (PBS), and mounted (Dako mounting medium).

Image capture and processing. Images of cross-sectionally oriented muscles stained with PAS or MHC were imaged (20X) using a Zeiss Apotome microscope capable of widefield fluorescent and brightfield illumination coupled to a high resolution axiocam black and white camera system with DAPI, GFP, TRITC, and Cy5 filters. For BODIPY-stained muscle sections

(and corresponding MHC sections), a Nikon Confocal A1 microscope was used at 60X magnification (20X for MHC imaging) to image fluorescently labeled LDs and MHC expression. Image capture settings and conditions were kept constant to minimize variability. At least three images from different regions of each muscle section were taken for fiber analysis. Two researchers independently identified MHC expression of each fiber to confirm accurate fiber typing. After the fiber type was identified for PAS-stained images, up to 10 fibers of each fiber type were manually traced and quantified for PAS stain intensity from each image. For BODIPY-stained images, regions of interest representing individual fibers were identified by the WGA lectin extracellular matrix marker using ImageJ. Fiber borders were automatically identified using the "Analyze Particles" feature, and up to 8 fibers of each fiber type were used for LD analysis from a given image. An automated threshold representing positive LD signal was set using ImageJ and applied uniformly to all images. LD density was quantified as the percent covered by BODIPY stain. The region 1μm below the cell border (subsarcolemmal) was quantified for lipid density using the "Enlarge" and "Make Band" tools in ImageJ. LD size was determined using the "Analyze Particles" tool in ImageJ. Fiber cross sectional area (CSA) was quantified using BODIPY-stained images.

Immunoblotting. To measure fiber type-specific GLUT4 abundance, all of the single fiber lysates (non-heated) expressing the same MHC from a muscle from each rat from each group (LFD-SED, HFD-SED and HFD-3hPEX) were pooled together for GLUT4 immunoblotting. Aliquots of pooled fiber lysates were separated by SDS-PAGE using 10% gels, and then transferred to polyvinyl difluoride membranes. After electrotransfer, gels were stained (SimplyBlue™ SafeStain,1h, room temperature), then destained (deionized water, 2h). SimplyBlue-stained MHC bands quantified by densitometry (AlphaView; ProteinSimple, San Leandro,CA) were the loading controls for immunoblotted proteins [47, 48]. Membranes were incubated with primary and secondary antibodies, and subjected to enhanced chemiluminescence to quantify protein bands by densitometry. Individual values were normalized to the mean value of all samples on the membrane and divided by the corresponding MHC loading control.

Statistics. Data are expressed as mean±95% confidence interval (95% CI), with two-tailed significance levels of $\alpha<0.05$. Two-tailed *t*-tests were used to determine the diet-effect on daily caloric intake, epididymal fat pad mass, and body mass. One-way ANOVA was used to determine the treatment group-effect for GLUT4 abundance in pooled fibers of each fiber type

from each muscle. Because single fiber glucose uptake, glycogen, LD-measurements, and CSA were collected from multiple individual fibers per rat, we analyzed these data using mixed-effects linear regression models, incorporating fixed parameters evaluating the contributions of treatment group (LFD-SED, HFD-SED, HFD-IPEX or HFD-3hPEX) and insulin (insulin, no insulin; for glucose uptake only) and interaction-effects, a random Y-intercepts to account for multiple observations within each rat. The analysis revealed main effects of insulin dose or treatment (diet or exercise) group [i.e., the effect of one independent variable (insulin or treatment group) on the dependent variable (e.g., glucose uptake) distinct from the other independent variables (insulin or treatment group)]. The analysis also revealed if there were significant Insulin x Group (diet or exercise) interaction effects (i.e., if the magnitude of the insulin effect on the dependent variable (e.g., glucose uptake) was different between the treatment groups). Analyses were performed using StataIC 14.2 (College Station,TX).

RESULTS

Caloric intake, body mass and fat pad mass. Estimated daily caloric intake (kcal/day) was 22% greater ($P<0.001$) in HFD (105.8±4.8) versus LFD (86.4±3.8) rats. Body mass (g) was not significantly different ($P=0.116$) for the HFD (313±12) versus LFD (299±10) animals. Epididymal fat pad mass (g) was greater ($P<0.001$) for HFD (6.1±0.7) versus LFD rats (4.0±0.4).

MHC isoform expression. MHC isoform expression in each of the isolated single fibers was determined using SDS PAGE followed by protein staining (Figure 4.1).

Glucose uptake. For the HFD-IPEX group versus HFD-SED controls, insulin-independent glucose uptake was increased ($P<0.05$) in all fiber types (Figure 4.2). For the 3hPEX-experiment there was a significant main effect of insulin ($P<0.001$) on glucose uptake in each fiber type (Figure 4.3). In LFD-SED versus HFD-SED muscles, there was a significant insulin x treatment-group interaction on glucose uptake in type IIAX, IIX, IIBX and IIB fibers, where HFD reduced insulin-stimulated glucose uptake in these fiber types. In HFD-SED versus HFD-3hPEX muscles, there was a significant insulin x treatment-group interaction in type IIA, IIAX, IIX, IIBX, and IIB fibers, where insulin-stimulated glucose uptake was greater for HFD-3hPEX. There was a significant insulin x treatment-group interaction for LFD-SED versus HFD-

3hPEX in type IIA and IIBX fibers, where insulin-stimulated glucose uptake was greater for HFD-3hPEX rats.

Glycogen. All fiber types had lower ($P<0.05$) glycogen in the HFD-IPEX group versus LFD-SED and HFD-SED groups (Figures 4.4 and 4.5). The greater insulin-independent glucose uptake and lower glycogen IPEX provide strong evidence that the exercise protocol caused recruitment of all fiber types.

Lipid droplet (LD) analysis. Representative images of BODIPY-stained cross sections used for LD density and size analyses are displayed in Figure 4.6. The LD density, indicated by the percentage of fiber CSA covered by BODIPY-stained LDs, was lower ($P<0.05$) in LFD-SED versus either HFD-SED or HFD-IPEX in type IIA and IIAX fibers (Figure 4.7). In type I fibers the LD density was lower ($P<0.01$) in LFD-SED versus HFD-SED fibers. In type IIX fibers the LD density was lower ($P<0.05$) in LFD-SED versus HFD-IPEX fibers. Subsarcolemmal LD density was greater ($P<0.01$) in HFD-SED versus other groups for type I fibers (Figure 4.8). Additionally, subsarcolemmal LD density was greater ($P<0.05$) in HFD-IPEX versus other groups in type IIX fibers. LD size was greater ($P<0.05$) in HFD-SED versus other groups in type I fibers, and was lower ($P<0.05$) in LFD-SED versus HFD-SED in type IIA fibers (Figure 4.9). Subsarcolemmal LD size was not different among the groups for any fiber type (results not shown).

Muscle fiber CSA. Fiber CSA was determined from the MHC-stained cross sections used for lipid analysis. There were no significant treatment-group differences within any fiber type (results not shown).

GLUT4 protein. GLUT4 abundance was not significantly different among the treatment-groups (LFD-SED, HFD-SED and HFD-3hPEX) for any fiber type (Figure 4.10).

DISCUSSION

The results revealed a number of novel insights with regard to muscle fiber-type selective effects of acute exercise on glucose uptake in insulin resistant muscle. The most important results were: 1) in SED rats, the HFD resulted in fiber type-selective insulin resistance (no HFD-related insulin resistance in type I fibers, a non-significant trend for slightly lower values for IIA

fibers from HFD-fed rats, and significantly lower insulin-stimulated glucose uptake for all other fiber types from the HFD group); 2) the HFD-related insulin resistance was not accompanied by greater values for any of the LD indices (total LD size or density, or subsarcolemmal LD size or density) or lower GLUT4 abundance; 3) the recruitment of each fiber type was indirectly evidenced by both greater insulin-independent glucose uptake IPEX and lower glycogen measured IPEX; and 4) prior exercise resulted in fiber type-selective improvements in insulin-stimulated glucose uptake (no significant increase in type I fibers versus either SED control group; greater values versus HFD-SED controls for IIAX, IIX and IIB fibers; and greater values versus both HFD-SED and LFD-SED controls for type IIA and IIBX fibers) without an exercise-related increase in GLUT4 abundance in any of the fiber types.

The fiber type-selective insulin resistance corresponded closely with the results of our earlier study using the same dietary protocol only in sedentary rats [30]. Pearson correlation analysis performed between the mean sedentary values for glucose uptake of each fiber type from the previous experiment versus the corresponding sedentary control values in the current experiment revealed an $R^2 = 0.926$ ($P < 0.001$). The mechanisms underlying skeletal muscle fiber type-selective insulin resistance are uncertain, but the current study provided new insights in this regard. We did not detect a significant HFD-induced change in GLUT4 abundance in any fiber type. These results are consistent with the findings of our earlier study [30] for type I, IIA, IIAX, IIX and IIBX fibers. Although GLUT4 abundance was also not significantly different between diet groups in IIB fibers in the current study, we previously reported GLUT4 abundance was significantly lower for IIB fibers from HFD versus LFD rats using the same dietary protocol. In the earlier study, we evaluated GLUT4 abundance in individual fibers of each fiber type, whereas in the current study we determined GLUT4 in a pooled sample of all of the fibers collected for each fiber type in each diet group. In the earlier study, a total of 19 individual fibers from each diet group were analyzed for GLUT4. In the current study, GLUT4 abundance was analyzed using a total of 143 pooled fibers from LFD rats and 99 pooled fibers from HFD rats. The results from the larger number of fibers in the current study suggest that the HFD-induced insulin resistance in the current study was not attributable to significantly lower GLUT4 abundance in any of the fiber types. It is notable that earlier studies have reported that HFD-induced insulin resistance in whole muscles can occur without a decrement in total GLUT4 abundance [19, 49-51]. The localization of GLUT4 at the cell surface membranes is crucial for

insulin-stimulated glucose uptake [52], and in whole muscles, the insulin resistance was secondary to reduced insulin-stimulated cell surface GLUT4 localization [49, 51]. Similarly, the current data suggest that the observed fiber type-specific insulin resistance is attributable to fiber type-selective effects of the HFD on GLUT4 translocation.

IMCLs have been reported to be positively associated with insulin resistance [32], but this relationship is not always observed [33, 53]. Some studies have suggested that LDs localized near the sarcolemma [34, 35] and/or LD size [36] are more closely linked to insulin resistance than total IMCL content. Therefore, we assessed multiple indicators of IMCL content and subcellular localization in each fiber type. The current study is apparently the first to report fiber type-specific values determined in single muscle fibers for both insulin-stimulated glucose uptake and indicators of LD density, size and subcellular localization. We anticipated that there might be greater LD size and/or localization near the sarcolemma in the fiber types which became insulin resistant during a HFD. However, there was no clear relationship between insulin-stimulated glucose uptake and any of the LD measurements. Although total LD density was greater in HFD-SED versus LFD-SED rats for some of the fiber types that became insulin resistant (IIAX and IIX), none of the LD indices differed between diet groups in other fiber types with substantial insulin resistance (IIBX and IIB). Furthermore, although neither type I nor type IIA fibers had significant HFD-induced insulin resistance, both fiber types had greater HFD-related values for several LD indices. These results argue that these LD indices were likely not responsible for the HFD-induced insulin resistance. Accumulation of specific lipid metabolites, such as ceramides and/or diacylglycerols, has been implicated in the processes leading to skeletal muscle insulin resistance [54-56]. Furthermore, recent evidence has suggested that the subcellular location of diacylglycerols and ceramides, rather than their total concentrations, may modulate whole body insulin sensitivity [57]. In this context, it would be valuable to develop the novel methods that will be necessary to assess HFD-induced subcellular changes in these lipid metabolites at a fiber type-specific level.

To interpret the fiber type-selective consequences of exercise on insulin-stimulated glucose uptake, it was important to evaluate the effects of the exercise protocol on the recruitment of each fiber type that was studied. Electromyography (EMG) can directly assess muscle recruitment, but determination of single fiber type-selective EMG during swim exercise

was not feasible. Glycogen depletion is widely used as an indirect indicator of fiber recruitment during exercise [58-60]. Accumulation of [^{3}H]-2-DG is another useful indirect indicator of fiber recruitment at the whole muscle, motor unit and single fiber level [29, 61, 62]. The current study is apparently the first to use both glycogen depletion and [^{3}H]-2-DG accumulation as indirect evidence for recruitment of individual fibers after *in vivo* exercise. There was a strong indication of fiber recruitment in every fiber type based on the increased insulin-independent glucose uptake and decreased glycogen in the IPEX group compared to SED controls.

Although there was evidence that each fiber type was recruited by the exercise, there were striking fiber type-related differences in exercise effects on insulin-stimulated glucose uptake determined in the 3hPEX experiment. The results revealed several distinct patterns with regard to exercise-effects on insulin-stimulated glucose uptake. In type IIB and IIX fibers, which were both characterized by HFD-induced insulin resistance, prior exercise increased insulin-stimulated glucose uptake to values that exceeded their HFD-SED controls, but exercise failed to increase insulin-stimulated glucose uptake by either fiber type above their respective LFD-SED controls. In type IIA and IIBX fibers, prior exercise increased insulin-stimulated glucose uptake to levels that not only exceeded their HFD-SED controls, but that also exceeded their LFD-SED controls. Insulin-stimulated glucose uptake of type IIAX fibers was also greater than HFD-SED controls, but they did not significantly exceed their LFD-SED controls. Prior exercise only failed to induce significantly greater insulin-stimulated glucose uptake versus HFD-SED controls in type I fibers. The explanation for the lack of an increase in insulin-stimulated glucose uptake in HFD-SED compared to HFD-3hPEX type I fibers is uncertain, but it is apparently not attributable to a lack of type I fiber recruitment, as evidenced by clear exercise-effects on both insulin-independent glucose uptake and glycogen determined IPEX.

It is useful to put the fiber type-specific results for glucose uptake into context based on earlier results for the whole muscles from rats using the same diet and exercise protocol. In whole epitrochlearis muscles, we previously found: 1) the HFD caused a moderate level of insulin resistance that was similar to the results in most of the individual fiber types; 2) insulin-independent glucose uptake was increased ~2-fold for IPEX versus HFD-SED controls, comparable to the ~2-3-fold increase in each of the fiber types; 3) exercise enhanced the insulin-stimulated glucose uptake of the HFD-3hPEX group to values ~30% greater than LFD-SED

controls, which roughly approximates the mid-point for the range of exercise-effects in the different fiber types; and 4) insulin-stimulated glucose uptake of the HFD-3hPEX rats was increased to values that were similar to their LFD-SED controls for each fiber type (i.e., prior exercise eliminated HFD-induced insulin resistance in the whole epitrochlearis) [19]. There was good correspondence between the glucose uptake by whole epitrochlearis and glucose uptake by single fibers with regard to the effects of diet and exercise (both IPEX and 3hPEX). The heterogeneity in diet- and exercise-effects among the fiber types for insulin-stimulated glucose uptake that was revealed by single fiber analysis would have been impossible to discern based only on the conventional analysis of whole muscles.

Although the current study was the first to assess the fiber type-selective effects of exercise on glucose uptake by single fibers from insulin resistant muscle, we recently reported the effects of the same exercise protocol on insulin-stimulated glucose uptake by single fibers from rats eating a LFD that were not insulin resistant [29]. As in the current study, insulin-independent glucose uptake was increased in each fiber type evaluated IPEX compared to SED controls. However, at ~3h post-exercise, insulin-stimulated glucose uptake was significantly increased in type I fibers and each of the type II fiber types evaluated except for type IIX fibers. Given that exercise increased insulin-stimulated glucose uptake by type I fibers in LFD rats [29], and that the HFD did not cause insulin resistance in type I fibers in either the current study or an earlier study [30], it was surprising that exercise did not enhance insulin-stimulated glucose uptake in type I fibers of HFD-fed rats in the current study. The results for type IIX fibers in the current study indicated that prior exercise increased insulin-stimulated glucose uptake above values for HFD-SED controls, but exercise failed to elevate values above those for the LFD-SED controls. The available results do not reveal the reason that LFD and HFD rats had different effects of exercise on insulin-stimulated glucose uptake in type I fibers, or why exercise failed to increase insulin-stimulated glucose uptake of type IIX fibers above LFD-SED controls in either diet group. A speculative scenario is that the time-course for exercise-induced increase in insulin-stimulated glucose uptake may not be identical for all fiber types. For example, perhaps the insulin sensitivity was transiently increased in type I fibers from HFD rats at an earlier time-point, but had reversed by 3hPEX. The time-course for post-exercise increases in insulin-stimulated glucose uptake by the whole epitrochlearis muscle has been reported at multiple times between 0.5 and 48 hours post-exercise, with peak values evident at ~3hPEX [11, 12, 63].

However, the current study is the first to evaluate post-exercise insulin sensitivity at the single fiber level in insulin resistant muscle, and only one earlier study assessed single fiber insulin sensitivity after exercise in normal muscle [29]. In both studies, insulin-stimulated glucose uptake was determined only at ~3hPEX, so the time-course for post-exercise effects on insulin sensitivity in individual fiber types has not been characterized.

An important next step will be to elucidate the specific, cellular mechanisms which underlie the differential post-exercise effects that we have discovered for insulin-stimulated glucose uptake in various fiber types. Our working hypothesis is based on our results in whole epitrochlearis muscles from LFD and HFD rats after the same exercise protocol. In several studies using LFD rats, we found that prior exercise resulted in greater phosphorylation of the Rab-GAP protein known as Akt substrate of 160 kDa (also called AS160 or TBC1D4) in insulin-stimulated muscles on sites that are important for GLUT4 glucose transporter translocation and glucose uptake [19, 63-65]. We also found that HFD resulted in attenuated AS160 phosphorylation, and that acute exercise by HFD-fed rats increased AS160 phosphorylation in insulin-stimulated muscles [19]. Results from multiple studies using rats, mice or humans have reported the increased insulin-stimulated glucose uptake can occur without alterations in proximal insulin signaling steps, from insulin receptor binding to Akt activation [15, 16, 19, 66-68]. We hypothesize that in insulin-stimulated muscles from both LFD- and HFD-fed rats, prior exercise will lead to greater phosphorylation of AS160 on key regulatory sites in a fiber type-specific manner by exercise, resulting in greater cell surface GLUT4 localization, leading in turn, to the fiber type-specific effects of exercise on insulin-stimulated glucose uptake.

In conclusion, glucose uptake occurs at the cellular level, and skeletal muscle is composed of fiber types with diverse metabolic properties [23], including their capacity for glucose uptake [28, 29, 69]. Accordingly, it is impossible to fully understand the effect of interventions on skeletal muscle glucose uptake without evaluating the possibility of differences at the cellular and fiber type-specific level. By doing so, we made the unexpected discovery that exercise robustly enhanced insulin-stimulated glucose uptake in each of the insulin resistant fiber types (including the fiber types with the greatest insulin resistance), but it did not significantly elevate insulin-stimulated glucose uptake above HFD-SED controls in the type I fibers (which did not become insulin resistant with the HFD). These unique results offer an opportunity for

future research aimed at delineating the cellular mechanisms that were responsible for the fiber type-selective effects of diet and exercise in glucose uptake.

ACKNOWLEDGEMENTS

These experiments were supported by a grant from the National Institutes of Health (R01 DK71771). This study has been published; Pataky MW, Yu CS, Nie Y, Arias EB, Singh M, Mendias CL, Ploutz-Snyder RJ, & Cartee GD. *American Journal of Physiology-Endocrinology and Metabolism, 316*(5), E695-E706. I would also like to thank Dr. Haiyan Wang and Dr. Xiaohua Zheng for their technical assistance with this study.

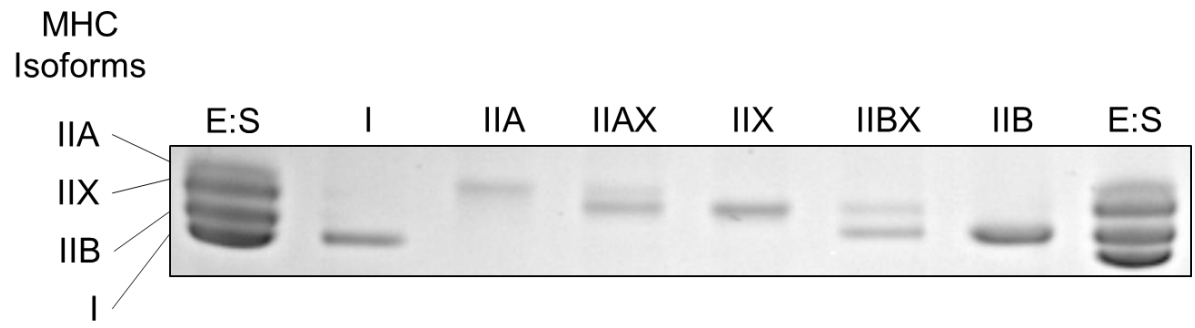

Figure 4.1

Representative image of SDS-PAGE gel of single fibers for the identification of fiber type. *Lanes 1 and 8*: E+S, pooled EDL + Soleus standard expressing MHC (myosin heavy chain) types I, IIA, IIX, and IIB. *Lane 2*: type I fiber. *Lane 3*: type IIA fiber. *Lane 4*: type IIAX fiber. *Lane 5*: type IIX fiber. *Lane 6*: type IIBX fiber. *Lane 7*: type IIB fiber.

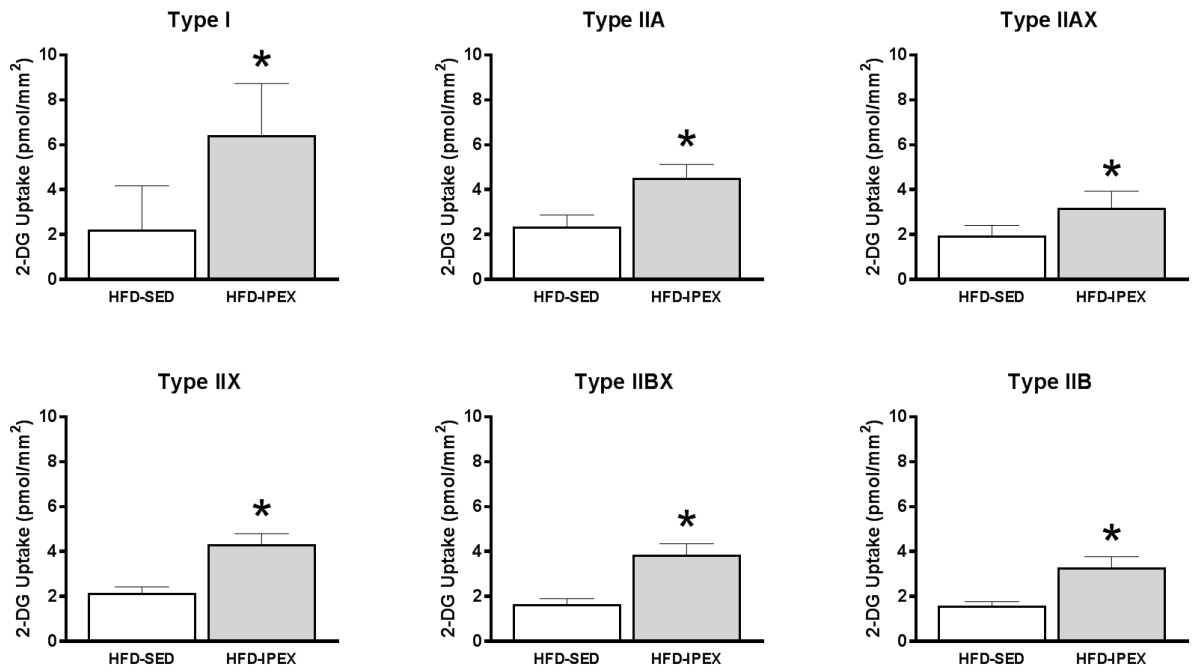

Figure 4.2

Insulin independent 2-DG uptake measured immediately post-exercise in single fibers of each fiber type from rats. Bars represent the mean of all fibers within a given treatment group (HFD-SED or HFD-IPEX). Error bars are means ± 95% confidence interval. *P<0.05, HFD-IPEX versus HFD-SED. The numbers of rats used for the groups in this experiment were; HFD-SED (n=8), and HFD-IPEX (n=8). All of the fibers isolated from each muscle (~40-56 fibers/muscle) were used to determine both 2DG uptake and MHC expression. However, not every fiber type was included in the fibers sampled from every muscle. Therefore, the number of rats (HFD-SED/HFD-IPEX) from which fibers were isolated of each fiber type were: type I (3/7), type IIA (7/7), type IIAX (7/7), type IIX (8/8), type IIBX (8/7), and type IIB (8/8). The numbers of fibers (HFD-SED/HFD-IPEX) isolated for each fiber type were: type I (8/17), type IIA (43/59), type IIAX (15/27), type IIX (94/94), type IIBX (72/75), and type IIB (144/120).

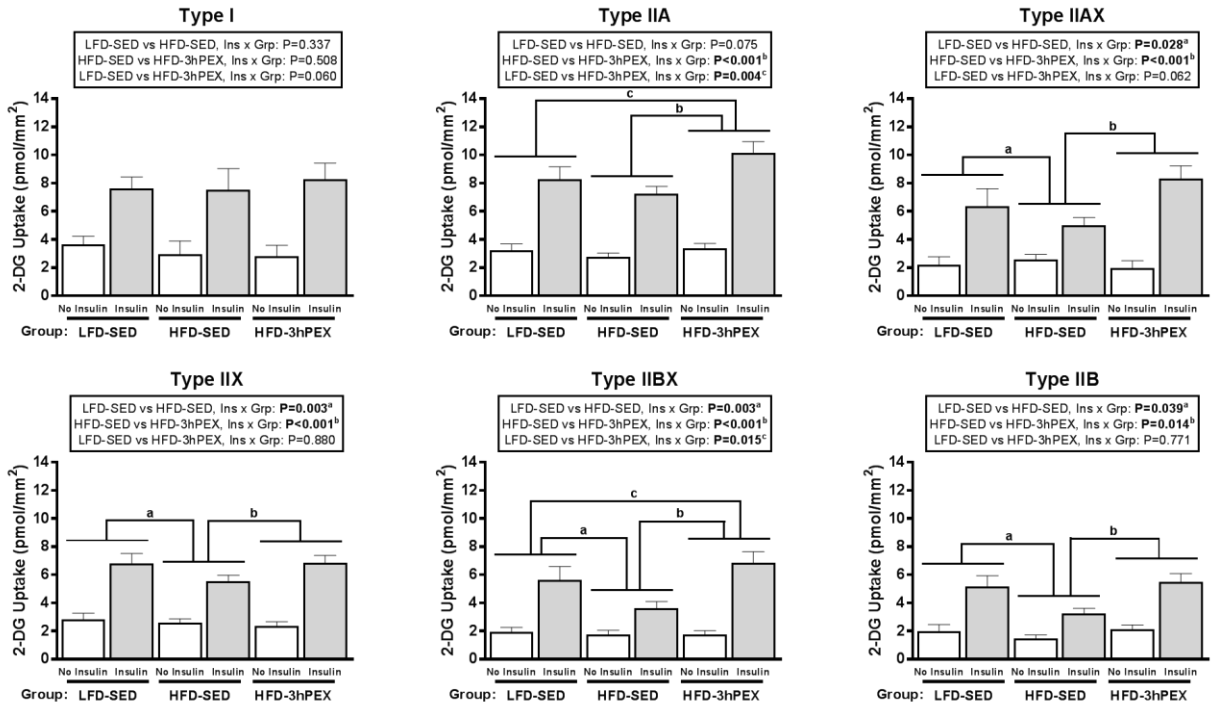

Figure 4.3

2-DG uptake measured in single fibers of each fiber type isolated from incubated paired rat muscles without or with insulin. Paired muscles were used within each treatment group (LFD-SED, HFD-SED, and HFD-3hPEX) for incubation without or with 100µU/ml insulin. Bars represent the mean of all fibers within a given insulin treatment and group. Error bars are means ± 95% confidence interval. P<0.05 was considered statistically significant. A main effect of insulin was detected for all fiber types. There was no significant main effect of group detected for any fiber type. Insulin x Group interaction effects are displayed above each fiber type and P-values are displayed. Insulin x Group interaction effects between LFD-SED vs HFD-SED, HFD-SED vs HFD-3hPEX, and LFD-SED vs HFD-3hPEX are indicated by symbols [a], [b], and [c], respectively. The numbers of rats used for the groups in this experiment were; LFD-SED (n=8), HFD-SED (n=12), and HFD-3hPEX (n=12). All of the fibers isolated from each muscle (~20-56 fibers/muscle) were used to determine both 2DG uptake and MHC expression. However, not every fiber type was included in the fibers sampled from every muscle. Therefore, the number of rats (LFD-SED no insulin/insulin, HFD-SED no insulin/insulin, HFD-3hPEX no insulin/insulin) from which fibers were isolated of each fiber type were: type I (5/5, 7/7, 7/7), type IIA (6/7, 12/12, 12/12), type IIAX (8/6, 10/9, 6/8), type IIX (8/8, 12/12, 12/12), type IIBX (8/8, 11/10, 12/10), and type IIB (8/8, 8/9, 12/8). The numbers of fibers (LFD-SED no insulin/insulin, HFD-SED no insulin/insulin, HFD-3hPEX no insulin/insulin) isolated for each fiber type were: type I (30/37, 16/12, 16/26), type IIA (114/103, 162/166, 142/165), type IIAX (38/33, 75/66, 38/35), type IIX (79/104, 156/183, 131/127), type IIBX (44/47, 59/53, 91/74), and type IIB (74/69, 48/62, 102/109).

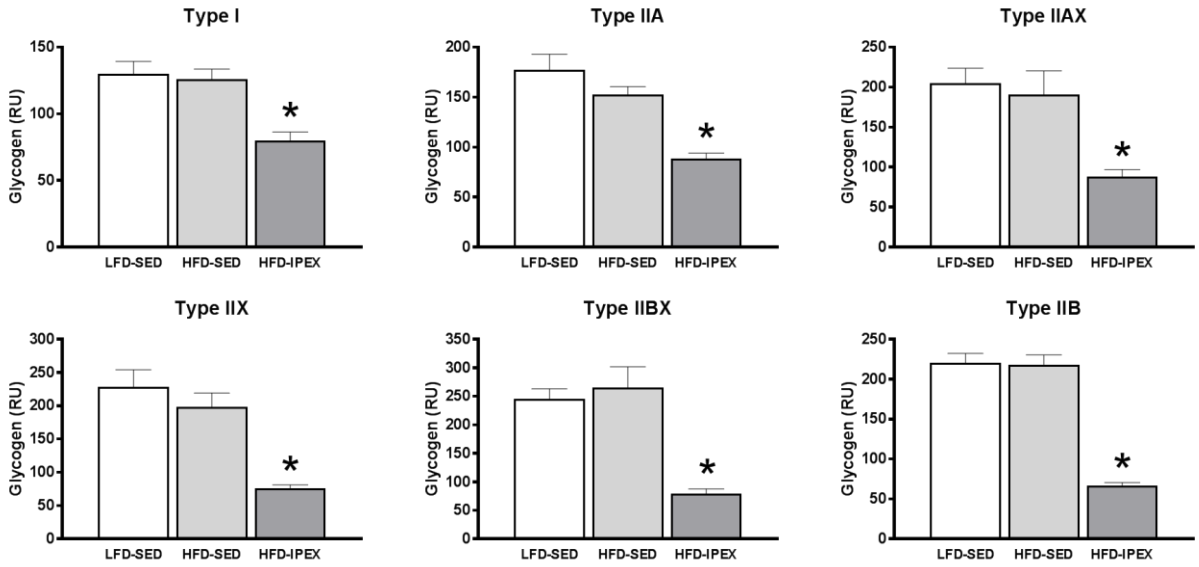

Figure 4.4

Glycogen content in single fibers of each fiber type measured by periodic acid-Schiff staining of histologically sectioned rat muscle. Bars represent the mean of all fibers within a given treatment group (LFD-SED, HFD-SED, or HFD-IPEX). Error bars are means ± 95% confidence interval. *P<0.05, HFD-IPEX versus LFD-SED and HFD-SED. The numbers of rats used for the groups in this experiment were: LFD-SED (n=4), HFD-SED (n=4), and HFD-IPEX (n=4). 39-116 fibers/muscle were used to determine glycogen content. There was one HFD-SED muscle and one LFD-SED muscle for which no type IIAX fibers were identified. Additionally, there was one HFD-SED muscle for which no type IIBX fibers were identified. The numbers of fibers (LFD-SED/HFD-SED/HFD-IPEX) used for glycogen measurement of each fiber type were: type I (56/22/54), type IIA (66/74/60), type IIAX (39/19/33), type IIX (25/50/72), type IIBX (28/18/25), and type IIB (72/79/107).

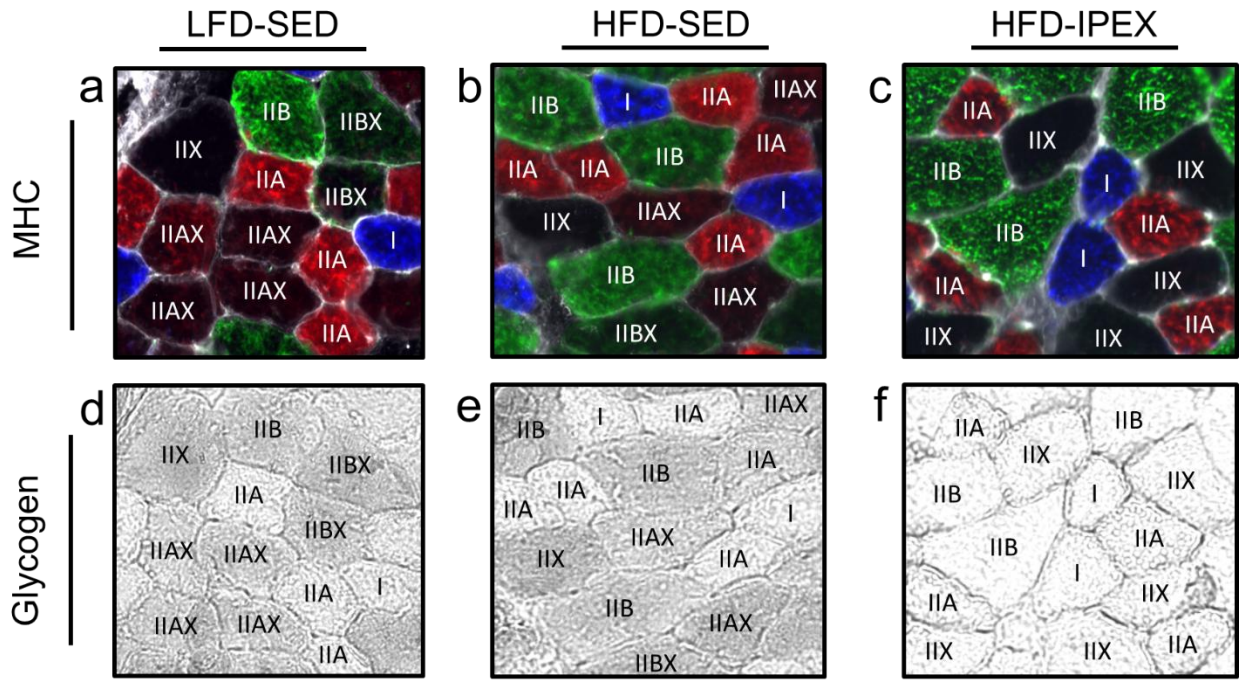

Figure 4.5

Representative images of serially cross sectioned rat muscle for the identification of glycogen content and fiber type. Serially sectioned muscle from LFD-SED (**a** and **d**), HFD-SED (**b** and **e**), and HFD-IPEX (**c** and **f**) are shown. Type I MHC is shown in blue, type IIA MHC is shown in red, type IIB MHC is shown in green, and type IIX MHC is represented by an absence of signal (black). Glycogen content was determined by the stain intensity (by grayscale) within each fiber.

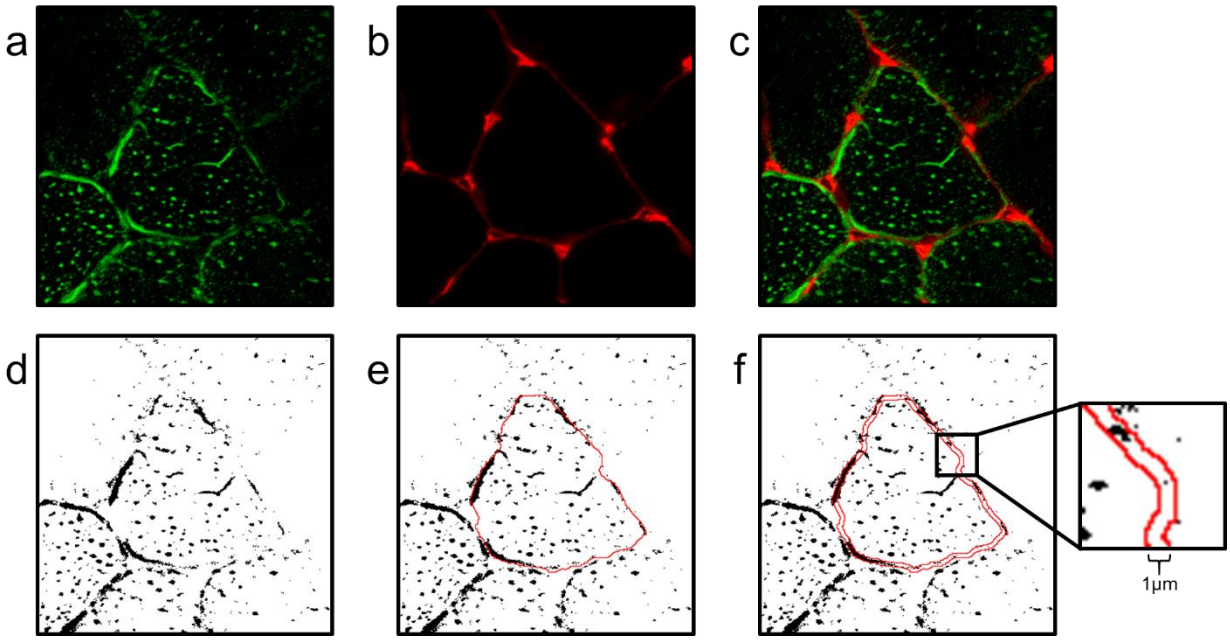

Figure 4.6

Representative images of a cross section of rat muscle used to identify fiber specific neutral lipids. Images were captured for the identification of neutral lipids (**a**) and the extracellular matrix (ECM) (**b**). Merged lipid and ECM images are shown (**c**). Using ImageJ an automated threshold (**d**) was applied and the border of each fiber was identified (**e**). A region 1µm from the border of each fiber was used for the quantification of subsarcolemmal lipids (**f**).

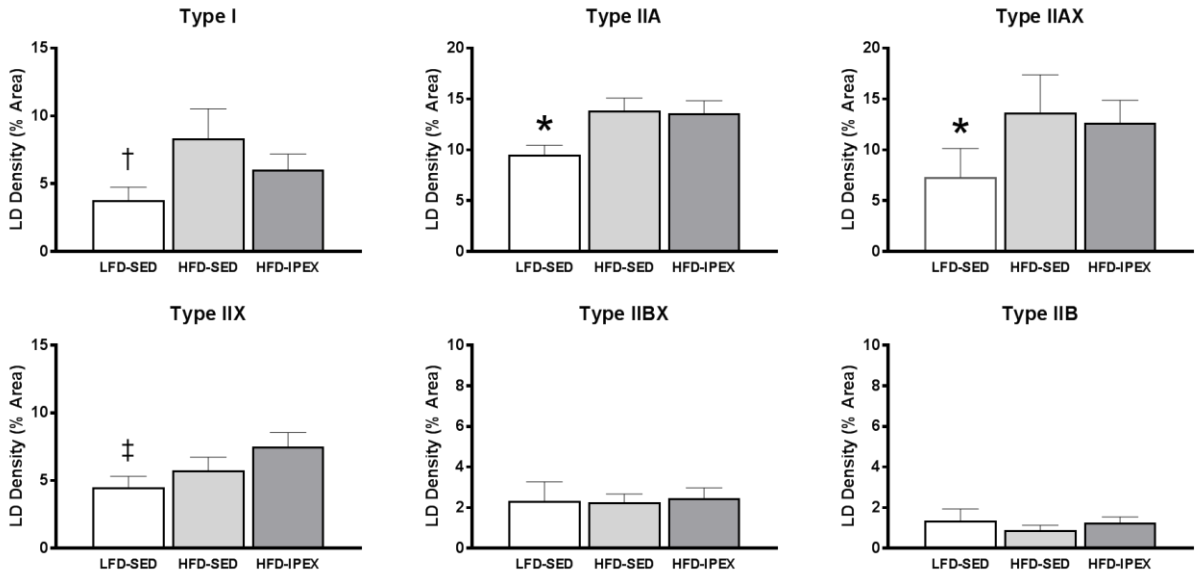

Figure 4.7

Quantification of lipid droplet density in single fibers of each fiber type measured by BODIPY staining of histologically sectioned rat muscle. Bars represent the mean of all fibers within a given treatment group (LFD-SED, HFD-SED, or HFD-IPEX). Error bars are means ± 95% confidence interval. *P<0.05, different from both other groups. †P<0.05, LFD-SED versus HFD-SED. ‡P<0.05, LFD-SED versus HFD-IPEX. The numbers of rats used for the groups in this experiment were: LFD-SED (n=4), HFD-SED (n=4), and HFD-IPEX (n=4). 24-77 fibers/muscle were used to determine lipid droplet density. There was one HFD-SED muscle for which no type IIAX fibers were identified. The numbers of fibers (LFD-SED/HFD-SED/HFD-IPEX) used for lipid droplet density of each fiber type were: type I (31/23/32), type IIA (61/43/54), type IIAX (12/9/17), type IIX (43/34/53), type IIBX (14/19/27), and type IIB (40/33/59).

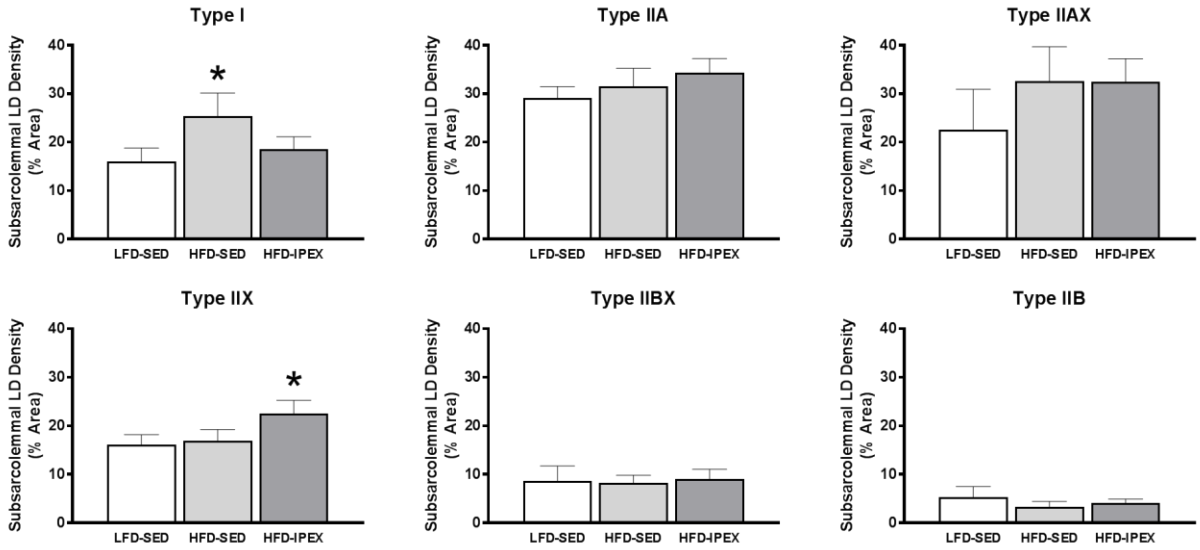

Figure 4.8

Quantification of the density of lipid droplets located <1µm from the sarcolemma in single fibers of each fiber type. Bars represent the mean of all fibers within a given treatment group (LFD-SED, HFD-SED, or HFD-IPEX). Error bars are means ± 95% confidence interval. *P<0.05, different from both other groups. Subsarcolemmal lipid droplet density was quantified from the same images as total lipid droplet density. Therefore, the rat numbers and fiber numbers are identical to those displayed in the Figure 4.7 legend.

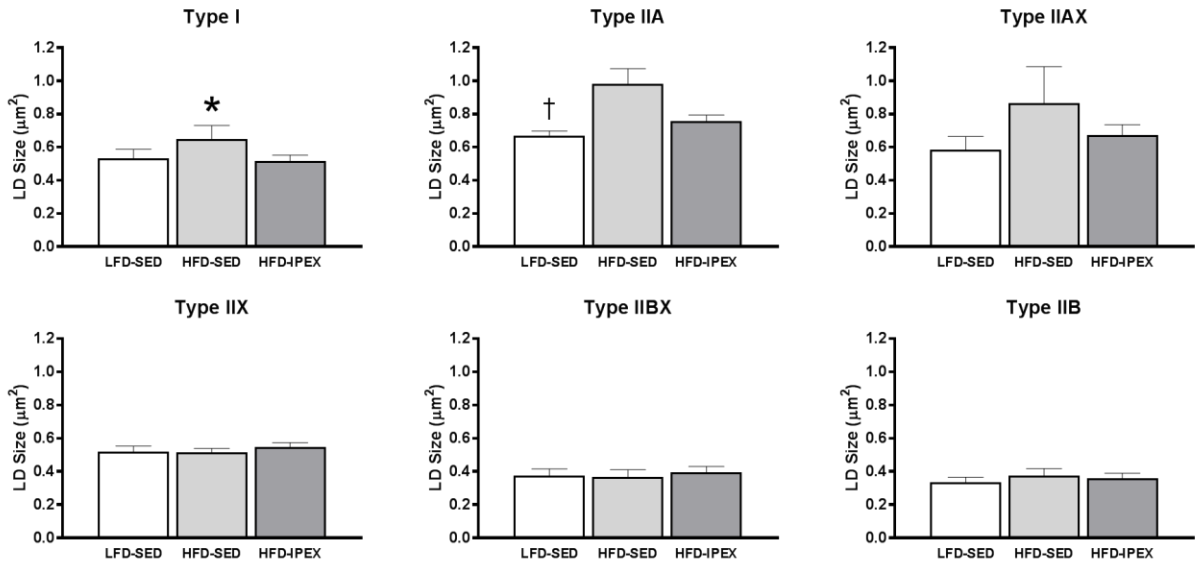

Figure 4.9

Quantification of lipid droplet size in single fibers of each fiber type measured by BODIPY staining of histologically sectioned rat muscle. Bars represent the mean of all fibers within a given treatment group (LFD-SED, HFD-SED, or HFD-IPEX). Error bars are means ± 95% confidence interval. *P<0.05, different from both other groups. †P<0.05, LFD-SED versus HFD-SED. Lipid droplet size was quantified from the same images as lipid droplet density. Therefore, the rat numbers and fiber numbers are identical to those displayed in the Figure 4.7 legend.

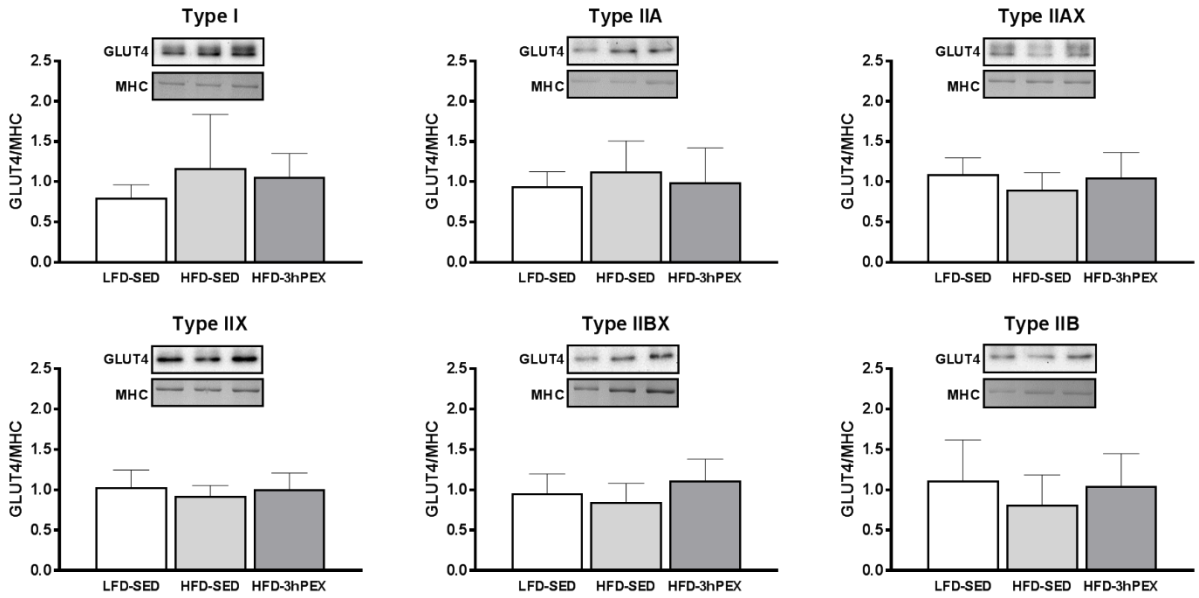

Figure 4.10

Glucose transporter protein, GLUT4, abundance in pooled single fibers of each fiber type. Bars represent the mean of fiber pools within a given treatment group (LFD-SED, HFD-SED, or HFD-3hPEX). Error bars are means ± 95% confidence interval; n = 6-8/group. There were no significant differences among treatment groups for any fiber type.

Antibodies and fluorescent probes

Antibody/Probe	Catalog #	Source	Primary or Secondary	Dilution	Use
Anti-GLUT4	CBL-243	EMD Millipore (Billerica, MA)	Primary	1:100	Immunoblotting
Anti-Rabbit IgG	7074	Cell Signaling Technology (Danvers, MA)	Secondary	1:20,000	Immunoblotting
Anti-MHC type IIB (IgM)	BF-F3	DSHB University of Iowa (Iowa City, IA)	Primary	1:100	Immunohistochemistry
Anti-MHC type IIA (IgG1)	SC-71	DSHB University of Iowa (Iowa City, IA)	Primary	1:500	Immunohistochemistry
Anti-MHC type I (IgG2b)	BA-D5	DSHB University of Iowa (Iowa City, IA)	Primary	1:50	Immunohistochemistry
Alexa Fluor 555 IgM	A-21043	ThermoFisher (Pittsburgh, PA)	Secondary	1:500	Immunohistochemistry
Alexa Fluor 647 IgG1	A-21240	ThermoFisher (Pittsburgh, PA)	Secondary	1:500	Immunohistochemistry
Alexa Fluor 350 IgG2b	A-21140	ThermoFisher (Pittsburgh, PA)	Secondary	1:500	Immunohistochemistry
BODIPY 493/503 (2mg/mL)	D3922	ThermoFisher (Pittsburgh, PA)	N/A	1:500	Fluorescent Probe
WGA-Alexa Fluor 488 (1mg/mL)	W11261	ThermoFisher (Pittsburgh, PA)	N/A	1:200	Fluorescent Probe
WGA-Alexa Fluor 555 (1mg/mL)	W32464	ThermoFisher (Pittsburgh, PA)	N/A	1:200	Fluorescent Probe

Table 4.1

Summary of antibodies and fluorescent probes used for immunoblotting and immunohistochemistry. All antibodies were validated by the vendor.

REFERENCES

1. *National diabetes statistics report, 2017*, in *Atlanta, GA: Centers for Disease Control and Prevention, US Dept of Health and Human Services*. 2017.
2. DeFronzo, R., E. Jacot, E. Jequier, E. Maeder, J. Wahren, and J. Felber, *The effect of insulin on the disposal of intravenous glucose: results from indirect calorimetry and hepatic and femoral venous catheterization.* Diabetes, 1981. **30**(12): p. 1000-1007.
3. Ng, J.M., K. Azuma, C. Kelley, R. Pencek, Z. Radikova, C. Laymon, J. Price, B.H. Goodpaster, and D.E. Kelley, *PET imaging reveals distinctive roles for different regional adipose tissue depots in systemic glucose metabolism in nonobese humans.* American Journal of Physiology-Endocrinology and Metabolism, 2012. **303**(9): p. E1134-E1141.
4. Facchini, F.S., N. Hua, F. Abbasi, and G.M. Reaven, *Insulin resistance as a predictor of age-related diseases.* The Journal of Clinical Endocrinology & Metabolism, 2001. **86**(8): p. 3574-3578.
5. Haffner, S.M., *Epidemiology of insulin resistance and its relation to coronary artery disease.* The American journal of cardiology, 1999. **84**(1): p. 11-14.
6. Kumari, M., E. Brunner, and R. Fuhrer, *Minireview: mechanisms by which the metabolic syndrome and diabetes impair memory.* The Journals of Gerontology Series A: Biological Sciences and Medical Sciences, 2000. **55**(5): p. B228-B232.
7. Richter, E.A., L.P. Garetto, M.N. Goodman, and N.B. Ruderman, *Muscle glucose metabolism following exercise in the rat: increased sensitivity to insulin.* Journal of Clinical Investigation, 1982. **69**(4): p. 785-793.
8. Bonen, A., M. Tan, and W. Watson-Wright, *Effects of exercise on insulin binding and glucose metabolism in muscle.* Canadian journal of physiology and pharmacology, 1984. **62**(12): p. 1500-1504.
9. Garetto, L.P., E.A. Richter, M.N. Goodman, and N.B. Ruderman, *Enhanced muscle glucose metabolism after exercise in the rat: the two phases.* American Journal of Physiology-Endocrinology And Metabolism, 1984. **246**(6): p. E471-E475.
10. Richter, E.A., T. Ploug, and H. Galbo, *Increased muscle glucose uptake after exercise: no need for insulin during exercise.* Diabetes, 1985. **34**(10): p. 1041-1048.
11. Wallberg-Henriksson, H., S. Constable, D. Young, and J. Holloszy, *Glucose transport into rat skeletal muscle: interaction between exercise and insulin.* Journal of applied physiology, 1988. **65**(2): p. 909-913.
12. Cartee, G.D., D.A. Young, M.D. Sleeper, J. Zierath, H. Wallberg-Henriksson, and J.O. Holloszy, *Prolonged increase in insulin-stimulated glucose transport in muscle after exercise.* Am J Physiol, 1989. **256**(4 Pt 1): p. E494-9.
13. Betts, J.J., W.M. Sherman, M.J. Reed, and J.P. Gao, *Duration of improved muscle glucose uptake after acute exercise in obese Zucker rats.* Obesity, 1993. **1**(4): p. 295-302.
14. Perseghin, G., T.B. Price, K.F. Petersen, M. Roden, G.W. Cline, K. Gerow, D.L. Rothman, and G.I. Shulman, *Increased glucose transport–phosphorylation and muscle glycogen synthesis after exercise training in insulin-resistant subjects.* New England Journal of Medicine, 1996. **335**(18): p. 1357-1362.
15. Cartee, G.D., *Roles of TBC1D1 and TBC1D4 in insulin-and exercise-stimulated glucose transport of skeletal muscle.* Diabetologia, 2015. **58**(1): p. 19-30.
16. Wojtaszewski, J.F., B.F. Hansen, B. Kiens, and E.A. Richter, *Insulin signaling in human skeletal muscle: time course and effect of exercise.* Diabetes, 1997. **46**(11): p. 1775-1781.

17. Richter, E.A., K. Mikines, H. Galbo, and B. Kiens, *Effect of exercise on insulin action in human skeletal muscle.* Journal of applied physiology, 1989. **66**(2): p. 876-885.
18. Annuzzi, G., G. Riccardi, B. Capaldo, and L. KAUSER, *Increased insulin-stimulated glucose uptake by exercised human muscles one day after prolonged physical exercise.* European journal of clinical investigation, 1991. **21**(1): p. 6-12.
19. Castorena, C.M., E.B. Arias, N. Sharma, and G.D. Cartee, *Postexercise improvement in insulin-stimulated glucose uptake occurs concomitant with greater AS160 phosphorylation in muscle from normal and insulin-resistant rats.* Diabetes, 2014. **63**(7): p. 2297-308.
20. Devlin, J.T., M. Hirshman, E.D. Horton, and E.S. Horton, *Enhanced peripheral and splanchnic insulin sensitivity in NIDDM men after single bout of exercise.* Diabetes, 1987. **36**(4): p. 434-439.
21. Devlin, J. and E. Horton, *Effects of prior high-intensity exercise on glucose metabolism in normal and insulin-resistant men.* Diabetes, 1985. **34**(10): p. 973-979.
22. Cartee, G.D., *Mechanisms for greater insulin-stimulated glucose uptake in normal and insulin-resistant skeletal muscle after acute exercise.* American Journal of Physiology-Endocrinology and Metabolism, 2015. **309**(12): p. E949-E959.
23. Pette, D. and R.S. Staron, *Cellular and molecular diversities of mammalian skeletal muscle fibers.* Rev Physiol Biochem Pharmacol, 1990. **116**: p. 1-76.
24. Caiozzo, V.J., M.J. Baker, K. Huang, H. Chou, Y.Z. Wu, and K.M. Baldwin, *Single-fiber myosin heavy chain polymorphism: how many patterns and what proportions?* Am J Physiol Regul Integr Comp Physiol, 2003. **285**(3): p. R570-80.
25. Stephenson, G.M., *Hybrid skeletal muscle fibres: a rare or common phenomenon?* Clin Exp Pharmacol Physiol, 2001. **28**(8): p. 692-702.
26. Zhang, M.Y., W.J. Zhang, and S. Medler, *The continuum of hybrid IIX/IIB fibers in normal mouse muscles: MHC isoform proportions and spatial distribution within single fibers.* Am J Physiol Regul Integr Comp Physiol, 2010. **299**(6): p. R1582-91.
27. Williamson, D.L., P.M. Gallagher, C.C. Carroll, U. Raue, and S.W. Trappe, *Reduction in hybrid single muscle fiber proportions with resistance training in humans.* J Appl Physiol (1985), 2001. **91**(5): p. 1955-61.
28. Mackrell, J.G. and G.D. Cartee, *A novel method to measure glucose uptake and myosin heavy chain isoform expression of single fibers from rat skeletal muscle.* Diabetes, 2012. **61**(5): p. 995-1003.
29. Cartee, G.D., E.B. Arias, S.Y. Carmen, and M.W. Pataky, *Novel single skeletal muscle fiber analysis reveals a fiber type-selective effect of acute exercise on glucose uptake.* American Journal of Physiology-Endocrinology and Metabolism, 2016. **311**(5): p. E818-E824.
30. Pataky, M.W., H. Wang, C.S. Yu, E.B. Arias, R.J. Ploutz-Snyder, X. Zheng, and G.D. Cartee, *High-Fat Diet-Induced Insulin Resistance in Single Skeletal Muscle Fibers is Fiber Type Selective.* Sci Rep, 2017. **7**(1): p. 13642.
31. Turner, N., G.M. Kowalski, S.J. Leslie, S. Risis, C. Yang, R.S. Lee-Young, J.R. Babb, P.J. Meikle, G.I. Lancaster, D.C. Henstridge, P.J. White, E.W. Kraegen, A. Marette, G.J. Cooney, M.A. Febbraio, and C.R. Bruce, *Distinct patterns of tissue-specific lipid accumulation during the induction of insulin resistance in mice by high-fat feeding.* Diabetologia, 2013. **56**(7): p. 1638-48.

32. Krssak, M., K.F. Petersen, A. Dresner, L. DiPietro, S. Vogel, D. Rothman, G. Shulman, and M. Roden, *Intramyocellular lipid concentrations are correlated with insulin sensitivity in humans: a 1H NMR spectroscopy study.* Diabetologia, 1999. **42**(1): p. 113-116.
33. Goodpaster, B.H., J. He, S. Watkins, and D.E. Kelley, *Skeletal muscle lipid content and insulin resistance: evidence for a paradox in endurance-trained athletes.* The Journal of Clinical Endocrinology & Metabolism, 2001. **86**(12): p. 5755-5761.
34. Chee, C., C.E. Shannon, A. Burns, A.L. Selby, D. Wilkinson, K. Smith, P.L. Greenhaff, and F.B. Stephens, *Relative contribution of intramyocellular lipid to whole-body fat oxidation is reduced with age but subsarcolemmal lipid accumulation and insulin resistance are only associated with overweight individuals.* Diabetes, 2016. **65**(4): p. 840-850.
35. Nielsen, J., M. Mogensen, B.F. Vind, K. Sahlin, K. Højlund, H.D. Schrøder, and N. Ørtenblad, *Increased subsarcolemmal lipids in type 2 diabetes: effect of training on localization of lipids, mitochondria, and glycogen in sedentary human skeletal muscle.* American Journal of Physiology-Endocrinology and Metabolism, 2010. **298**(3): p. E706-E713.
36. Nielsen, J., A.E. Christensen, B. Nellemann, and B. Christensen, *Lipid droplet size and location in human skeletal muscle fibers are associated with insulin sensitivity.* American Journal of Physiology-Endocrinology and Metabolism, 2017: p. ajpendo. 00062.2017.
37. Huang, S. and M.P. Czech, *The GLUT4 glucose transporter.* Cell metabolism, 2007. **5**(4): p. 237-252.
38. Lauritzen, H.P. and J.D. Schertzer, *Measuring GLUT4 translocation in mature muscle fibers.* American Journal of Physiology-Endocrinology and Metabolism, 2010. **299**(2): p. E169-E179.
39. Kraniou, G.N., D. Cameron-Smith, and M. Hargreaves, *Acute exercise and GLUT4 expression in human skeletal muscle: influence of exercise intensity.* Journal of applied physiology, 2006. **101**(3): p. 934-937.
40. Wang, H., E.B. Arias, M.W. Pataky, L.J. Goodyear, and G.D. Cartee, *Postexercise improvement in glucose uptake occurs concomitant with greater γ3-AMPK activation and AS160 phosphorylation in rat skeletal muscle.* American Journal of Physiology-Endocrinology and Metabolism, 2018.
41. Pataky, M.W., E.B. Arias, and G.D. Cartee, *Measuring Both Glucose Uptake and Myosin Heavy Chain Isoform Expression in Single Rat Skeletal Muscle Fibers.* Methods Mol Biol, 2019. **1889**: p. 283-300.
42. Schaart, G., R.P. Hesselink, H.A. Keizer, G. van Kranenburg, M.R. Drost, and M.K. Hesselink, *A modified PAS stain combined with immunofluorescence for quantitative analyses of glycogen in muscle sections.* Histochemistry and cell biology, 2004. **122**(2): p. 161-169.
43. Bloemberg, D. and J. Quadrilatero, *Rapid determination of myosin heavy chain expression in rat, mouse, and human skeletal muscle using multicolor immunofluorescence analysis.* PloS one, 2012. **7**(4): p. e35273.
44. Spangenburg, E.E., S.J. Pratt, L.M. Wohlers, and R.M. Lovering, *Use of BODIPY (493/503) to visualize intramuscular lipid droplets in skeletal muscle.* BioMed Research International, 2011. **2011**.

45. Wohlers, L.M., B.L. Powers, E.R. Chin, and E.E. Spangenburg, *Using a novel coculture model to dissect the role of intramuscular lipid load on skeletal muscle insulin responsiveness under reduced estrogen conditions.* American Journal of Physiology-Endocrinology and Metabolism, 2013. **304**(11): p. E1199-E1212.
46. Dalen, K.T., T. Dahl, E. Holter, B. Arntsen, C. Londos, C. Sztalryd, and H.I. Nebb, *LSDP5 is a PAT protein specifically expressed in fatty acid oxidizing tissues.* Biochimica et Biophysica Acta (BBA)-Molecular and Cell Biology of Lipids, 2007. **1771**(2): p. 210-227.
47. Murphy, R.M., *Enhanced technique to measure proteins in single segments of human skeletal muscle fibers: fiber-type dependence of AMPK-α1 and-β1.* Journal of Applied Physiology, 2011. **110**(3): p. 820-825.
48. Murphy, R.M., E. Verburg, and G.D. Lamb, *Ca2+ activation of diffusible and bound pools of μ-calpain in rat skeletal muscle.* The Journal of physiology, 2006. **576**(2): p. 595-612.
49. Zierath, J.R., K.L. Houseknecht, L. Gnudi, and B.B. Kahn, *High-fat feeding impairs insulin-stimulated GLUT4 recruitment via an early insulin-signaling defect.* Diabetes, 1997. **46**(2): p. 215-223.
50. Han, D.-H., P.A. Hansen, H.H. Host, and J.O. Holloszy, *Insulin resistance of muscle glucose transport in rats fed a high-fat diet: a reevaluation.* Diabetes, 1997. **46**(11): p. 1761-1767.
51. Hansen, P.A., D.H. Han, B.A. Marshall, L.A. Nolte, M.M. Chen, M. Mueckler, and J.O. Holloszy, *A high fat diet impairs stimulation of glucose transport in muscle functional evaluation of potential mechanisms.* Journal of Biological Chemistry, 1998. **273**(40): p. 26157-26163.
52. Garvey, W.T., L. Maianu, J.-H. Zhu, G. Brechtel-Hook, P. Wallace, and A.D. Baron, *Evidence for defects in the trafficking and translocation of GLUT4 glucose transporters in skeletal muscle as a cause of human insulin resistance.* Journal of Clinical Investigation, 1998. **101**(11): p. 2377.
53. Nadeau, K., L. Ehlers, L. Aguirre, J. Reusch, and B. Draznin, *Discordance between intramuscular triglyceride and insulin sensitivity in skeletal muscle of Zucker diabetic rats after treatment with fenofibrate and rosiglitazone.* Diabetes, Obesity and Metabolism, 2007. **9**(5): p. 714-723.
54. Samuel, V.T. and G.I. Shulman, *Mechanisms for insulin resistance: common threads and missing links.* Cell, 2012. **148**(5): p. 852-871.
55. Holland, W.L., T.A. Knotts, J.A. Chavez, L.P. Wang, K.L. Hoehn, and S.A. Summers, *Lipid mediators of insulin resistance.* Nutrition reviews, 2007. **65**(s1).
56. Coen, P.M. and B.H. Goodpaster, *Role of intramyocelluar lipids in human health.* Trends in Endocrinology & Metabolism, 2012. **23**(8): p. 391-398.
57. Perreault, L., S.A. Newsom, A. Strauss, A. Kerege, D.E. Kahn, K.A. Harrison, J.K. Snell-Bergeon, T. Nemkov, A. D'Alessandro, and M.R. Jackman, *Intracellular localization of diacylglycerols and sphingolipids influences insulin sensitivity and mitochondrial function in human skeletal muscle.* JCI insight, 2018. **3**(3).
58. Armstrong, R.B., C.W.t. Saubert, W.L. Sembrowich, R.E. Shepherd, and P.D. Gollnick, *Glycogen depletion in rat skeletal muscle fibers at different intensities and durations of exercise.* Pflugers Arch, 1974. **352**(3): p. 243-56.

59. Ianuzzo, C.D., M.J. Spalding, and H. Williams, *Exercise-induced glycogen utilization by the respiratory muscles.* J Appl Physiol (1985), 1987. **62**(4): p. 1405-9.
60. Kernell, D., A. Lind, A.B. van Diemen, and A. De Haan, *Relative degree of stimulation-evoked glycogen degradation in muscle fibres of different type in rat gastrocnemius.* J Physiol, 1995. **484 (Pt 1)**: p. 139-53.
61. James, D.E., E.W. Kraegen, and D.J. Chisholm, *Muscle glucose metabolism in exercising rats: comparison with insulin stimulation.* Am J Physiol, 1985. **248**(5 Pt 1): p. E575-80.
62. Nemeth, P.M., B.J. Norris, O.H. Lowry, D.A. Gordon, R.M. Enoka, and D.G. Stuart, *Activation of muscle fibers in individual motor units revealed by 2-deoxyglucose-6-phosphate.* J Neurosci, 1988. **8**(11): p. 3959-66.
63. Funai, K., G.G. Schweitzer, N. Sharma, M. Kanzaki, and G.D. Cartee, *Increased AS160 phosphorylation, but not TBC1D1 phosphorylation, with increased postexercise insulin sensitivity in rat skeletal muscle.* American Journal of Physiology-Endocrinology and Metabolism, 2009. **297**(1): p. E242-E251.
64. Arias, E.B., J. Kim, K. Funai, and G.D. Cartee, *Prior exercise increases phosphorylation of Akt substrate of 160 kDa (AS160) in rat skeletal muscle.* American Journal of Physiology-Endocrinology and Metabolism, 2007. **292**(4): p. E1191-E1200.
65. Schweitzer, G.G., E.B. Arias, and G.D. Cartee, *Sustained postexercise increases in AS160 Thr 642 and Ser 588 phosphorylation in skeletal muscle without sustained increases in kinase phosphorylation.* Journal of applied physiology, 2012. **113**(12): p. 1852-1861.
66. Hamada, T., E.B. Arias, and G.D. Cartee, *Increased submaximal insulin-stimulated glucose uptake in mouse skeletal muscle after treadmill exercise.* Journal of applied physiology, 2006. **101**(5): p. 1368-1376.
67. Pehmøller, C., N. Brandt, J.B. Birk, L.D. Høeg, K.A. Sjøberg, L.J. Goodyear, B. Kiens, E.A. Richter, and J.F. Wojtaszewski, *Exercise alleviates lipid-induced insulin resistance in human skeletal muscle–signaling interaction at the level of TBC1 domain family member 4.* Diabetes, 2012. **61**(11): p. 2743-2752.
68. Wojtaszewski, J.F., B.F. Hansen, B. Kiens, J. Markuns, L. Goodyear, and E. Richter, *Insulin signaling and insulin sensitivity after exercise in human skeletal muscle.* Diabetes, 2000. **49**(3): p. 325-331.
69. Mackrell, J.G., E.B. Arias, and G.D. Cartee, *Fiber type-specific differences in glucose uptake by single fibers from skeletal muscles of 9- and 25-month-old rats.* J Gerontol A Biol Sci Med Sci, 2012. **67**(12): p. 1286-94.

CHAPTER V

Study 3

Exercise Effects on γ3-AMPK Activity, Phosphorylation of Akt2 and AS160, and Insulin-stimulated Glucose Uptake in Insulin-Resistant Rat Skeletal Muscle

ABSTRACT

One exercise session can increase subsequent insulin-stimulated glucose uptake (ISGU) by skeletal muscle. Prior research in healthy muscle suggests that enhanced post-exercise ISGU depends on elevation in γ3-AMPK activity leading to greater phosphorylation of Akt substrate of 160 kDa (pAS160) on an AMPK-phosphomotif (Ser^{704}), in turn favoring greater insulin-stimulated pAS160 on an Akt-phosphomotif (Thr^{642}) that regulates ISGU. Accordingly, we tested if exercise-induced increases in γ3-AMPK activity and pAS160 on key regulatory sites accompany improved ISGU at 3-hours post-exercise (3hPEX) in insulin resistant muscle. Rats fed a high-fat diet (HFD; 2-wk) known to induce insulin resistance either performed acute swim-exercise (2h) or were sedentary (SED). SED rats fed a low-fat diet (LFD; 2-wk) served as healthy controls. Isolated epitrochlearis muscles from 3hPEX and SED rats were analyzed for ISGU, pAS160, pAkt2 (Akt-isoform that phosphorylates $pAS160^{Thr642}$), and γ1-AMPK and γ3-AMPK activity. ISGU was lower in HFD-SED muscles versus LFD-SED, but this decrement was eliminated in the HFD-3hPEX group. γ3-AMPK activity, but not γ1-AMPK activity, was elevated in HFD-3hPEX muscles versus both SED controls. Furthermore, insulin-stimulated $pAS160^{Thr642}$, $pAS160^{Ser704}$, and $pAkt2^{Ser474}$ in HFD-3hPEX muscles were elevated above HFD-SED controls and equal to values in LFD-SED muscles, but insulin-independent $pAS160^{Ser704}$ was unaltered at 3hPEX. These results demonstrated, for the first time in an insulin-resistant model, that the post-exercise increase in ISGU was accompanied by sustained enhancement of γ3-AMPK activation and greater $pAkt2^{Ser474}$. Our working hypothesis is that these changes along with enhanced insulin-stimulated pAS160 increase ISGU of insulin-resistant muscles to values equaling healthy controls.

INTRODUCTION

Insulin resistance is a primary and essential defect in the process leading to type 2 diabetes. Skeletal muscle accounts for up to 85% of insulin mediated glucose disposal [1], making it a prime target for combating insulin resistance. It is well established that exercise or muscle contractions can increase subsequent insulin-stimulated glucose uptake of skeletal muscle from either insulin-sensitive or insulin-resistant subjects [2-6]. The effect of acute exercise on insulin sensitivity is evident ~2-4 hours post-exercise, and can persist for up to 48 hours later [7-9]. Understanding how exercise regulated insulin-stimulated glucose uptake in insulin-sensitive subjects is important, but there is a more urgent need to identify the mechanisms responsible for enhanced insulin-stimulated glucose uptake after exercise during insulin-resistance.

The post-exercise enhancement in insulin-stimulated glucose uptake by skeletal muscle has been observed in the absence of altered insulin signaling at a number of proximal steps including insulin binding to the insulin receptor [10], insulin receptor phosphorylation [2, 11], IRS-1 phosphorylation [11, 12], PI3-kinase activity [2, 13, 14], and Akt phosphorylation [13-18] in insulin-sensitive rodents and humans. These results suggest that exercise might improve insulin sensitivity via regulation of a more distal insulin signaling step.

Akt substrate of 160 kDa (AS160; also known as TBC1D4) is the most distal signaling protein that has been clearly linked to insulin-stimulated glucose uptake in skeletal muscle [19]. Multiple lines of evidence have suggested that altered AS160 phosphorylation is a strong candidate for mediating the improved insulin-stimulated glucose uptake by skeletal muscle following acute exercise [20-23]. In 2003, Gustav Lienhard's group discovered that mutations preventing phosphorylation of two Akt-phosphomotifs of AS160 (Thr642 to Ala642 and Ser588 to Ala588) markedly reduced insulin-stimulated GLUT4 translocation in adipocytes [24]. Enhanced insulin-stimulated phosphorylation of AS160 on Thr642 and Ser588 in exercised compared to unexercised skeletal muscle, concomitant with increased glucose uptake, has been reported in a number of previous experiments in skeletal muscle from rats with normal insulin sensitivity [22, 23, 25-28]. Acute exercise has also been reported to enhance subsequent AS160 phosphorylation on Thr642 and/or Ser588 in insulin-stimulated skeletal muscles from insulin resistant rats or humans independent of greater Akt activation [2, 18]. Compelling new evidence was recently published supporting the idea that AS160 is essential for increased insulin-

stimulated glucose uptake in skeletal muscle after acute contractile activity. Kjøbsted et al. reported that insulin-stimulated glucose uptake by muscle several hours after in situ contraction was increased in wild type mice, but not in AS160 muscle-specific knockout mice [29].

The mechanisms accounting for a sustained, post-exercise increase in pAS160^{Thr642} and/or pAS160^{Ser588} of insulin-stimulated skeletal muscle are unknown. However, the phosphorylation of AS160 on Ser704, an AMPK-phosphomotif, has recently emerged as a potentially important step for enhanced insulin-stimulated glucose uptake after exercise. In human [18, 30] and rat [31] skeletal muscle with normal insulin sensitivity, the insulin-independent phosphorylation of AS160^{Ser704} has been reported to be increased immediately post-exercise and to remain elevated for hours after exercise, when insulin-stimulated glucose uptake is enhanced [7, 32]. Additionally, multiple studies have reported enhanced insulin-stimulated pAS160^{Ser704} in skeletal muscle after exercise or contraction [18, 31, 33-35]. Preventing the phosphorylation of AS160^{Ser704} in mouse muscle by mutating Ser704 to Ala704 attenuates the insulin-stimulated phosphorylation of AS160^{Thr642}, an Akt phosphomotif which regulates insulin-stimulated glucose uptake [36]. These data suggest that the enhanced phosphorylation of AS160^{Ser704} after exercise may prime Thr642, and possibly other AS160 phosphosites, to be more easily phosphorylated, a potentially critical event for enhancing insulin sensitivity. It will be important to identify exercise effects on pAS160^{Ser704} during insulin resistance to better understand the mechanisms which govern enhanced post-exercise insulin sensitivity in insulin resistant subjects. Therefore, our first major aim was to investigate the acute post-exercise effect on AS160 phosphorylation sites (Ser588, Thr642, and Ser704) in muscles from insulin-resistant rats fed a high-fat diet (HFD) after exercise, compared to sedentary HFD- and low-fat diet-fed (LFD) controls. We employed a 2 week high-fat diet which has been shown to induce insulin resistance in rat skeletal muscle prior to major changes in body mass and body composition [2, 37, 38].

AS160^{Ser704} is an AMPK phosphosite, and AMPK is a heterotrimeric complex composed of a catalytic α subunit (α1 or α2 isoform) and two regulatory subunits (β1 or β2 isoform; and γ1, γ2, or γ3 isoform). The expression of γ1 and γ3 isoform-containing heterotrimers of AMPK has been reported in skeletal muscle [39], but γ2-containing AMPK heterotrimers have not been detected in skeletal muscle [39]. γ3-AMPK has been shown to be activated in muscle by exercise

in humans [30, 40] and rats [31] or by electrically stimulated contractions in mice [35, 40]. In human skeletal muscle, prolonged exercise resulted in a modest increase in γ1-AMPK along with a larger increase in γ3-AMPK activity [41]. Prior incubation of isolated muscles from wild-type mice with 5-aminoimidazole-4-carboxamide ribonucleotide (AICAR) resulted in enhanced insulin-stimulated glucose uptake, but this AICAR-effect on insulin sensitivity was absent in muscles from γ3-AMPK knockout mice [36]. Moreover, electrically stimulated in situ contractile activity which enhances insulin-stimulated pAS160^{Ser704} in wild type (WT) mice did not increase insulin-stimulated pAS160^{Ser704} in γ3-AMPK knockout mice [35]. These findings suggest γ3-AMPK activation and pAS160^{Ser704} may be critical steps for enhancing insulin-stimulated glucose uptake after AICAR or contraction in insulin sensitive animals. However, neither prior AICAR treatment nor in situ contractions completely recapitulate in vivo exercise, and no published study has evaluated γ3-AMPK activity after exercise in insulin-resistant rats. Furthermore, apparently neither γ1- nor γ3-AMPK activity have been evaluated in rat skeletal muscle after acute exercise. Therefore, the second major aim of this experiment was to investigate the post-exercise effect on γ3-AMPK activity in muscles from insulin-resistant rats fed a high-fat diet (HFD), compared to sedentary HFD- and low-fat diet-fed (LFD) controls.

Earlier research has reported that acute exercise can lead to subsequently elevated insulin-stimulated AS160 phosphorylation on key regulatory sites and glucose uptake in skeletal muscle independent of enhanced Akt phosphorylation [2, 18, 20, 25, 26]. However, these studies have not included evaluation of Akt2 phosphorylation, the Akt isoform implicated in insulin-stimulated AS160 phosphorylation [42] and insulin-stimulated glucose uptake [43, 44]. Accordingly, the third major aim of the current study was to determine in insulin resistant skeletal muscle the effects of acute exercise on the phosphorylation of Akt2 on its key regulatory sites, Ser474 and Thr309.

METHODS

Materials. The reagents and apparatus for SDS-PAGE and nonfat dry milk (#170-6404) were from Bio-Rad (Hercules, CA). [^{3}H]-2-deoxyglucose (NET328001MC), [^{14}C]-mannitol (NEC314250UC), and [γ-^{32}P]-ATP were from PerkinElmer (Waltham, MA). Tissue Protein Extraction Reagent, (T-PER; #PI78510), Bicinchoninic Acid Protein Assay Kit (#PI23223),

MemCode Reversible Protein Stain Kit (#PI24585), and Protein G magnetic beads (#10004D), DynaMag^{TM-2} magnet (#12321D) were from ThermoFisher (Pittsburgh, PA). Anti-rabbit IgG horseradish peroxidase conjugate (#7074), anti-phospho Akt Ser^{473} (pAkt^{Ser473}; #4060; recognizes Akt1 when phosphorylated at Ser473, Akt2 when phosphorylated at Ser474 or Akt3 when phosphorylated at Ser472), anti-phospho Akt Thr^{308} (pAkt^{Thr308}; #13038; recognizes Akt1 when phosphorylated at Thr308, Akt2 when phosphorylated at Thr309 or Akt3 when phosphorylated at Thr305), anti-panAkt (#4691; recognizes all Akt isoforms), anti-phospho Akt2 Ser^{474} (pAkt2^{Ser474}; #8599), anti-Akt2 (#3063), anti-phospho AS160 Thr^{642} (pAS160^{Thr642}; #4288), anti-phospho AS160 Ser^{588} (pAS160^{Ser588}; #8730), anti-phospho AMPKα Thr^{172} (pAMPKα^{Thr172}; #2535), anti-AMP-activated protein kinase-α (AMPKα; #2532), anti-AMP-activated protein kinase-β1 (AMPK-β1; #12063), anti-AMP-activated protein kinase-β2 (AMPK-β2; #4148), anti-acetyl CoA carboxylase (ACC; #3676), and anti-phospho ACC Ser^{79} (pACC^{Ser79}; #3661) were from Cell Signaling Technology (Danvers, MA). Skeletal muscle expresses two isoforms of ACC (ACC1 and ACC2). ACC1 has a relatively low expression in skeletal muscle and is phosphorylated by AMPK on Ser^{79}. ACC2 has a relatively high expression in skeletal muscle and is phosphorylated by AMPK on Ser^{212} [45]. Since the pACC^{Ser79} antibody (#3661) detects both pACC1^{Ser79} and pACC2^{Ser212} [46], we hereafter refer to the results with this antibody as pACC$^{Ser79/212}$. Anti-phospho AS160^{Ser704} was provided by Dr. Jonas Treebak (University of Copenhagen, Denmark). Anti-AMP-activated protein kinase γ1 (γ1-AMPK; #32508) was from Abcam. Anti-AMP-activated protein kinase γ3 (γ3-AMPK) was provided by Dr. David Thomson (Brigham Young University, USA) [47]. Liquid scintillation cocktail (#111195-CS) was from Research Products International (Mount Prospect, IL). Anti-Akt substrate of 160kDa (AS160; #ABS54), anti-AMP-activated protein kinase α1 (AMPK-α1; #07-350), anti-AMP-activated protein kinase α2 (AMPK-α2; #07-363), P81 phosphocellulose squares (#20-134), and enhanced chemiluminescence Luminata Forte Western HRP Substrate (#WBLUF0100) were from EMD Millipore (Billerica, MA).

Animal treatment and muscle preparation. Procedures for animal care were approved by the University of Michigan Committee on Use and Care of Animals. Male Wistar rats (6-7 weeks old; Charles River Laboratories, Boston, MA) were individually housed and provided with standard rodent chow (Laboratory Diet no. 5L0D; LabDiet, St. Louis, MO) or high-fat chow (Laboratory Diet no. D12492; ResearchDiets, New Brunswick, NJ) and water *ad libitum* for two

weeks until they were fasted the night before the experiment at ~1700. Caloric intake for each rat during the two week diet period was estimated based on the difference between the food provided on day one and the food remaining at ~1700 on the night prior to the experiment. Beginning at 0700 on the day of the experiment rats either remained sedentary or swam in a barrel filled with water (35°C) for four 30-min bouts with a 5-min rest between bouts. Immediately following exercise, some rats (IPEX and Sedentary) were anesthetized (intraperitoneal sodium pentobarbital, 50 mg/kg weight), weighed, and their epitrochlearis muscles dissected. Other rats (3hPEX and Sedentary) were anesthetized approximately 3 hours following swimming, weighed, and their epitrochlearis muscle dissected. After muscle dissections, the epididymal fat pads were dissected and weighed.

Ex vivo incubations of muscles for glucose uptake. Muscles were incubated, as previously described [48], in glass vials gassed (95% O_2, 5% CO_2) in a temperature controlled bath by a two-step incubation process (35°C during both steps). For the IPEX experiments, muscles were placed in vials for 10 min containing 2 ml of incubation step 1 media (Krebs Henseleit Buffer, KHB, supplemented with 0.1% bovine serum albumin, BSA, 2 mM sodium pyruvate and 6 mM mannitol). For incubation step 2 (15 min) these muscles were transferred to vials containing 2 ml of incubation step 2 media (KHB supplemented with 0.1% BSA, 0.1 mM 2-DG (2.25 mCi/mmol [^{3}H]-2-DG), 2 mM sodium pyruvate and 6 mM mannitol (2 mCi/mmol [^{14}C] mannitol)). For the 3hPEX experiment, paired muscles were placed in vials containing 2 ml of incubation step 1 media for 30 min with or without 100 µU/ml insulin. These muscles were then transferred to vials containing 2 ml of incubation step 2 media for 20 min with or without 100 µU/ml insulin. After step 2, whole muscles were blotted, freeze clamped, and stored at -80°C until further processing.

Whole muscle glucose uptake. Frozen muscles used for 2-DG uptake were weighed and homogenized in ice-cold lysis buffer (T-PER supplemented with 1mM Na_3VO_4, 1mM EDTA, 1mM EGTA, 2.5mM sodium pyrophosphate tetrabasic decahydrate, 1mM β-glycerophosphate, 1µg/ml leupeptin, and 1mM phenylmethylsulfonyl fluoride). Homogenates were then rotated at 4°C for 1 h before centrifugation at 15,000g for 15 min at 4°C. Aliquots (200 µl) of supernatant were added to vials along with 8 ml of scintillation cocktail. 2-[^{3}H]-DG and 2-[^{14}C]-mannitol disintegrations per min were measured by scintillation counter, and then 2-DG uptake was calculated as previously described [49].

Immunoblotting. Total protein concentrations for whole muscle lysates were determined by bicinchoninic acid assay, and equal amounts of protein for each sample were separated via SDS-PAGE, and transferred to polyvinyl difluoride membranes. After electrotransfer, the MemCode protein stain was used to confirm equal loading [50]. Membranes were then blocked with 5% BSA or nonfat milk in TBST (Tris-buffered saline, pH 7.5 plus 0.1% Tween-20) for 1 h, incubated with appropriate concentrations of primary (1:1000; overnight) and secondary (1:20,000; 1 h) antibodies, and subjected to enhanced chemiluminescence to quantify protein bands by densitometry (FluorChem E Imager, AlphaView software; ProteinSimple, San Jose, CA). Individual values were normalized to the mean value of all samples on the membrane. Because no commercial phospho-antibody is currently available for the selective detection of pAkt2^{Thr309}, we assessed this phosphophosite essentially as previously described [51]. In brief, muscle lysates were subjected to inmmunoprecipitation using an antibody that selectively recognizes Akt2 (Cell Signaling Technology #3063) and subsequently blotted with an antibody that recognizes pThr309 on Akt2 (Cell Signaling Technology #13038).

AMPK-γ1 and -γ3 Isoform Activity. We confirmed the specificity of γ1-AMPK and γ3-AMPK antibodies used for immunoprecipitation as previously described by immunoblotting muscle samples from wild type, γ1 knockout, and γ3- knockout animals following immunoprecipitation with each of the isoform-specific antibodies [31]. AMPK isoform-specific activity was determined as previously described [36]. Briefly, 300μg (for γ3-AMPK assay) or 600μg (for γ1-AMPK assay) of protein from each sample was rotated at 4°C overnight with appropriate AMPK γ isoform antibody (1:1000). Then 50 μl of protein G-magnetic beads were added to the muscle lysate/antibody mixture and rotated for 2 h at 4°C. A DynaMag^{TM}-2 magnet was used to precipitate the protein G-immunocomplex. Each pellet was washed one time in buffer A [50 mmol/L NaCl, 1% Triton X-100, 50 mmol/L sodium fluoride, 5 mmol/L sodium-pyrophosphate, 20 mmol/L Tris-base (pH 7.5), 500 μmol/L PMSF, 2 mmol/L dithiothreitol (DTT), 4 μg/mL leupeptin, 4 μg/mL aprotinin, and 250 mmol/L sucrose], once in 6X assay buffer (240 mmol/L HEPES, 480 mmol/L NaCl, pH 7.0), and two times in 3X assay buffer. The activity assay was then performed in 30 μl of kinase reaction buffer [40 mmol/L HEPES, pH 7.5, 80 mmol/L NaCl, 800μmol/L DTT, 200 μmol/L AMP, 100μmol/L AMARA peptide, 5 mmol/L magnesium chloride ($MgCl_2$), 200 μmol/L ATP, and 10 μCi of [γ- ^{32}P]-ATP] for 30 min at 30°C. The reaction was stopped by the addition of 10 μl of 1% phosphoric acid and then 40 μl of

supernatant was transferred to phosphocellulose paper. After 4 x 15 min washes with 1% phosphoric acid, the phosphocellulose paper was dried for 5 min and placed in the vials containing scintillation cocktail for scintillation counting. Results are expressed relative to the normalized mean of all the samples from each experiment.

Statistics. Data are expressed as mean ± 95% confidence interval (95% CI), with two-tailed significance levels of $\alpha<0.05$. Two-tailed t-tests were performed to compare means from two groups. One-way ANOVAs were used to determine the treatment group effect of IPEX experiments. Two-way ANOVAs were used to compare means among more than two groups from 3hPEX experiments, and Bonferroni post-hoc tests were performed to identify the source of significant differences.

RESULTS

Body mass, epididymal fat mass and estimated caloric intake. Following the 2-week diet intervention, the HFD rats versus LFD rats had a significantly greater body mass (299 ± 4 versus 290 ± 6 g; $P < 0.05$), epididymal fat mass (2318 ± 128 versus 1297 ± 81 mg; $P < 0.001$) and estimated caloric intake (97 ± 2 versus 82 ± 2 kcal/day; $P < 0.001$).

Glucose uptake. Insulin-independent glucose uptake was significantly greater in the HFD-IPEX group compared to both sedentary control groups ($P<0.001$; Figure 5.1A). In the 3hPEX experiment, muscles incubated with insulin had a greater glucose uptake than paired muscles incubated without insulin in all treatment groups ($P<0.001$; Figure 5.1B). Within the insulin-treated muscles, glucose uptake was lower in the HFD-SED group compared to either the LFD-SED or HFD-3hPEX groups ($P<0.01$), but there was not a significant difference between insulin-treated LFD-SED and HFD-3hPEX muscles. There were significant main effects of diet and exercise treatment ($P<0.01$) and insulin ($P<0.001$), and a significant treatment x insulin interaction effect ($P<0.05$) for glucose uptake.

γ1-AMPK and γ3-AMPK activity. There was not a significant effect of exercise on γ1-AMPK activity in HFD-IPEX or HFD-3hPEX groups compared to either sedentary control group (Figures 5.2A and 5.2C). Increased γ3-AMPK activity was observed in both HFD-IPEX and

HFD-3hPEX rats compared to both HFD-SED and LFD-SED controls ($P<0.05$; Figures 5.2B and 5.2D).

AMPK isoform abundance. There was no significant effect of treatment group on the abundance of α1-AMPK, α2-AMPK, β1-AMPK, β2-AMPK, γ1-AMPK, or γ3-AMPK (Figures 5.3A-F). Because γ2-containing AMPK heterotrimers have been reported to be undetectable in skeletal muscle [52], γ2-AMPK was not measured.

AMPKα and ACC phosphorylation. For the IPEX experiment, pAMPKα^{Thr172} calculated relative to total AMPKα (pAMPKα^{Thr172}/ AMPKα) was significantly greater in the HFD-IPEX group compared to both SED controls ($P<0.001$; Figure 5.4A). At 3hPEX there was a significant main effect of exercise for increased pAMPKα^{Thr172}/ AMPKα ($P<0.001$; Figure 5.4C). pACC$^{Ser79/212}$ was significantly increased in the HFD-IPEX group compared to SED controls ($P<0.005$; Figure 5.4B), but there was no effect of insulin or treatment group on pACC$^{Ser79/212}$ at 3hPEX (Figure 5.4D).

AS160 phosphorylation. For the IPEX experiment, pAS160^{Ser588} calculated relative to total AS160 (pAS160^{Ser588}/AS160) was significantly greater in the HFD-IPEX group compared to the HFD-SED control ($P<0.005$; Figure 5.5A), but not compared to the LFD-SED control. pAS160^{Thr642} and pAS160^{Ser704} expressed relative to total AS160 were significantly greater in the HFD-IPEX group compared to both SED controls ($P<0.005$; Figures 5.5B, and 5.5C). For the 3hPEX experiment, insulin-stimulated pAS160^{Ser588} was significantly greater in the HFD-3hPEX group compared to HFD-SED control ($P<0.01$; Figure 5.5D), but not compared to LFD-SED control. Insulin stimulated pAS160^{Thr642} and pAS160^{Ser704} were lower in the HFD-SED group compared to either LFD-SED and HFD-3hPEX ($P<0.01$; Figures 5.5E and 5.5F). There were significant main effects of diet and exercise treatment ($P<0.01$) and insulin ($P<0.001$) for pAS160^{Ser588}, pAS160^{Thr642}, and pAS160^{Ser704}. There was a significant treatment x insulin interaction effect ($P<0.05$) for pAS160^{Thr642}.

Akt phosphorylation. Insulin-stimulated pAkt^{Thr308} and pAkt^{Ser473} relative to total Akt (pAkt^{Thr308}/Akt and pAkt^{Ser473}/Akt) were significantly lower in the HFD-SED group compared to the LFD-SED group and the HFD-3hPEX group (Figures 5.6A and 5.6C). Insulin-stimulated pAkt2^{Thr309} relative to total Akt2 (pAkt2^{Thr309}/Akt2) was lower in HFD-SED versus LFD-SED (Figure 5.6B). Insulin-stimulated pAkt2^{Ser474} relative to total Akt2 (pAkt2^{Ser474}/Akt2) was greater

in the HFD-3hPEX group compared to both the LFD-SED and HFD-SED control groups (Figure 5.6D). There was a significant main effect of insulin ($P<0.001$) for $pAkt^{Thr308}$, $pAkt2^{Thr309}$, $pAkt^{Ser473}$, and $pAkt2^{Ser474}$. There was a significant main effect of diet and exercise treatment ($P<0.005$) for $pAkt^{Thr308}$, $pAkt^{Ser473}$, $pAkt2^{Ser474}$. There was a significant treatment x insulin interaction effect ($P<0.005$) for $pAkt^{Thr308}$, $pAkt^{Ser473}$, and $pAkt2^{Ser474}$.

DISCUSSION

It is important to better understand the biological processes that underlie the exercise-induced improvement in insulin sensitivity of insulin resistant skeletal muscle. The current study used a two week HFD protocol that has been shown to induce skeletal muscle insulin resistance in rats [2, 38, 53]. In this insulin resistance model, we assessed key post-exercise signaling events that have been proposed to be critical for enhancing insulin-stimulated glucose uptake in insulin sensitive muscle. The main new findings of the study were: 1) γ3-AMPK activity, but not γ1-AMPK activity, in skeletal muscle was elevated both IPEX and 3hPEX compared to sedentary controls, 2) at 3hPEX insulin-stimulated $pAS160^{Ser704}$ was increased, but insulin-independent $pAS160^{Ser704}$ was unaltered compared to HFD-SED controls, 3) insulin-stimulated $pAkt2^{Ser474}$ was elevated at 3hPEX compared to HFD-SED control, and 4) insulin-stimulated $pAkt2^{Thr309}$ was decreased in sedentary muscle following a 2 week HFD versus LFD-SED control. In addition, insulin-independent glucose uptake, $pAS160^{Thr642}$, and $pAS160^{Ser704}$ were elevated above sedentary (LFD and HFD) values IPEX. Furthermore, the abundance of α1, α2, β1, β2, γ1, and γ3 AMPK-subunits were unaltered by either HFD or exercise. These results support the idea that γ3-AMPK activity and AS160 phosphorylation are critical steps for enhancing insulin stimulated glucose uptake in insulin resistant skeletal muscle.

We recently proposed a model to help elucidate the processes underlying increased insulin-stimulated glucose uptake by skeletal muscle post-exercise [6]. In this model, triggers are initiating events that activate downstream memory elements, which store the information that can be passed on to the mediators, which convert the memory into action that ultimately results in greater insulin-stimulated glucose uptake.

Skeletal muscle AMPK activation is a hallmark response to exercise [54-57] and a potential trigger for increased insulin sensitivity. Exercise results in the reversible phosphorylation of AMPKα^{Thr172} which markedly increases AMPK's enzymatic activity [39]. Increased pAMPKα^{Thr172} and phosphorylation of AMPK's substrate, acetyl CoA carboxylase (ACC), are widely used as indicators of AMPK activity [36, 58-61]. As expected, we observed increased pAMPKα^{Thr172} and pACC^{Ser79} IPEX. However, AMPK is a heterotrimeric protein complex that contains one catalytic (α) and two regulatory (β and γ) subunits, and values for pAMPK^{Thr172} and pACC^{Ser79} do not provide information regarding the isoform-specific activity of AMPK. The activation of various heterotrimeric combinations of AMPK can have differential responses to exercise [41, 60]. In humans and rats, the effect of in vivo exercise has consistently been shown to increase γ3-containing AMPK activity [30, 31, 41, 60, 61]. However, exercise-induced enhancement of γ1-AMPK activity in skeletal muscle has been less consistent. The current results, which are the first assessment of isoform-selective effects of exercise on AMPK activity in insulin resistant rat skeletal muscle, show elevated γ3-AMPK activity, but unaltered γ1-AMPK activity, both IPEX and 3hPEX. It seemed possible that the effect of exercise to increase γ3-AMPK activity could have been secondary to changes in the abundance of γ3-AMPK post-exercise, but we found that the exercise-mediated increase in γ3-AMPK activity occurred in the absence of altered abundance of γ3 or other AMPK subunits.

Earlier research provides several lines of evidence implicating γ3-AMPK activation as being potentially important for increased insulin sensitivity. Results using γ3-AMPK knockout mice, revealed that γ3-AMPK is essential for the effect of prior exposure of skeletal muscle to AICAR, an AMPK-activator, on insulin-stimulated glucose uptake [36]. Furthermore, γ3-AMPK activity was elevated 3h after in situ muscle contraction along with greater insulin-stimulated glucose uptake in mouse skeletal muscle [35]. Similar to the results for insulin resistant rats in the current study, we recently reported in muscles from rats with normal insulin sensitivity that γ3-AMPK activity was increased (both IPEX and 3hPEX), and insulin-stimulated glucose uptake was enhanced 3hPEX [31].

What are possible cellular events that may serve as the memory elements that connect exercise-induced γ3-AMPK activation and insulin-stimulated glucose uptake? Increased post-exercise pAS160^{Ser704} has emerged as a candidate memory element that is linked to AMPK

because Ser704 is an AMPK phosphomotif, and because mutating AS160 Ser704 to Ala704, which prevents its phosphorylation, results in decreased insulin-stimulated pAS160^{Thr642} [36]. Although insulin-independent pAS160^{Ser704} remained elevated for several hours after exercise in some studies [18, 31], in the current study, pAS160^{Ser704} was no longer significantly increased above sedentary values at 3hPEX. Therefore, the current results do not support the idea that a sustained elevation in insulin-independent pAS160^{Ser704} is a likely memory element for greater insulin-stimulated glucose uptake in insulin resistant rat skeletal muscle. An increase in insulin-stimulated pAS160^{Ser704} at 3hPEX was also observed, but the mechanisms for the effect of insulin on pAS160^{Ser704} remain to be elucidated. Treebak et al. found that the insulin-stimulated increase in pAS160^{Ser704} required a PI 3-kinase-dependent mechanism that was apparently not attributable to phosphorylation by Akt2, AMPK, or mTOR [62]. Therefore, some unidentified PI 3-kinase regulated protein kinase may be involved in the post-exercise effect on insulin-stimulated pAS160^{Ser704}.

Given that greater activity of γ3-AMPK 3hPEX in insulin-resistant muscle was not accompanied by a sustained increase in insulin-independent pAS160^{Ser704}, what are other possible memory elements that might rely on elevated γ3-AMPK activity? Mass spectrometry analysis identified several other sites that became phosphorylated in skeletal muscles from mice that had been injected with the AMPK-activator AICAR [62]. Validated antibodies do not appear to be available for these sites, and it is unknown if they are responsive to in vivo exercise or if they have any effect on insulin-stimulated glucose uptake. However, it seems possible that AMPK-regulated phosphomotifs on AS160 other than Ser704 might influence insulin-stimulated glucose uptake in insulin resistant muscle after exercise. Because various proteins can bind to AS160 (e.g., 14-3-3, RUVBL2, RIP140, and ClipR-59) [63-66], an alternative possibility is that γ3-AMPK might phosphorylate these or other proteins, and thus indirectly regulate AS160's function. Alternatively, γ3-AMPK may lead to inhibition of protein phosphatase-1α or other phosphatases that regulate AS160 dephosphorylation [28, 67]. Finally, γ3-AMPK activity remained elevated 3hPEX in insulin resistant muscle, and we previously also observed a similar, long-lasting increase in γ3-AMPK activity in muscles from normal rats [31]. Others have also reported that γ3-AMPK activity in skeletal muscle can remain elevated several hours after exercise by humans [30, 68, 69], in situ contraction [35], or ex vivo incubation with AICAR [36]. Thus, it is possible that a sustained increase in muscle γ3-AMPK activity serves as a

memory element that can lead to enhanced insulin sensitivity, and the mechanism may not necessarily involve AS160-dependent processes.

Insulin-stimulated phosphorylation of Akt is often reported to be unchanged following acute exercise [2, 15, 16, 18, 25, 70, 71]. However, some studies have reported elevated insulin-stimulated Akt phosphorylation after exercise [20, 22, 26]. Similarly, insulin-stimulated pAkt^{Ser473} and pAkt^{Thr308} were greater in insulin-stimulated muscle post-exercise compared to SED controls. It is important to note that Akt2 is the isoform of Akt that is primarily responsible for insulin-stimulation of both pAS160^{Thr642} and glucose uptake [43, 72, 73]. Apparently no earlier research has evaluated acute exercise effects on the insulin-stimulated phosphorylation of Akt2 in skeletal muscle with a physiological insulin dose. Accordingly, we also measured insulin-stimulated pAkt2 and found that exercise increased insulin-stimulated pAkt2^{Ser474}, but not pAkt2^{Thr309} in HFD-fed rats. These novel results suggest that the exercise-induced enhancement in insulin-stimulated pAS160^{Thr642} and glucose uptake may have been attributable, at least in part, to greater Akt2^{Ser474} phosphorylation.

It is well-established that a single bout of exercise can increase insulin-stimulated glucose uptake in both normal and insulin resistant skeletal muscle. Although enhanced AS160 phosphorylation on insulin-regulated Akt-phosphomotifs (Ser588 and Thr642) has been identified as a potential mediator of this effect, the results of the current study provided several important new insights in insulin resistant skeletal muscle. A prolonged post-exercise increase in pAS160^{Ser704} has been suggested as part of the process leading to greater insulin sensitivity, but in contrast to recent research with muscles from healthy rats undergoing the same exercise protocol [31], we did not detect a sustained increase in phosphorylation on this site in insulin resistant muscle. However, the current results are consistent with the notion that greater post-exercise γ3-AMPK activity may be relevant as a trigger and/or memory element for elevated insulin-stimulated glucose uptake by insulin-resistant skeletal muscle. It will be important to test if elevated post-exercise γ3-AMPK activity plays a causal role in insulin-stimulated AS160 phosphorylation and/or glucose uptake in insulin resistant muscle. In light of the discovery of greater Akt2 phosphorylation in insulin resistant muscle after acute exercise, it would also be worthwhile to evaluate exercise effects on Akt2 in healthy skeletal muscle. Finally, recent research has demonstrated that effects of prior exercise on insulin-stimulated glucose uptake are

variable in different muscle fiber types, and the fiber type-selective differences are not identical in muscles from normal compared to insulin resistant muscle [53, 74]. The fiber type-selective effects on post-exercise insulin-stimulated glucose uptake tracked closely with fiber type-selective effects on insulin-stimulated AS160 phosphorylation [27]. Future research should also probe the possibility of fiber type-selective effects of exercise on key signaling events in insulin resistant skeletal muscle.

ACKNOWLEDGEMENTS

These experiments were supported by a grant from the National Institutes of Health (R01 DK71771). I would like to thank Ed Arias, Haiyan Wang, and Xiaohua Zheng for their technical assistance. I also want to thank Dr. Jonas Treebak for generously supplying the pAS160^{Ser704} antibody and Dr. David Thomson for generously supplying the γ3-AMPK antibody.

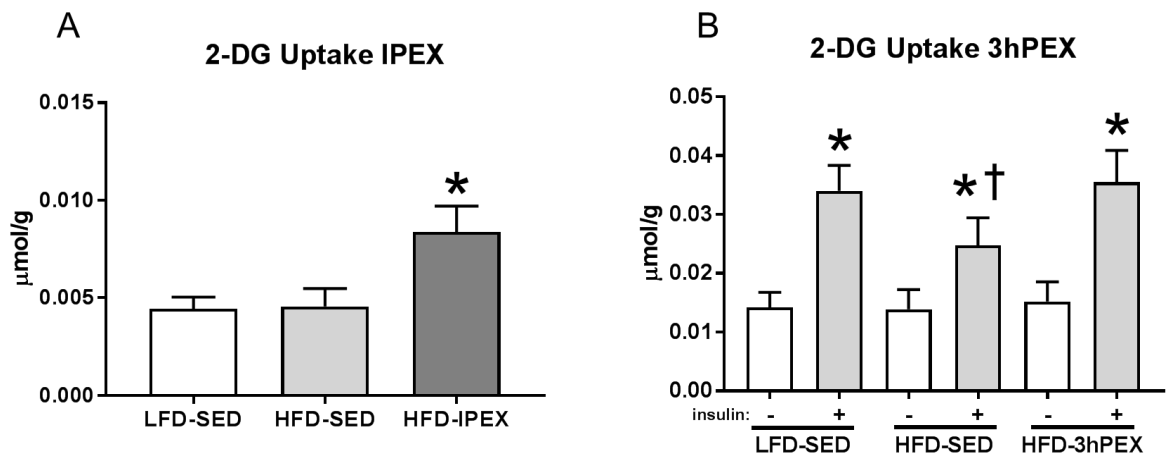

Figure 5.1

Effect of 2-week high-fat feeding plus acute exercise on skeletal muscle 2-DG uptake. A) Epitrochlearis 2-DG uptake immediately post-exercise. Data were analyzed by one-way ANOVA. *P < 0.001, HFD-IPEX vs both LFD-SED and HFD-SED. Values are mean ± 95% confidence interval; n = 14/group. B) 2-DG uptake from paired epitrochlearis muscles incubated ± 100µU/mL insulin at 3 hours post-exercise. Data were analyzed by two-way ANOVA. *P < 0.001, insulin vs no insulin. †P < 0.005, within insulin treated muscles HFD-SED vs both LFD-SED and HFD-3hPEX. Values are mean ± 95% confidence interval; n = 15/group. 2-DG, 2-deoxy-D-glucose; HFD, high-fat diet; LFD, low-fat diet; SED, sedentary; IPEX, immediately post-exercise; 3hPEX, 3 hours post-exercise.

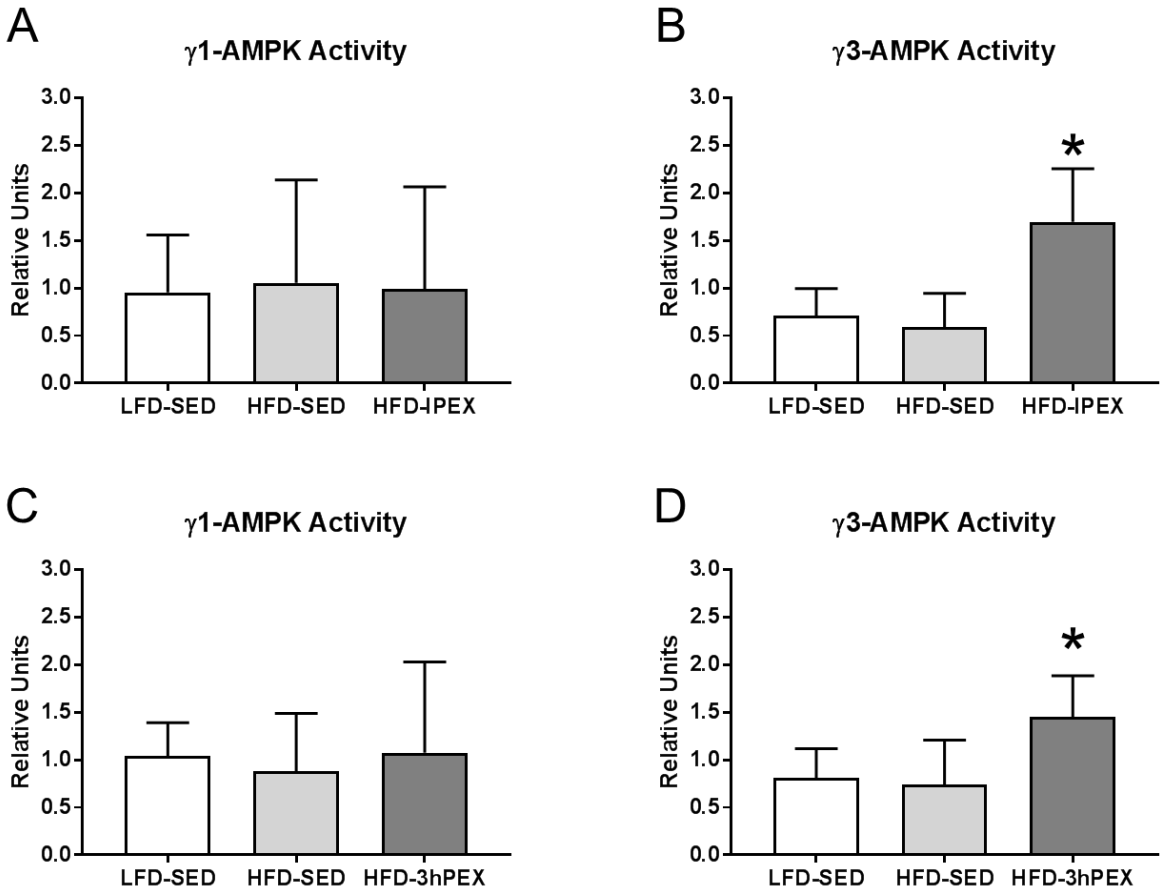

Figure 5.2

Effect of 2-week high-fat feeding plus acute exercise on γ-isoform-specific AMPK activity in rat epitrochlearis muscle. A) γ1-AMPK activity immediately post-exercise. B) γ3-AMPK activity immediately post-exercise. C) γ1-AMPK activity 3 hours post-exercise. D) γ1-AMPK activity 3 hours post-exercise. For γ1-AMPK activity assays n = 5/group. For γ3-AMPK activity assays n = 8/group. Data were analyzed by one-way ANOVA. *P < 0.01, significantly greater than both other treatment groups. Values are expressed as mean ± 95% confidence interval. HFD, high-fat diet; LFD, low-fat diet; SED, sedentary; IPEX, immediately post-exercise; 3hPEX, 3 hours post-exercise.

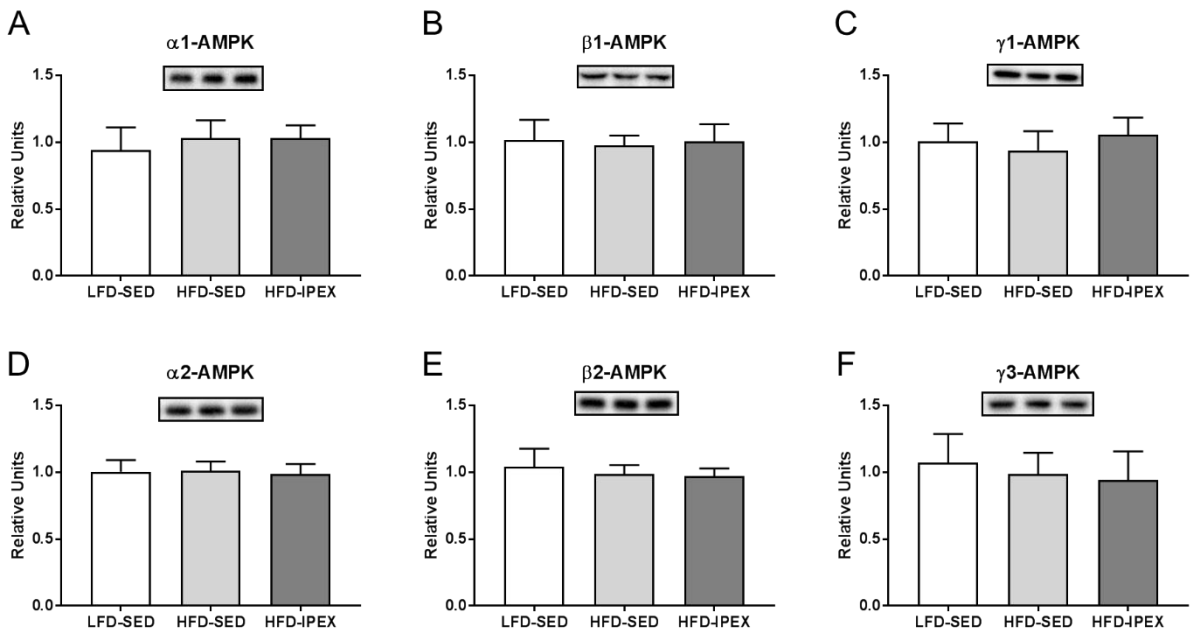

Figure 5.3

AMPK isoform abundance in epitrochlearis muscle from rats fed a low or high fat diet and acutely exercised. A-F) Abundance of α1, α2, β1, β2, γ1, and γ3 AMPK isoforms in epitrochlearis muscles immediately post-exercise. Data were analyzed by one-way ANOVA. No significant differences were detected. Values are expressed as mean ± 95% confidence interval; n = 8/group. HFD, high-fat diet; LFD, low-fat diet; SED, sedentary; IPEX, immediately post-exercise.

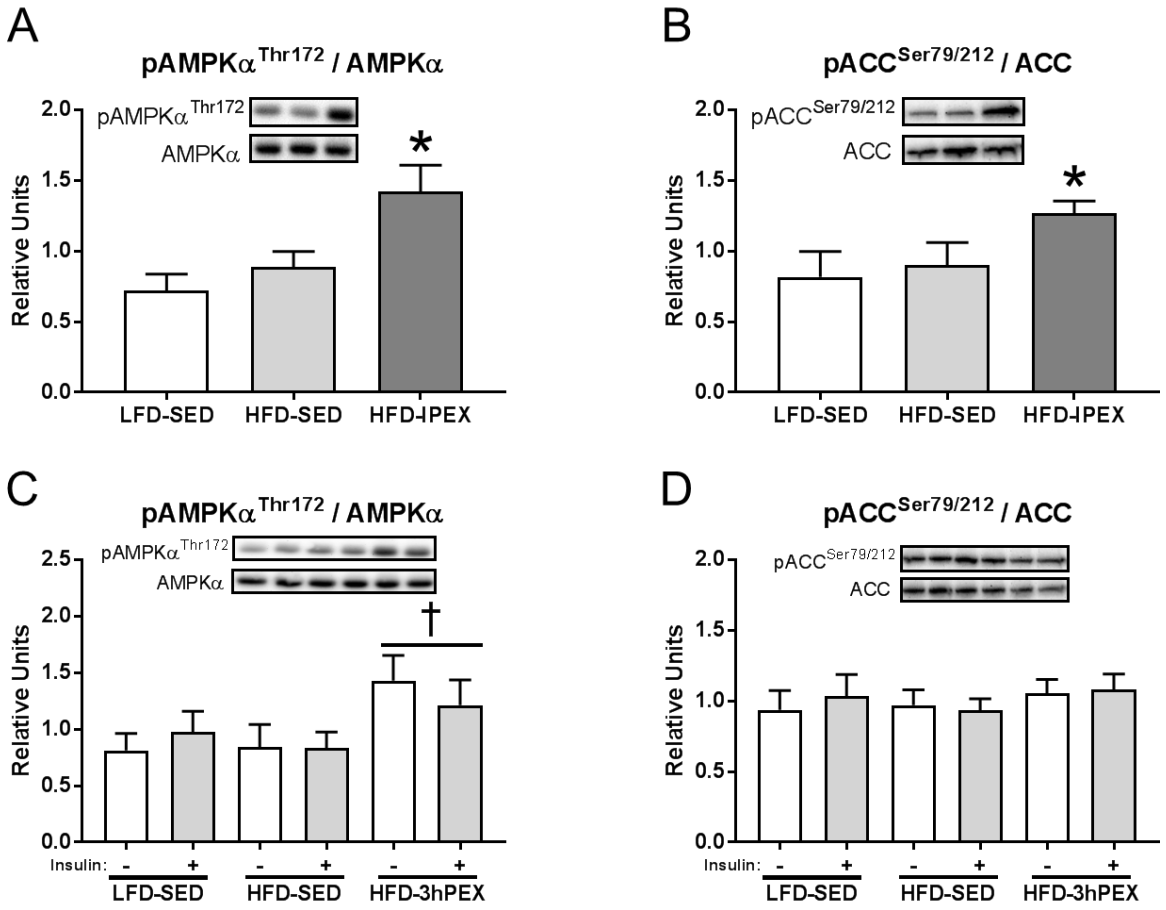

Figure 5.4

Post-exercise AMPK and ACC phosphorylation in epitrochlearis muscle from high fat-fed rats versus sedentary controls. A) Phosphorylated AMPKα^{Thr172}/AMPKα immediately post-exercise. B) phosphorylated ACC$^{Ser79/212}$/ACC immediately post-exercise. C) phosphorylated AMPKα^{Thr172}/AMPKα 3 hours post-exercise. D) phosphorylated ACC$^{Ser79/212}$/ACC 3 hours post-exercise. IPEX data were analyzed by one-way ANOVA and 3hPEX data were analyzed by two-way ANOVA. *P < 0.005, HFD-IPEX greater than both other groups. †P < 0.01, Main effect of 3hPEX vs both LFD-SED and HFD-SED. Values are expressed as mean ± 95% confidence interval; n = 8-17/group. HFD, high-fat diet; LFD, low-fat diet; SED, sedentary; IPEX, immediately post-exercise; 3hPEX, 3 hours post-exercise.

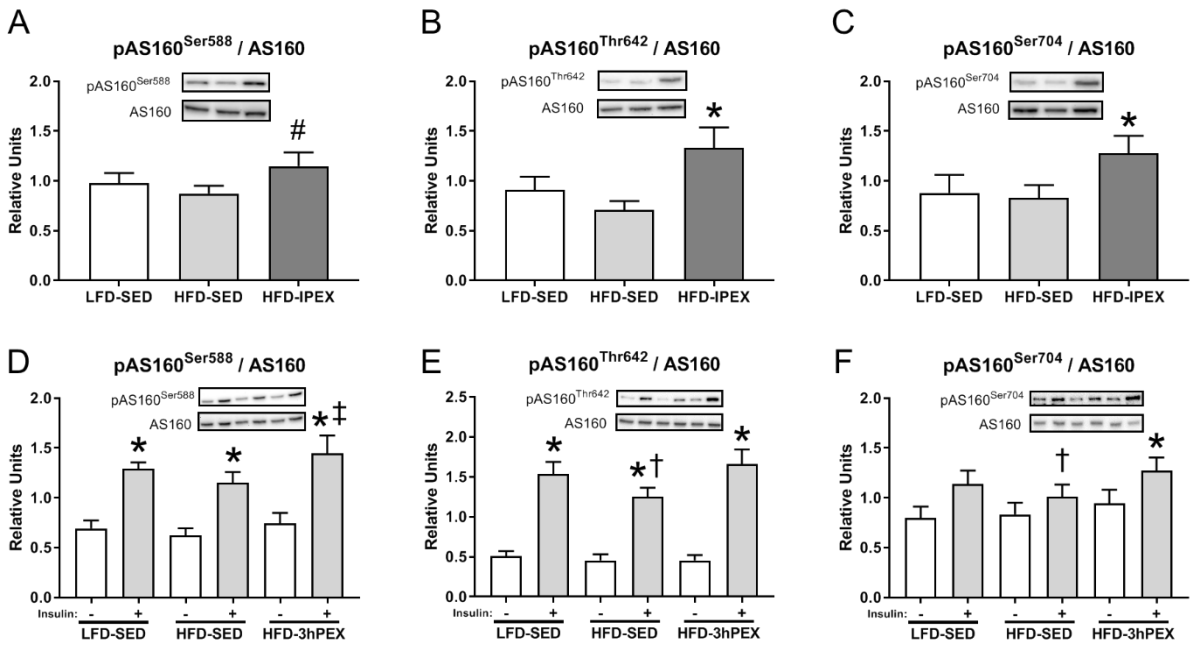

Figure 5.5

Post-exercise AS160 phosphorylation in epitrochlearis muscle from high fat-fed rats versus sedentary controls. A-C) Phosphorylated AS160^{Ser588}, AS160^{Thr642}, and AS160^{Ser704}/AS160 immediately post-exercise. Data were analyzed by one-way ANOVA. *P < 0.005, HFD-IPEX vs both LFD-SED and HFD-SED. #P < 0.01, HFD-IPEX vs HFD-SED only. Values are expressed as mean ± 95% confidence interval; n = 17/group. D-F) phosphorylated AS160^{Ser588}, AS160^{Thr642}, and AS160^{Ser704}/AS160 at 3 hours post-exercise. Data were analyzed by two-way ANOVA. *P < 0.001, insulin vs no insulin. †P < 0.001, HFD-SED vs both LFD-SED and HFD-3hPEX within insulin treated muscles. ‡P < 0.01, HFD-3hPEX vs HFD-SED within insulin treated muscles. Values are expressed as mean ± 95% confidence interval; n = 10-17/group. HFD, high-fat diet; LFD, low-fat diet; SED, sedentary; IPEX, immediately post-exercise; 3hPEX, 3 hours post-exercise.

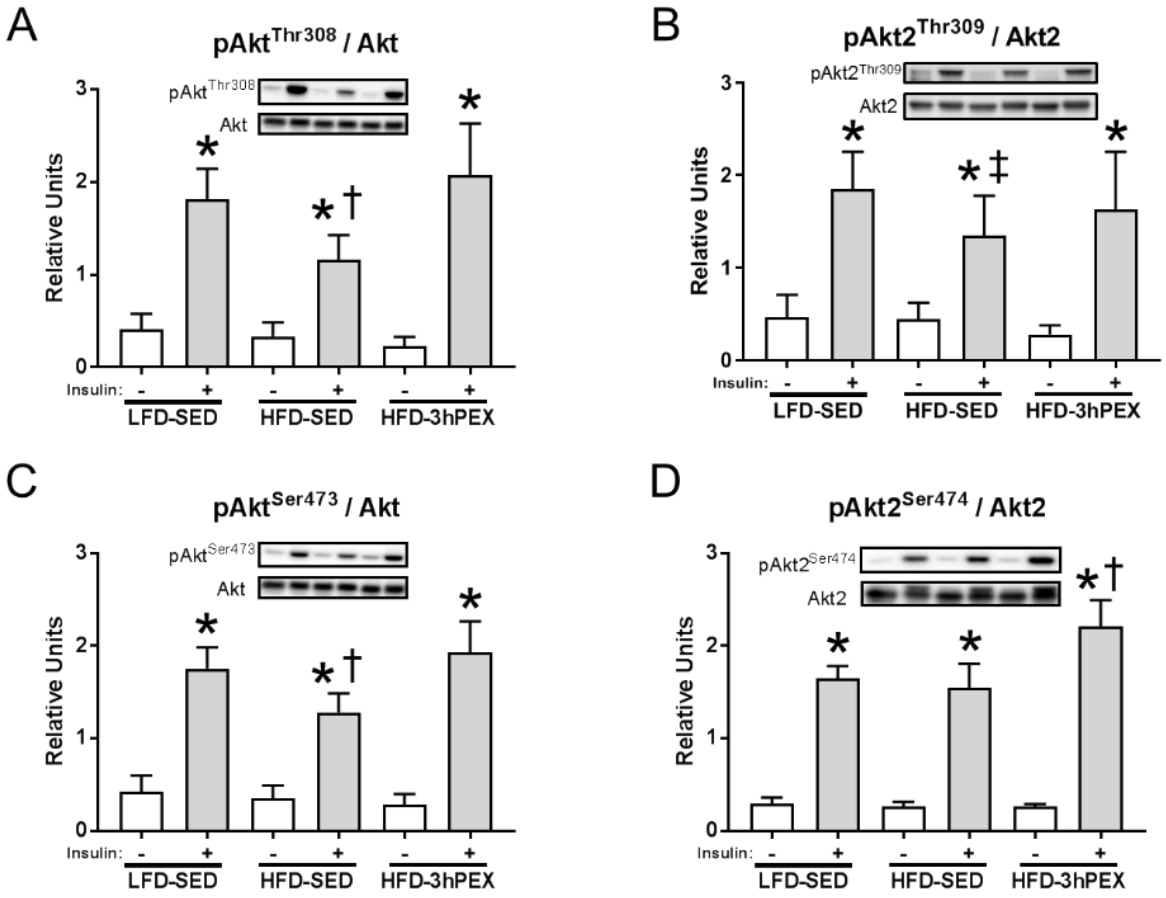

Figure 5.6

Post-exercise insulin-stimulated Akt and Akt2 phosphorylation in epitrochlearis muscle from high fat-fed rats versus sedentary controls. A-D) Phosphorylated Akt^{Thr308}/Akt, Akt^{Ser473}/Akt, $Akt2^{Thr309}$/Akt2 and $Akt2^{Ser474}$/Akt2 at 3 hours post-exercise. Data were analyzed by two-way ANOVA. *P < 0.001, insulin vs no insulin. †P < 0.01, significantly different than both other treatment groups within insulin treated muscles. ‡P < 0.05, significantly different than LFD-SED within insulin treated muscles. Values are expressed as mean ± 95% confidence interval; n = 10/group. HFD, high-fat diet; LFD, low-fat diet; SED, sedentary; 3hPEX, 3 hours post-exercise.

REFERENCES

1. DeFronzo, R., E. Jacot, E. Jequier, E. Maeder, J. Wahren, and J. Felber, *The effect of insulin on the disposal of intravenous glucose: results from indirect calorimetry and hepatic and femoral venous catheterization.* Diabetes, 1981. **30**(12): p. 1000-1007.
2. Castorena, C.M., E.B. Arias, N. Sharma, and G.D. Cartee, *Postexercise improvement in insulin-stimulated glucose uptake occurs concomitant with greater AS160 phosphorylation in muscle from normal and insulin-resistant rats.* Diabetes, 2014. **63**(7): p. 2297-308.
3. Ropelle, E.R., J.R. Pauli, P.O. Prada, C.T. De Souza, P.K. Picardi, M.C. Faria, D.E. Cintra, M.F.d.A. Fernandes, M.B. Flores, and L.A. Velloso, *Reversal of diet-induced insulin resistance with a single bout of exercise in the rat: the role of PTP1B and IRS-1 serine phosphorylation.* The Journal of Physiology, 2006. **577**(3): p. 997-1007.
4. Richter, E.A., L.P. Garetto, M.N. Goodman, and N.B. Ruderman, *Muscle glucose metabolism following exercise in the rat: increased sensitivity to insulin.* Journal of Clinical Investigation, 1982. **69**(4): p. 785-793.
5. Richter, E.A., K. Mikines, H. Galbo, and B. Kiens, *Effect of exercise on insulin action in human skeletal muscle.* Journal of Applied Physiology, 1989. **66**(2): p. 876-885.
6. Cartee, G.D., *Mechanisms for greater insulin-stimulated glucose uptake in normal and insulin-resistant skeletal muscle after acute exercise.* American Journal of Physiology-Endocrinology and Metabolism, 2015. **309**(12): p. E949-E959.
7. Wallberg-Henriksson, H., S. Constable, D. Young, and J. Holloszy, *Glucose transport into rat skeletal muscle: interaction between exercise and insulin.* Journal of applied physiology, 1988. **65**(2): p. 909-913.
8. Cartee, G.D., D.A. Young, M.D. Sleeper, J. Zierath, H. Wallberg-Henriksson, and J.O. Holloszy, *Prolonged increase in insulin-stimulated glucose transport in muscle after exercise.* Am J Physiol, 1989. **256**(4 Pt 1): p. E494-9.
9. Mikines, K.J., B. Sonne, P. Farrell, B. Tronier, and H. Galbo, *Effect of physical exercise on sensitivity and responsiveness to insulin in humans.* American Journal of Physiology-Endocrinology And Metabolism, 1988. **254**(3): p. E248-E259.
10. Cartee, G. and J. Holloszy, *Exercise increases susceptibility of muscle glucose transport to activation by various stimuli.* American Journal of Physiology-Endocrinology And Metabolism, 1990. **258**(2): p. E390-E393.
11. Hansen, P.A., L.A. Nolte, M.M. Chen, and J.O. Holloszy, *Increased GLUT-4 translocation mediates enhanced insulin sensitivity of muscle glucose transport after exercise.* Journal of Applied Physiology, 1998. **85**(4): p. 1218-1222.
12. Wojtaszewski, J.F., B.F. Hansen, B. Kiens, and E.A. Richter, *Insulin signaling in human skeletal muscle: time course and effect of exercise.* Diabetes, 1997. **46**(11): p. 1775-1781.
13. Fisher, J.S., J. Gao, D.-H. Han, J.O. Holloszy, and L.A. Nolte, *Activation of AMP kinase enhances sensitivity of muscle glucose transport to insulin.* American Journal of Physiology-Endocrinology And Metabolism, 2002. **282**(1): p. E18-E23.
14. Thong, F.S., W. Derave, B. Kiens, T.E. Graham, B. Ursø, J.F. Wojtaszewski, B.F. Hansen, and E.A. Richter, *Caffeine-induced impairment of insulin action but not insulin signaling in human skeletal muscle is reduced by exercise.* Diabetes, 2002. **51**(3): p. 583-590.

15. Wojtaszewski, J.F., B.F. Hansen, B. Kiens, J. Markuns, L. Goodyear, and E. Richter, *Insulin signaling and insulin sensitivity after exercise in human skeletal muscle.* Diabetes, 2000. **49**(3): p. 325-331.
16. Hamada, T., E.B. Arias, and G.D. Cartee, *Increased submaximal insulin-stimulated glucose uptake in mouse skeletal muscle after treadmill exercise.* Journal of Applied Physiology, 2006. **101**(5): p. 1368-1376.
17. Tanaka, S., T. Hayashi, T. Toyoda, T. Hamada, Y. Shimizu, M. Hirata, K. Ebihara, H. Masuzaki, K. Hosoda, and T. Fushiki, *High-fat diet impairs the effects of a single bout of endurance exercise on glucose transport and insulin sensitivity in rat skeletal muscle.* Metabolism, 2007. **56**(12): p. 1719-1728.
18. Pehmøller, C., N. Brandt, J.B. Birk, L.D. Høeg, K.A. Sjøberg, L.J. Goodyear, B. Kiens, E.A. Richter, and J.F. Wojtaszewski, *Exercise alleviates lipid-induced insulin resistance in human skeletal muscle–signaling interaction at the level of TBC1 domain family member 4.* Diabetes, 2012. **61**(11): p. 2743-2752.
19. Cartee, G.D., *Roles of TBC1D1 and TBC1D4 in insulin-and exercise-stimulated glucose transport of skeletal muscle.* Diabetologia, 2015. **58**(1): p. 19-30.
20. Arias, E.B., J. Kim, K. Funai, and G.D. Cartee, *Prior exercise increases phosphorylation of Akt substrate of 160 kDa (AS160) in rat skeletal muscle.* American Journal of Physiology-Endocrinology and Metabolism, 2007. **292**(4): p. E1191-E1200.
21. Treebak, J.T., C. Frøsig, C. Pehmøller, S. Chen, S.J. Maarbjerg, N. Brandt, C. MacKintosh, J. Zierath, D. Hardie, and B. Kiens, *Potential role of TBC1D4 in enhanced post-exercise insulin action in human skeletal muscle.* Diabetologia, 2009. **52**(5): p. 891-900.
22. Funai, K., G.G. Schweitzer, N. Sharma, M. Kanzaki, and G.D. Cartee, *Increased AS160 phosphorylation, but not TBC1D1 phosphorylation, with increased postexercise insulin sensitivity in rat skeletal muscle.* American Journal of Physiology-Endocrinology and Metabolism, 2009. **297**(1): p. E242-E251.
23. Funai, K., G.G. Schweitzer, C.M. Castorena, M. Kanzaki, and G.D. Cartee, *In vivo exercise followed by in vitro contraction additively elevates subsequent insulin-stimulated glucose transport by rat skeletal muscle.* American Journal of Physiology-Endocrinology and Metabolism, 2010. **298**(5): p. E999-E1010.
24. Sano, H., S. Kane, E. Sano, C.P. Mîinea, J.M. Asara, W.S. Lane, C.W. Garner, and G.E. Lienhard, *Insulin-stimulated phosphorylation of a Rab GTPase-activating protein regulates GLUT4 translocation.* Journal of Biological Chemistry, 2003. **278**(17): p. 14599-14602.
25. Iwabe, M., E. Kawamoto, K. Koshinaka, and K. Kawanaka, *Increased postexercise insulin sensitivity is accompanied by increased AS160 phosphorylation in slow-twitch soleus muscle.* Physiological Reports, 2014. **2**(12): p. e12162.
26. Schweitzer, G.G., E.B. Arias, and G.D. Cartee, *Sustained postexercise increases in AS160 Thr 642 and Ser 588 phosphorylation in skeletal muscle without sustained increases in kinase phosphorylation.* Journal of Applied Physiology, 2012. **113**(12): p. 1852-1861.
27. Wang, H., E.B. Arias, K. Oki, M.W. Pataky, J.A. Almallouhi, and G.D. Cartee, *Fiber Type-selective Exercise Effects on AS160 Phosphorylation.* American Journal of Physiology-Endocrinology and Metabolism, 2019. **316**: p. E837-E851.

28. Arias, E.B., H. Wang, and G.D. Cartee, *Akt substrate of 160 kDa dephosphorylation rate is reduced in insulin-stimulated rat skeletal muscle after acute exercise.* Physiological research, 2018. **67**(1): p. 143-147.
29. Kjøbsted, R., A. Chadt, N.O. Jørgensen, K. Kido, J.K. Larsen, C. de Wendt, H. Al-Hasani, and J.F. Wojtaszewski, *TBC1D4 is Necessary for Enhancing Muscle Insulin Sensitivity in Response to AICAR and Contraction.* Diabetes, 2019: p. db180769.
30. Kjøbsted, R., A.J. Pedersen, J.R. Hingst, R. Sabaratnam, J.B. Birk, J.M. Kristensen, K. Højlund, and J.F. Wojtaszewski, *Intact regulation of the AMPK signaling network in response to exercise and insulin in skeletal muscle of male patients with type 2 diabetes: illumination of AMPK activation in recovery from exercise.* Diabetes, 2016. **65**(5): p. 1219-1230.
31. Wang, H., E.B. Arias, M.W. Pataky, L.J. Goodyear, and G.D. Cartee, *Postexercise improvement in glucose uptake occurs concomitant with greater γ3-AMPK activation and AS160 phosphorylation in rat skeletal muscle.* American Journal of Physiology-Endocrinology and Metabolism, 2018. **315**: p. E859-E871.
32. Richter, E.A., L.P. Garetto, M.N. Goodman, and N.B. Ruderman, *Enhanced muscle glucose metabolism after exercise: modulation by local factors.* American Journal of Physiology-Endocrinology And Metabolism, 1984. **246**(6): p. E476-E482.
33. Vendelbo, M.H., A.B. Møller, J.T. Treebak, L.C. Gormsen, L.J. Goodyear, J.F. Wojtaszewski, J.O.L. Jørgensen, N. Møller, and N. Jessen, *Sustained AS160 and TBC1D1 phosphorylations in human skeletal muscle 30 min after a single bout of exercise.* Journal of Applied Physiology, 2014. **117**(3): p. 289-296.
34. Sjøberg, K.A., C. Frøsig, R. Kjøbsted, L. Sylow, M. Kleinert, A.C. Betik, C.S. Shaw, B. Kiens, J.F. Wojtaszewski, and S. Rattigan, *Exercise increases human skeletal muscle insulin sensitivity via coordinated increases in microvascular perfusion and molecular signaling.* Diabetes, 2017. **66**(6): p. 1501-1510.
35. Kjøbsted, R., N. Munk-Hansen, J.B. Birk, M. Foretz, B. Viollet, M. Björnholm, J.R. Zierath, J.T. Treebak, and J.F. Wojtaszewski, *Enhanced muscle insulin sensitivity after contraction/exercise is mediated by AMPK.* Diabetes, 2017. **66**(3): p. 598-612.
36. Kjøbsted, R., J.T. Treebak, J. Fentz, L. Lantier, B. Viollet, J.B. Birk, P. Schjerling, M. Björnholm, J.R. Zierath, and J.F. Wojtaszewski, *Prior AICAR stimulation increases insulin sensitivity in mouse skeletal muscle in an AMPK-dependent manner.* Diabetes, 2015. **64**(6): p. 2042-2055.
37. Turner, N., G.M. Kowalski, S.J. Leslie, S. Risis, C. Yang, R.S. Lee-Young, J.R. Babb, P.J. Meikle, G.I. Lancaster, D.C. Henstridge, P.J. White, E.W. Kraegen, A. Marette, G.J. Cooney, M.A. Febbraio, and C.R. Bruce, *Distinct patterns of tissue-specific lipid accumulation during the induction of insulin resistance in mice by high-fat feeding.* Diabetologia, 2013. **56**(7): p. 1638-48.
38. Pataky, M.W., H. Wang, C.S. Yu, E.B. Arias, R.J. Ploutz-Snyder, X. Zheng, and G.D. Cartee, *High-Fat Diet-Induced Insulin Resistance in Single Skeletal Muscle Fibers is Fiber Type Selective.* Scientific Reports, 2017. **7**(1): p. 13642.
39. Kjøbsted, R., J.R. Hingst, J. Fentz, M. Foretz, M.-N. Sanz, C. Pehmøller, M. Shum, A. Marette, R. Mounier, and J.T. Treebak, *AMPK in skeletal muscle function and metabolism.* The FASEB Journal, 2018. **32**(4): p. 1741-1777.
40. Treebak, J.T., C. Pehmøller, J.M. Kristensen, R. Kjøbsted, J.B. Birk, P. Schjerling, E.A. Richter, L.J. Goodyear, and J.F. Wojtaszewski, *Acute exercise and physiological insulin*

induce distinct phosphorylation signatures on TBC1D1 and TBC1D4 proteins in human skeletal muscle. The Journal of Physiology, 2014. **592**(2): p. 351-375.
41. Treebak, J.T., J.B. Birk, A.J. Rose, B. Kiens, E.A. Richter, and J.F. Wojtaszewski, *AS160 phosphorylation is associated with activation of α2β2γ1-but not α2β2γ3-AMPK trimeric complex in skeletal muscle during exercise in humans.* American Journal of Physiology-Endocrinology and Metabolism, 2007. **292**(3): p. E715-E722.
42. Kramer, H.F., C.A. Witczak, N. Fujii, N. Jessen, E.B. Taylor, D.E. Arnolds, K. Sakamoto, M.F. Hirshman, and L.J. Goodyear, *Distinct signals regulate AS160 phosphorylation in response to insulin, AICAR, and contraction in mouse skeletal muscle.* Diabetes, 2006. **55**(7): p. 2067-2076.
43. McCurdy, C.E. and G.D. Cartee, *Akt2 is essential for the full effect of calorie restriction on insulin-stimulated glucose uptake in skeletal muscle.* Diabetes, 2005. **54**(5): p. 1349-1356.
44. Cho, H., J. Mu, J.K. Kim, J.L. Thorvaldsen, Q. Chu, E.B. Crenshaw, K.H. Kaestner, M.S. Bartolomei, G.I. Shulman, and M.J. Birnbaum, *Insulin resistance and a diabetes mellitus-like syndrome in mice lacking the protein kinase Akt2 (PKBβ).* Science, 2001. **292**(5522): p. 1728-1731.
45. Abu-Elheiga, L., D.B. Almarza-Ortega, A. Baldini, and S.J. Wakil, *Human acetyl-CoA carboxylase 2 molecular cloning, characterization, chromosomal mapping, and evidence for two isoforms.* Journal of Biological Chemistry, 1997. **272**(16): p. 10669-10677.
46. O'Neill, H.M., J.S. Lally, S. Galic, T. Pulinilkunnil, R.J. Ford, J.R. Dyck, B.J. Denderen, B.E. Kemp, and G.R. Steinberg, *Skeletal muscle ACC2 S212 phosphorylation is not required for the control of fatty acid oxidation during exercise.* Physiological Reports, 2015. **3**(7): p. e12444.
47. Hardman, S.E., D.E. Hall, A.J. Cabrera, C.R. Hancock, and D.M. Thomson, *The effects of age and muscle contraction on AMPK activity and heterotrimer composition.* Experimental gerontology, 2014. **55**: p. 120-128.
48. Pataky, M.W., E.B. Arias, and G.D. Cartee, *Measuring Both Glucose Uptake and Myosin Heavy Chain Isoform Expression in Single Rat Skeletal Muscle Fibers*, in *Myogenesis* 2019, Springer. p. 283-300.
49. Cartee, G. and E. Bohn, *Growth hormone reduces glucose transport but not GLUT-1 or GLUT-4 in adult and old rats.* American Journal of Physiology-Endocrinology And Metabolism, 1995. **268**(5): p. E902-E909.
50. Antharavally, B.S., B. Carter, P.A. Bell, and A.K. Mallia, *A high-affinity reversible protein stain for Western blots.* Analytical biochemistry, 2004. **329**(2): p. 276-280.
51. Sharma, N., E.B. Arias, A.D. Bhat, D.A. Sequea, S. Ho, K.K. Croff, M.P. Sajan, R.V. Farese, and G.D. Cartee, *Mechanisms for increased insulin-stimulated Akt phosphorylation and glucose uptake in fast-and slow-twitch skeletal muscles of calorie-restricted rats.* American Journal of Physiology-Endocrinology and Metabolism, 2011. **300**(6): p. E966-E978.
52. Treebak, J.T., J.B. Birk, B.F. Hansen, G.S. Olsen, and J.F. Wojtaszewski, *A-769662 activates AMPK β1-containing complexes but induces glucose uptake through a PI3-kinase-dependent pathway in mouse skeletal muscle.* American Journal of Physiology-Cell Physiology, 2009. **297**(4): p. C1041-C1052.
53. Pataky, M.W., C.S. Yu, Y. Nie, E.B. Arias, M. Singh, C.L. Mendias, R.J. Ploutz-Snyder, and G.D. Cartee, *Skeletal Muscle Fiber Type-selective Effects of Acute Exercise on*

Insulin-stimulated Glucose Uptake in Insulin Resistant, High Fat-fed Rats. American Journal of Physiology-Endocrinology and Metabolism, 2019. **316**: p. E695-E706.
54. Winder, W. and D. Hardie, *Inactivation of acetyl-CoA carboxylase and activation of AMP-activated protein kinase in muscle during exercise.* American Journal of Physiology-Endocrinology And Metabolism, 1996. **270**(2): p. E299-E304.
55. Chen, Z.-P., G.K. McConell, B.J. Michell, R.J. Snow, B.J. Canny, and B.E. Kemp, *AMPK signaling in contracting human skeletal muscle: acetyl-CoA carboxylase and NO synthase phosphorylation.* American Journal of Physiology-Endocrinology And Metabolism, 2000. **279**(5): p. E1202-E1206.
56. Fujii, N., T. Hayashi, M.F. Hirshman, J.T. Smith, S.A. Habinowski, L. Kaijser, J. Mu, O. Ljungqvist, M.J. Birnbaum, and L.A. Witters, *Exercise induces isoform-specific increase in 5′ AMP-activated protein kinase activity in human skeletal muscle.* Biochemical and biophysical research communications, 2000. **273**(3): p. 1150-1155.
57. Wojtaszewski, J.F., P. Nielsen, B.F. Hansen, E.A. Richter, and B. Kiens, *Isoform-specific and exercise intensity-dependent activation of 5'-AMP-activated protein kinase in human skeletal muscle.* J Physiol, 2000. **528 Pt 1**: p. 221-6.
58. Hawley, S.A., M. Davison, A. Woods, S.P. Davies, R.K. Beri, D. Carling, and D.G. Hardie, *Characterization of the AMP-activated protein kinase kinase from rat liver and identification of threonine 172 as the major site at which it phosphorylates AMP-activated protein kinase.* Journal of Biological Chemistry, 1996. **271**(44): p. 27879-27887.
59. Stein, S.C., A. Woods, N.A. Jones, M.D. Davison, and D. Carling, *The regulation of AMP-activated protein kinase by phosphorylation.* Biochemical Journal, 2000. **345**(3): p. 437-443.
60. Birk, J.B. and J. Wojtaszewski, *Predominant α2/β2/γ3 AMPK activation during exercise in human skeletal muscle.* The Journal of Physiology, 2006. **577**(3): p. 1021-1032.
61. Kristensen, D.E., P.H. Albers, C. Prats, O. Baba, J.B. Birk, and J.F. Wojtaszewski, *Human muscle fibre type-specific regulation of AMPK and downstream targets by exercise.* The Journal of Physiology, 2015. **593**(8): p. 2053-2069.
62. Treebak, J.T., E.B. Taylor, C.A. Witczak, D. An, T. Toyoda, H.-J. Koh, J. Xie, E.P. Feener, J.F. Wojtaszewski, M.F. Hirshman, and L.J. Goodyear, *Identification of a novel phosphorylation site on TBC1D4 regulated by AMP-activated protein kinase in skeletal muscle.* American Journal of Physiology-Cell Physiology, 2009. **298**(2): p. C377-C385.
63. Geraghty, K.M., S. Chen, J.E. Harthill, A.F. Ibrahim, R. Toth, N.A. Morrice, F. Vandermoere, G.B. Moorhead, D.G. Hardie, and C. MacKintosh, *Regulation of multisite phosphorylation and 14-3-3 binding of AS160 in response to IGF-1, EGF, PMA and AICAR.* Biochemical Journal, 2007. **407**(2): p. 231-241.
64. Consitt, L.A., J. Van Meter, C.A. Newton, D.N. Collier, M.S. Dar, J.F. Wojtaszewski, J.T. Treebak, C.J. Tanner, and J.A. Houmard, *Impairments in site-specific AS160 phosphorylation and effects of exercise training.* Diabetes, 2013. **62**(10): p. 3437-3447.
65. Xie, X., Y. Chen, P. Xue, Y. Fan, Y. Deng, G. Peng, F. Yang, and T. Xu, *RUVBL2, a novel AS160-binding protein, regulates insulin-stimulated GLUT4 translocation.* Cell research, 2009. **19**(9): p. 1090.
66. Ren, W., S. Cheema, and K. Du, *The association of ClipR-59 protein with AS160 modulates AS160 protein phosphorylation and adipocyte Glut4 protein membrane translocation.* Journal of Biological Chemistry, 2012. **287**(32): p. 26890-26900.

67. Sharma, P., E.B. Arias, and G.D. Cartee, *Protein phosphatase 1-α regulates AS160 Ser588 and Thr642 dephosphorylation in skeletal muscle.* Diabetes, 2016. **65**(9): p. 2606-2617.
68. Steenberg, D.E., N.B. Jørgensen, J.B. Birk, K.A. Sjøberg, B. Kiens, E.A. Richter, and J.F. Wojtaszewski, *Exercise training reduces the insulin-sensitizing effect of a single bout of exercise in human skeletal muscle.* The Journal of physiology, 2019. **597**(1): p. 89-103.
69. Hingst, J.R., L. Bruhn, M.B. Hansen, M.F. Rosschou, J.B. Birk, J. Fentz, M. Foretz, B. Viollet, K. Sakamoto, and N.J. Færgeman, *Exercise-induced molecular mechanisms promoting glycogen supercompensation in human skeletal muscle.* Molecular metabolism, 2018. **16**: p. 24-34.
70. Frøsig, C., M.P. Sajan, S.J. Maarbjerg, N. Brandt, C. Roepstorff, J.F. Wojtaszewski, B. Kiens, R.V. Farese, and E.A. Richter, *Exercise improves phosphatidylinositol-3, 4, 5-trisphosphate responsiveness of atypical protein kinase C and interacts with insulin signalling to peptide elongation in human skeletal muscle.* The Journal of Physiology, 2007. **582**(3): p. 1289-1301.
71. Wang, H., N. Sharma, E.B. Arias, and G.D. Cartee, *Insulin signaling and glucose uptake in the soleus muscle of 30-month-old rats after calorie restriction with or without acute exercise.* Journals of Gerontology Series A: Biomedical Sciences and Medical Sciences, 2015. **71**(3): p. 323-332.
72. Bae, S.S., H. Cho, J. Mu, and M.J. Birnbaum, *Isoform-specific regulation of insulin-dependent glucose uptake by Akt/protein kinase B.* Journal of Biological Chemistry, 2003. **278**(49): p. 49530-49536.
73. Sakamoto, K., D.E. Arnolds, N. Fujii, H.F. Kramer, M.F. Hirshman, and L.J. Goodyear, *Role of Akt2 in contraction-stimulated cell signaling and glucose uptake in skeletal muscle.* American Journal of Physiology-Endocrinology and Metabolism, 2006. **291**(5): p. E1031-E1037.
74. Cartee, G.D., E.B. Arias, S.Y. Carmen, and M.W. Pataky, *Novel single skeletal muscle fiber analysis reveals a fiber type-selective effect of acute exercise on glucose uptake.* American Journal of Physiology-Endocrinology and Metabolism, 2016. **311**(5): p. E818-E824.

CHAPTER VI

Study 4

Fiber Type-specific Effects of Acute Exercise on Insulin-stimulated AS160 Phosphorylation in Insulin-Resistant Rat Skeletal Muscle

ABSTRACT

Muscle is a heterogeneous tissue composed of multiple fiber types. Earlier research revealed fiber type-selective post-exercise-effects on insulin-stimulated glucose uptake (ISGU) from insulin-resistant rats (increased for type IIA, IIB, IIBX and IIX, but not type I). In whole muscle from insulin-resistant rats, the exercise-effect on ISGU corresponds to the exercise-effect on insulin-stimulated AS160 phosphorylation (pAS160), an ISGU-regulating protein. We hypothesized that, in insulin-resistant muscle, the fiber type-selective exercise-effects on ISGU would correspond to the fiber type-selective exercise-effects on pAS160. Rats were fed a two-week high-fat diet (HFD) and remained sedentary (SED) or were exercised before epitrochlearis muscles were dissected either immediately post-exercise (IPEX) or at 3-hours post-exercise (3hPEX) using an exercise protocol that previously revealed fiber type-selective effects on ISGU. 3hPEX muscles and SED controls were incubated ±100μU/mL insulin. Individual myofibers were isolated, pooled based on myosin heavy chain expression (MHC), and key phosphoproteins were measured. Myofiber glycogen and MHC expression were evaluated in muscles from other SED, IPEX and 3hPEX rats. Insulin-stimulated $pAkt^{Ser473}$ and $pAkt^{Thr308}$ were unaltered by exercise in all fiber types. Insulin-stimulated pAS160 was greater for 3hPEX versus SED on at least one phosphosite (Ser588, Thr642 and/or Ser704) in type IIA, IIBX, and IIB fibers, but not in type I or IIX fibers. Both IPEX and 3hPEX glycogen were decreased versus SED in all fiber types. These results provided evidence that fiber type-specific pAS160 in insulin-resistant muscle may play a role in the previously reported fiber type-specific elevation in ISGU in some, but not all fiber types.

INTRODUCTION

Type 2 diabetes is a global health epidemic which costs the United States upwards of $133 billion annually [1]. Even in the absence of diabetes, insulin resistance is associated with many negative health outcomes [2]. Skeletal muscle accounts for up to 85% of insulin mediated glucose disposal making it a prime target for combating insulin resistance [3]. It is well documented that exercise can enhance insulin-stimulated glucose uptake into skeletal muscle from either healthy or insulin-resistant individuals [4-7]. The robust impact of exercise on insulin-stimulated glucose uptake by skeletal muscle has prompted the pursuit of mechanisms which link exercise to enhanced insulin sensitivity.

Extensive research has previously evaluated the potential effects of acute exercise on insulin signaling in skeletal muscle tissue as a possible mechanism for enhanced insulin sensitivity. The results of numerous studies suggest that insulin signaling events distal to Akt phosphorylation are likely important for increased insulin sensitivity after exercise [8-19]. In particular, the Rab GAP protein, AS160 (Akt Substrate of 160 kDa; also known as TBC1D4), has emerged as a leading candidate for mediating the effect of prior exercise on insulin sensitivity. In an unphosphorylated state, AS160 is believed to elevate GLUT4 translocation by maintaining Rab proteins in an inactive GDP bound state. Site-selective phosphorylation of AS160 results in GTP bound Rab, leading to greater GLUT4 vesicle exocytosis [20] and increased glucose uptake. The insulin-stimulated phosphorylation of AS160 on Ser588 [12, 13, 16, 21] and Thr642 [10, 11, 13, 14] has been reported to be enhanced in skeletal muscle several hours after exercise, concomitant with elevated insulin-stimulated glucose uptake. In addition, the time-course of the reversal of enhanced post-exercise insulin-stimulated AS160 phosphorylation tracks with the reversal of glucose uptake [10]. Taken together, these previous findings support the idea that greater pAS160^{Ser588} and pAS160^{Thr642} may be important for enhanced insulin sensitivity observed in the hours after exercise. Recent research has also reported increased insulin-stimulated pAS160^{Ser704} several hours after exercise in human and rat skeletal muscle [12, 18, 22, 23]. These results are intriguing given that Kjøbsted et al. found that mutating Ser704 on AS160 to Ala704, thereby preventing phosphorylation on this site, reduces the insulin-stimulated increase in pAS160^{Thr642} in mouse skeletal muscle [19]. These

observations suggest the possibility that phosphorylation of AS160^{Ser704} may contribute to enhanced phosphorylation of AS160^{Thr642} and insulin-stimulated glucose uptake [24, 25].

Although there is substantial evidence suggesting that increased site-selective AS160 phosphorylation may play a role in mediating the effect of exercise on insulin sensitivity, almost all of this previous research has been performed in whole muscle tissue. Skeletal muscle is a heterogeneous tissue composed of multiple fiber types, characterized by myosin heavy chain (MHC) isoform expression, that vary in metabolic and contractile properties [26]. Recent findings from our laboratory indicated that the effect of acute exercise on insulin-stimulated glucose uptake is fiber type-specific in skeletal muscle from healthy rats [27]. We subsequently evaluated fiber type-selective AS160 phosphorylation in insulin-stimulated muscles from healthy rats and reported that those fiber types with exercise-induced improvement in insulin-stimulated glucose uptake were also characterized by greater AS160 phosphorylation [28]. These findings provided evidence at the fiber type-specific and cellular levels consistent with the idea that AS160 plays a role in the increased insulin sensitivity after exercise in insulin-sensitive muscle. Although studying exercise effects on insulin sensitivity in healthy muscle is important, a more urgent need is to understand these processes in insulin resistance.

We recently found that a 2-week high-fat diet (HFD) can induce significant insulin resistance in the whole rat epitrochlearis muscle [16, 29], but analysis of single fibers from rats revealed that the insulin resistance was not uniform across all fiber types [29, 30]. Insulin resistance was detected in type II fibers (including IIA, IIAX, IIX, IIBX and IIB), but not in type I fibers [29]. Furthermore, when HFD-fed rats performed an acute bout of exercise, insulin-stimulated glucose uptake was increased in whole epitrochlearis muscles [16]. However, this exercise-benefit on insulin-stimulated glucose uptake occurred only in type II fibers, and not in type I fibers in HFD-fed rats [30]. Earlier research indicated that acute exercise can increase AS160 phosphorylation in muscles from insulin resistant rats and humans [12, 16], but the effects of exercise on fiber type-specific AS160 phosphorylation have not been reported. The evidence that exercise effects on AS160 phosphorylation are fiber type-specific in muscles from healthy rats [28], and that exercise effects on insulin-stimulated glucose uptake is fiber type-specific in muscles from insulin resistant rats [30], provides a clear rationale for evaluating fiber-type-specific signaling processes in insulin resistant muscle after exercise. Therefore our first

aim was to evaluate fiber-type-specific effects of exercise (both immediately post-exercise and 3-hours post-exercise with and without insulin) on the phosphorylation of key signaling proteins (AMPK, Akt, and AS160) that have been implicated in the regulation of exercise effects on skeletal muscle glucose uptake. We also evaluated the phosphorylation of acetyl CoA-carboxylase, an AMPK substrate, which is often used as an indicator of AMPK activity [19, 31, 32].

A striking finding in earlier research was that exercise resulted in increased insulin-stimulated glucose uptake in each of the insulin-resistant type II fiber types from HFD-fed rats [30], but exercise did not lead to greater insulin-stimulated glucose uptake in the only fiber type which that did not become insulin-resistant on a HFD [29]. The exercise protocol resulted in a significant reduction in muscle glycogen in all fiber types of HFD-fed rats immediately post-exercise, but glycogen concentration was not determined 3 h post-exercise, when insulin-stimulated glucose uptake was measured [30]. Previous research has suggested that the post-exercise restoration of muscle glycogen concentration might be important for the reversal of the post-exercise increase in insulin sensitivity [10, 33, 34]. Therefore, it seemed possible that in type I fibers glycogen concentration might have recovered by 3 h post-exercise. Accordingly, our second aim was to determine fiber type-specific glycogen content in epitrochlearis muscles from HFD-fed rats both immediately and 3-hours post-exercise compared to sedentary controls.

Hexokinase II (HKII) abundance has been suggested to be important for insulin-stimulated glucose uptake by skeletal muscle [35]. HKII mRNA expression [36, 37] and activity [36] of HKII have been shown to be increased in whole muscle several hours after one exercise session. Furthermore, HKII protein abundance is elevated in all fiber types after acute exercise in insulin-sensitive rats [28]. Therefore, our final aim was to assess the abundance of HKII after acute exercise in different fiber types from insulin-resistant rat skeletal muscle.

METHODS

Materials. The reagents and apparatus for SDS-PAGE, nonfat dry milk (#170-6404), and Clarity Max Western ECL Substrate (#1705062) were from Bio-Rad (Hercules, CA). Tissue Protein Extraction Reagent T-PER (#PI78510), Simply Blue SafeStain (#LC6065), Alexa Fluor

555 IgM (#A-21043), Alexa Fluor 647 IgG1 (#A-21240), Alexa Fluor 350 IgG2b (#A-21140), and WGA-Alexa Fluor 488 (#W11261) were from ThermoFisher (Pittsburgh, PA). Anti-MHC type IIB IgM (#BF-F3), anti-MHC type IIA IgG1 (#SC-71), and anti-MHC type I IgG2b (#BA-D5) were from Developmental Studies Hybridoma Bank, University of Iowa (Iowa City, IA). PhosStop^{TM} (#4906845001), Protease Inhibitor Cocktail (#P8340), periodic acid-Schiff (PAS) kit (#395B), and bovine liver glycogen type IX (#G0885) were from Sigma-Aldrich (St. Louis, MO). Anti-rabbit IgG horseradish peroxidase conjugate (#7074), anti-phospho Akt Ser^{473} (pAkt^{Ser473}; #4060), anti-phospho Akt Thr^{308} (pAkt^{Thr308}; #13038), anti-Akt (#4691), anti-phospho AS160 Thr^{642} (pAS160^{Thr642}; #4288), anti-phospho AS160 Ser^{588} (pAS160^{Ser588}; #8730), anti-AS160 (AS160; #2447), anti-phospho AMPKα Thr^{172} (pAMPKα^{Thr172}; #2535), anti-AMP-activated protein kinase-α (AMPKα; #2532), anti-acetyl CoA carboxylase (ACC; #3676), anti-phospho ACC Ser^{79} (pACC^{Ser79}; #3661), and anti-Hexokinase II (HKII; #2867) were from Cell Signaling Technology (Danvers, MA). Skeletal muscle expresses two isoforms of ACC (ACC1 and ACC2). ACC1 has a relatively low expression in skeletal muscle and is phosphorylated by AMPK on Ser^{79}. ACC2 has a relatively high expression in skeletal muscle and is phosphorylated by AMPK on Ser^{212} [38]. Since the pACC^{Ser79} antibody (#3661) detects both pACC1^{Ser79} and pACC2^{Ser212} [39], we hereafter refer to the results with this antibody as pACC$^{Ser79/212}$. Anti-phospho AS160^{Ser704} was provided by Dr. Jonas Treebak (University of Copenhagen, Denmark).

Animal treatment and muscle preparation. Procedures for animal care were approved by the University of Michigan Committee on Use and Care of Animals. Male Wistar rats (6-7 weeks old; Charles River Laboratories, Wilmington, MA) were individually housed and provided with high-fat chow (Laboratory Diet no. D12492; ResearchDiets, New Brunswick, NJ) and water *ad libitum* for two weeks until they were fasted on the night before the experiment at ~1700. Caloric intake for each rat during the two week diet period was estimated based on the difference between the food provided on day one and the food remaining at ~1700 on the night prior to the experiment. At ~0700 on the day of the experiment rats either remained sedentary or swam in a barrel filled with water (35°C) for four 30-minute bouts with 5-minutes of rest between bouts. Rats were anesthetized (intraperitoneal injection: 50mg/kg ketamine, 5mg/kg xylazine) either immediately post-exercise (IPEX) or at 3-hours post-exercise (3hPEX) with time matched sedentary controls. Rats were then weighed and epitrochlearis muscles were dissected. After muscle dissections, the epididymal fat pads were dissected and weighed.

Muscle storage and incubation. Muscles that were dissected IPEX (and sedentary controls) were immediately frozen in liquid N_2 and stored at -80°C until further processing. In the 3hPEX experiment, after dissection muscles underwent a two-step incubation process. First muscles were incubated in media 1 (Krebs Henseleit Buffer, KHB, supplemented with 0.1% BSA, 2mM sodium pyruvate, and 6mM mannitol) for 30min in glass vials gassed (95% O_2, 5% CO_2) in a temperature-controlled bath (35°C) with or without 100μU/mL insulin. Then muscles were transferred to other vials (35°C) containing fresh media 1 at the same insulin concentration (0 or 100μU/mL) for 20 minutes. After the second incubation, muscles were blotted, frozen in liquid N_2, and stored at -80°C until further processing.

Freeze-drying and isolation of single muscle fibers. Frozen muscles were processed as previously described [28, 40]. In brief, muscles were freeze-dried for 48 h and then individual fiber segments (~1-5mm in length) were isolated under a dissecting microscope (EZ4D; Leica; Buffalo Grove, IL) using fine forceps in a humidity-controlled room (30-35% humidity). Fibers were placed in individual PCR tubes and then 6μl of lysis buffer (T-PER, 1mM Na_3VO_4, 1mM EDTA, 1mM EGTA, 2.5mM sodium pyrophosphate tetrabasic decahydrate, 1mM β-glycerophosphate, 1μg/ml leupeptin, 1mM phenylmethylsulfonyl fluoride, 100μl/ml Protease Inhibitor Cocktail and 1 tablet/5ml PhosSTOP™) and 6μl of 6X Laemmli sample buffer were added to each tube. Tubes were placed on ice for at least 15minutes before heating at 95-100°C for 5min. Fiber lysates were then stored at -80°C until further processing.

Pooled freeze-dried fiber preparation and protein quantification. An aliquot (6μl) of each fiber lysate was used to determine fiber type by myosin heavy chain (MHC) isoform expression using SDS-PAGE as previously described [41, 42]. The remaining fiber lysate (6μl) of each sample was then pooled with other samples from the same muscle that expressed the same fiber type. This resulted in 5 pools of lysed fiber from each muscle containing samples which expressed type I, IIA, IIX, IIBX and IIB MHC. Although type IIAX hybrid fibers were detected, there was an insufficient amount of fibers (and thus protein) for subsequent immunoblotting.

A total of 1503 fibers isolated from 16 muscles (1 muscle per rat; 8 SED and 8 IPEX rats) was analyzed for the IPEX experiment. The means ± SE for number of pooled fibers used from each muscle of each fiber type from SED/IPEX groups were: type I (12 ± 2 / 12 ± 1), type IIA (13 ± 2 / 12 ± 1), type IIX (24 ± 5 / 17 ± 3), type IIBX (14 ± 1 / 18 ± 2), and type IIB (35 ± 5 / 34

± 4). A total of 4084 fibers isolated from 40 muscles (paired muscles of each rat were incubated with or without insulin; 10 SED and 10 3hPEX rats) was analyzed for the 3hPEX experiment. The means ± SE for number of pooled fibers used from each muscle of each fiber type from SED no insulin/SED insulin and 3hPEX no insulin/3hPEX insulin groups were: type I (16 ± 1 / 18 ± 1 and 18 ± 2 / 23 ± 2), type IIA (17 ± 2 / 20 ± 2 and 22 ± 2 / 23 ± 2), type IIX (21 ± 2 / 22 ± 2 and 25 ± 2 / 26 ± 2), type IIBX (20 ± 2 / 21 ± 2 and 23 ± 1 / 21 ± 2), and type IIB (38 ± 3 / 30 ± 3 and 39 ± 4 / 39 ± 3).

A 10µl aliquot of each pooled sample was loaded on 10% SDS-PAGE gels to determine the MHC protein concentration. On each gel there was a standard curve of known protein concentration (ranging from 0.2µg-3.2µg) made from homogenized epitrochlearis muscle. After electrophoresis, gels were stained for 1 h using Simply Blue SafeStain and destained for 2-3 h in deionized water. Stained MHC band intensity was quantified by densitrometry and protein concentration was determined using the standard curve (R^2=0.95-0.99).

Immunoblotting. Samples were heated (95-100°C) for 5 minutes, equal amount of pooled fiber lysate protein was subjected to SDS-PAGE, and then samples were transferred to polyvinylidene difluoride membranes. Following electrotransfer, gels were stained for 1hr (Simply Blue SafeStain), destained for 2-3hr (deionized water), and then MHC bands were quantified by densitometry to serve as loading controls. Membranes were blocked (3% BSA or nonfat milk in TBST, 45 minutes, room temperature), incubated in appropriate primary antibodies (3% BSA or nonfat milk in TBST, overnight, 4°C), and washed (3 X 5 minutes with TBST) before incubation in secondary antibody (3% BSA or nonfat milk in TBST, 1hr, room temperature). Membranes were then washed in TBST (3 X 5 minutes) and TBS (3 X 5 minutes) before exposure to Clarity Max Western ECL Substrate for 5 minutes. After imaging (Fluorchem E Imager, ProteinSimple, San Leandro, CA) proteins were quantified by densitometry and each sample value was expressed relative to the normalized average of all samples on the blot and divided by the respective MHC loading control. Phosphorylated protein data were expressed as a ratio of phosphorylated:total protein. The signal for pAS160^{Ser588} in type I fibers was insufficient to quantify, therefore the data are not shown.

Histochemical glycogen analysis. External standards of known glycogen concentration were created using bovine liver glycogen type IX as previously described [30, 43]. Serial muscle

cross-sections (10μm) were used for PAS staining and MHC detection. Each PAS slide also contained external glycogen standards (10μm) to reliably compare staining of muscle sections on separate slides. Slides were fixed in 10% formalin, treated with periodic acid and Schiff's reagent, washed, and mounted as previously described [30]. MHC identification was performed using standard procedures, as previously described [44]. Images of cross-sectionally oriented muscles were captured using a Keyence BZ-X700 microscope capable of fluorescent and bright-field illumination. DAPI, GFP, TRITC, and Cy5 filter cubes were used for the fluorescent detection of MHC isoforms and extracellular matrix at 10X magnification. PAS stained sections were captured using bright-field illumination at 10X magnification and converted to 8-bit for quantification of stain intensity. Image capture settings and conditions remained constant for PAS slide imaging to minimize variability between slides. Two researchers independently identified MHC isoform expression of all analyzed fibers to confirm accurate fiber typing. After fiber type was identified, the corresponding fibers in PAS images were manually traced (excluding the cell border) and quantified by mean grayscale value using ImageJ.

Statistics. Data are expressed as means ± standard error (SEM), with two-tailed significance levels of $\alpha \leq 0.05$. Two-tailed *t*-tests were used to determine the exercise effect in IPEX samples compared to sedentary. Two-way ANOVA was used to determine the effect of exercise and insulin on protein phosphorylation or abundance in the 3hPEX experiments. Because glycogen was collected from multiple individual fibers per rat, we analyzed these data using mixed-effects linear regression models, incorporating fixed parameters evaluating the contributions of treatment group (SED, IPEX, or 3hPEX) and interaction effects, random Y-intercepts to account for multiple observations within each rat. Analyses were performed using StataIC 14.2 (College Station, TX).

RESULTS

Signaling immediately post-exercise. Phosphorylation of AMPKα^{Thr172} divided by total AMPKα (pAMPKα^{Thr172}/AMPKα) was significantly greater ($P < 0.05$) immediately post-exercise (IPEX) compared to sedentary (SED) controls in type I, IIX, and IIB fibers (Figure 6.1). There was not a statistically significant IPEX-induced increase in pAMPKα^{Thr172}/AMPKα in

type IIA or IIBX fibers IPEX. The phosphorylation of $ACC^{Ser79/212}$ divided by total ACC ($pACC^{Ser79/212}$/ACC) was significantly greater ($P < 0.05$) in all fiber types IPEX versus SED controls (Figure 6.2). Phosphorylation of $AS160^{Ser704}$ divided by total AS160 ($pAS160^{Ser704}$/AS160) was significantly greater ($P < 0.01$) in all fiber types IPEX versus SED controls (Figure 6.3).

Insulin signaling 3-hours post-exercise. There was a significant main effect of insulin ($P < 0.001$) on the phosphorylation of Akt^{Ser473} divided by total Akt ($pAkt^{Ser473}$/Akt) in all fiber types. Post-hoc analyses revealed significant effects of insulin on $pAkt^{Ser473}$/Akt within both SED and 3hPEX muscles of all fiber types ($P < 0.05$) (Figure 6.4).

There was a significant main effect of insulin ($P < 0.005$) on the phosphorylation of Akt^{Thr308} divided by total Akt ($pAkt^{Thr308}$/Akt) in all fiber types. Post-hoc analyses revealed significant effects of insulin on $pAkt^{Thr308}$/Akt within both SED and 3hPEX muscles of all fiber types ($P \leq 0.05$) (Figure 6.5). We did not detect significant exercise-induced changes in Akt phosphorylation (on Ser473 or Thr308) in any fiber type.

There was a significant main effect of insulin ($P < 0.005$) on the phosphorylation of $AS160^{Ser704}$ divided by total AS160 ($pAS160^{Ser704}$/AS160) in type I, IIA, IIBX, and IIB fibers at 3hPEX. A significant main effect of exercise ($P < 0.05$) was detected for $pAS160^{Ser704}$/AS160 in type IIBX and IIB fibers. A significant insulin by exercise interaction ($P < 0.05$) was detected for $pAS160^{Ser704}$/AS160 in type I and IIBX fibers. Post-hoc analyses revealed that insulin-stimulated $pAS160^{Ser704}$/AS160 at 3hPEX was greater versus SED in type IIBX and IIB fibers ($P < 0.05$). The insulin-stimulated increase in $pAS160^{Ser704}$/AS160 was significant in type I, IIA and IIB fiber from SED rats ($P < 0.05$), and in type IIA, IIBX, and IIB 3hPEX fibers from 3hPEX rats ($P < 0.05$) (Figure 6.6).

There was a significant main effect of insulin ($P < 0.001$) on the phosphorylation of $AS160^{Thr642}$ divided by total AS160 ($pAS160^{Thr642}$/AS160) in all fiber types at 3hPEX. A significant insulin by exercise interaction ($P < 0.05$) was detected for $pAS160^{Thr642}$/AS160 in type I fibers. Post-hoc analyses revealed that insulin-stimulated $pAS160^{Thr642}$/AS160 at 3hPEX was greater versus SED in type IIA and IIBX fibers ($P < 0.05$), but was lower versus SED in type I fibers ($P < 0.05$). Insulin-stimulated $pAS160^{Thr642}$/AS160 was significantly greater in all

fiber types from SED rats ($P < 0.005$), and in type IIA, IIX, IIBX and IIB fibers from 3hPEX rats ($P < 0.001$) (Figure 6.7).

There was a significant main effect of insulin ($P < 0.005$) on the phosphorylation of $AS160^{Ser588}$ divided by total AS160 ($pAS160^{Ser588}$/AS160) in type IIA, IIX, IIBX, and IIB fibers at 3hPEX. A significant main effect of exercise ($P < 0.01$) was detected for $pAS160^{Ser588}$/AS160 in type IIA fibers. Post-hoc analyses revealed that insulin-stimulated $pAS160^{Ser588}$/AS160 at 3hPEX was greater versus SED in type IIA fibers ($P < 0.05$). Insulin-stimulated $pAS160^{Ser588}$/AS160 was significantly greater in type IIA, IIX, IIBX and IIB fiber from SED rats ($P < 0.05$), and 3hPEX rats ($P < 0.05$) (Figure 6.8).

Glycogen. Glycogen values was significantly decreased ($P < 0.001$) at both IPEX and 3hPEX groups when compared to SED in all fiber types (Figures 6.9 & 6.10). At 3hPEX versus IPEX the type IIX, IIBX, and IIB fibers had significantly greater glycogen values ($P < 0.001$), but glycogen levels at 3hPEX remained significantly lower than the SED group.

Hexokinase II abundance. The abundance of hexokinase II (HKII) was significantly greater ($P < 0.05$) at 3hPEX versus SED in all fiber types (Figure 6.11).

DISCUSSION

Improved insulin-stimulated glucose uptake is a critical health benefit of exercise that is observed in both healthy and insulin resistant skeletal muscle. The specific molecular and cellular processes responsible for this important outcome are not completely understood. In whole muscle tissue, increased AS160 phosphorylation has emerged as an attractive candidate for mediating the effects of exercise on insulin-stimulated glucose uptake. Recently we observed in healthy rats that exercise-induced fiber type-specific increases in insulin-stimulated glucose uptake correspond to fiber type-specific insulin-stimulated AS160 phosphorylation on multiple sites [28]. However, the mechanisms which lead to increased insulin-stimulated glucose uptake after exercise in insulin resistant muscle fibers may differ from those in insulin sensitive muscle. Therefore, we assessed the effects of exercise and insulin on signaling differences at a fiber type-specific level in insulin resistant rat muscle. In different fiber types from insulin resistant muscle we discovered: 1) recruitment of all fiber types was strongly evidenced by decreased glycogen

along with increased pACC$^{Ser79/212}$ and pAS160^{Ser704} for IPEX versus SED rats; 2) insulin-stimulated pAkt^{Ser473} and pAkt^{Thr308} were unaffected by exercise in all fiber types; 3) a fiber type-specific effect of exercise on insulin-stimulated pAS160^{Ser704}, pAS160^{Thr642}, and pAS160^{Ser588} for 3hPEX versus SED; 4) glycogen levels were lower for 3hPEX compared to SED in all fiber types; and 5) HKII abundance was greater in all fiber types for 3hPEX versus SED.

Multiple lines of evidence indicate that all fiber types were recruited by the exercise protocol. Glycogen levels were significantly reduced for all fiber types in IPEX compared to SED rats. We also observed increased pAMPKα^{Thr172} IPEX in type IIB, IIX, and I fibers, but unaltered pAMPKα^{Thr172} IPEX in type IIBX, and IIA fibers. Although pAMPKα^{Thr172} was not elevated IPEX in every fiber type, the phosphorylation of AMPK may not completely reflect its enzymatic activity because AMPK can be allosterically activated by AMP binding [45]. In this context, there is evidence that AMPK was activated in all fiber types from IPEX versus SED rats based on an increase in pACC$^{Ser79/212}$, an AMPK substrate and widely used indicator for greater AMPK activity [46, 47]. Greater activation of AMPK was also evidenced by enhanced pAS160^{Ser704} in all fiber types from IPEX compared to SED rats. The current results, along with our earlier report that the same exercise protocol significantly increased insulin-independent glucose uptake in all fiber types of IPEX versus SED rats [30], provide substantial evidence that all fiber types were recruited by the exercise protocol. It is unlikely that the lack of an exercise-induced increase in AS160 phosphorylation at 3hPEX in type I fibers was attributable to a lack of type I fiber recruitment by the exercise protocol.

Our recent determination of both glucose uptake and fiber type in single fibers from rats undergoing the same diet and exercise treatment as in the current study revealed that the exercise effect on insulin-stimulated glucose uptake is not uniform across all fiber types [30]. In that study, insulin-stimulated glucose uptake in type II fibers (IIA, IIB, IIBX and IIX) from HFD-3hPEX rats exceeded HFD-SED values, but no exercise-effect on insulin-stimulated glucose uptake was evident for type I fibers [30]. The current study offers new insights into possible reasons for the differential fiber-type specific increases in insulin-stimulated glucose uptake after acute exercise by HFD-fed rats. In type IIB, IIBX, and IIA fibers we observed post-exercise enhancement of insulin-stimulated AS160 phosphorylation on one or more phosphosites (IIB on Ser704; IIBX on Ser704 and Thr642; and IIA on Thr642 and Ser588) in HFD-fed rats at 3hPEX.

The elevated AS160 phosphorylation may play a role in the enhanced post-exercise insulin-stimulated glucose uptake found in these fiber types. In contrast, in type IIX fibers the insulin-stimulated AS160 phosphorylation was unaltered after exercise on all of the measured phosphosites, suggesting that other mechanisms are responsible for the improved post-exercise insulin-stimulated glucose uptake in IIX fibers. In type I fibers the current study found decreased insulin-stimulated pAS160^{Ser704} and pAS160^{Thr642} after exercise in HFD-fed rats. The decrease in insulin-stimulated AS160 site-selective phosphorylation in type I fibers after exercise may contribute to the absence of an effect of exercise on insulin-stimulated glucose uptake.

A striking observation from our previous study using the same diet and exercise protocol was that insulin-stimulated glucose uptake was not increased in type I fibers from HFD-3hPEX versus HFD-SED rats [30]. Because it has been suggested that recovery of muscle glycogen after exercise may be important for the reversal of insulin-stimulated glucose uptake [10, 33, 34], it seemed possible that glycogen might have been rapidly restored in type I fibers from HFD-3hPEX rats. Accordingly, we tested this idea by measuring fiber type-specific glycogen values of epitrochlearis muscles from SED, IPEX, and 3hPEX rats. Glycogen levels at 3hPEX in type I fibers remained significantly below SED values, and not different from IPEX levels. The current glycogen results together with the previously reported fiber type-specific glucose uptake data in HFD-fed rats after the same exercise protocol are consistent with the results from earlier research suggesting that a sustained decrease in glycogen after exercise may be necessary, but is not sufficient for the post-exercise increase in insulin sensitivity [19, 48].

Given that glycogen values had not been resynthesized to SED control levels at 3hPEX in type I fibers, what are other possible mechanisms that might account for the absence of improved insulin-stimulated glucose uptake in type I fibers? AMPK activation has been proposed to play an important role in triggering events that lead to insulin-stimulated glucose uptake. AMPK is a heterotrimeric protein complex composed of one catalytic (α) and two regulatory (β and γ) subunits. γ3-containing AMPK is essential for the effect of AICAR, an AMPK activator, on insulin-stimulated glucose uptake [19]. Furthermore, substantial evidence has consistently shown that γ3-containing AMPK is activated after exercise [31, 32, 49, 50] and remains elevated hours later concomitant with insulin-stimulated glucose uptake in both chow-fed [23] and HFD-fed rats (manuscript in review). It is possible that type I fibers from HFD-fed rats do not have sustained

post-exercise elevations in γ3-AMPK activity, which in turn might be responsible for the lack of a post-exercise effect on insulin-stimulated glucose uptake. Our preliminary experiments used ~100 fibers to measure γ3-AMPK activity (unpublished data). For this experiment, we typically collected ~12-18 type I fibers/muscle, suggesting we would need to pool type I fibers from up to ~6-8 rats for each data-point. Accordingly, evaluating γ3-AMPK in pooled fiber samples will be quite challenging because of the quantity of muscle that is required for determination of γ3-AMPK activity.

Earlier research on rats with normal insulin sensitivity subjected to the same exercise protocol as used in the current study found that insulin-stimulated glucose uptake was increased at 3hPEX above SED values for type I, IIA, IIB, and IIBX fibers, but not for type IIX fibers [27]. AS160 phosphorylation was also increased in each of the fiber types with post-exercise elevation in insulin-stimulated glucose uptake (I, IIA, IIB and IIBX), but not in type IIX fibers from 3hPEX compared to SED rats with normal insulin sensitivity [28]. Thus, type IIA, IIB and IIBX fibers from either insulin sensitive or insulin resistant rats had increased post-exercise insulin-stimulated glucose uptake concomitant with greater AS160 phosphorylation. In contrast, exercise effects on type I fibers were different for insulin sensitive (both insulin-stimulated glucose uptake and AS160 phosphorylation increased) compared to insulin resistant (insulin-stimulated glucose uptake unchanged and AS160 phosphorylation decreased) rats. However, the results for type I fibers in both diet groups support the idea that increased insulin-stimulated AS160 phosphorylation is linked to post-exercise effects on insulin sensitivity. The results for type IIX fibers in insulin sensitive rats provide further evidence for an association between greater insulin-stimulated AS160 phosphorylation and greater insulin-stimulated glucose uptake (i.e., neither was increased after exercise). Among the five fiber types evaluated in both normal and insulin resistant rats, only type IIX fibers from HFD rats were characterized by greater insulin-stimulated glucose uptake for 3hPEX versus diet-matched SED controls without an exercise-induced improvement in AS160 phosphorylation. Taking together all of the observations from the earlier and current research provides considerable evidence for a relationship between post-exercise effects on AS160 phosphorylation and glucose uptake in insulin-stimulated fibers.

What might account for the improved insulin-stimulated glucose uptake in type IIX fibers from the HFD-3hPEX rats in which AS160 phosphorylation was not increased? Overexpression

of HKII can lead to elevated post-exercise glucose uptake in mouse skeletal muscle [51]. In chow-fed rats with normal insulin sensitivity performing the same exercise protocol as used in this study, HKII protein expression was either significantly increased (type I, IIB, IIBX and IIX) or tended to increase (type IIA) at 3hPEX compared to SED values [28]. Similarly, HKII abundance of HFD-3hPEX rats exceeded HFD-SED values in all fiber types. Taking together the exercise-induced increase in HKII abundance in type I fibers in the current study with earlier results indicating that insulin-stimulated glucose uptake was not increased in type I fibers of HFD-3hPEX rats suggests that increased HKII expression after exercise is not sufficient for the elevation in insulin-stimulated glucose uptake in type I fibers. However, it remains possible that greater HKII abundance has a role in the improved insulin-stimulated glucose uptake that was previously reported for IIX fibers, and possibly other type II fiber types, from HFD-3hPEX rats [30].

Exercise did not significantly alter insulin-stimulated $pAkt^{Ser473}$ or $pAkt^{Thr308}$ after exercise in any fiber type, indicating that enhanced Akt phosphorylation was not responsible for the elevated insulin-stimulated glucose uptake in any of the fiber types. The lack of an effect of exercise on insulin-stimulated Akt phosphorylation in all fiber types is consistent with the results from previous studies that analyzed whole muscle tissue [12, 18, 52-55]. However, we recently observed in whole epitrochlearis muscle from rats undergoing the same diet and exercise protocols as the current study that insulin-stimulated $pAkt^{Ser473}$ and $pAkt^{Thr308}$ were increased at 3hPEX (manuscript in review). Skeletal muscle includes many cell types other than muscle fibers, so whole muscle analysis reflects the sum total for all cells types. Other cell types that are included in whole skeletal muscle analysis (including adipocytes, smooth muscle cells, endothelial cells, nerve cells, fibroblasts, erythrocytes, platelets, neutrophils) are known to express Akt [56-61]. Thus, interpreting together the results of the current study and our unpublished data from HFD-fed whole muscles (manuscript in review), an intriguing possibility is that acute exercise may enhance Akt phosphorylation in cell types other than myofibers. Future research will be required to test this provocative idea.

By definition, glucose uptake is a cellular process, so evaluating fiber type differences is essential to fully understand the regulation of glucose uptake. Previous data using whole muscle [8, 10, 13, 23] or single fibers [28] from insulin-sensitive rats demonstrated a strong relationship

between increased AS160 phosphorylation and improved insulin-stimulated glucose uptake after exercise. This relationship was also observed in whole muscle from insulin resistant rats [16] (manuscript in review). However, the lack of a uniform effect of prior exercise on insulin-stimulated AS160 phosphorylation across all fiber types in the current study using insulin resistant muscle revealed novel and important information about the complexity of this relationship that could not have been discovered using only whole muscle analysis. These data provide further evidence for a possible role of AS160 in post-exercise insulin-stimulated glucose uptake, but this relationship was notably absent in insulin-resistant type IIX fibers. The underlying biological basis for the different post-exercise responses in various fiber types with regard to insulin-stimulated glucose uptake or pAS160 remains to be elucidated, but the current results indicate that the fiber type-differences are not attributable to differences in post-exercise effects on Akt phosphorylation, glycogen levels or HKII abundance. The current results revealed the need for future research to test the possible causal relationships between post-exercise outcomes (including site-selective AS160 phosphorylation, increased HKII abundance, and other post-exercise events such as γ3-AMPK activity) and post-exercise insulin-stimulated glucose uptake in each fiber type from insulin resistant animals.

ACKNOWLEDGEMENTS

These experiments were supported by a grant from the National Institutes of Health (R01 DK71771). I would like to thank Sydney Van Acker, Rhea Dhingra, Marina Freeburg, Ed Arias, Haiyan Wang, Ken Oki, Ed Arias, Jalal Almallouhi, and Manak Singh for their technical assistance. I also appreciate Dr. Jonas Treebak for generously supplying the pAS160^{Ser704} antibody.

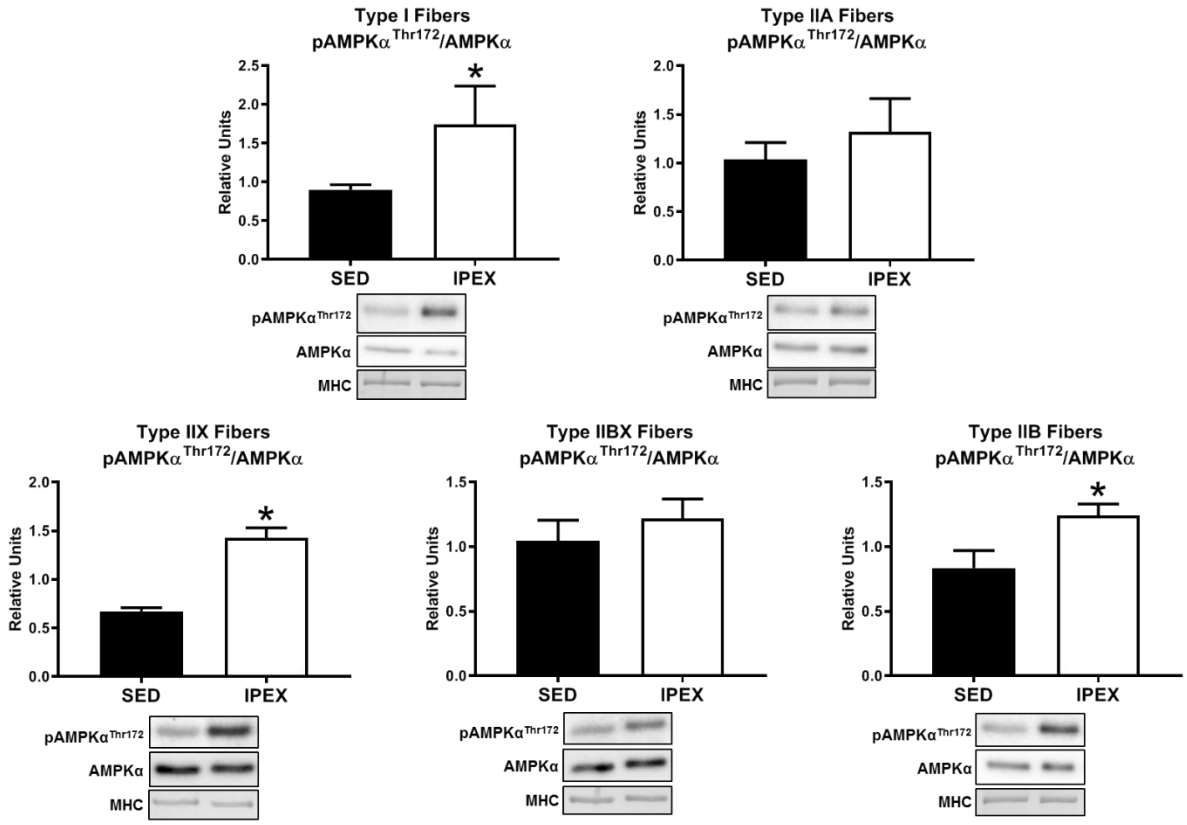

Figure 6.1

Fiber type-specific pAMPKα^{Thr172}/AMPKα immediately post-exercise from high-fat diet fed rats. *P ≤ 0.05, indicates IPEX significantly greater than SED. Values are mean ± SEM, n = 7-8 per group. Representative blots and loading controls are included for each fiber type. SED, sedentary; IPEX, immediately post-exercise; MHC, myosin heavy chain.

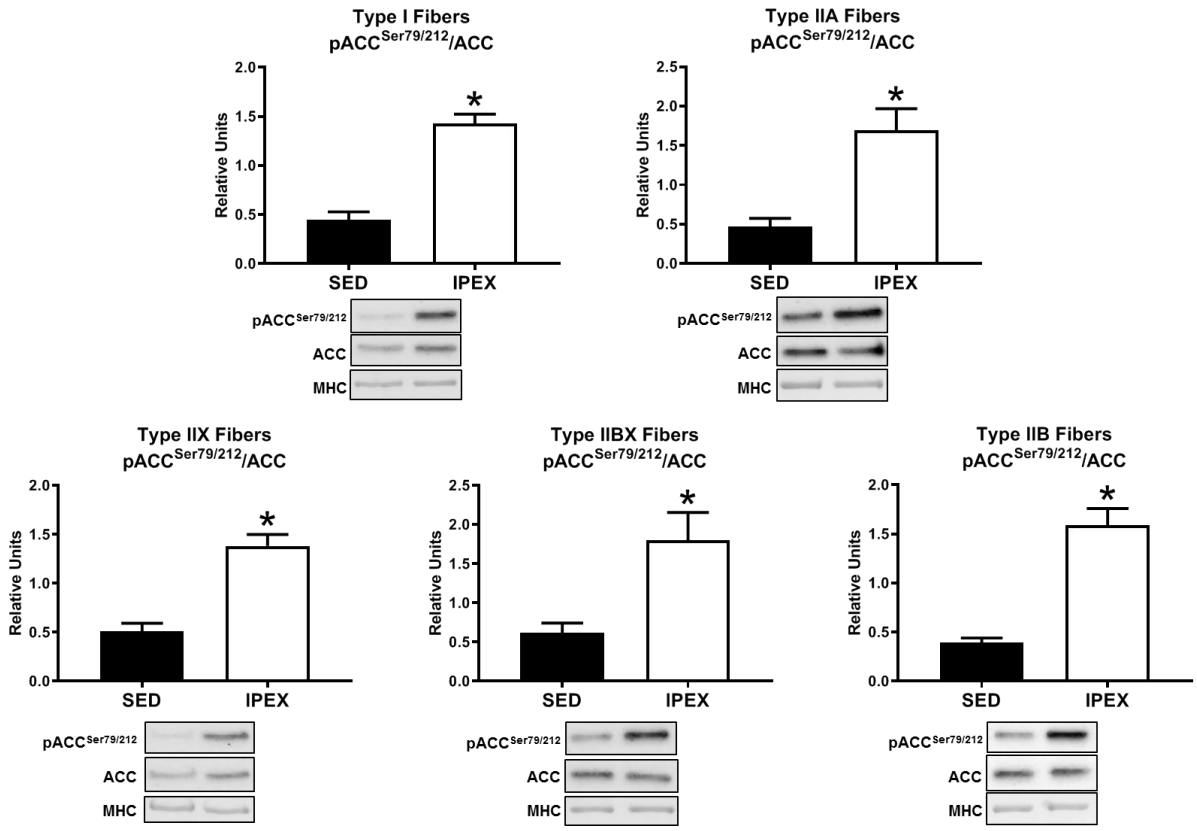

Figure 6.2

Fiber type-specific pACC$^{Ser79/212}$/ACC immediately post-exercise from high-fat diet fed rats. *P ≤ 0.05, indicates IPEX significantly greater than SED. Values are mean ± SEM, n = 6-8 per group. Representative blots and loading controls are included for each fiber type. SED, sedentary; IPEX, immediately post-exercise; MHC, myosin heavy chain.

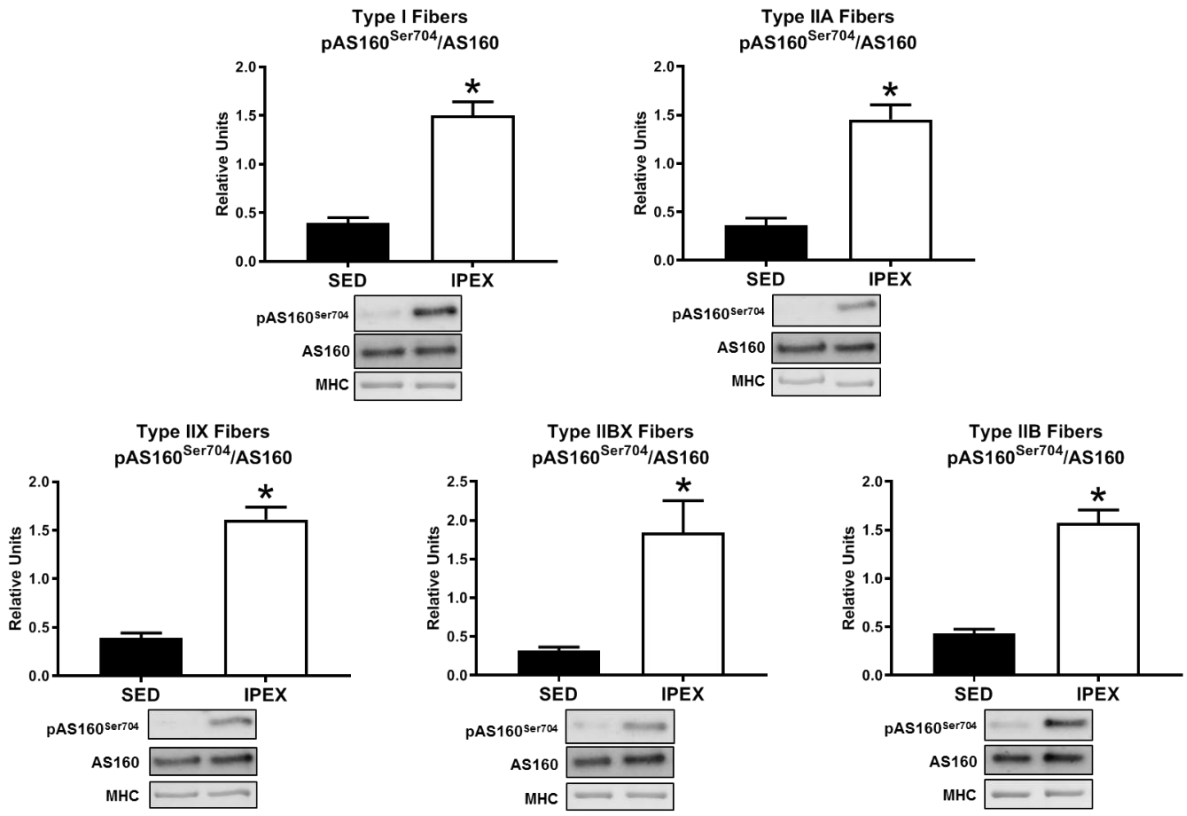

Figure 6.3

Fiber type-specific pAS160^{Ser704}/AS160 immediately post-exercise from high-fat diet fed rats. *P ≤ 0.01, indicates IPEX significantly greater than SED. Values are mean ± SEM, n = 7-8 per group. Representative blots and loading controls are included for each fiber type. SED, sedentary; IPEX, immediately post-exercise; MHC, myosin heavy chain.

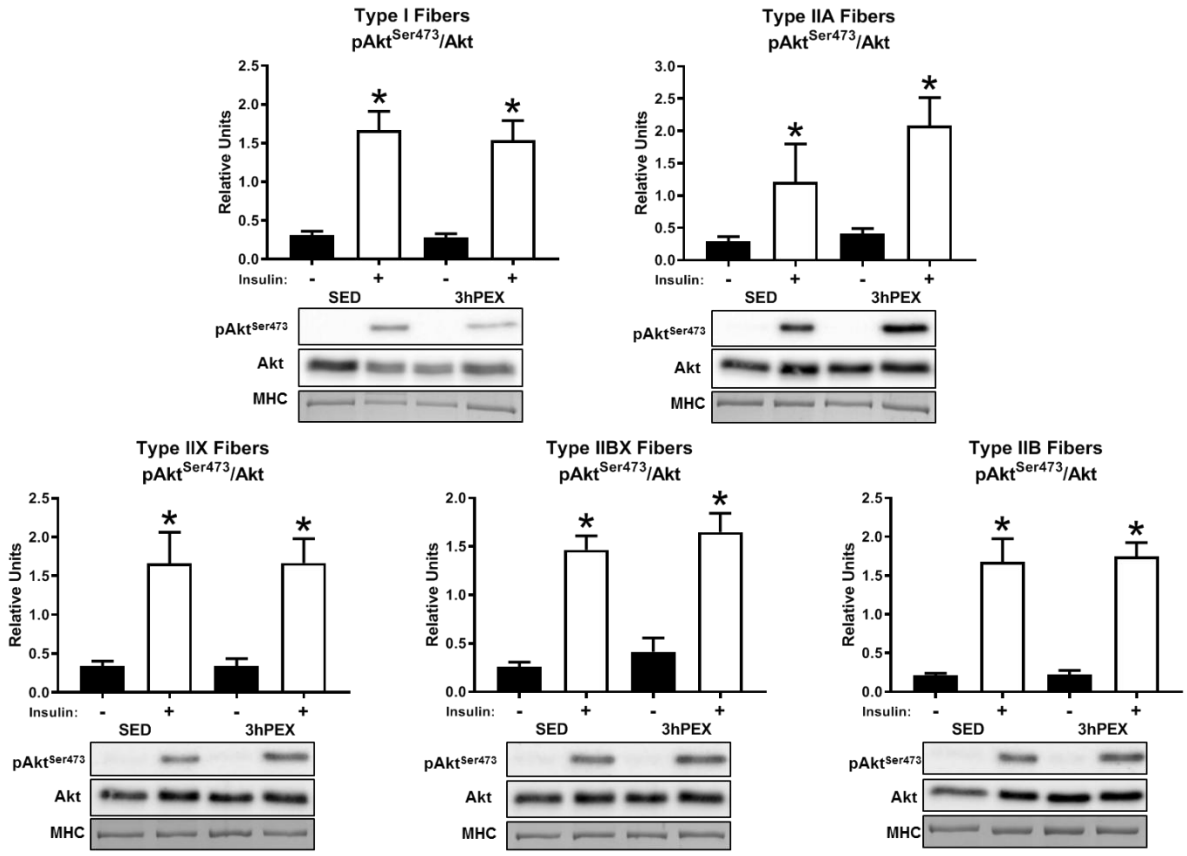

Figure 6.4

Insulin-stimulated pAkt^{Ser473}/Akt at 3hPEX vs SED controls in different fiber types from high-fat diet fed rats. *$P \leq 0.05$, indicates insulin significantly greater than no insulin within the same treatment group (SED or 3hPEX). Values are mean ± SEM, n = 7-10 per group. Representative blots and loading controls are included for each fiber type. SED, sedentary; 3hPEX, 3-hours post-exercise; MHC, myosin heavy chain.

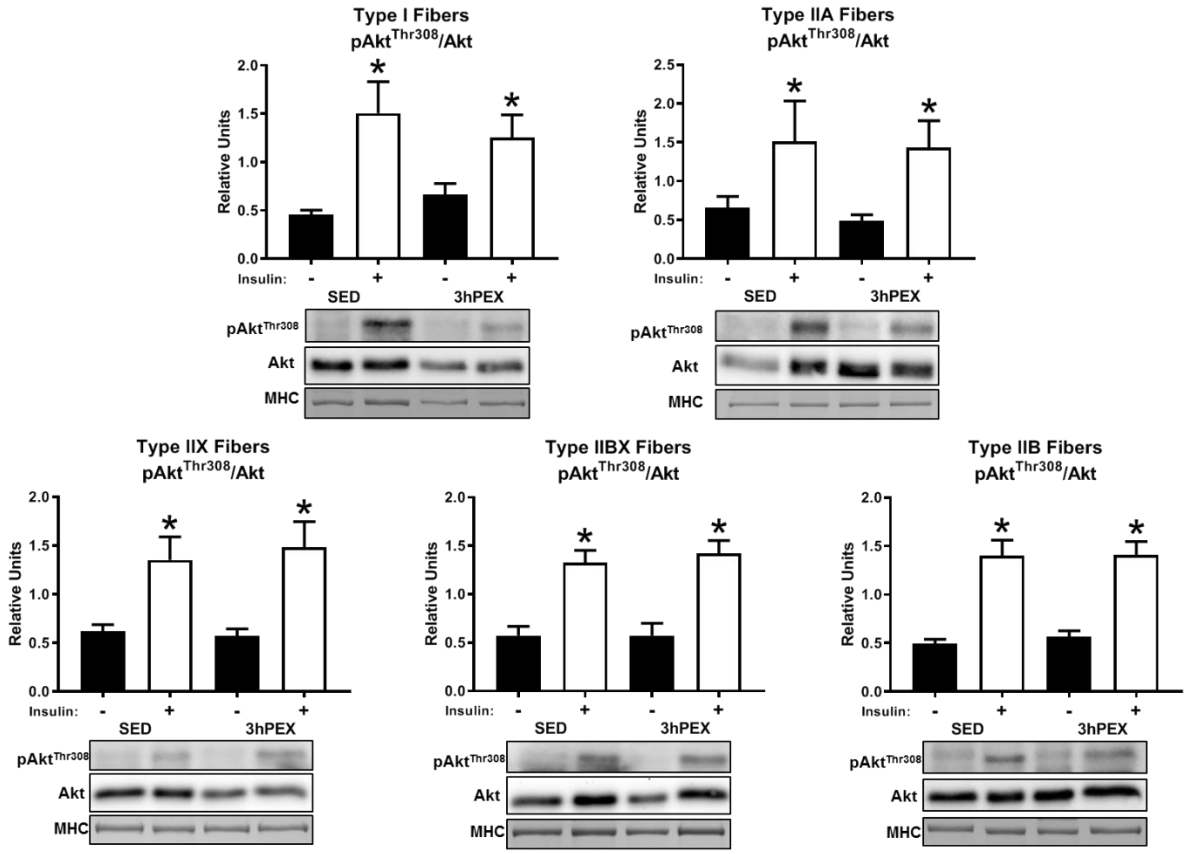

Figure 6.5

Insulin-stimulated pAkt^{Thr308}/Akt at 3hPEX vs SED controls in different fiber types from high-fat diet fed rats. *$P \leq 0.05$, indicates insulin significantly greater than no insulin within the same treatment group (SED or 3hPEX). Values are mean ± SEM, n = 7-10 per group. Representative blots and loading controls are included for each fiber type. SED, sedentary; 3hPEX, 3-hours post-exercise; MHC, myosin heavy chain.

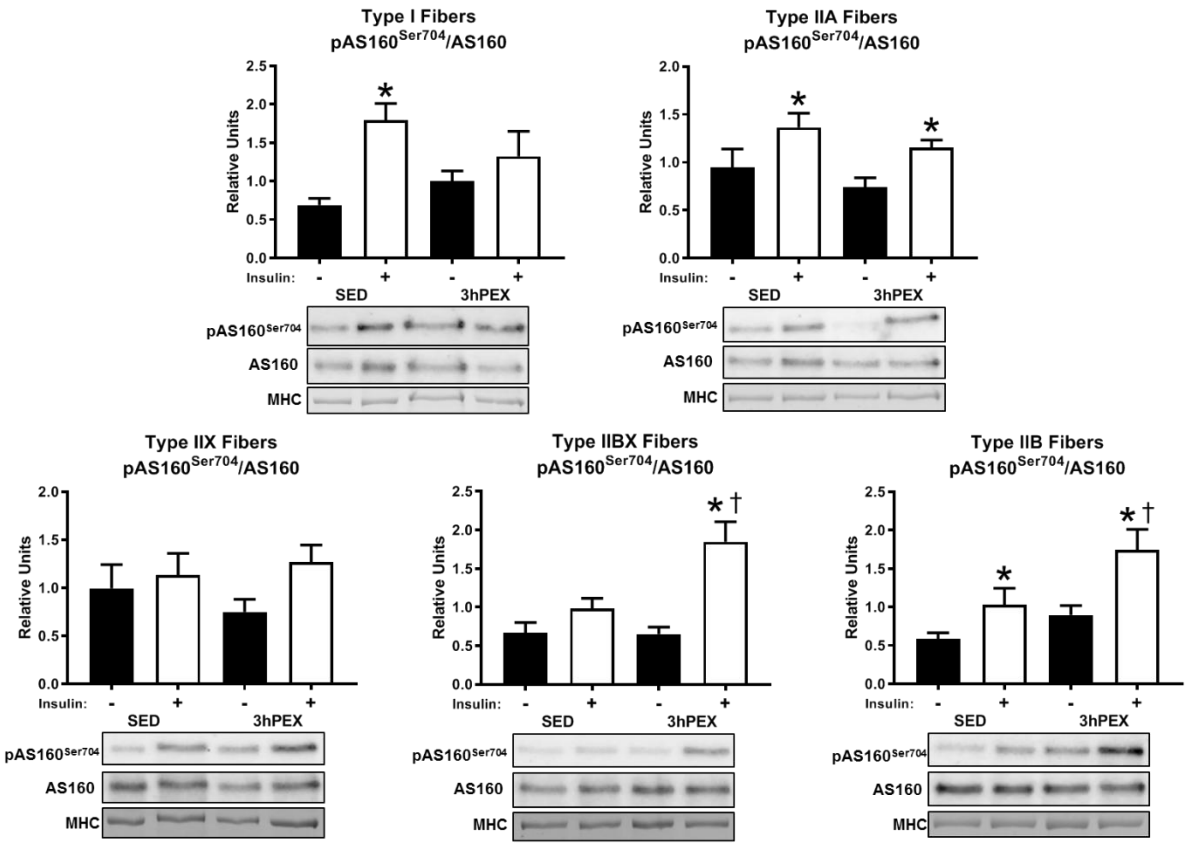

Figure 6.6

Insulin-stimulated pAS160^{Ser704}/AS160 at 3hPEX vs SED controls in different fiber types from high-fat diet fed rats. *P ≤ 0.05, indicates insulin significantly greater than no insulin within the same treatment group (SED or 3hPEX). †P ≤ 0.05, indicates 3hPEX significantly different than SED within insulin treated fibers. Values are mean ± SEM, n = 6-10 per group. Representative blots and loading controls are included for each fiber type. SED, sedentary; 3hPEX, 3-hours post-exercise; MHC, myosin heavy chain.

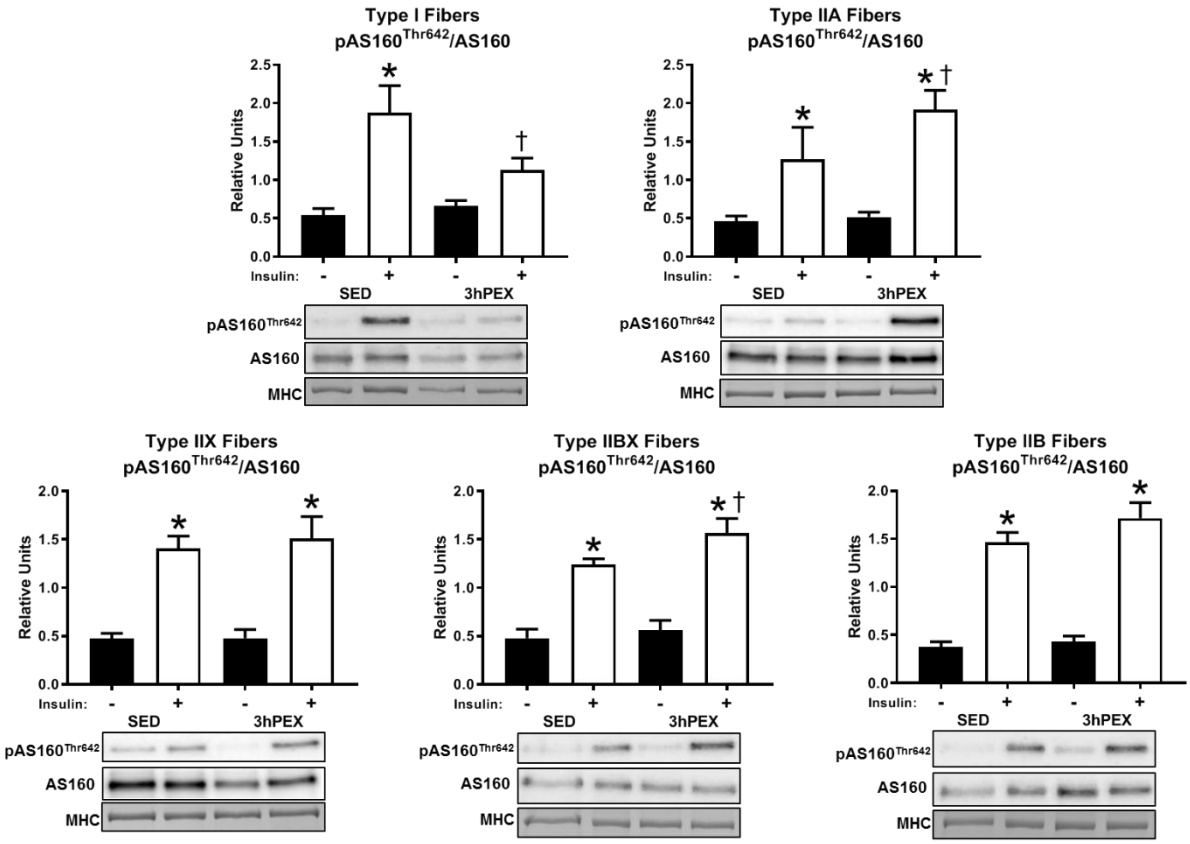

Figure 6.7

Insulin-stimulated pAS160^{Thr642}/AS160 at 3hPEX vs SED controls in different fiber types from high-fat diet fed rats. *$P \leq 0.05$, indicates insulin significantly greater than no insulin within the same treatment group (SED or 3hPEX). $^{\dagger}P \leq 0.05$, indicates 3hPEX significantly different than SED within insulin treated fibers. Values are mean ± SEM, n = 6-10 per group. Representative blots and loading controls are included for each fiber type. SED, sedentary; 3hPEX, 3-hours post-exercise; MHC, myosin heavy chain.

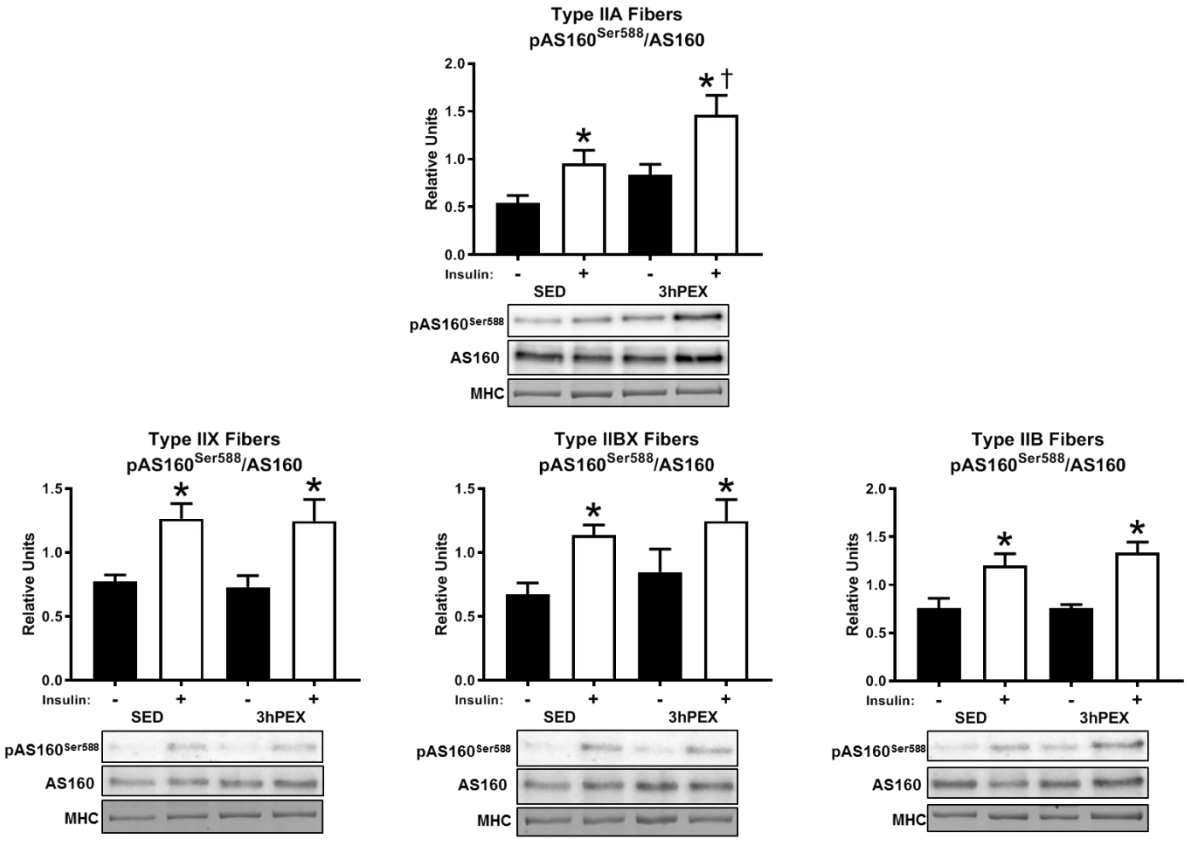

Figure 6.8

Insulin-stimulated pAS160^{Ser588}/AS160 at 3hPEX vs SED controls in different fiber types from high-fat diet fed rats. *P ≤ 0.05, indicates insulin significantly greater than no insulin within the same treatment group (SED or 3hPEX). †P ≤ 0.05, indicates 3hPEX significantly different than SED within insulin treated fibers. Values are mean ± SEM, n = 7-10 per group. Representative blots and loading controls are included for each fiber type. SED, sedentary; 3hPEX, 3-hours post-exercise; MHC, myosin heavy chain.

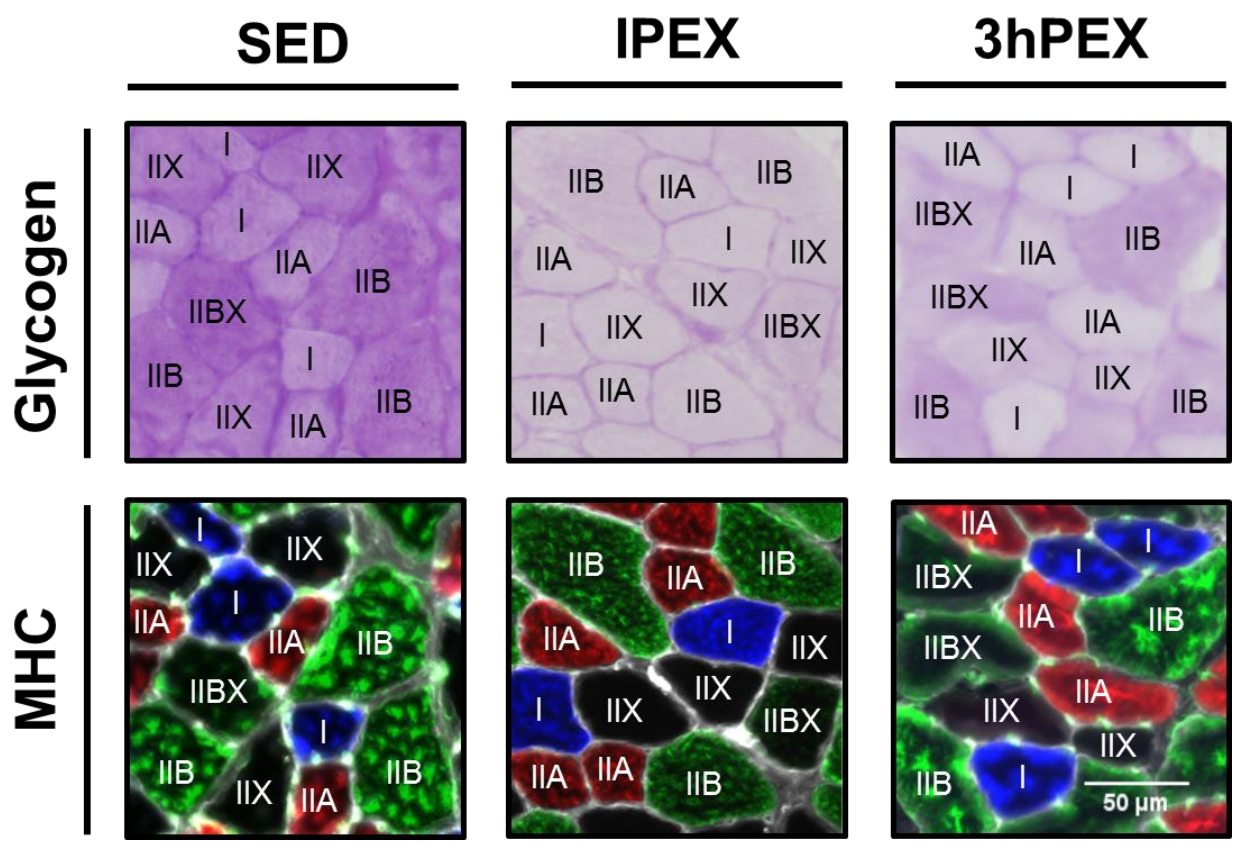

Figure 6.9

Representative images of serially cross-sectioned rat muscle for identification of glycogen content and fiber type. Glycogen content was determined by PAS stain intensity (darker stain represents higher glycogen content). MHC type I is shown in blue, MHC type IIA is shown in red, MHC type IIB is shown in green, and MHC type IIX is represented by the absence of signal (black).

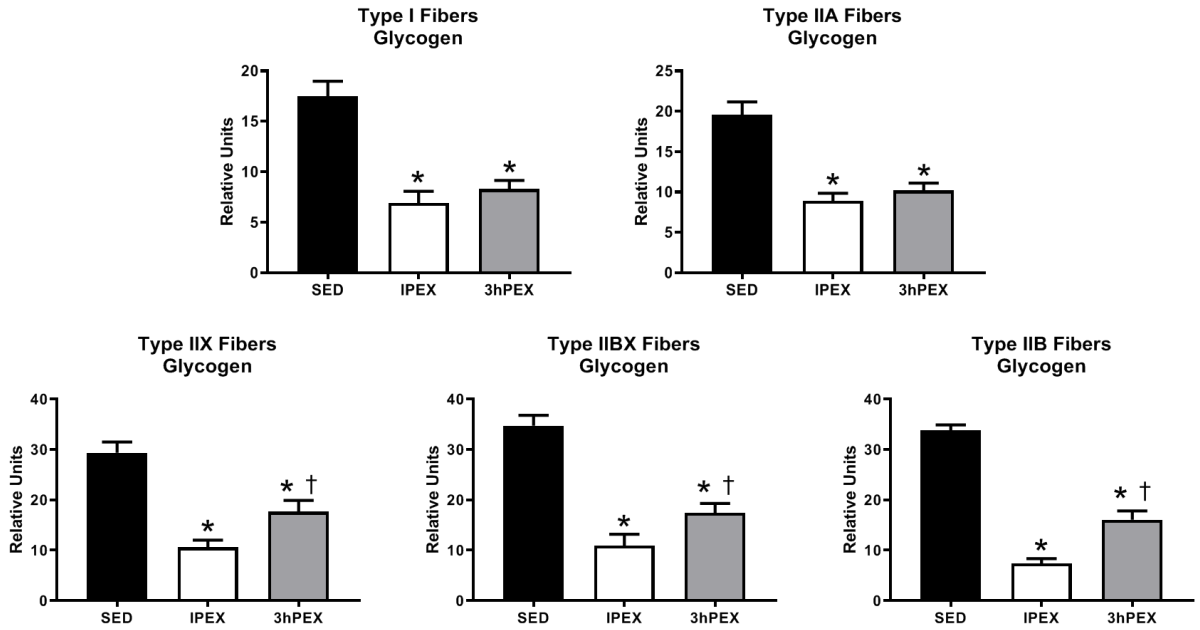

Figure 6.10

Post-exercise fiber type-specific glycogen content. *P ≤ 0.001, indicates SED significantly greater than both IPEX and 3hPEX. †P ≤ 0.001, indicates 3hPEX significantly greater than IPEX. Values are mean ± SEM. The number of rats used for each group in this experiment was n=6; 51-108 fibers/muscle were used to determine glycogen content. Numbers of fibers (SED, IPEX, 3hPEX) used for glycogen measurement of each fiber type were: type I (100, 76, 106), type IIA (117, 133, 123), type IIX (45, 83, 81), type IIBX (42, 37, 54), type IIB (146, 163, 175).

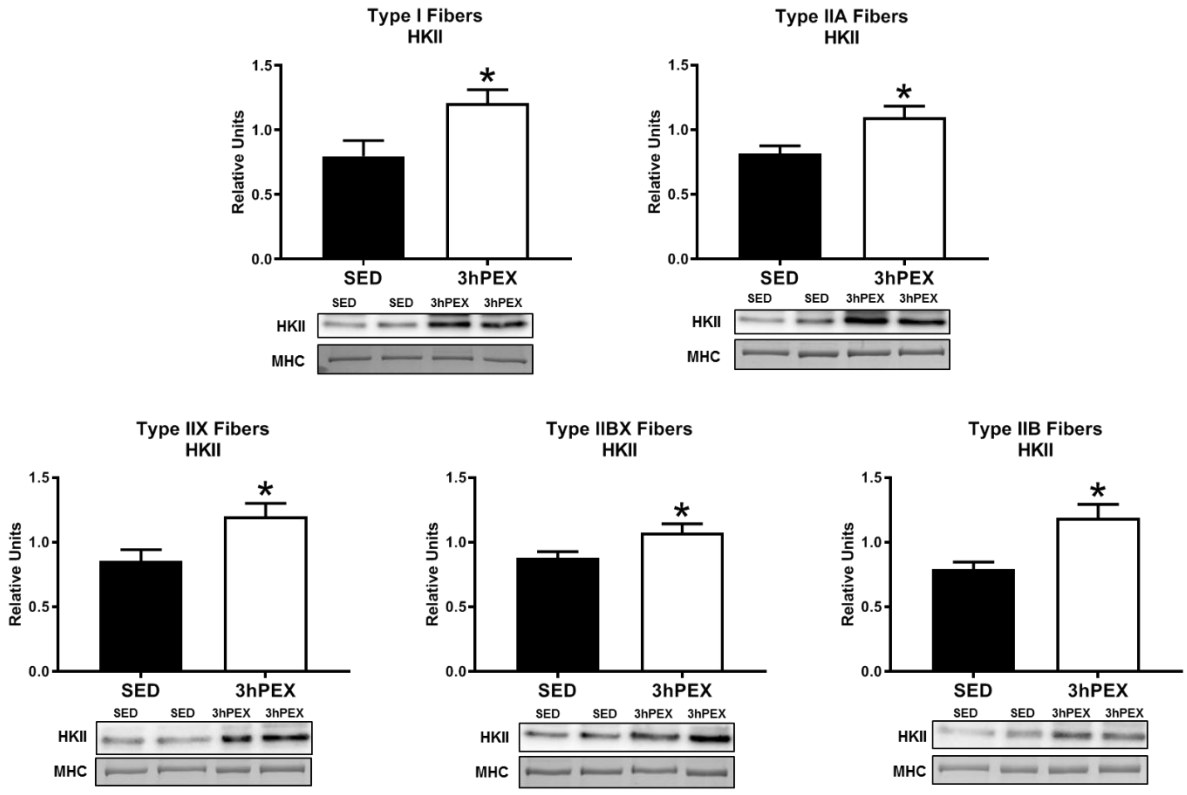

Figure 6.11

Fiber type-specific Hexokinase II abundance 3-hours post-exercise. *$P \leq 0.05$, indicates 3hPEX significantly greater than SED. Values are mean ± SEM, n = 12-20 per group. Representative blots and loading controls are included for each fiber type. SED, sedentary; 3hPEX, 3-hours post-exercise; MHC, myosin heavy chain.

REFERENCES

1. Huang, E.S., A. Basu, M. O'grady, and J.C. Capretta, *Projecting the future diabetes population size and related costs for the US.* Diabetes Care, 2009. **32**(12): p. 2225-2229.
2. Facchini, F.S., N. Hua, F. Abbasi, and G.M. Reaven, *Insulin resistance as a predictor of age-related diseases.* The Journal of Clinical Endocrinology & Metabolism, 2001. **86**(8): p. 3574-3578.
3. DeFronzo, R., E. Jacot, E. Jequier, E. Maeder, J. Wahren, and J. Felber, *The effect of insulin on the disposal of intravenous glucose: results from indirect calorimetry and hepatic and femoral venous catheterization.* Diabetes, 1981. **30**(12): p. 1000-1007.
4. Richter, E.A., L.P. Garetto, M.N. Goodman, and N.B. Ruderman, *Muscle glucose metabolism following exercise in the rat: increased sensitivity to insulin.* Journal of Clinical Investigation, 1982. **69**(4): p. 785-793.
5. Richter, E.A., K. Mikines, H. Galbo, and B. Kiens, *Effect of exercise on insulin action in human skeletal muscle.* Journal of Applied Physiology, 1989. **66**(2): p. 876-885.
6. Ropelle, E.R., J.R. Pauli, P.O. Prada, C.T. De Souza, P.K. Picardi, M.C. Faria, D.E. Cintra, M.F.d.A. Fernandes, M.B. Flores, and L.A. Velloso, *Reversal of diet-induced insulin resistance with a single bout of exercise in the rat: the role of PTP1B and IRS-1 serine phosphorylation.* The Journal of Physiology, 2006. **577**(3): p. 997-1007.
7. Tanaka, S., T. Hayashi, T. Toyoda, T. Hamada, Y. Shimizu, M. Hirata, K. Ebihara, H. Masuzaki, K. Hosoda, and T. Fushiki, *High-fat diet impairs the effects of a single bout of endurance exercise on glucose transport and insulin sensitivity in rat skeletal muscle.* Metabolism, 2007. **56**(12): p. 1719-1728.
8. Arias, E.B., J. Kim, K. Funai, and G.D. Cartee, *Prior exercise increases phosphorylation of Akt substrate of 160 kDa (AS160) in rat skeletal muscle.* American Journal of Physiology-Endocrinology and Metabolism, 2007. **292**(4): p. E1191-E1200.
9. Treebak, J.T., C. Frøsig, C. Pehmøller, S. Chen, S.J. Maarbjerg, N. Brandt, C. MacKintosh, J. Zierath, D. Hardie, and B. Kiens, *Potential role of TBC1D4 in enhanced post-exercise insulin action in human skeletal muscle.* Diabetologia, 2009. **52**(5): p. 891-900.
10. Funai, K., G.G. Schweitzer, N. Sharma, M. Kanzaki, and G.D. Cartee, *Increased AS160 phosphorylation, but not TBC1D1 phosphorylation, with increased postexercise insulin sensitivity in rat skeletal muscle.* American Journal of Physiology-Endocrinology and Metabolism, 2009. **297**(1): p. E242-E251.
11. Funai, K., G.G. Schweitzer, C.M. Castorena, M. Kanzaki, and G.D. Cartee, *In vivo exercise followed by in vitro contraction additively elevates subsequent insulin-stimulated glucose transport by rat skeletal muscle.* American Journal of Physiology-Endocrinology and Metabolism, 2010. **298**(5): p. E999-E1010.
12. Pehmøller, C., N. Brandt, J.B. Birk, L.D. Høeg, K.A. Sjøberg, L.J. Goodyear, B. Kiens, E.A. Richter, and J.F. Wojtaszewski, *Exercise alleviates lipid-induced insulin resistance in human skeletal muscle–signaling interaction at the level of TBC1 domain family member 4.* Diabetes, 2012. **61**(11): p. 2743-2752.
13. Schweitzer, G.G., E.B. Arias, and G.D. Cartee, *Sustained postexercise increases in AS160 Thr 642 and Ser 588 phosphorylation in skeletal muscle without sustained increases in kinase phosphorylation.* Journal of Applied Physiology, 2012. **113**(12): p. 1852-1861.

14. Xiao, Y., N. Sharma, E.B. Arias, C.M. Castorena, and G.D. Cartee, *A persistent increase in insulin-stimulated glucose uptake by both fast-twitch and slow-twitch skeletal muscles after a single exercise session by old rats.* Age, 2013. **35**(3): p. 573-582.
15. Iwabe, M., E. Kawamoto, K. Koshinaka, and K. Kawanaka, *Increased postexercise insulin sensitivity is accompanied by increased AS160 phosphorylation in slow-twitch soleus muscle.* Physiological Reports, 2014. **2**(12): p. e12162.
16. Castorena, C.M., E.B. Arias, N. Sharma, and G.D. Cartee, *Postexercise improvement in insulin-stimulated glucose uptake occurs concomitant with greater AS160 phosphorylation in muscle from normal and insulin-resistant rats.* Diabetes, 2014. **63**(7): p. 2297-308.
17. Levinger, I., G. Jerums, N.K. Stepto, L. Parker, F.R. Serpiello, G.K. McConell, M. Anderson, D.L. Hare, E. Byrnes, and P.R. Ebeling, *The effect of acute exercise on undercarboxylated osteocalcin and insulin sensitivity in obese men.* Journal of Bone and Mineral Research, 2014. **29**(12): p. 2571-2576.
18. Vendelbo, M.H., A.B. Møller, J.T. Treebak, L.C. Gormsen, L.J. Goodyear, J.F. Wojtaszewski, J.O.L. Jørgensen, N. Møller, and N. Jessen, *Sustained AS160 and TBC1D1 phosphorylations in human skeletal muscle 30 min after a single bout of exercise.* Journal of Applied Physiology, 2014. **117**(3): p. 289-296.
19. Kjøbsted, R., J.T. Treebak, J. Fentz, L. Lantier, B. Viollet, J.B. Birk, P. Schjerling, M. Björnholm, J.R. Zierath, and J.F. Wojtaszewski, *Prior AICAR stimulation increases insulin sensitivity in mouse skeletal muscle in an AMPK-dependent manner.* Diabetes, 2015. **64**(6): p. 2042-2055.
20. Klip, A., Y. Sun, T.T. Chiu, and K.P. Foley, *Signal transduction meets vesicle traffic: the software and hardware of GLUT4 translocation.* American Journal of Physiology-Cell Physiology, 2014. **306**(10): p. C879-C886.
21. Treebak, J.T., C. Pehmøller, J.M. Kristensen, R. Kjøbsted, J.B. Birk, P. Schjerling, E.A. Richter, L.J. Goodyear, and J.F. Wojtaszewski, *Acute exercise and physiological insulin induce distinct phosphorylation signatures on TBC1D1 and TBC1D4 proteins in human skeletal muscle.* The Journal of Physiology, 2014. **592**(2): p. 351-375.
22. Sjøberg, K.A., C. Frøsig, R. Kjøbsted, L. Sylow, M. Kleinert, A.C. Betik, C.S. Shaw, B. Kiens, J.F. Wojtaszewski, and S. Rattigan, *Exercise increases human skeletal muscle insulin sensitivity via coordinated increases in microvascular perfusion and molecular signaling.* Diabetes, 2017. **66**(6): p. 1501-1510.
23. Wang, H., E.B. Arias, M.W. Pataky, L.J. Goodyear, and G.D. Cartee, *Postexercise improvement in glucose uptake occurs concomitant with greater γ3-AMPK activation and AS160 phosphorylation in rat skeletal muscle.* American Journal of Physiology-Endocrinology and Metabolism, 2018. **315**: p. E859-E871.
24. Sano, H., S. Kane, E. Sano, C.P. Mîinea, J.M. Asara, W.S. Lane, C.W. Garner, and G.E. Lienhard, *Insulin-stimulated phosphorylation of a Rab GTPase-activating protein regulates GLUT4 translocation.* Journal of Biological Chemistry, 2003. **278**(17): p. 14599-14602.
25. Chen, S., D.H. Wasserman, C. MacKintosh, and K. Sakamoto, *Mice with AS160/TBC1D4-Thr649Ala knockin mutation are glucose intolerant with reduced insulin sensitivity and altered GLUT4 trafficking.* Cell Metabolism, 2011. **13**(1): p. 68-79.
26. Pette, D. and R.S. Staron, *Cellular and molecular diversities of mammalian skeletal muscle fibers.* Rev Physiol Biochem Pharmacol, 1990. **116**: p. 1-76.

27. Cartee, G.D., E.B. Arias, S.Y. Carmen, and M.W. Pataky, *Novel single skeletal muscle fiber analysis reveals a fiber type-selective effect of acute exercise on glucose uptake.* American Journal of Physiology-Endocrinology and Metabolism, 2016. **311**(5): p. E818-E824.
28. Wang, H., E.B. Arias, K. Oki, M.W. Pataky, J.A. Almallouhi, and G.D. Cartee, *Fiber Type-selective Exercise Effects on AS160 Phosphorylation.* American Journal of Physiology-Endocrinology and Metabolism, 2019. **316**: p. E837-E851.
29. Pataky, M.W., H. Wang, C.S. Yu, E.B. Arias, R.J. Ploutz-Snyder, X. Zheng, and G.D. Cartee, *High-Fat Diet-Induced Insulin Resistance in Single Skeletal Muscle Fibers is Fiber Type Selective.* Scientific Reports, 2017. **7**(1): p. 13642.
30. Pataky, M.W., C.S. Yu, Y. Nie, E.B. Arias, M. Singh, C.L. Mendias, R.J. Ploutz-Snyder, and G.D. Cartee, *Skeletal Muscle Fiber Type-selective Effects of Acute Exercise on Insulin-stimulated Glucose Uptake in Insulin Resistant, High Fat-fed Rats.* American Journal of Physiology-Endocrinology and Metabolism, 2019. **316**: p. E695-E706.
31. Birk, J.B. and J. Wojtaszewski, *Predominant α2/β2/γ3 AMPK activation during exercise in human skeletal muscle.* The Journal of Physiology, 2006. **577**(3): p. 1021-1032.
32. Kristensen, D.E., P.H. Albers, C. Prats, O. Baba, J.B. Birk, and J.F. Wojtaszewski, *Human muscle fibre type-specific regulation of AMPK and downstream targets by exercise.* The Journal of Physiology, 2015. **593**(8): p. 2053-2069.
33. Cartee, G.D., D.A. Young, M.D. Sleeper, J. Zierath, H. Wallberg-Henriksson, and J. Holloszy, *Prolonged increase in insulin-stimulated glucose transport in muscle after exercise.* American Journal of Physiology-Endocrinology And Metabolism, 1989. **256**(4): p. E494-E499.
34. Gulve, E.A., G.D. Cartee, J.R. Zierath, V. Corpus, and J. Holloszy, *Reversal of enhanced muscle glucose transport after exercise: roles of insulin and glucose.* American Journal of Physiology-Endocrinology And Metabolism, 1990. **259**(5): p. E685-E691.
35. Fueger, P.T., H.S. Hess, D.P. Bracy, R.R. Pencek, K.A. Posey, M.J. Charron, and D.H. Wasserman, *Regulation of insulin-stimulated muscle glucose uptake in the conscious mouse: role of glucose transport is dependent on glucose phosphorylation capacity.* Endocrinology, 2004. **145**(11): p. 4912-4916.
36. O'Doherty, R.M., D.P. Bracy, H. Osawa, D.H. Wasserman, and D.K. Granner, *Rat skeletal muscle hexokinase II mRNA and activity are increased by a single bout of acute exercise.* American Journal of Physiology-Endocrinology And Metabolism, 1994. **266**(2): p. E171-E178.
37. Pilegaard, H., B. Saltin, and P.D. Neufer, *Exercise induces transient transcriptional activation of the PGC-1α gene in human skeletal muscle.* The Journal of Physiology, 2003. **546**(3): p. 851-858.
38. Abu-Elheiga, L., D.B. Almarza-Ortega, A. Baldini, and S.J. Wakil, *Human acetyl-CoA carboxylase 2 molecular cloning, characterization, chromosomal mapping, and evidence for two isoforms.* Journal of Biological Chemistry, 1997. **272**(16): p. 10669-10677.
39. O'Neill, H.M., J.S. Lally, S. Galic, T. Pulinilkunnil, R.J. Ford, J.R. Dyck, B.J. Denderen, B.E. Kemp, and G.R. Steinberg, *Skeletal muscle ACC2 S212 phosphorylation is not required for the control of fatty acid oxidation during exercise.* Physiological Reports, 2015. **3**(7): p. e12444.

40. Albers, P.H., A.J. Pedersen, J.B. Birk, D.E. Kristensen, B.F. Vind, O. Baba, J. Nøhr, K. Højlund, and J.F. Wojtaszewski, *Human Muscle Fiber Type–Specific Insulin Signaling: Impact of Obesity and Type 2 Diabetes.* Diabetes, 2015. **64**(2): p. 485-497.
41. Pataky, M.W., E.B. Arias, and G.D. Cartee, *Measuring Both Glucose Uptake and Myosin Heavy Chain Isoform Expression in Single Rat Skeletal Muscle Fibers*, in *Myogenesis* 2019, Springer. p. 283-300.
42. Mizunoya, W., J.-i. Wakamatsu, R. Tatsumi, and Y. Ikeuchi, *Protocol for high-resolution separation of rodent myosin heavy chain isoforms in a mini-gel electrophoresis system.* Analytical Biochemistry, 2008. **377**(1): p. 111-113.
43. Schaart, G., R.P. Hesselink, H.A. Keizer, G. van Kranenburg, M.R. Drost, and M.K. Hesselink, *A modified PAS stain combined with immunofluorescence for quantitative analyses of glycogen in muscle sections.* Histochemistry and Cell Biology, 2004. **122**(2): p. 161-169.
44. Bloemberg, D. and J. Quadrilatero, *Rapid determination of myosin heavy chain expression in rat, mouse, and human skeletal muscle using multicolor immunofluorescence analysis.* PloS one, 2012. **7**(4): p. e35273.
45. Hardie, D.G. and M.L. Ashford, *AMPK: regulating energy balance at the cellular and whole body levels.* Physiology, 2014. **29**(2): p. 99-107.
46. Hardie, D.G., *Regulation of fatty acid and cholesterol metabolism by the AMP-activated protein kinase.* Biochimica et Biophysica Acta (BBA)-Lipids and Lipid Metabolism, 1992. **1123**(3): p. 231-238.
47. Scott, J.W., D.G. Norman, S.A. Hawley, L. Kontogiannis, and D.G. Hardie, *Protein kinase substrate recognition studied using the recombinant catalytic domain of AMP-activated protein kinase and a model substrate.* Journal of Molecular Biology, 2002. **317**(2): p. 309-323.
48. Kim, J., R.S. Solis, E.B. Arias, and G.D. Cartee, *Postcontraction insulin sensitivity: relationship with contraction protocol, glycogen concentration, and 5' AMP-activated protein kinase phosphorylation.* Journal of Applied Physiology, 2004. **96**(2): p. 575-583.
49. Treebak, J.T., J.B. Birk, A.J. Rose, B. Kiens, E.A. Richter, and J.F. Wojtaszewski, *AS160 phosphorylation is associated with activation of α2β2γ1-but not α2β2γ3-AMPK trimeric complex in skeletal muscle during exercise in humans.* American Journal of Physiology-Endocrinology and Metabolism, 2007. **292**(3): p. E715-E722.
50. Kjøbsted, R., A.J. Pedersen, J.R. Hingst, R. Sabaratnam, J.B. Birk, J.M. Kristensen, K. Højlund, and J.F. Wojtaszewski, *Intact regulation of the AMPK signaling network in response to exercise and insulin in skeletal muscle of male patients with type 2 diabetes: illumination of AMPK activation in recovery from exercise.* Diabetes, 2016. **65**(5): p. 1219-1230.
51. Fueger, P.T., H.S. Hess, K.A. Posey, D.P. Bracy, R.R. Pencek, M.J. Charron, and D.H. Wasserman, *Control of exercise-stimulated muscle glucose uptake by GLUT4 is dependent on glucose phosphorylation capacity in the conscious mouse.* Journal of Biological Chemistry, 2004. **279**(49): p. 50956-50961.
52. Cartee, G.D., *Mechanisms for greater insulin-stimulated glucose uptake in normal and insulin-resistant skeletal muscle after acute exercise.* American Journal of Physiology-Endocrinology and Metabolism, 2015. **309**(12): p. E949-E959.
53. Wang, H., N. Sharma, E.B. Arias, and G.D. Cartee, *Insulin signaling and glucose uptake in the soleus muscle of 30-month-old rats after calorie restriction with or without acute*

exercise. Journals of Gerontology Series A: Biomedical Sciences and Medical Sciences, 2015. **71**(3): p. 323-332.
54. Frøsig, C., M.P. Sajan, S.J. Maarbjerg, N. Brandt, C. Roepstorff, J.F. Wojtaszewski, B. Kiens, R.V. Farese, and E.A. Richter, *Exercise improves phosphatidylinositol-3, 4, 5-trisphosphate responsiveness of atypical protein kinase C and interacts with insulin signalling to peptide elongation in human skeletal muscle.* The Journal of Physiology, 2007. **582**(3): p. 1289-1301.
55. Hamada, T., E.B. Arias, and G.D. Cartee, *Increased submaximal insulin-stimulated glucose uptake in mouse skeletal muscle after treadmill exercise.* Journal of Applied Physiology, 2006. **101**(5): p. 1368-1376.
56. Grote, C.W., A.L. Groover, J.M. Ryals, P.C. Geiger, E.L. Feldman, and D.E. Wright, *Peripheral nervous system insulin resistance in ob/ob mice.* Acta Neuropathologica Communications, 2013. **1**(1): p. 15.
57. Yu, H., T. Littlewood, and M. Bennett, *Akt isoforms in vascular disease.* Vascular Pharmacology, 2015. **71**: p. 57-64.
58. Cong, L.-N., H. Chen, Y. Li, L. Zhou, M.A. McGibbon, S.I. Taylor, and M.J. Quon, *Physiological role of Akt in insulin-stimulated translocation of GLUT4 in transfected rat adipose cells.* Molecular Endocrinology, 1997. **11**(13): p. 1881-1890.
59. Park, C.S., I.C. Schneider, and J.M. Haugh, *Kinetic analysis of platelet-derived growth factor receptor/phosphoinositide 3-kinase/Akt signaling in fibroblasts.* Journal of Biological Chemistry, 2003. **278**(39): p. 37064-37072.
60. Woulfe, D.S., *Akt signaling in platelets and thrombosis.* Expert Review of Hematology, 2010. **3**(1): p. 81-91.
61. Suhr, F., J. Brenig, R. Müller, H. Behrens, W. Bloch, and M. Grau, *Moderate exercise promotes human RBC-NOS activity, NO production and deformability through Akt kinase pathway.* PloS one, 2012. **7**(9): p. e45982.

CHAPTER VII

Discussion

Focus of this Discussion

This discussion chapter will: 1) provide a summary of the key findings from each study; 2) provide an integrated interpretation of the results from all studies; 3) suggest directions for future research, including a proposal for a specific future research projects to build on the results in this dissertation; and 4) summarize the overall conclusions of the research presented in this dissertation.

Summary of Key Findings

The results from this dissertation provide novel insights into the mechanisms for enhanced insulin-stimulated glucose uptake in insulin-resistant skeletal muscle after acute exercise. Although previous research related to the insulin signaling events that lead to enhanced post-exercise insulin-stimulated glucose uptake have been relatively well studied in healthy muscle [1-8], considerably less work had been performed on this topic in insulin-resistant skeletal muscle. It is important to recognize that skeletal muscle is a heterogeneous tissue composed of multiple fiber types with differing metabolic and contractile properties [9]. By evaluating glucose uptake and signaling events in various muscle fiber types, this dissertation has provided unique insight into the effects of *in vivo* exercise during insulin resistance on insulin sensitivity at the myocellular level. A brief summary of the key findings from each study of this dissertation is provided below.

Study 1: *High-Fat Diet-Induced Insulin Resistance in Single Skeletal Muscle Fibers is Fiber Type Selective*

Male Wistar rats were fed either a normal chow diet (LFD; low-fat diet) or a high-fat diet (HFD) which can induce muscle insulin resistance. Paired epitrochlearis muscles were

dissected and incubated with or without 100μU/mL insulin and [^{3}H]-2-DG for glucose uptake measurement. Some muscles were used for whole muscle analysis while other muscles were incubated in collagenase and single fibers were isolated for glucose uptake analysis. After fiber typing and glucose uptake measurement, the remaining fiber lysate sample was used for blotting of GLUT4 and mitochondrial proteins.

- There was greater body mass (8%), estimated caloric intake (16%), and epididymal fat mass (57%) in rats fed a HFD for 2-weeks compared to LFD-fed rats.
- Insulin-stimulated glucose uptake was decreased (40%) in whole epitrochlearis muscle from HFD-fed rats compared to LFD-fed rats.
- In HFD-fed versus LFD-fed rats, insulin-stimulated glucose uptake was significantly diminished in type II fibers, including IIA (12%), IIAX (49%), IIX (34%), IIBX (44%), and IIB (45%), without a significant effect in type I fibers.
- MHC expression of whole muscle tissue did not differ between LFD and HFD. If the relative abundance of each MHC isoform in whole muscle (8% type I, 16% type IIA, 27% type IIX, and 49% type IIB) is multiplied by the respective decrements in glucose uptake for each fiber type (non-significant 4% lower value for type I and significant decrements of 12% for type IIA, 34% for type IIX, and 45% for type IIB) then an estimated sum of isoform-selective values results in an approximate 33.5% decrease in insulin-stimulated glucose uptake. This value compares favorably to the directly measured 40% decrease in whole muscle insulin-stimulated glucose uptake.
- GLUT4 protein abundance was not significantly altered by a HFD in the whole epitrochlearis muscle or type I, IIA, IIAX, IIX, or IIBX fibers. However, GLUT4 abundance was significantly decreased in type IIB fibers from HFD-fed rats compared to LFD-fed rats.
- There were fiber type-selective HFD-effects on the abundance of 6 mitochondrial proteins. Type I fibers, the sole fiber type that did not become insulin-resistant with the HFD, had a significant HFD-induced decrease in several of these mitochondrial proteins. However, the lack of uniform results among the different type II fibers (which became insulin-resistant) did not point toward a simple relationship between changes in mitochondrial protein abundance and the induction of insulin resistance.

Study 2: *Skeletal Muscle Fiber Type-selective Effects of Acute Exercise on Insulin-stimulated Glucose Uptake in Insulin-Resistant, High Fat-fed Rats*

Male Wistar rats were either fed a LFD or a HFD for 2-weeks. LFD-fed rats remained sedentary and HFD-fed rats were either sedentary or acutely swim exercised (2h). Epitrochlearis muscles were dissected from some rats immediately post-exercise (IPEX), along with HFD and LFD sedentary controls, and incubated with [^{3}H]-2-DG. Epitrochlearis muscles from other rats were dissected at 3h post-exercise (3hPEX), along with HFD and LFD sedentary controls, and paired muscles were incubated in [^{3}H]-2-DG with or without 100μU/mL insulin. Single fibers were isolated from all muscles and used to measure fiber type, glucose uptake, and GLUT4 abundance. Muscles from other rats were frozen IPEX for histochemical analysis of glycogen and neutral lipids.

- In sedentary rats there was a significant decrease in insulin-stimulated glucose uptake in type IIB (37%), IIBX (36%), IIX (20%), and IIAX (19%) fibers from HFD-fed rats compared to LFD-fed rats. In type IIA (11%) fibers there was a non-significant trend for a decrease in insulin-stimulated glucose uptake with a HFD. Insulin-stimulated glucose uptake was not significantly different for type I fibers from LFD versus HFD rats.
- In HFD-fed rats there was a significant increase in insulin-stimulated glucose uptake from type IIB (68%), IIBX (89%), IIX (28%), IIAX (61%), and IIA (46%) fibers from muscles dissected 3hPEX compared to sedentary HFD controls. Insulin-stimulated glucose uptake in type I fibers was not greater in muscles from 3hPEX rats compared to SED rats.
- In HFD-fed rats there was a significant increase (64-187%) in insulin-independent glucose uptake immediately post-exercise (IPEX) in all fiber types.
- In HFD-IPEX muscles there was a significant decrease (37-70%) in glycogen content in all fiber types compared to sedentary HFD and LFD controls.
- In sedentary rats the total lipid droplet (LD) density was significantly greater in the IIAX and IIX fibers from HFD-fed versus LFD-fed rats, but none of the other LD indices (subsarcolemmal LD density, LD size, and subsarcolemmal LD size) differed among treatment groups (LFD-SED, HFD-SED, and HFD-IPEX) in other fiber types with substantial insulin resistance (IIBX and IIB). Type I and IIA fibers, which did not have

significant insulin resistance, had greater values for multiple LD indices in HFD-fed versus LFD-fed rats.

- GLUT4 abundance was unaltered by diet or exercise in all fiber types.
- There were no statistically significant differences among treatment groups for muscle fiber cross-sectional area (CSA) within any fiber type.

Study 3: *Exercise Effects on γ3-AMPK Activity, Phosphorylation of Akt2 and AS160, and Insulin-stimulated Glucose Uptake in Insulin-Resistant Rat Skeletal Muscle*

Male Wistar rats were either fed a LFD or a HFD for 2-weeks. LFD-fed rats remained sedentary and HFD-fed rats were either sedentary or acutely swim exercised (2h). Epitrochlearis muscles were dissected from some rats immediately post-exercise (IPEX), along with HFD and LFD sedentary controls, and incubated with [^{3}H]-2-DG. Muscles from other rats were dissected at 3h post-exercise (3hPEX), along with HFD and LFD sedentary controls, and paired muscles were incubated in [^{3}H]-2-DG with or without 100μU/mL insulin. Glucose uptake was determined in isolated muscles. In addition, Akt, AS160, AMPK, and ACC phosphorylation was evaluated in skeletal muscle. AMPK isoform-specific activity was also determined in skeletal muscle.

- Insulin-independent glucose uptake was greater in the HFD-IPEX muscles versus both LFD-SED (91%) and HFD-SED (83%) controls.
- Insulin-stimulated muscle glucose uptake was lower in HFD-SED (28%) compared to LFD-SED. When HFD-fed rats were exercised and muscles were dissected 3 hours later, insulin-stimulated glucose uptake was enhanced (43%) compared to HFD-SED.
- There was not a significant effect of acute exercise on γ1-AMPK activity either IPEX or 3hPEX. However, γ3-AMPK activity at both IPEX and 3hPEX in HFD-fed rats was increased versus LFD-SED and HFD-SED controls.
- There was no effect of diet or exercise on the skeletal muscle abundance of any of the AMPK isoforms evaluated (α1, α2, β1, β2, γ1, and γ3).
- The phosphorylation of AMPK^{Thr172} and the AMPK substrate, pACC^{Ser79}, were significantly elevated IPEX in HFD-fed rat muscle compared to LFD- and HFD-SED controls. At 3hPEX versus LFD- and HFD-SED, only pAMPK^{Thr172} was elevated, and not its substrate pACC^{Ser79}.

- There was an increase in pAS160^{Thr642} and pAS160^{Ser704} in the HFD-IPEX group compared to LFD-SED and HFD-SED groups. pAS160^{Ser588} was elevated in the HFD-IPEX compared to the HFD-SED group only.
- There was an increase in pAS160^{Ser588} and pAS160^{Thr642} in all groups when exposed to insulin. There was an increase in pAS160^{Ser704} only in the HFD-3hPEX group when exposed to insulin compared to basal. In muscles from HFD-fed rats there was a significant exercise-induced increase compared to sedentary in insulin-stimulated pAS160 on all three sites. Insulin-stimulated pAS160 was lower for HFD-SED versus LFD-SED rats for Thr642 and Ser704, but not Ser588.
- The phosphorylation of Akt (Ser473 and Thr308) and Akt2 (Ser474 and Thr309) were elevated by insulin versus basal in all treatment groups. Insulin-stimulated pAkt^{Thr308}, pAkt^{Ser473}, and pAkt2^{Thr309} were lower for HFD versus LFD rats. Insulin-stimulated pAkt^{Thr308}, pAkt^{Ser473}, and pAkt2^{Ser474} were greater for HFD-3hPEX versus HFD-SED rats.

Study 4: *Fiber Type-specific Effects of Acute Exercise on Insulin-stimulated AS160 Phosphorylation in Insulin-Resistant Rat Skeletal Muscle*

Male Wistar rats were fed a HFD for 2-weeks and either acutely swim exercised (2h) or remained sedentary. Epitrochlearis muscles were dissected from some rats immediately post-exercise (IPEX), along with sedentary controls, and immediately frozen in liquid nitrogen or embedded in OCT medium. Muscles from other rats were dissected at 3h post-exercise (3hPEX), along with sedentary controls, and paired muscles were incubated with or without 100µU/mL insulin before being frozen in liquid nitrogen or embedded in OCT medium. Muscles were lyophilized and then single fibers were isolated, fiber typed, pooled with fibers of the same type, and used for western blotting. Fiber type-specific glycogen was determined from muscles embedded in OCT by periodic acid-Schiff staining.

- Type I, IIX and IIB fibers from IPEX versus SED rats had increased pAMPK^{Thr172}, but there was not a significant increase in pAMPK^{Thr172} IPEX in type IIA or IIBX fibers.
- pACC^{Ser79} and pAS160^{Ser704} were significantly increased IPEX compared to SED in all fiber types.

- In both SED and 3hPEX muscles there was an insulin-stimulated increase compared to basal for $pAkt^{Ser473}$ and $pAkt^{Thr308}$ in all fiber types. There was no significant difference for 3hPEX versus SED on insulin-stimulated $pAkt^{Ser473}$ or $pAkt^{Thr308}$ in any fiber type.
- Exercise versus SED groups had greater insulin-stimulated AS160 phosphorylation on at least one of the three sites measured (Ser704, Thr642, and Ser588) in type IIB, IIBX, and IIA fibers. There was no effect of exercise compared to SED in type IIX fibers on insulin-stimulated pAS160. In type I fibers there was lower insulin-stimulated $pAS160^{Ser704}$ and $pAS160^{Thr642}$ in 3hPEX versus SED ($pAS160^{Ser588}$ was not quantifiable in type I fibers).
- Glycogen content was significantly lower for both IPEX and 3hPEX rats compared to SED rats in all fiber types. In type IIB, IIBX, and IIX fibers, there was a small, but significant increase in glycogen content at 3hPEX compared to IPEX.
- Hexokinase II abundance was significantly increased in all fiber types of 3hPEX versus SED rats.

Integrated Interpretation of Results

Reliable method for measuring fiber type-specific insulin resistance

Study 1 of this dissertation discovered striking fiber type-specific results for insulin-stimulated glucose uptake. Following a 2-week HFD, type IIB, IIBX, IIX, IIAX, and IIA fibers became significantly insulin-resistant. However, type I fibers maintained normal insulin sensitivity following a 2-week HFD. Study 2 performed the same fiber type-specific glucose uptake analyses in sedentary LFD and HFD rats, but also included an additional HFD-fed group that was exercised. The results from the sedentary fibers from Study 2 were similar to the results from Study 1. The type IIB, IIBX, IIX, and IIAX fibers all became significantly insulin-resistant, the type IIA fibers showed a non-significant trend (P=0.075) for insulin resistance, and the type I fibers did not become insulin-resistant when fed a HFD. The mean glucose uptake for each fiber type from insulin and non-insulin treated fibers from LFD and HFD rats was used to perform a correlation analysis between Study 1 and Study 2. The correlation for glucose uptake from these two studies, which were performed in completely different fibers from different rats nearly a year apart, was $R^2 = 0.926$ (Figure 7.1).

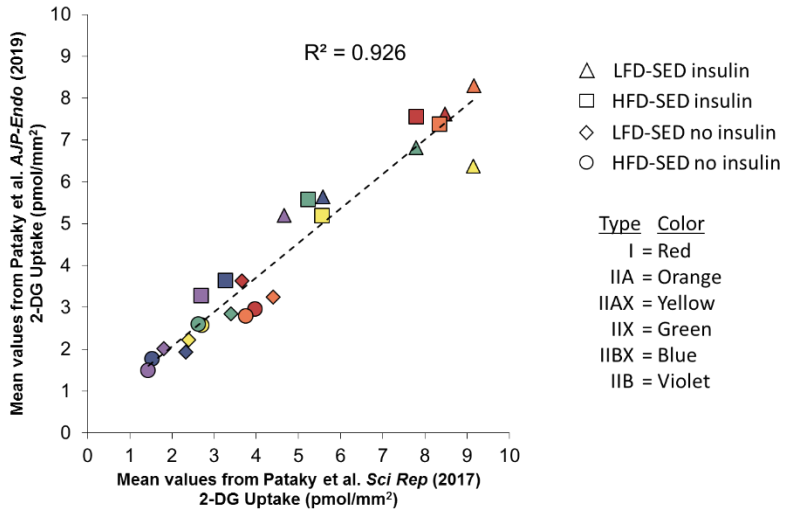

Figure 7.1

Reproducibility of glucose uptake by single fibers. Each data point represents the mean 2-DG uptake values of a given fiber type incubated with or without insulin from muscles of LFD or HFD rats. Colors represent different fiber types; type I (Red), type IIA (Orange), type IIAX (Yellow), type IIX (green), type IIBX (blue), and type IIB (violet). Shapes represent different treatment groups; LFD-SED insulin (triangle), HFD-SED insulin (square), LFD-SED no insulin (diamond), and HFD-SED no insulin (circle). An R^2 value correlating our previously published results (Pataky et al. 2017; x-axis) and the current study (y-axis) is shown. A significant ($P < 0.001$) correlation of $R^2 = 0.926$ was detected.

In 2012, MacKrell et al. first described the method for measuring glucose uptake and MHC isoform expression in the same individual muscle fiber [10]. This seminal publication included multiple experiments which validated the described technique. They showed that collagenase incubation did not alter glucose uptake, and Cytochlasin B incubation (a glucose transport inhibitor) completely eliminated insulin-stimulated glucose transport in single fibers. Comparing the results from Study 1 and Study 2 of this dissertation provides evidence of high reproducibility using this method to measure glucose uptake and fiber type in the same muscle fiber types. Not only do these findings provide unique insight into insulin resistance at a cellular level, but they are a useful demonstration of high reliability of this valuable technique.

Comparing fiber type and whole muscle glucose uptake results

Study 1 measured insulin-stimulated glucose uptake in different fiber types and whole muscles from LFD- and HFD-fed rats. When the relative abundance of each MHC isoform in whole muscle (8% type I, 16% type IIA, 27% type IIX, and 49% type IIB) was multiplied by the respective decrements in glucose uptake of HFD versus LFD (non-significant 4% lower value in type I and significant decrements of 12% for type IIA, 34% for type IIX, and 45% for type IIB), this resulted in an estimated 33.5% decrease. This result compared favorably to the directly measured 40% decrease in whole HFD versus LFD muscles.

Study 2 measured the fiber type-specific effect of exercise on insulin-stimulated glucose uptake in HFD-fed rats. When the relative abundance of each MHC isoform in whole muscle

(8% type I, 16% type IIA, 27% type IIX, and 49% type IIB) was multiplied by the respective increase in insulin-stimulated glucose uptake post-exercise (non-significant 9% greater value in type I and significant increases of 46% for type IIA, 28% for type IIX, and 68% for type IIB), this resulted in an estimated 49% increase. This relative increase compared favorably to the directly measured 43% increase in whole muscle insulin-stimulated glucose uptake that was measured after exercise in HFD-fed rats in Study 3.

The results for insulin-stimulated glucose uptake directly measured in whole muscle and estimated by the sum of multiple fiber types are strikingly similar. However, it is important to recognize that although the sums of the fiber type results for glucose uptake approximately equal the glucose uptake results in whole muscle, the whole muscle results do not necessarily reflect what is occurring in individual fiber types. A complete understanding of insulin resistance or the effect of exercise on insulin sensitivity, therefore, cannot be determined by exclusively assessing whole muscle tissue. It is critical to additionally assess fiber type-specific glucose uptake to fully understand these processes. Furthermore, the striking differences in glucose uptake that were observed in different fiber types in Study 1 and Study 2 warranted additional investigation into the mechanisms which may be regulating glucose uptake (Study 4).

Mechanisms responsible for fiber type-specific exercise effect on insulin-stimulated glucose uptake

Many earlier studies have reported that insulin-stimulated AS160 phosphorylation corresponds to insulin-stimulated glucose uptake in insulin-sensitive or insulin-resistant muscle tissue [6-8, 11, 12]. Additionally, in different fiber types from insulin-sensitive rat muscle the effect of exercise on insulin-stimulated glucose uptake tracks with AS160 phosphorylation [13]. However, fiber type-specific AS160 phosphorylation had never been assessed in insulin-resistant muscle for which fiber type-specific glucose uptake results were also known. Study 4 expanded on the interesting fiber type-specific glucose uptake results from Study 2 by measuring key insulin signaling events (including pAkt and pAS160) in HFD-fed rats after exercise.

In type IIB, IIBX, and IIA fibers the increase in insulin-stimulated glucose uptake after exercise was elevated above that of HFD-SED controls. The effect of exercise may be partially

explained by elevated AS160 phosphorylation in these fiber types (pAS160^{Ser704} for type IIB and IIBX, pAS160^{Thr642} for type IIBX and IIA, and pAS160^{Ser588} for type IIA). Conversely, type I fibers from HFD-fed rats did not increase insulin-stimulated glucose uptake after exercise compared to HFD-SED, and there was a decrease in insulin-stimulated pAS160^{Thr642} post-exercise. Therefore, since both insulin-stimulated glucose uptake and pAS160 in type I fibers were not increased, the hypothesis that that pAS160 can lead in post-exercise increases in insulin-stimulated glucose uptake is also supported in type I fibers. However, the effect of exercise on insulin-stimulated glucose uptake in type IIX fibers in HFD-fed rats was also elevated above HFD-SED, but was not matched by an effect of exercise to enhance AS160 phosphorylation on any of the three sites that were measured. Thus, type IIX fibers from HFD-fed rats do not support the concept that AS160 phosphorylation corresponds to insulin-stimulated glucose uptake following acute exercise. In contrast to earlier research using myofibers from rats with normal insulin sensitivity, the fiber type-specific glucose uptake corresponds to the fiber type-specific AS160 phosphorylation only for some AS160 phosphosites and some fiber types.

The full effect of exercise on insulin sensitivity, at least in some fiber types from muscles made insulin-resistant by a HFD, does not appear to be entirely due to enhancements in AS160 phosphorylation on the sites measured in this dissertation. Mass spectrometry analysis has identified several other sites on AS160 that can become phosphorylated in muscle that was exposed to the AMPK-activator AICAR [14]. One possible scenario for the disconnect between AS160 phosphorylation and glucose uptake is that the effect of exercise on insulin-stimulated glucose uptake in type IIX fibers may be related to exercise effects on the phosphorylation of AS160 on sites that were not measured in this dissertation. Additionally, since other fiber types characterized by increased insulin-stimulated glucose uptake after exercise versus SED controls (type IIA, IIBX, and IIB) only displayed elevated phosphorylation on some sites of AS160, other phosphomotifs of AS160 that were not measured may also contribute to the full effect of exercise. Finally, the differences among fiber types in subcellular localization of AS160 has never been studied. It is possible that the co-localization of AS160 with Rab proteins, Akt, GLUT4, AMPK, or other important mediators of insulin-stimulated glucose uptake may be particularly important for its post-exercise effect.

It also remains possible that other mechanisms, besides elevated AS160 phosphorylation, may be responsible for the effect of exercise on enhanced insulin sensitivity. The amount of sample obtained from our fiber type-specific analyses in Study 4 did not allow for the measurement of γ-isoform-specific AMPK activity. An important question remains: Is γ3-AMPK activity elevated in all fiber types which also have elevated insulin-stimulated glucose uptake following exercise? This question is particularly important with regards to type IIX fibers, which did not have increased AS160 phosphorylation. It would also be interesting to measure insulin-stimulated cell surface GLUT4 content after exercise in different fiber types from HFD-fed rats. The amount of cell surface GLUT4 is assumed to be elevated when insulin-stimulated glucose uptake is also elevated based on results in whole muscle tissue, but this has not been shown at a fiber type-specific level. Finally, it will be important to identify other proteins which may be playing a role in the effect of exercise on insulin-stimulated glucose uptake in insulin-resistant muscle. Mass spectrometry-based discovery analyses could be a useful tool to identify fiber type-specific changes in various post-translation modifications that may influence insulin-stimulated glucose uptake.

A particularly interesting finding from Study 2 was that the insulin-stimulated glucose uptake in type I fibers was maintained in sedentary HFD-fed rats, but was unchanged at 3hPEX in HFD-fed rats compared to HFD or LFD sedentary controls. Because the insulin-stimulated glucose uptake in Study 2 was measured at 3-hours post-exercise, it is conceivable that the type I fibers experienced transiently elevated *in vivo* glucose uptake while the rat rested for 3-hours post-exercise. Thus, when insulin-stimulated glucose uptake was measured in fibers from isolated epitrochlearis muscles at 3-hours post-exercise, it seemed possible that the type I fibers had already replenished glycogen stores, and the restoration or supercompensation of muscle glycogen has been proposed to be an event favoring the reversal of post-exercise insulin-stimulated glucose uptake [15].Therefore, in Study 4 we measured glycogen content in different fiber types from sedentary and exercised (IPEX and 3hPEX) rats fed a HFD. Our hypothesis was that all fiber types would have decreased glycogen content IPEX, but that at 3hPEX the type I fibers would have subsequently elevated glycogen content due to a rapid post-exercise glucose uptake *in vivo*. However, our results showed that the glycogen content of all fiber types at 3hPEX remained below the values in SED fibers. This finding from Study 4 suggested that the

lack of an effect of exercise to enhance insulin-stimulated glucose uptake in type I fibers in Study 2, was not due to a rapid glycogen resynthesis in the hours post-exercise.

Unique insights gained by measuring signaling events at both fiber type-specific and whole muscle levels

The glucose uptake results from Studies 1, 2, and 3 clearly demonstrated that although the sum of all fiber types may correspond to what is observed in whole muscle, values for whole muscle analysis may not be representative of the values for a given fiber type. It is possible to make similar comparisons for signaling events related to insulin sensitivity post-exercise based on the results of Studies 3 and 4. Study 3 measured key post-exercise signaling events in whole muscles that were made insulin-resistant by a HFD. Study 4 assessed some of these same post-exercise signaling events in different fiber types that were made insulin-resistant by a HFD. Consolidated comparisons of these results are displayed in Tables 7.1 (HFD-IPEX versus HFD-SED) and 7.2 (insulin-stimulated condition HFD-3hPEX versus HFD-SED).

Table 7.1

Insulin-independent glucose uptake and signaling events in whole muscle and different fiber types from 2-week HFD-fed rats at IPEX versus sedentary. Data are based on results from Studies 2, 3, and 4 of this dissertation. "↑" indicates increased value post-exercise. "↔" indicates no detectable change in value post-exercise.

	Glucose Uptake	pAMPK^{Thr172}	pACC^{Ser79}	pAS160^{Ser704}
Whole Muscle	↑	↑	↑	↑
Type I Fibers	↑	↑	↑	↑
Type IIA Fibers	↑	↔	↑	↑
Type IIX Fibers	↑	↑	↑	↑
Type IIBX Fibers	↑	↔	↑	↑
Type IIB Fibers	↑	↑	↑	↑

A significant increase in pAMPK^{Thr172} was observed IPEX compared to sedentary in whole muscles from HFD-fed rats in Study 3. In Study 4 only types IIB, IIX, and I showed significantly elevated pAMPK^{Thr172} IPEX versus SED. It is unclear why type IIBX and IIA fibers did not also have a statistically significant increase in pAMPK^{Thr172}. Study 3 included measurement in whole muscle of γ isoform-specific AMPK activity, which is a more direct measurement of AMPK activity than pAMPK^{Thr172}. However, it was impractical to determine γ3-AMPK activity in different fiber types because of the large number of fibers that would be required for the assay. The results revealed that γ3-containing AMPK heterotrimers, not γ1-containing heterotrimers, were likely responsible for the increased AMPK activity IPEX in

whole muscle. However, γ3-containing AMPK accounts for less than 20% of the AMPK in muscle [16]. Therefore differences in fiber type-specific AMPK phosphorylation could reflect differences in AMPK isoform-specific abundance and activity. Although some fiber type differences were observed in pAMPK^{Thr172} IPEX, two downstream substrates of AMPK, pACC^{Ser79} and pAS160^{Ser704}, were significantly elevated in all fiber types and whole muscles IPEX. The uniform results for all fiber types for multiple AMPK substrates suggest that AMPK activity was elevated in all fiber types, despite the lack of a significant increase in pAMPK^{Thr172} in each fiber type. The results observed for signaling events IPEX are similar for whole muscle and most fiber types. However, the differences in IPEX effects on pAMPK^{Thr172} between some fiber types and whole muscle could have never been identified without these single fiber analyses.

	Glucose Uptake	pAkt^{Ser473}	pAkt^{Thr308}	pAkt2^{Ser474}	pAkt2^{Thr309}	pAS160^{Ser704}	pAS160^{Thr642}	pAS160^{Ser588}
Whole Muscle	↑	↑	↑	↑	↔	↑	↑	↑
Type I Fibers	↔	↔	↔	?	?	↔	↓	Insufficient Signal
Type IIA Fibers	↑	↔	↔	?	?	↔	↑	↑
Type IIX Fibers	↑	↔	↔	?	?	↔	↔	↔
Type IIBX Fibers	↑	↔	↔	?	?	↑	↑	↔
Type IIB Fibers	↑	↔	↔	?	?	↑	↔	↔

Table 7.2

Insulin-stimulated glucose uptake and phosphorylation of Akt and AS160 in whole muscle and different fiber types from 2-week HFD-fed rats at 3hPEX versus sedentary. Data are based on results from Studies 2, 3, and 4 of this dissertation. "↑" indicates increased insulin-stimulated value with exercise. "↓" indicates decreased insulin-stimulated value with exercise. "↔" indicates no detectable change in insulin-stimulated value with exercise. "?" indicates measurement not made. "Insufficient Signal" indicates measurement made, but signal too weak for accurate quantification.

Insulin-stimulated pAkt^{Ser473} and pAkt^{Thr308} were increased at 3hPEX versus sedentary whole muscles from HFD-fed rats in Study 3. However, in Study 4 the effect of exercise was absent on insulin-stimulated pAkt^{Ser473} and pAkt^{Thr308} in all fiber types from HFD-fed rats (Table 7.2). What is responsible for the differential effect of exercise on insulin-stimulated pAkt at the whole muscle and fiber type level? Akt is present not only in myofibers, but also in multiple other cell types [17-22]. However, it is unknown if exercise alters the amount of pAkt in cell types other than myofibers. One speculative explanation for the exercise effect on whole muscle pAkt in the absence of an increase in pAkt in myofibers is that other cell types in whole muscle (e.g., vascular, neural, adipose, erythrocytes, neutrophils, etc.) may be largely responsible for the exercise-induced increase in insulin-stimulated pAkt observed in whole muscles in Study 3. It would be useful to evaluate the effects of prior exercise on pAkt in these other cells, e.g., by

analyzing blood cells or by using immunohistochemical analysis to evaluate non-skeletal muscle cells in muscle tissue. In the event that exercise effects were detected, it would be important to determine if these changes had any functional consequences. This provocative idea was stimulated by performing experiments that included both whole muscle and fiber type-specific analyses.

In Study 4 the effect of exercise on insulin-stimulated AS160 phosphorylation in different fiber types revealed that the pattern of pAS160 on the three phosphosites differed among all of the five fiber types studied (Table 7.2). Moreover, none of the five fiber types had an exercise-induced pattern on pAS160 that was the same as whole muscle (i.e., increased on all three phosphosites). Insulin-stimulated AS160 phosphorylation on at least one of the measured phosphosites ($pAS160^{Ser588}$, $pAS160^{Thr642}$, and $pAS160^{Ser704}$) of 3hPEX versus SED muscle was either increased (type IIB, IIBX, and IIA), unaltered (type IIX), or decreased (type I) in the different fiber types. Had we performed only whole muscle analysis, we would have failed to recognize that, at least in type IIX fibers, there is no evidence that greater pAS160 at 3hPEX versus SED rats. These unexpected outcomes provide strong evidence that mechanisms other than increased pAS160 on the sites evaluated should be considered to explain the improved insulin-stimulated glucose uptake in IIX fibers at 3hPEX. Additionally, type I fibers had unaltered insulin-stimulated glucose uptake post-exercise, but pAS160 was decreased. The increased pAS160 in type IIB, IIBX, and IIA did correspond to insulin-stimulated glucose uptake after exercise from single fibers in Study 2 and from whole muscles in Study 3. Therefore, it is possible that AS160 phosphorylation is partially responsible for the enhanced insulin sensitivity that is observed post-exercise in insulin-resistant muscle, but it is also certainly possible that other factors also contribute to the full effect of exercise on insulin sensitivity. The findings from these studies provided important new information regarding the influence of AS160 in post-exercise insulin-stimulated glucose uptake that could have never been determined by only investigating whole muscle tissue.

Directions for Future Research

The results from this dissertation provide unique insights into the mechanisms that lead to increased post-exercise insulin-stimulated glucose uptake in insulin-resistant skeletal muscle.

The enhanced post-exercise insulin sensitivity requires that the muscle "remembers" that exercise occurred for several hours after completion of the exercise bout. This phenomenon can occur in the absence of or after the reversal of a number of classic responses to exercise (elevated AMP/ATP ratio, increased AMPK activity, increased blood flow, increased O_2 uptake, etc.). What, then, is the "memory element" within skeletal muscle that serves to enhance insulin sensitivity hours to days after exercise? A previously proposed hypothesis was that activation of AMPK immediately after exercise would lead to greater pAS160^{Ser704} which would remain elevated at 3hPEX, and subsequently favor greater insulin-stimulated pAS160^{Thr642}, leading to increased glucose uptake. This hypothesis was supported by results in insulin-sensitive tissue [23]. Study 3 and Study 4 found that there was not an increase in insulin-independent pAS160^{Ser704} at 3hPEX in insulin-resistant whole muscle or any fiber type. Therefore, the evidence from this dissertation suggested pAS160^{Ser704} is not a memory element in insulin-resistant muscle for enhanced post-exercise insulin sensitivity. Study 3 found that γ3-AMPK activity, but not γ1-AMPK activity, was increased IPEX and at 3hPEX in whole muscles from rats fed a HFD. This result has also been observed in chow-fed rats [23] and γ3-containing AMPK heterotrimers are consistently shown to be activated after exercise [5, 23-28]. It was not feasible to test γ3-AMPK activity in different fiber types from Study 4, due to the limited available sample from isolated single fibers. In prior-AICAR treated muscles from whole body γ3-AMPK knockout mice, the insulin-stimulated increase in glucose uptake was completely abolished [29]. Therefore, substantial evidence suggests that elevated γ3-AMPK activity is an attractive "memory element" candidate for the increase in insulin sensitivity hours after exercise. However, a direct relationship between post-exercise γ3AMPK-activity and insulin-stimulated glucose uptake has yet to be explicitly shown. Accordingly, the following questions should be addressed:

> Question 1: Is elevated γ3-AMPK activity in skeletal muscle required for the post-exercise effect of insulin-stimulated glucose uptake in insulin-sensitive and insulin-resistant muscle?
>
> Question 2: Is elevated γ3-AMPK activity in skeletal muscle required for the fiber type-specific effect of exercise on insulin-stimulated glucose uptake in insulin-sensitive muscle?

The possibility that increased γ3-AMPK activity is essential for enhanced insulin-stimulated glucose uptake by muscle following *in vivo* exercise on insulin-stimulated glucose uptake has never been assessed using a genetic knockout of γ3-AMPK. The following section will address these questions using a rat model genetically deficient in muscle-specific γ3-AMPK.

Specific Research Projects

Specific Aims:

Currently there is no pharmacological γ3-specific AMPK inhibitor or activator, so testing the direct effect of γ3-AMPK activity using pharmacological means is not possible. The AICAR effect on insulin-stimulated glucose uptake is absent in γ3-AMPK knockout mice [29], but AICAR does not completely recapitulate *in vivo* exercise. It would seem logical to test the effect of *in vivo* exercise on insulin-stimulated glucose uptake using these γ3-AMPK knockout mice. However, the effect of exercise on muscle insulin sensitivity has been less frequently studied and characterized in much less detail in mice [30-32] than in either rats [2, 8, 15, 33-43] or humans [1, 3, 12, 44-47]. Furthermore, the method for measuring glucose uptake and fiber type from the same individual muscle fiber has only been described in rat epitrochlearis muscle, and would be extremely challenging using much mouse myofibers. Additionally, although it appears that γ3-AMPK expression is almost exclusively limited to skeletal muscle [48-50], low levels of expression may be present in other tissues as well. Therefore, γ3-AMPK muscle-specific knockout (mKO) rats will be generated to perform a series of experiments aimed to identify the role of γ3-AMPK activity in the effect of exercise on insulin-stimulated glucose uptake in skeletal muscle. The specific aims of these experiments are:

Aim 1: *Determine the extent to which the acute exercise effect on insulin-stimulated glucose uptake and key signaling events are altered in **whole muscle** from mKO-γ3-AMPK rats compared to wildtype (WT) controls.*

- Hypothesis 1A: mKO-*γ3-AMPK will result in an elimination of post-exercise insulin-stimulated glucose uptake by whole muscles from chow-fed and HFD-fed rats.*
- Hypothesis 1B: *Post-exercise increases in key signaling events will be impaired in both diet groups of mKO-γ3-AMPK versus WT rats.*

Aim 2: *Determine if there is a **fiber type-specific** effect of exercise on insulin-stimulated glucose uptake in mKO-γ3-AMPK rats.*

- Hypothesis 2: *Post-exercise increases in insulin-simulated glucose uptake will be impaired in all fiber types of mKO-γ3-AMPK versus WT rats.*

Research Design and Methods:

Rats carrying loxP inserts bracketing the γ3-AMPK locus (γ3-AMPK$^{fl/fl}$) will be generated using the CRISPR/Cas9 system. Muscle-specific γ3-AMPK knockout (mKO-γ3-AMPK) rats will be generated by mating γ3-AMPK$^{fl/fl}$ rats with rats expressing Cre recombinase under the control of the human alpha skeletal actin promotor (HSA-Cre). The offspring containing the desired genotype will then be backcrossed to wild type rats for 4 generations.

Experiment 1 (Aim 1): At 6 weeks of age mKO-γ3-AMPK$^{-/-}$ and their wild type controls (γ3-AMPK$^{+/+}$) will be fed either a low-fat diet (LFD; chow) or a high-fat diet (HFD) for two weeks. Subsequently, at 8 weeks of age rats will be fasted overnight and randomly assigned to either the exercise (4 x 30min bouts of swim exercise) or sedentary group. At 3-hours post-exercise (3hPEX) rats will be anesthetized and contralateral epitrochlearis muscles will be dissected and incubated ± 100μU/mL insulin and 2-deoxyglucose for the measurement of insulin-stimulated glucose uptake and key signaling events (γ1-isoform and γ3-isoform AMPK activity, pAMPK^{Thr172}, pAS160^{Ser704}, pAS160^{Thr642}, and pAS160^{Ser588}). A graphical depiction of the treatment groups used for Experiment 1 are displayed in Figure 7.2.

Experiment 2 (Aim 2): chow-fed mKO-γ3-AMPK$^{-/-}$ and γ3-AMPK$^{+/+}$ control rats will be fasted overnight at 8 weeks of age. The following morning, rats from each genotype will be randomly assigned to either the exercise (4 x 30min bouts of swim exercise) or sedentary group. At 3-hours post-exercise (3hPEX) rats will be anesthetized and contralateral epitrochlearis muscles will be dissected and incubated ± 100μU/mL insulin and 2-deoxyglucose. Muscles will then be incubated in collagenase and individual fibers will be isolated for the measurement of myosin heavy chain (MHC) and insulin-stimulated glucose uptake as previously described (Appendix A). A graphical depiction of the treatment groups used for Experiment 2 are displayed in Figure 7.3.

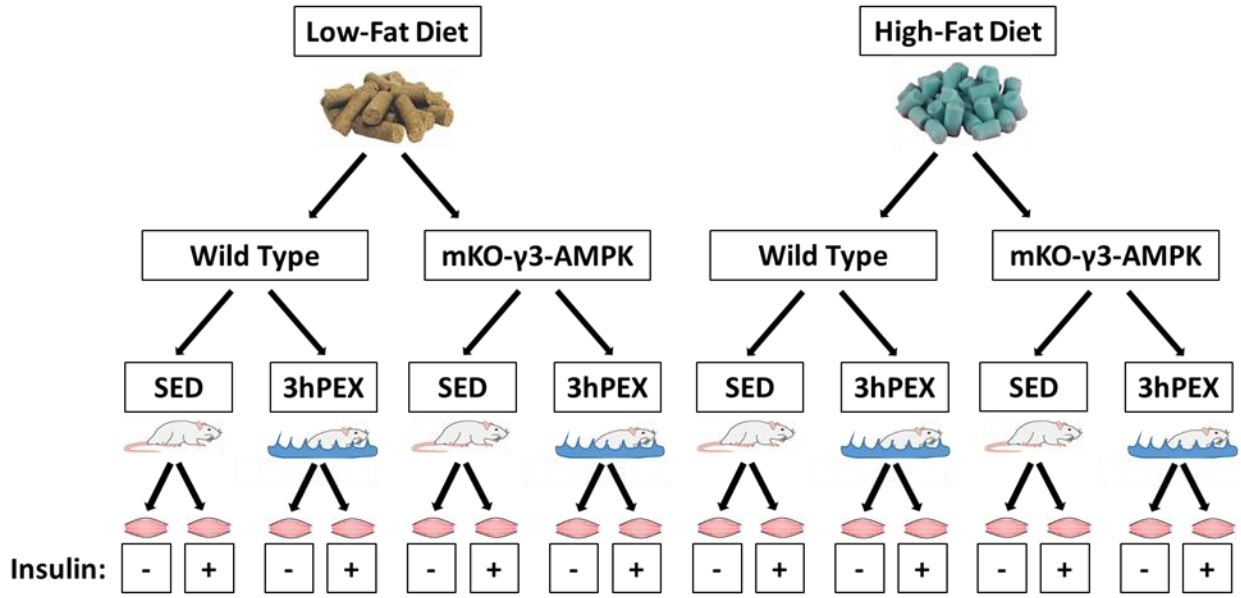

Figure 7.2

Treatment groups to be used for Experiment 1 of proposed Specific Research Projects. Wild type and muscle-specific γ3-AMPK knockout (mKO- γ3-AMPK) rats will be fed either a low- or high-fat diet. Epitrochlearis muscles will be dissected either 3-hours post-exercise (3hPEX) or from time-matched sedentary (SED) controls and incubated with (+) or without (-) 100μU/mL insulin.

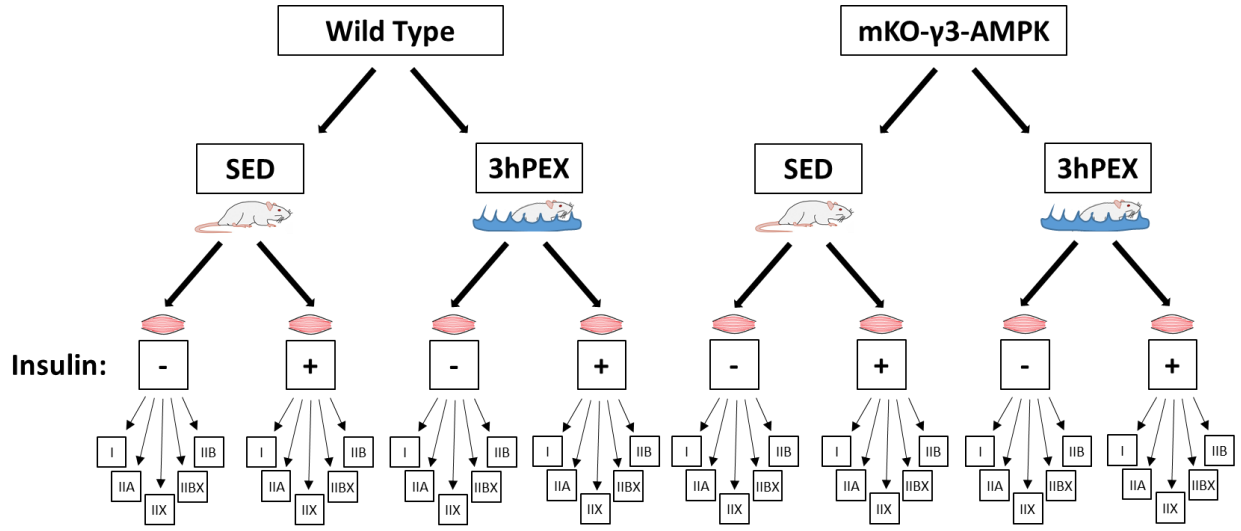

Figure 7.3

Treatment groups to be used for Experiment 2 of proposed Specific Research Projects. Wild type and muscle-specific γ3-AMPK knockout (mKO- γ3-AMPK) rats will be fed a low-fat diet. Epitrochlearis muscles will be dissected either 3-hours post-exercise (3hPEX) or from time-matched sedentary (SED) controls and incubated with (+) or without (-) 100μU/mL insulin. After collagenase incubation individual fibers will be isolated and fiber typed for myosin heavy chain expression (I, IIA, IIX, IIBX, and IIB).

Anticipated Results:

I predict that muscle-specific knockout of γ3-AMPK will alter several exercise effects that are found in whole muscle tissue from wild type rats, including the elimination of exercise effects on: 1) insulin-stimulated glucose uptake in muscles from LFD- and HFD-fed rats, 2) insulin-independent pAS160^{Ser704} at 3hPEX in LFD-fed rats, and 3) insulin-stimulated pAS160^{Ser704}, pAS160^{Thr642}, and pAS160^{Ser588} at 3hPEX in LFD- and HFD-fed rat muscle. I also predict that muscle-specific knockout of γ3-AMPK will result in reduced post-exercise insulin-stimulated glucose uptake in all fiber types.

Interpretation of Experiment 1:

The post-exercise effect on insulin-stimulated glucose uptake in mKO-γ3-AMPK$^{-/-}$ rats compared to sedentary mKO-γ3-AMPK$^{-/-}$ controls from Experiment 1 may be: 1) completely absent; 2) increased, but not to the level of wild type controls; or 3) increased to the same extent of wild type controls.

If the post-exercise enhancement in insulin-stimulated glucose uptake that is observed in wild type rats is completely absent in mKO-γ3-AMPK$^{-/-}$ rats, then the hypothesis that γ3-AMPK activity is required for enhanced post-exercise insulin-stimulated glucose uptake will be supported. If this phenomenon is additionally observed in HFD-fed rats, then the hypothesis that γ3-AMPK activity is required for enhanced post-exercise insulin-stimulated glucose uptake will also be supported in insulin-resistant muscle. This is an important distinction, since the potential for pharmacologically treating insulin-resistant muscle with γ3-AMPK activators would require insulin-resistant muscle to also exhibit this reliance on γ3-AMPK activity for its post-exercise benefit.

If exercise increases insulin-stimulated glucose uptake above sedentary in mKO-γ3-AMPK$^{-/-}$ rats, but not to the level of exercised wild type rats, then γ3-AMPK activity is only partially responsible for the effect of exercise on insulin sensitivity. It is possible that γ3-AMPK activity is required for the effect of exercise on insulin sensitivity in LFD-fed rats, but is only partially responsible for the effect of exercise on insulin sensitivity in HFD-fed rats. If this outcome occurs, then it would suggest that during muscle insulin resistance there are other

compensatory mechanisms, independent of γ3-AMPK activity, that contribute to elevating insulin-stimulated glucose uptake.

If the effect of exercise on insulin-stimulated glucose uptake is unaltered in whole muscle from mKO-γ3-AMPK$^{-/-}$ rats compared to wild type controls, then the results would suggest that γ3-AMPK activity is not required for the effect of exercise on insulin sensitivity. However, this outcome would not rule out the possibility that some fiber types require γ3-AMPK activity for the full effect of exercise on insulin-stimulated glucose uptake. It is possible that there is a decreased post-exercise effect on insulin-stimulated glucose uptake which occurs in some fiber types from mKO-γ3-AMPK$^{-/-}$ rats that only account for a small percentage of the whole muscle. Furthermore, when assessing glucose uptake at the whole muscle level, the decreased insulin-stimulated glucose uptake in some fiber types may be obscured by other fiber types with a normal response to exercise that comprise the majority of the whole muscle tissue. Therefore, equally increased insulin-stimulated glucose uptake following exercise in whole muscle from mKO-γ3-AMPK$^{-/-}$ and wild type rats would still require follow-up analyses in individual fiber types (Experiment 2).

It will also be important to identify the downstream signaling steps that are regulated by γ3-AMPK which influence insulin-stimulated glucose uptake. AS160 phosphorylation is a strong candidate for mediating the effect of exercise on insulin-sensitivity. In healthy muscle pAS160^{Ser704}, an AMPK phosphomotif on AS160, has been implicated as a potential "memory element" which remains elevated hours after exercise and enhances the insulin-stimulated phosphorylation of insulin-sensitive sites on AS160 (such as pAS160^{Thr642}). A decrease in insulin-independent pAS160^{Ser704} in chow-fed mKO-γ3-AMPK rats would provide further evidence that pAS160^{Ser704} may serve as a post-exercise memory element to increase insulin-stimulated glucose uptake. However, in Studies 3 and 4 we found that in insulin-resistant whole muscle and different fiber types the insulin-independent pAS160^{Ser704} had reversed to basal values by 3hPEX despite elevated γ3-AMPK activity (at least in whole muscle). Therefore, at least in insulin-resistant muscle, pAS160^{Ser704} would presumably not play a role as a memory element post-exercise.

Insulin-sensitive phosphosites on AS160 (pAS160^{Thr642} and pAS160^{Ser588}) may be indirectly regulated post-exercise by γ3-AMPK activity. If a post-exercise increase in insulin-

stimulated pAS160^{Thr642} and pAS160^{Ser588} did not occur in mKO-γ3-AMPK rats, then the hypothesis that these sites are indirectly influenced by post-exercise γ3-AMPK activity would be supported. It would be expected that this would occur in both LFD and HFD rats. Testing AS160 phosphorylation in these experiments will provide useful insight with regard to the differential downstream effects of post-exercise γ3-AMPK activity in healthy and insulin-resistant muscle. However, the mechanisms connecting γ3-AMPK activity and insulin-sensitive AS160 phosphorylation would remain uncertain. Thus, follow-up studies using site-specific mutation of AS160 would be warranted.

Interpretation of Experiment 2:

If the effect of exercise to enhance insulin-stimulated glucose uptake that is observed in wild type rats is absent in all fiber types from mKO-γ3-AMPK rats, then the hypothesis that γ3-AMPK activity is required for enhanced post-exercise insulin-stimulated glucose uptake would be supported at a fiber type specific level. This will be an important experiment because, as has been shown in wild type rats, responses to exercise from whole muscle do not always reflect the responses of individual fiber types. However, it is possible that in some fiber types from mKO-γ3-AMPK$^{-/-}$ rats that the effect of exercise to enhance insulin-stimulated glucose uptake is present. This would provide evidence for mechanisms independent from γ3-AMPK activity for enhancing insulin-stimulated glucose uptake following exercise. If in Experiment 1 the effect of exercise on insulin-stimulated glucose uptake was equal in whole muscle from mKO-γ3-AMPK$^{-/-}$ rats and wild type rats, then it does not rule out the possibility that some fiber types from mKO-γ3-AMPK$^{-/-}$ rats display blunted insulin-stimulated glucose uptake post-exercise. In this scenario, one possibility is that the sum of all fiber types that display an exercise effect on insulin-stimulated glucose uptake from mKO-γ3-AMPK$^{-/-}$ rats outweigh the detection of an increase in a single fiber type from the whole muscle analysis. Thus, in order to fully understand the effect of a muscle-specific deletion of γ3-AMPK on post-exercise insulin-stimulated glucose uptake it is necessary to make these fiber type-specific measures.

Potential Pitfalls and Alternative Experiments:

We expect that γ3-AMPK activity will be required for the effect of exercise on insulin sensitivity. However, if we discover that the γ3-AMPK knockout model does not influence the effect of exercise on insulin-stimulated glucose uptake, then it could be possible that the other γ-

isoform of AMPK in skeletal muscle (γ1) compensates for γ3-AMPK. Therefore, in a follow up experiment we will use an AMPK inhibitor [51] to prevent not only γ3-AMPK activity, but also γ1-AMPK activity. *Ex vivo* incubation in this AMPK inhibitor followed by glucose uptake measurement and γ-isoform AMPK activity measures would then determine if the effect of exercise on insulin sensitivity in the γ3-AMPK knockout model was due to compensatory γ1-AMPK activity or another unknown mechanism.

Although genetic knockout models are useful techniques for studying the function of certain proteins or genes of interest, it is possible that compensatory physiological effects of genetic knockouts can occur that may confound results. By using a muscle-specific knockout we have diminished, but not eliminated the possibility of compensatory physiological effects of a γ3-AMPK knockout. Therefore, it will be important to study the expression of other proteins that may be related to insulin-stimulated glucose uptake such as GLUT4, AS160, and Akt. It will additionally be important to make other measures such as body weight, fat mass, food intake, resting energy expenditure, respiratory exchange ratio, glucose tolerance, body composition, muscle fiber type composition, and muscle glycogen content to confirm that the γ3-AMPK knockout does not alter the general physiology of mKO-γ3-AMPK rats compared to wild type rats.

The exercise capacity of γ3-AMPK knockout mice seems to be unaltered compared to wild type mice. In fact, it has been shown that γ3-AMPK knockout mice can perform swim exercise for 2h, similar to the proposed experiments in rats [49]. However, if the mKO-γ3-AMPK rats have unexpectedly low exercise capacity then it will be possible to decrease the swim exercise time to accomplish the experiments. Funai et al. found that either 1h or 2h swim exercise in rats results in subsequently enhanced insulin-stimulated glucose uptake [52]. Therefore, decreasing exercise time is a possible solution for reduced exercise capacity to study post-exercise insulin-stimulated glucose uptake in rat muscle.

It was proposed that Experiment 1 would use both chow-fed and HFD-fed rats. However, because of the resources required for the single fiber analyses in Experiment 2, it was proposed that the assessment of single fibers would only use chow-fed rats. It will be necessary to perform Experiment 2 to identify potential fiber type differences in insulin-sensitive muscle from mKO-γ3-AMPK$^{-/-}$ rats. If we find fiber-type selective effects in healthy muscle from mKO-γ3-AMPK$^{-/-}$

rats, then a follow up study in HFD-fed muscle may be warranted. However, it is possible that no fiber type-selective effects of exercise will be discovered in healthy mKO-γ3-AMPK$^{-/-}$ rats after exercise. Although we have detected distinct differences between LFD and HFD wild type rats with regards to fiber type-specific glucose uptake, there were also clear fiber type-specific differences within each diet treatment. Therefore, before performing the extensive fiber type analyses in HFD-fed mKO-γ3-AMPK$^{-/-}$ rats the value of these experiments should be re-evaluated if there is no fiber type-specific exercise effect in chow-fed mKO-γ3-AMPK$^{-/-}$ rats.

Overall Conclusions

The findings from this dissertation have provided novel and important information regarding potential mechanisms for the post-exercise effect on insulin-stimulated glucose uptake in insulin-resistant skeletal muscle. The results demonstrated that: 1) the effect of a 2-week high-fat diet (HFD) on insulin-stimulated glucose uptake is fiber type-specific, 2) in muscle made insulin-resistant by a HFD, the effect of exercise on insulin-stimulated glucose uptake is also fiber type-specific, 3) although many of the effects of prior exercise on insulin signaling in insulin-resistant compared to healthy whole muscle are similar, there are notable exceptions, and 4) the effect of exercise on insulin-stimulated AS160 phosphorylation is fiber type-specific in insulin-resistant muscle. These findings revealed a need to consider the effects of exercise on insulin sensitivity at a fiber type level. Studying whole muscle is important, but a complete understanding of what is happening at a cellular level requires assessing fiber type-specific mechanisms. Furthermore, the differential effect of exercise that has been observed between LFD-and HFD-fed rats at the whole muscle and fiber type-specific levels emphasizes the need to understand the mechanisms of post-exercise insulin sensitivity in both healthy and insulin-resistant muscle.

To determine if the relationship between site-specific AS160 phosphorylation and post-exercise insulin-stimulated glucose uptake is causal, genetic manipulation studies should be performed. The recent creation of a recently generated AS160 knockout rat [53], will enable these types of experiments to be performed. Additionally, evidence of a causal relationship between post-exercise γ3-AMPK activity and insulin-stimulated glucose uptake will require the use of genetic studies. Mounting evidence of a possible role of γ3-AMPK on exercise-mediated

increases in insulin sensitivity [23, 27-29, 54] may warrant the generation of γ3-AMPK knockout rats to test this hypothesis, and also provide an impetus for efforts to develop a γ3-AMPK agonist for experimental and possible therapeutic use. The novel results from this dissertation research will help lay the foundation for subsequent research to further understand the complexities of exercise's effect on muscle insulin sensitivity.

REFERENCES

1. Wojtaszewski, J.F., B.F. Hansen, B. Kiens, and E.A. Richter, *Insulin signaling in human skeletal muscle: time course and effect of exercise.* Diabetes, 1997. **46**(11): p. 1775-1781.
2. Hansen, P.A., L.A. Nolte, M.M. Chen, and J.O. Holloszy, *Increased GLUT-4 translocation mediates enhanced insulin sensitivity of muscle glucose transport after exercise.* Journal of Applied Physiology, 1998. **85**(4): p. 1218-1222.
3. Wojtaszewski, J.F., B.F. Hansen, B. Kiens, J. Markuns, L. Goodyear, and E. Richter, *Insulin signaling and insulin sensitivity after exercise in human skeletal muscle.* Diabetes, 2000. **49**(3): p. 325-331.
4. Thong, F.S., W. Derave, B. Kiens, T.E. Graham, B. Ursø, J.F. Wojtaszewski, B.F. Hansen, and E.A. Richter, *Caffeine-induced impairment of insulin action but not insulin signaling in human skeletal muscle is reduced by exercise.* Diabetes, 2002. **51**(3): p. 583-590.
5. Treebak, J.T., J.B. Birk, A.J. Rose, B. Kiens, E.A. Richter, and J.F. Wojtaszewski, *AS160 phosphorylation is associated with activation of α2β2γ1-but not α2β2γ3-AMPK trimeric complex in skeletal muscle during exercise in humans.* American Journal of Physiology-Endocrinology and Metabolism, 2007. **292**(3): p. E715-E722.
6. Schweitzer, G.G., E.B. Arias, and G.D. Cartee, *Sustained postexercise increases in AS160 Thr 642 and Ser 588 phosphorylation in skeletal muscle without sustained increases in kinase phosphorylation.* Journal of applied physiology, 2012. **113**(12): p. 1852-1861.
7. Arias, E.B., J. Kim, K. Funai, and G.D. Cartee, *Prior exercise increases phosphorylation of Akt substrate of 160 kDa (AS160) in rat skeletal muscle.* American Journal of Physiology-Endocrinology and Metabolism, 2007. **292**(4): p. E1191-E1200.
8. Funai, K., G.G. Schweitzer, N. Sharma, M. Kanzaki, and G.D. Cartee, *Increased AS160 phosphorylation, but not TBC1D1 phosphorylation, with increased postexercise insulin sensitivity in rat skeletal muscle.* American Journal of Physiology-Endocrinology and Metabolism, 2009. **297**(1): p. E242-E251.
9. Pette, D. and R.S. Staron, *Myosin isoforms, muscle fiber types, and transitions.* Microsc Res Tech, 2000. **50**(6): p. 500-9.
10. Mackrell, J.G. and G.D. Cartee, *A novel method to measure glucose uptake and myosin heavy chain isoform expression of single fibers from rat skeletal muscle.* Diabetes, 2012. **61**(5): p. 995-1003.
11. Castorena, C.M., E.B. Arias, N. Sharma, and G.D. Cartee, *Postexercise improvement in insulin-stimulated glucose uptake occurs concomitant with greater AS160 phosphorylation in muscle from normal and insulin-resistant rats.* Diabetes, 2014. **63**(7): p. 2297-308.
12. Pehmøller, C., N. Brandt, J.B. Birk, L.D. Høeg, K.A. Sjøberg, L.J. Goodyear, B. Kiens, E.A. Richter, and J.F. Wojtaszewski, *Exercise alleviates lipid-induced insulin resistance in human skeletal muscle–signaling interaction at the level of TBC1 domain family member 4.* Diabetes, 2012. **61**(11): p. 2743-2752.
13. Wang, H., E.B. Arias, K. Oki, M.W. Pataky, J.A. Almallouhi, and G.D. Cartee, *Fiber Type-selective Exercise Effects on AS160 Phosphorylation.* American Journal of Physiology-Endocrinology and Metabolism, 2019.

14. Treebak, J.T., E.B. Taylor, C.A. Witczak, D. An, T. Toyoda, H.-J. Koh, J. Xie, E.P. Feener, J.F. Wojtaszewski, and M.F. Hirshman, *Identification of a novel phosphorylation site on TBC1D4 regulated by AMP-activated protein kinase in skeletal muscle.* American Journal of Physiology-Cell Physiology, 2009. **298**(2): p. C377-C385.
15. Cartee, G.D., D.A. Young, M.D. Sleeper, J. Zierath, H. Wallberg-Henriksson, and J. Holloszy, *Prolonged increase in insulin-stimulated glucose transport in muscle after exercise.* American Journal of Physiology-Endocrinology And Metabolism, 1989. **256**(4): p. E494-E499.
16. Kjøbsted, R., J.R. Hingst, J. Fentz, M. Foretz, M.-N. Sanz, C. Pehmøller, M. Shum, A. Marette, R. Mounier, and J.T. Treebak, *AMPK in skeletal muscle function and metabolism.* The FASEB Journal, 2018. **32**(4): p. 1741-1777.
17. Cong, L.-N., H. Chen, Y. Li, L. Zhou, M.A. McGibbon, S.I. Taylor, and M.J. Quon, *Physiological role of Akt in insulin-stimulated translocation of GLUT4 in transfected rat adipose cells.* Molecular endocrinology, 1997. **11**(13): p. 1881-1890.
18. Grote, C.W., A.L. Groover, J.M. Ryals, P.C. Geiger, E.L. Feldman, and D.E. Wright, *Peripheral nervous system insulin resistance in ob/ob mice.* Acta neuropathologica communications, 2013. **1**(1): p. 15.
19. Park, C.S., I.C. Schneider, and J.M. Haugh, *Kinetic analysis of platelet-derived growth factor receptor/phosphoinositide 3-kinase/Akt signaling in fibroblasts.* Journal of Biological Chemistry, 2003. **278**(39): p. 37064-37072.
20. Suhr, F., J. Brenig, R. Müller, H. Behrens, W. Bloch, and M. Grau, *Moderate exercise promotes human RBC-NOS activity, NO production and deformability through Akt kinase pathway.* PloS one, 2012. **7**(9): p. e45982.
21. Woulfe, D.S., *Akt signaling in platelets and thrombosis.* Expert review of hematology, 2010. **3**(1): p. 81-91.
22. Yu, H., T. Littlewood, and M. Bennett, *Akt isoforms in vascular disease.* Vascular pharmacology, 2015. **71**: p. 57-64.
23. Wang, H., E.B. Arias, M.W. Pataky, L.J. Goodyear, and G.D. Cartee, *Postexercise improvement in glucose uptake occurs concomitant with greater γ3-AMPK activation and AS160 phosphorylation in rat skeletal muscle.* American Journal of Physiology-Endocrinology and Metabolism, 2018.
24. Birk, J.B. and J. Wojtaszewski, *Predominant α2/β2/γ3 AMPK activation during exercise in human skeletal muscle.* The Journal of physiology, 2006. **577**(3): p. 1021-1032.
25. Kristensen, D.E., P.H. Albers, C. Prats, O. Baba, J.B. Birk, and J.F. Wojtaszewski, *Human muscle fibre type-specific regulation of AMPK and downstream targets by exercise.* The Journal of physiology, 2015. **593**(8): p. 2053-2069.
26. Kjøbsted, R., A.J. Pedersen, J.R. Hingst, R. Sabaratnam, J.B. Birk, J.M. Kristensen, K. Højlund, and J.F. Wojtaszewski, *Intact regulation of the AMPK signaling network in response to exercise and insulin in skeletal muscle of male patients with type 2 diabetes: illumination of AMPK activation in recovery from exercise.* Diabetes, 2016. **65**(5): p. 1219-1230.
27. Hingst, J.R., L. Bruhn, M.B. Hansen, M.F. Rosschou, J.B. Birk, J. Fentz, M. Foretz, B. Viollet, K. Sakamoto, and N.J. Færgeman, *Exercise-induced molecular mechanisms promoting glycogen supercompensation in human skeletal muscle.* Molecular metabolism, 2018. **16**: p. 24-34.

28. Steenberg, D.E., N.B. Jørgensen, J.B. Birk, K.A. Sjøberg, B. Kiens, E.A. Richter, and J.F. Wojtaszewski, *Exercise training reduces the insulin-sensitizing effect of a single bout of exercise in human skeletal muscle.* The Journal of physiology, 2019. **597**(1): p. 89-103.
29. Kjøbsted, R., J.T. Treebak, J. Fentz, L. Lantier, B. Viollet, J.B. Birk, P. Schjerling, M. Björnholm, J.R. Zierath, and J.F. Wojtaszewski, *Prior AICAR stimulation increases insulin sensitivity in mouse skeletal muscle in an AMPK-dependent manner.* Diabetes, 2015. **64**(6): p. 2042-2055.
30. Hamada, T., E.B. Arias, and G.D. Cartee, *Increased submaximal insulin-stimulated glucose uptake in mouse skeletal muscle after treadmill exercise.* Journal of applied physiology, 2006. **101**(5): p. 1368-1376.
31. Bonen, A., M. Tan, and W. Watson-Wright, *Effects of exercise on insulin binding and glucose metabolism in muscle.* Canadian journal of physiology and pharmacology, 1984. **62**(12): p. 1500-1504.
32. Schweitzer, G.G., C.M. Castorena, T. Hamada, K. Funai, E.B. Arias, and G.D. Cartee, *The B2 receptor of bradykinin is not essential for the post-exercise increase in glucose uptake by insulin-stimulated mouse skeletal muscle.* Physiological research/Academia Scientiarum Bohemoslovaca, 2011. **60**(3): p. 511.
33. Richter, E.A., L.P. Garetto, M.N. Goodman, and N.B. Ruderman, *Muscle glucose metabolism following exercise in the rat: increased sensitivity to insulin.* Journal of Clinical Investigation, 1982. **69**(4): p. 785.
34. Richter, E.A., L.P. Garetto, M.N. Goodman, and N.B. Ruderman, *Enhanced muscle glucose metabolism after exercise: modulation by local factors.* American Journal of Physiology-Endocrinology And Metabolism, 1984. **246**(6): p. E476-E482.
35. Richter, E.A., T. Ploug, and H. Galbo, *Increased muscle glucose uptake after exercise: no need for insulin during exercise.* Diabetes, 1985. **34**(10): p. 1041-1048.
36. Richter, E.A., K. Mikines, H. Galbo, and B. Kiens, *Effect of exercise on insulin action in human skeletal muscle.* Journal of applied physiology, 1989. **66**(2): p. 876-885.
37. Garetto, L.P., E.A. Richter, M.N. Goodman, and N.B. Ruderman, *Enhanced muscle glucose metabolism after exercise in the rat: the two phases.* American Journal of Physiology-Endocrinology And Metabolism, 1984. **246**(6): p. E471-E475.
38. Fisher, J.S., J. Gao, D.-H. Han, J.O. Holloszy, and L.A. Nolte, *Activation of AMP kinase enhances sensitivity of muscle glucose transport to insulin.* American Journal of Physiology-Endocrinology And Metabolism, 2002. **282**(1): p. E18-E23.
39. Dumke, C., J. Kim, E. Arias, and G. Cartee, *Role of kallikrein-kininogen system in insulin-stimulated glucose transport after muscle contractions.* Journal of Applied Physiology, 2002. **92**(2): p. 657-664.
40. Davis, T.A., S. Klahr, E.D. Tegtmeyer, D.F. Osborne, T.L. Howard, and I.E. Karl, *Glucose metabolism in epitrochlearis muscle of acutely exercised and trained rats.* American Journal of Physiology-Endocrinology And Metabolism, 1986. **250**(2): p. E137-E143.
41. Wallberg-Henriksson, H., S. Constable, D. Young, and J. Holloszy, *Glucose transport into rat skeletal muscle: interaction between exercise and insulin.* Journal of applied physiology, 1988. **65**(2): p. 909-913.
42. Cartee, G. and J. Holloszy, *Exercise increases susceptibility of muscle glucose transport to activation by various stimuli.* American Journal of Physiology-Endocrinology And Metabolism, 1990. **258**(2): p. E390-E393.

43. Funai, K. and G.D. Cartee, *Inhibition of contraction-stimulated AMP-activated protein kinase inhibits contraction-stimulated increases in PAS-TBC1D1 and glucose transport without altering PAS-AS160 in rat skeletal muscle.* Diabetes, 2009. **58**(5): p. 1096-104.
44. Annuzzi, G., G. Riccardi, B. Capaldo, and L. KAUSER, *Increased insulin-stimulated glucose uptake by exercised human muscles one day after prolonged physical exercise.* European journal of clinical investigation, 1991. **21**(1): p. 6-12.
45. Frøsig, C., M.P. Sajan, S.J. Maarbjerg, N. Brandt, C. Roepstorff, J.F. Wojtaszewski, B. Kiens, R.V. Farese, and E.A. Richter, *Exercise improves phosphatidylinositol-3, 4, 5-trisphosphate responsiveness of atypical protein kinase C and interacts with insulin signalling to peptide elongation in human skeletal muscle.* The Journal of physiology, 2007. **582**(3): p. 1289-1301.
46. Frøsig, C. and E.A. Richter, *Improved insulin sensitivity after exercise: focus on insulin signaling.* Obesity, 2009. **17**(S3).
47. Treebak, J.T., C. Frøsig, C. Pehmøller, S. Chen, S.J. Maarbjerg, N. Brandt, C. MacKintosh, J. Zierath, D. Hardie, and B. Kiens, *Potential role of TBC1D4 in enhanced post-exercise insulin action in human skeletal muscle.* Diabetologia, 2009. **52**(5): p. 891-900.
48. Mahlapuu, M., C. Johansson, K. Lindgren, G. Hjalm, B.R. Barnes, A. Krook, J.R. Zierath, L. Andersson, and S. Marklund, *Expression profiling of the γ-subunit isoforms of AMP-activated protein kinase suggests a major role for γ3 in white skeletal muscle.* American Journal of Physiology-Endocrinology and Metabolism, 2004. **286**(2): p. E194-E200.
49. Barnes, B.R., S. Marklund, T.L. Steiler, M. Walter, G. Hjälm, V. Amarger, M. Mahlapuu, Y. Leng, C. Johansson, and D. Galuska, *The 5'-AMP-activated protein kinase γ3 isoform has a key role in carbohydrate and lipid metabolism in glycolytic skeletal muscle.* Journal of Biological Chemistry, 2004. **279**(37): p. 38441-38447.
50. Yu, H., N. Fujii, M.F. Hirshman, J.M. Pomerleau, and L.J. Goodyear, *Cloning and characterization of mouse 5'-AMP-activated protein kinase γ3 subunit.* American Journal of Physiology-Cell Physiology, 2004. **286**(2): p. C283-C292.
51. Dite, T.A., C.G. Langendorf, A. Hoque, S. Galic, R.J. Rebello, A.J. Ovens, L.M. Lindqvist, K.R. Ngoei, N.X. Ling, and L. Furic, *AMP-activated protein kinase selectively inhibited by the type II inhibitor SBI-0206965.* Journal of Biological Chemistry, 2018. **293**(23): p. 8874-8885.
52. Funai, K., G.G. Schweitzer, C.M. Castorena, M. Kanzaki, and G.D. Cartee, *In vivo exercise followed by in vitro contraction additively elevates subsequent insulin-stimulated glucose transport by rat skeletal muscle.* American Journal of Physiology-Endocrinology and Metabolism, 2010. **298**(5): p. E999-E1010.
53. Arias, E., X. Zheng, S. Agrawal, and G. Cartee, *Whole body glucoregulation and tissue-specific glucose uptake in a novel Akt substrate of 160 kDa knockout rat model.* PloS one, 2019. **14**(4): p. e0216236-e0216236.
54. Kjøbsted, R., N. Munk-Hansen, J.B. Birk, M. Foretz, B. Viollet, M. Björnholm, J.R. Zierath, J.T. Treebak, and J.F. Wojtaszewski, *Enhanced muscle insulin sensitivity after contraction/exercise is mediated by AMPK.* Diabetes, 2017. **66**(3): p. 598-612.

APPENDICES

Appendix A is a published book chapter describing the method used for measuring fiber type and glucose uptake in the same muscle fiber. This method was used in Chapters I and II of this dissertation. Appendices B and C are data mentioned in Chapter IV, but not published in the manuscript.

Appendix A

Measuring Both Glucose Uptake and Myosin Heavy Chain Isoform Expression in Single Rat Skeletal Muscle Fibers

ABSTRACT

Glucose uptake by skeletal muscle is important for metabolic health. Because skeletal muscle is composed of multiple fiber types that have differing metabolic and contractile properties, studying glucose uptake in whole muscle tissue does not elucidate differences at the cellular level. Here we describe a procedure which enables the measurement of both glucose uptake and fiber type (by myosin heavy chain isoform expression) in individual rat epitrochlearis muscle fibers.

INTRODUCTION

Skeletal muscle is a heterogeneous tissue composed of hundreds to many thousands of individual muscle cells (muscle fibers). Different muscle fibers can have strikingly different metabolic and contractile properties [1]. Measuring the myosin heavy chain (MHC) expression via SDS-PAGE is the gold standard for classifying muscle fiber type at both the tissue and single fiber levels [2]. Four MHC isoforms are expressed in adult rat or mouse skeletal muscle (MHC type I, IIA, IIX, and IIB) and three MHC isoforms are expressed in adult human skeletal muscle (MHC type I, IIA, and IIX) [1]. Additionally, muscle fibers that express more than one MHC isoform are classified as “hybrid” fibers which typically possess characteristics that are intermediate to the values of the individual MHC isoforms that they express. There is evidence that certain conditions such as chronic exercise training [3, 4], and old age [5, 6] may alter fiber type composition, and this may have an impact on metabolic health.

In skeletal muscle, glucose transport into the cell is a rate-limiting step for glucose disposal. Glucose uptake in whole skeletal muscle tissue is often measured using radiolabeled

glucose analogs such as 2-deoxyglucose (2-DG; which can be phosphorylated by hexokinase with limited subsequent metabolism) or 3-O-methylglucose (3-MG; which is not metabolized after cell entry) in response to insulin [7, 8], exercise [9, 10], contraction [11, 12], or various other stimuli [8, 12]. Conventionally, researchers have attempted to evaluate fiber type-related differences for glucose uptake by comparing whole muscle or regions of whole muscle which have enriched expression of a given fiber type. However, comparing glucose uptake at the whole muscle level is not ideal from the perspective of understanding fiber type-specific differences because: 1) no whole muscle is only comprised of one fiber type, 2) hybrid fibers cannot be evaluated using whole muscle tissue analysis, 3) whole muscles contain multiple cell types (including neural, vascular, connective, and adipose) which contribute to tissue glucose uptake, and 4) no whole muscle in rat has been identified that is primarily composed of type IIX fibers.

In 2012 MacKrell et al. developed and validated a novel method for measuring glucose uptake and fiber type in the same single fiber from rat skeletal muscle [13]. 2-DG was the glucose analog used because 2-DG that enters myofibers is rapidly phosphorylated by hexokinase, and the resultant 2-DG-6P is trapped in the fiber. A fundamental feature of measuring glucose uptake in isolated whole muscles involves the calculation of [^{3}H]-2-DG within the muscle fibers with correction of extracellular [^{3}H]-2-DG, e.g., using [^{14}C] mannitol to estimate the extracellular space. Because isolated muscle fibers do not have extracellular space, extracellular [^{14}C] mannitol is not required for single fiber glucose uptake. Therefore, the conventional whole muscle glucose uptake method (with [^{3}H]-2-DG and extracellular [^{14}C] mannitol) was compared with incubation of whole muscle in [^{3}H]-2-DG followed by three washing steps to remove extracellular [^{3}H]-2-DG that was not trapped in the muscle cells, and no differences were detected [13]. Because the procedure to measure single fiber glucose uptake requires enzymatic digestion of the collagen surrounding muscle fibers by collagenase treatment, a control experiment was performed which demonstrated that collagenase did not alter glucose uptake by isolated muscle tissue. Finally, incubation in cytochalasin B, a fungal metabolite which inhibits glucose transporter-mediated glucose transport [14], completely blocked insulin-stimulated glucose uptake in all fiber types, indicating that the glucose uptake measured in single fibers was attributable to glucose transporter-mediated transport.

After validating this single fiber method, our laboratory performed a series of experiments to characterize the fiber type-specific effects of various conditions and interventions on glucose uptake. The seminal publication by MacKrell et al. which evaluated type IIA, IIB, IIX, and IIBX fibers demonstrated that glucose uptake was increased by insulin in a fiber type-specific manner, where type IIA fibers displayed the greatest insulin-stimulated glucose uptake and type IIX and IIB fibers had the lowest insulin-stimulated glucose uptake [13]. In the original study, we failed to isolate any type I fibers, but we subsequently modified the protocol and were successful in isolating type I fibers from the epitrochlearis muscle. With the modified protocol, we recently found that insulin-stimulated glucose uptake was similar for type I fibers versus type IIA fibers, and values for each of these fiber types significantly exceeded the values for other fiber types (IIB, IIX, and IIBX) [15]. Using the single fiber method we have discovered that some conditions or interventions do not result in fiber type-selective effects on glucose uptake. For example, in a comparison of obese versus lean Zucker rats, insulin-stimulated glucose uptake was substantially reduced to a similar extent in each fiber type studied (type IIA, IIB, IIX, and IIBX) [13]. We also found that old rats eating a calorie restricted diet (40% below ad libitum, AL, intake) compared to AL controls had greater insulin-stimulated glucose uptake in each fiber type studied (type I, IIA, IIB, IIX, IIAX, and IIBX) [16]. However, we have also discovered fiber type-selective differences on insulin-stimulated glucose uptake induced by either acute exercise (increased for rats at 3.5h post-exercise versus sedentary controls in all fiber types except IIX) [15], or a high-fat diet (values for rats consuming a high-fat diet were reduced versus low-fat diet-fed controls for all fiber types except type I) [17].

Insulin is the most important physiologic stimulator of glucose transport, but there are also insulin-independent mechanisms to increase glucose transport in skeletal muscle. Using muscle incubated with AMP-activated kinase stimulating compound, AICAR, we found a relatively greater increase in glucose uptake in type IIB fibers compared to type IIA fibers [13]. In response to electrical stimulation-induced muscle contraction, we observed similar increases in glucose uptake in each fiber type studied (type IIA, IIB, IIX, and IIBX) [18]. Whether or not the method has revealed fiber type-selective responses to a given intervention, the ability to interrogate muscle at the single fiber level has offered valuable insights at the cellular and fiber type-specific level that would have otherwise been impossible to determine based solely on tissue-level analysis.

For several reasons, we have exclusively used rat epitrochlearis muscles in all of our publications that evaluated glucose uptake and fiber type in single muscle fibers. We initially used the rat epitrochlearis for single fiber glucose uptake because we and many other researchers have frequently used the epitrochlearis for analysis of whole muscle glucose uptake, resulting in and extensive foundation of information regarding this muscle. The epitrochlearis is a thin forelimb muscle that originates at the distal tendon of the latissimus dorsi and inserts at the medial epicondyle of the humerus [19]. Because the epitrochlearis is only ~25 fibers thick, it has a relatively thin diffusion distance that facilitates the access of extracellular nutrients to the fibers. The epitrochlearis expresses each of the MHC isoforms that are expressed in adult rat skeletal muscle, and the fiber type proportion of the epitrochlearis muscle is comparable to the fiber type profile that has been reported for 76 skeletal muscles or muscle regions that were sampled from the rat neck, trunk, forelimbs, and hindlimbs [20], making it a representative muscle from the perspective of fiber type. When we initially developed this method, we made very limited attempts to isolate single fibers from rat soleus and extensor digitorum (EDL) muscles. These limited efforts suggested that the epitrochlearis was superior to these muscles with regard to the ease of fiber isolation using our approach, so we discontinued further attempts using these muscles. It remains possible that others will identify modifications of our methods or other muscles that are suitable for single fiber glucose uptake analysis.

Here, we describe the procedure which enables the measurement of both glucose uptake and fiber type in the same individual rat epitrochlearis muscle fiber. The following description incorporates improvements to the original method that have been noted in several subsequent publications, as well as providing more details than have been previously documented [15, 17, 18, 21, 22].

MATERIALS

2.1 Experimental Set-up

1. Temperature controlled shaking water bath capable of 35°C and 45 revolutions per minute (rpm)

2. 20 mL glass scintillation vials (used for both incubating muscles and for scintillation counting)

3. Krebs-Henseleit Buffer (KHB): Prepare 10X KHB Stock #1 (1 L deionized H_2O, 67.8 g NaCl, 3.4 g KCl, 1.58 g KH_2PO_4, and 21.5 g NaH_3CO_3) and 10X KHB Stock #2 (1 L deionized H_2O, 2.82 g $CaCl_2$, and 1.4 g $MgSO_4$). 10X KHB Stock #1 and #2 can be stored at 4°C for at least 1 month. To make KHB add 50 mL of 10X KHB Stock #1 to 400 mL deionized ultrapure H_2O and gas with 95% O_2/5% CO_2 with stainless steel aeration stone for 15 minutes on ice, then add 50 mL of 10X KHB Stock #2 and mix.

4. Incubation Media #1: KHB supplemented with 0.1% RIA-grade bovine serum albumin (BSA), 2 mM sodium pyruvate, and 6 mM mannitol (*see* **Note 1**)

5. Incubation Media #2: KHB supplemented with 0.1% BSA, 2 mM sodium pyruvate, 6 mM mannitol, and 0.1 mM 2-deoxy-D-glucose (2-DG) [specific activity of 13.5 mCi/mmol [^{3}H]-2-DG] (*see* **Note 2**)

6. Wash Media: Ca^{2+}-free KHB (*see* **Note 3**) supplemented with 0.1% BSA and 8 mM glucose

7. 2.5% type II Collagenase Media: Ca^{2+}-free KHB supplemented with 0.1% BSA, 8 mM glucose, and 2.5% type II collagenase (*see* **Note 4**)

8. Gas washing bottle with gas dispersion disc

9. 95% O_2/5% CO_2 compressed gas cylinder

10. Gas regulator appropriate for 95% O_2/5% CO_2

11. Gas manifold apparatus (with sufficient number of ports to accommodate the number of incubation vials used in the experiment)

12. Support stand setups (base and rods) with appropriate clamps to secure each manifold apparatus

13. 3/8” x 1/16” wall flexible polyethylene tubing (enough to reach from the compressed gas cylinder to the gas washing bottle and manifold apparatus)

14. Flexible polyethylene microbore tubing (size 0.04 x 0.07; 1 ft per vial to reach from manifold to incubation vials)

15. 1.5 inch blunt tip 18 gauge needles (sufficient number to accommodate for the number of incubation vials used in the experiment)

16. Rubber stoppers for vials (size 0; sufficient number to accommodate the number of incubation vials used in the experiment)

2.2 Muscle Dissection and Incubation

1. Surgical instruments for rat epitrochlearis dissection

2. Stainless steel Gerald forceps

3. Stainless steel laboratory spatula

4. Orbital Shaker capable of 90 rpm

5. Glass petri dishes

6. 30 mm culture dish

2.3 Single Fiber Isolation and Processing

1. Camera enabled dissecting microscope capable of 8-20X magnification

2. Fine surgical forceps (*see* **Note 5)**

3. 200 µl microcentrifuge tubes

4. Lysis Buffer: tissue protein extraction reagent (T-PER; *see* **Note 6**) supplemented with 1 mM Na_3VO_4, 1 mM EGTA, 2.5 mM sodium pyrophosphate tetrabasic decahydrate, 1 mM β-glycerophosphate, 1 µg/mL leupeptin, and 1 mM phenylmethylsulfonyl fluoride

5. 2X Laemmli Buffer

6. Vortex mixer

7. Heating block

8. Benchtop mini-centrifuge

2.4 Measuring Glucose Uptake

1. Liquid scintillation cocktail

2. Scintillation counter

3. Computer with ImageJ software (NIH, Bethesda, MD)

2.5 MHC Isoform Identification

1. 6.5% Polyacrylamide Resolving Gel (volumes for 16 gels): 14.7 mL 30% acrylamide/bis-acrylamide (50:1 ratio), 20.25 mL glycerol, 9.45 mL 1.5 M Tris-HCl (pH 8.8), 7.08 mL 1 M glycine, 2.7 mL 10% sodium dodecyl sulfate (SDS), 12.612 mL deionized H_2O, 0.675 mL 10% ammonium persulfate, and 0.04 mL TEMED

2. 4% Polyacrylamide Stacking Gel (volumes for 16 gels): 5.332 mL 30% acrylamide/bis-acrylamide (37.5:1 ratio), 12 mL glycerol, 5.6 mL 0.5 M Tris-HCl (pH 6.7), 1.6 mL 100 mM EDTA (pH 7.0), 1.6 mL 10% SDS, 13.448 mL deionized H_2O, 0.4 mL 10% ammonium persulfate, and 0.025 mL TEMED

3. 10X Running Buffer: 0.25 M Tris base, 1.92 M glycine, 34.7 mM SDS.

4. 1X Running Buffer: 900 mL deionized H_2O and 100 mL of 10X Running Buffer

5. Rat extensor digitorum longus (EDL) muscle (for positive MHC control)

6. Rat soleus muscle (for positive MHC control)

7. High molecular weight (HMW) protein ladder standard

8. Equipment used for SDS-PAGE

9. Plastic tupperware to be filled with ice that can also hold SDS-PAGE boxes

10. SimplyBlue™ SafeStain

11. Bicinchoninic acid (BCA) Protein Assay Kit

12. Microplate reader with absorbance detection capability and appropriate filters

METHODS

3.1 Experimental Set-up

1. On the day of the experiment prepare KHB solution as described in **section 2.1 step 3**.

2. Prepare Incubation Media #1 and Incubation Media #2 fresh on the day of the experiment (*see* **steps 4 and 5 in section 2.1**). When the incubation media #2 is prepared, an aliquot of ~200-500 µl should be removed and stored at -20°C until it is thawed and used for liquid scintillation counting and the calculation of glucose uptake measurement (*see* **step 3 in section 3.4**).

3. Pipette 2 ml of Incubation Media #1 into an incubation vial for each muscle that will be isolated (*see* **Note 7**). Pre-gas and pre-warm the vials containing Incubation Media #1 for at least 5 minutes in the shaking, heated water bath as shown in **Figure A-1.1** (*see* **Note 8**).

4. Pipette 2 ml of Incubation Media #2 into a separate incubation vial for each muscle, and pre-gas and pre-warm the media.

5. Prepare Wash Media and 2.5% type II Collagenase Media (*see* **steps 6 and 7 in section 2.1**) and add to appropriate vials. Wash Media and 2.5% type II Collagenase Media should be stored at 4°C until just prior to use. Incubations in Wash Media will be performed on ice. For incubation steps using 2.5% type II Collagenase Media, vials should be placed in the shaking, heated water bath ~5 minutes prior to muscle incubation (*see* **Note 9)**.

3.2 Muscle Dissection and Incubation

1. Remove skin from the forelimb of a deeply anesthetized rat.

2. Carefully dissect the whole epitrochlearis muscle from the rat. Take care to avoid damaging the epitrochlearis fibers. Retain the connective tissue at the proximal and distal ends of the epitrochlearis.

3. Briefly (2-3 seconds) wash excess blood from the isolated epitrochlearis muscle (handling only by the connective tissue) in a glass petri dish with KHB at room temperature.

4. Prior to transferring isolated muscles into vials for incubation, the vials should have been pre-warmed and pre-gassed for at least 5 minutes using the gassing apparatus in the heated, shaking water bath (Figure A-1.1). Using Gerald forceps, grasp the adjacent connective tissue on the end

of the epitrochlearis, and transfer the muscle to a glass vial containing 2 mL of Incubation Media #1 (*see* **Note 10**). During this incubation step each vial should be continually gassed with 95% O_2/5% CO_2 from above with an individual line. Additionally, vials should be shaken at 45 rpm (*see* **Note 11**) in a heated (35°C) water bath for 10-30 minutes (*see* **Note 12**).

5. Using Gerald forceps, gently transfer the muscle into a pre-gassed and pre-warmed glass vial containing 2 mL of Incubation Media #2. Vials containing isolated muscles should be continually gassed with 95% O_2/5% CO_2 while being shaken at 45 rpm in a heated (35°C) water bath for 30-60 minutes (*see* **Note 13**).

6. To clear extracellular space of 2-DG, rinse the muscle 3 X 5 min in 5 mL of ice-cold Wash Media in glass vials with shaking at 90 rpm.

7. After washing, place the muscle in a continually gassed (95% O_2/5% CO_2) glass vial containing 2 mL of 2.5% type II Collagenase Media for 60 minutes (*see* **Note 14)**. The vials should be placed in a water bath at 35°C with shaking at 45 rpm. The enzymatic digestion of collagen results in loosely connected fibers, which are hereafter referred to as fiber bundles.

8. Transfer Collagenase Media and fiber bundle by carefully pouring into a 30 mm culture dish. Under a dissecting microscope, trim the proximal and distal connective tissue from the fiber bundle using a scalpel (*see* **Note 15**). Gently remove fiber bundle from collagenase media with a stainless steel laboratory spatula and place in a glass petri dish containing Wash Media at room temperature (*see* **Note 16**). Fibers will be isolated from the fiber bundle in this dish.

3.3 Single Fiber Isolation and Processing

1. Using fine surgical forceps, gently tease apart individual fibers from the fiber bundle by grasping a fiber from one end and gently pulling away it from the fiber bundle. Then release the fiber in an area of the petri dish free from debris.

2. After isolating each fiber under the microscope, capture an image of the fiber to be analyzed for fiber area (*see* **step 8 in section 3.4**). Include a scale bar in the image based on the magnification being used (typically 16X or 20X magnification). A representative image of an isolated fiber is shown in Figure A-1.2.

3. After image capture, transfer each fiber by pipette, along with 20 µl of the Wash Media that the fibers are being isolated in, to a microcentrifuge tube (*see* **Note 17**).

4. After completing the imaging of all of the fibers that were isolated from a given muscle (typically 50-60 fibers for our experiments), and after each isolated fiber has been transferred into an individual microcentrifuge tube, add 30 µl of Lysis Buffer and 50 µl of 2X Laemmli Buffer to each microcentrifuge tube. The final volume of each tube will now be 100 µl.

5. Vortex and then lyse the fibers by heating tubes for 10 minutes at 95-100°C in a heating block (*see* **Note 18**). Vortex tubes again, flash spin with mini-centrifuge and store lysed fibers at -20°C until processing for glucose uptake and MHC expression.

3.4 Measuring Glucose Uptake

1. Aliquot 40 µl of each fiber lysate into separate glass scintillation vials.

2. Add 8 mL of liquid scintillation cocktail to each vial, and tightly cap and vortex the vials.

3. Dilute 100 µl of Incubation Media #2 (*saved from* **step 2 in section 3.1**) in 900 µl of Lysis Buffer. Aliquot 200 µl of the diluted Incubation Media #2 into 4 separate scintillation vials, followed with 8 mL of liquid scintillation cocktail.

4. Aliquot 200 µl of non-radioactive KHB into 4 separate scintillation vials, along with 8 mL of liquid scintillation cocktail.

5. Place the individual scintillation vials containing lysate from each single fiber sample (after steps 1 & 2), quadruplicate incubation media (step 3), and quadruplicate KHB background samples (step 4) into carrier racks that are placed in a scintillation counter to determine 2-[^{3}H]-DG disintegrations per minute (dpm).

6. The total ^{3}H dpm per fiber can then be used to calculate 2-DG accumulation in individual fibers using the following equation (*see* **Note 19**):

$$\text{total } ^{3}\text{H dpm per fiber} \times \frac{\text{µmol 2-DG per mL incubation media}}{^{3}\text{H dpm per mL incubation media}} = \text{2-DG accumulation per fiber}$$

7. 2-DG accumulation should be expressed relative to fiber area (picomoles x mm^2) which is determined based on the captured image from individual fibers.

8. Images of each fiber (*captured during* **step 2 of section 3.3**) can be manually traced in ImageJ using the "Polygon Selections" or "Freehand Selections" tools for an estimate of fiber area (*see* **Notes 20-22**).

3.5 MHC Isoform Identification

1. Prepare 15-well self-cast 6.5% polyacrylamide gels (*see* **1 and 2 in section 2.4**) and 1X running buffer.

2. Preparation of MHC Standards: Homogenize ~30 g of rat EDL and ~20 g of rat soleus muscles together in 1 mL of Lysis Buffer. Do not centrifuge to remove insoluble protein which include the MHC isoforms. Perform a BCA protein assay in quadruplicate for protein concentration in the lysate and then dilute the lysate to a concentration of 1 µg/µl with lysis buffer. Add equal volume of 2X Laemmli buffer to bring the final protein concentration to 0.5 µg/µl and then boil heat sample for 10 minutes at 95-100°C and store at 20°C. 12 µl (6 µg) of this 3:2 EDL:Soleus standard will be used for each MHC standard lane (*see* **Note 23**).

3. When ready to run the MHC fiber-typing gel, heat the 3:2 EDL:Soleus standard and single fiber lysates for 10 minutes at 95-100° prior to loading on gel (*see* **Note 24**).

4. Add 1X Running Buffer to SDS-PAGE boxes.

5. In well #1 load 6-10 µl of a HMW protein ladder standard. In wells #2, #9, and #15 load 12 µl of heated 3:2 EDL:Soleus standard. In the remaining 11 wells load 18 µl of the heated fiber lysates (*see* **Note 25**).

6. Pack SDS-PAGE boxes in a container with ice and run for 1 hour at 50V in a 4°C refrigerator.

7. After 1 hour, re-set the voltage to ~40V and run for 22-24 hours, or until the 200 kDa marker is almost at the bottom of the gel (*see* **Note 26**).

8. After the gel is finished running, remove the gels from the glass plates and wash gels in a shaking container with deionized water at room temperature for 4-5 minutes to rinse off excess glycerol (*see* **Note 27**).

9. Remove gels from deionized water and place in a shaking container with SimplyBlue^{TM} SafeStain for 1-2 hours (*see* **Note 28**).

10. Remove gels from SimplyBlue^{TM} SafeStain and place in a shaking container with deionized water for ≥ 2 hours (*see* **Note 29**) for de-staining.

11. Gels can now be imaged and MHC expression determined by the migration of MHC isoforms in each lane. Images of representative gels with labeled MHC isoforms are shown in Figure A-1.3.

12. MHC isoform and 2-DG uptake (*from* **section 3.4**) can be used to determine fiber type specific glucose uptake.

NOTES

1. If the experiment requires evaluating the effect of insulin on glucose uptake, then Incubation Media #1 and Incubation Media #2 should each be divided into two equal portions. One portion for each Media will be used for the muscles incubated without insulin, and the second portion will be used for insulin-treated muscles. Add insulin (at the desired concentration) to the second portions of Incubation Media #1 and #2. One epitrochlearis muscle from each rat can then be incubated in Incubation Media #1 and #2 without insulin, and the contralateral epitrochlearis from each rat can be incubated in Incubation Media #1 and #2 with insulin.
2. The greater specific activity of [^{3}H]-2-DG for these single fiber experiments than is used for whole muscle experiments is necessary for the detectable accumulation of [^{3}H]-2-DG in single fibers. Additionally, the initial single fiber experiments from our group used 1 mM 2-DG in the incubation media. Although we have no evidence that 1 mM 2-DG causes problems, we have since reduced the 2-DG in the incubation media to 0.1 mM to minimize the possibility of metabolic stress related to using a higher 2-DG concentration.

3. To make Ca^{2+}-free KHB do not include $CaCl_2$ in the KHB Stock #2 (*see* **step 3 section 2.1**).
4. The Type II collagenase used for previously performed experiments was from Worthington Biochemical Corporation (CAT#: LS004177). For our experiments, the activity of the type II collagenase was 295 u/mg dw. Because the activity of collagenase can vary from lot-to-lot, researchers should be aware of the collagenase activity that they are using, and they should perform some preliminary experiments to confirm it is optimal for their experiments.
5. Multiple types of fine surgical forceps may be used. We recommend Dumont #5 Forceps Inox Tip Size .10 X .06 mm.
6. Tissue protein extraction reagent (T-PER) is a proprietary detergent from ThermoFisher, Pittsburgh, PA (PI78510). Because we have not tested other detergents, we do not know which other detergents may also be suitable.
7. The volume of media that should be added to each vial will depend on the size of vial being used. There should be enough media to fully cover the muscle. We use 2 mL of media in 20 mL glass scintillation vials. The size of these vials is relatively small and allows for a small volume of media (2 mL), which reduces the cost of reagents. Additionally, when small vials are used then a larger number of vials can be placed in the shaking water bath, which makes larger experiments possible.
8. A gas washing bottle including deionized water is used to ensure humidification of gasses, and thereby minimize evaporation of the incubation media during gassing. The length of microbore tubing which connects the manifold to each vial is equal length (12 inches) to ensure equal gas flow to all vials. The needle that is attached to the microbore tubing and placed in each vial serves as a rigid tube that will not be constricted by the rubber stopper, allowing gas to flow into the vial. When positioned inside the vial, and held in place by inserting the rubber stopper, the hub of the needle should remain above the surface of the incubation media in the vial, to maintain an oxygen-enriched atmosphere above the media's surface. Bubbling the gas directly into media that contains bovine serum albumin would cause problems, including foaming of the media as well as cross-contamination between the needle and the media.

9. Placing the vials which contain 2.5% type II Collagenase Media into the 35°C heated water bath at least 5 minutes prior to the transfer of muscles into these vials ensures that the muscle will be incubated at the temperature for appropriate collagenase activity.
10. It is important to transfer the muscles from one vial to another vial by gently grasping the muscle with Gerald forceps by the connective tissue on either end of the muscle to minimize damage to the muscle fibers.
11. Shaking vials during muscle incubations is important for maintaining a more homogenous oxygen gradient and for helping to dissociate/ dilute metabolic waste products away from the incubating muscle.
12. For incubation step #1 we have had successful results using incubation times ranging from 10-30 minutes. For experiments that have evaluated 2-DG uptake immediately following exercise the step #1 incubation was shortened to 10 minutes to measure [^{3}H]-2-DG uptake (incubation step #2) as soon after exercise as possible (because the insulin-independent effect of 2-DG uptake is relatively transient). When evaluating insulin-stimulated 2-DG uptake, the duration of step #1 in other experiments has typically been 20-30 minutes.
13. Similar to incubation step #1, the duration of incubation step #2 may be altered depending on the experiment. We have successfully used incubations of 30-60 minutes in duration. Longer duration will enable greater accumulation of [^{3}H]-2-DG, and we have used 30 or 60 minutes for both basal and insulin-treated conditions. However, we have used 30 minutes duration for the insulin-independent effect immediately after *ex vivo* contractions or *in vivo* exercise because of the relatively transient nature of the effects of these treatments.
14. We have found that 2.5% type II collagenase allows for effective enzymatic digestion of collagen using the rat epitrochlearis muscle. In our initial experiments using 1.5% collagenase, MHC type I fibers were rarely isolated. It is possible that greater collagen levels surrounding type I fibers requires a greater concentration of collagenase for proper digestion. In subsequent experiments using 2.5% collagenase, we have succeeded in increasing the number of type I fibers isolated from the epitrochlearis muscle. If future researchers aim to use other rat skeletal muscles, they may need to perform exploratory analysis to identify the optimal collagenase concentration.

15. It is important to trim the adjacent connective tissue on the proximal and distal ends of the epitrochlearis as closely to the end of the epitrochlearis fibers as possible to minimize damage to the fibers and loss of intracellular [^{3}H]-2-DG.
16. It is not recommended to grasp fiber bundles by the connective tissue. The fiber bundles are very fragile and fibers will easily tear if grasped by the proximal or distal connective tissue. We pour Collagenase Media into a 30 mm culture dish to easily remove fiber bundles with a stainless steel laboratory spatula. This approach also minimizes the debris that is transferred with the fiber bundles.
17. Fibers can easily adhere to pipette tips or the surface tension of the meniscus. To avoid this problem, flush the pipette tip once with Ca^{2+}-free KHB solution and then draw up ~5 µl into the pipette tip before drawing up the remaining ~15 µl with the muscle fiber into the pipette tip. Eject the fiber and Ca^{2+}-free KHB into the microcentrifuge tube quickly or the fiber will adhere to the side of the pipette tip. Not gassing KHB (which will result in a high pH) or not adding 0.1% BSA will also cause issues with fibers adhering to forceps and pipette tips.
18. Because glucose uptake and MHC isoform identification require 40 and 18 µl of sample respectively, there will be 42 µl of sample remaining (42% of the lysed fiber) following these procedures. The remaining sample can be used for blotting for the abundance of proteins of interest. However, we have found that some proteins (GLUT4, MTCO1, and COXIV) are affected by heating. If western blotting is to be performed on proteins affected by heating, then it is recommended that an aliquot of the lysed fiber sample is removed before heating.
19. The "total ^{3}H dpm per fiber" value is determined by taking the dpm measured in each fiber lysate (**step 5 of section 3.4**) and subtracting the average background dpm (**step 4 of section 3.4**). The resulting value should be divided by 0.4 to account for the 40% (or 40 µl of sample, **step 1 of section 3.4**) of the fiber that was used for 2-DG uptake assay. The "µmol 2-DG per mL incubation media" represents the 0.1 µmol of 2-DG used in the incubation media (from **step 5 of section 2.1)**. The "^{3}H dpm per ml incubation media" represents the average dpm taken from the quadruplicate incubation media samples in **step 5 of section 3.4**, and this value should be multiplied by 50 due to the dilutions performed in **step 3 of section 3.4**.

20. In the original publication, we expressed glucose uptake relative to the estimated value for fiber volume ($V = \pi r^2 l$) using the mean width (mean value of the width measured at three locations per fiber) and the length of each fiber [13]. However, reproducibility in the measurement of muscle width was challenging. When two experienced researchers analyzed an identical set of fiber images using this procedure the coefficient of determination of estimated fiber volume was $r^2 = 0.9317$. Subsequently, we modified and improved our method for determining fiber size using ImageJ by calculating fiber area based on the traced perimeter of each fiber [15]. When two experienced researchers analyzed an identical set of fiber images to determine fiber area the coefficient of determination was $r^2 = 0.9885$. Because the fiber area is a more reliable measure of fiber size than estimate fiber volume, we recommend that glucose uptake be expressed relative to fiber area rather than estimated fiber volume.
21. Because of the reflective glare from the microscope lighting and the uneven brightness of captured images across the length of the fiber, we have been unable to create an automated method for measuring fiber area that is as reproducible and accurate as manual tracing. Development of an accurate automated thresholding and fiber area analysis method would save time and eliminate the tedious, but crucial step of manual fiber tracing.
22. Accuracy and reliability of fiber tracing is essential for meaningful quantification, and the training and quality control of fiber tracing is crucial. When a new researcher performs these techniques it is important to confirm the reproducibility of fiber area measurements within each researcher. We have a set of imaged fibers that each new researcher will trace multiple times to confirm internal reproducibility. Furthermore, after the trainee establishes his/her internal consistency, his/her results are compared to the values obtained by experienced researchers using the same images. We also recommend spot checking fiber tracing accuracy by having two experienced researchers independently trace the same fibers. Researchers should be blinded to the group and treatment identities of the fibers being traced.
23. EDL:Soleus standard can be made in large volumes (~10-15 mL) and stored at -20^{o}C in aliquots. We have freeze-thawed and re-frozen these MHC standards up to 4 times

without issue. We have not tested if more freeze-thaw cycles cause problems for the MHC standard.

24. The EDL:Soleus standard is used as a MHC isoform marker guide to identify fiber type of lysed fibers in adjacent lanes. The MHC isoform expression in rat EDL is <5% type I, ~10% type IIA, ~30% type IIX, and ~55% type IIB; and in rat soleus is ~90% type I, ~10% type IIA, and <1% types IIX and IIB [23]. By loading a sample containing EDL:Soleus standard beside wells containing single fiber lysates, the fiber type can be determined based on the MHC migration in the EDL:Soleus well (**Figure A-1.3** *above*).
25. The EDL:Soleus standard is loaded into 3 different lanes with spacing between the standard lanes to ensure accurate fiber typing of single fiber lysates. Some MHC isoforms migrate relatively close to one another (for example: type IIA and type IIX). It can be difficult to determine the fiber type if an EDL:Soleus standard is loaded in a lane that is a number of lanes from the sample. For this reason we recommend that the EDL:Soleus standard is loaded in multiple lanes.
26. The distinct separation of MHC isoforms in the EDL:Soleus standard is crucial for determining fiber type. We have found that running the MHC (~220 kDa) approximately 2/3 of the way down the gel allows for optimal separation of these bands.
27. After radioactive samples are loaded in the gels, the 1X running buffer will now be contaminated. It is essential to dispose of this buffer in the appropriate radioactive waste container. Additionally, sufficiently rinse the SDS-PAGE apparatus with water for decontamination and dispose of rinsing water in the appropriate radioactive waste container.
28. Typically MHC bands are stained by the SimplyBlue^{TM} SafeStain within 1 hour, but if less protein is added then staining may require up to 2 hours. Coomassie Stain can also be used for this procedure, but requires a longer duration of staining with more steps.
29. Typically destaining in water takes 2 hours, but gels can be left in shaking water for > 48 hours and the MHC protein bands will remain stained.

ACKNOWLEDGEMENTS

This work was supported by grants from the National Institutes of Health (R01 DK71771 and R01 AG10026). This methods paper has been published; Pataky MW, Arias EB, & Cartee GD. *Methods in Molecular Biology* 1889, 283-300, 2019. I also would like to thank Jim MacKrell and Haiyan Wang for providing valuable suggestions about the manuscript.

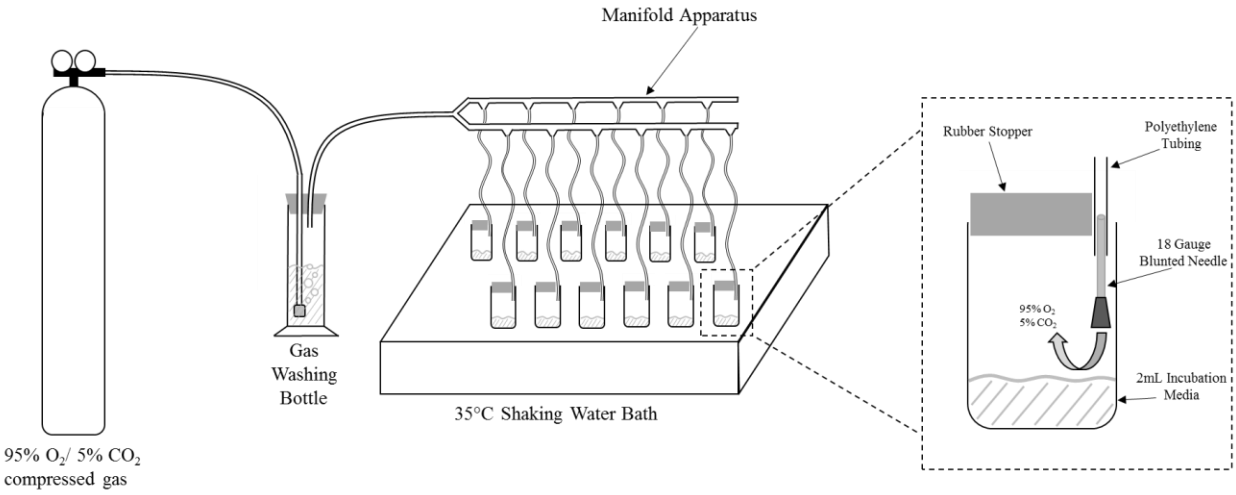

Figure A-1.1

Schematic diagram illustrating the system used to gas the vials during isolated muscle incubation steps. The 95% O_2/ 5% CO_2 gas cylinder with a gas regulator is attached by polyethylene tubing to the inlet tube of a gas washing bottle including deionized water. The gas washing bottle's outlet tube is attached via polyethylene tubing to a manifold that has multiple gassing ports, each of which is connected to individual segments of polyethylene tubing. The distal end of the tubing is connected to stainless steel 18 gauge blunt tip needles that are inserted into the mouth of glass scintillation vials. A size 0 rubber stopper is inserted into the vial's opening and holds each needle in place above the surface of the media that has been pipetted into the vial, which is placed in a shaking, heated water bath. During muscle incubation, individual isolated muscles are submerged in the media in the vials, and the vials are returned water bath. See Section 2.1 and Note 8 for details.

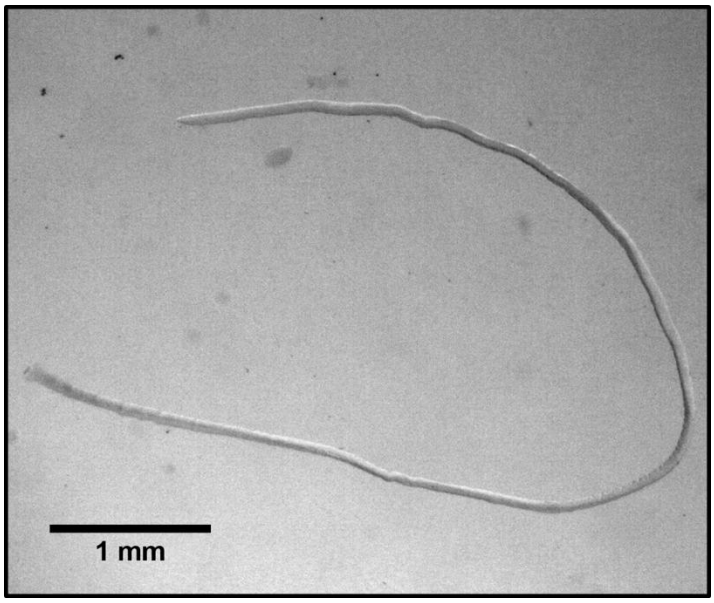

Figure A-1.2

Representative image of an isolated single rat epitrochlearis muscle fiber (16X magnification). The scale bar in the lower left of image is used for calibration when measuring fiber area.

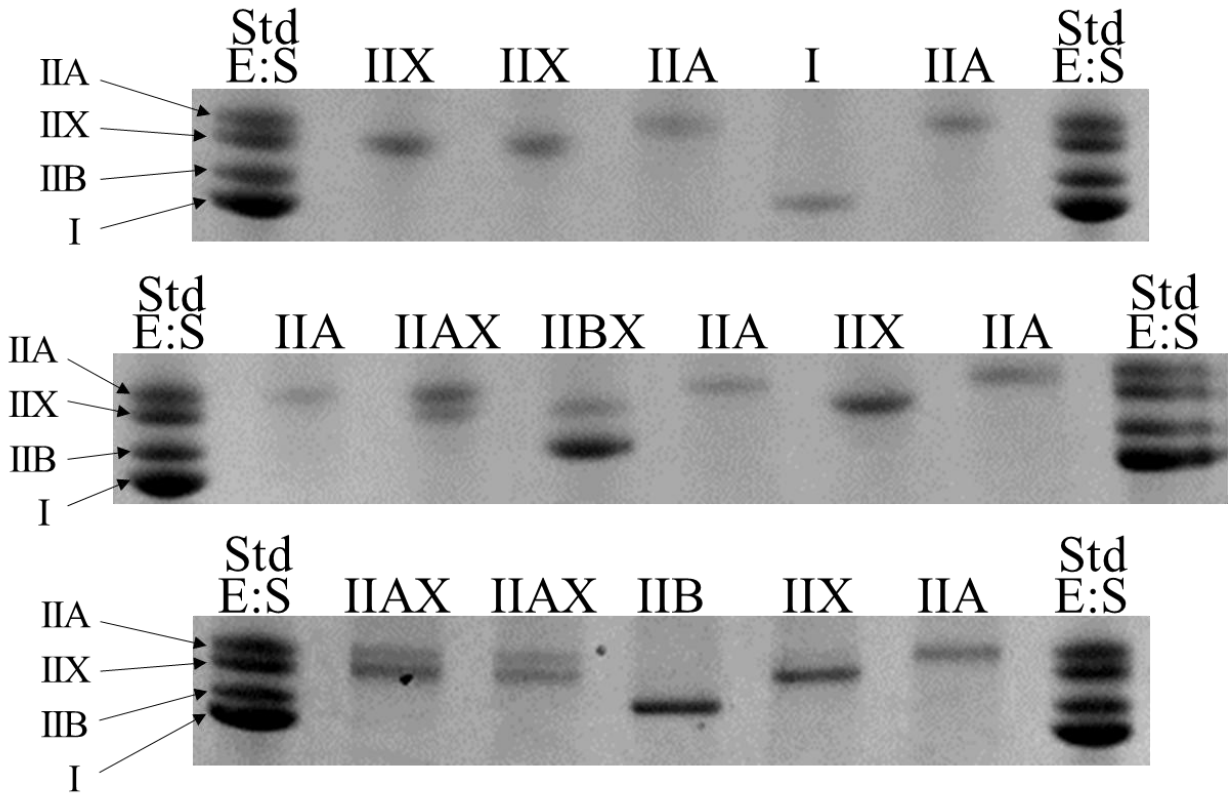

Figure A-1.3

Representative myosin heavy chain (MHC) single fiber gels. The 3:2 EDL:Soleus standard (Std E:S) is located on either side of all fibers. The migration of the Std E:S MHC allows for a guide to determine the MHC isoform expression of each single fiber which have been loaded in all other lanes. Fibers of all isolated fiber types (types I, IIA, IIAX, IIX, IIBX, and IIB) are displayed in the representative gels.

Appendix A References

1. Pette, D. and R.S. Staron, *Cellular and molecular diversities of mammalian skeletal muscle fibers.* Rev Physiol Biochem Pharmacol, 1990. **116**: p. 1-76.
2. Pandorf, C.E., T. Garland, W. Aoi, C. Handschin, L. Gorza, P.M. Garcia-Roves, S.W. Copp, C.M. Tipton, V.J. Caiozzo, and F. Haddad, *A Rationale for SDS-PAGE of MHC Isoforms as a Gold Standard for Determining Contractile Phenotype.* Journal of Applied Physiology, 2010. **108**(1): p. 222-225.
3. Fitzsimons, D.P., G.M. Diffee, R.E. Herrick, and K.M. Baldwin, *Effects of endurance exercise on isomyosin patterns in fast-and slow-twitch skeletal muscles.* Journal of Applied Physiology, 1990. **68**(5): p. 1950-1955.
4. Röckl, K.S., M.F. Hirshman, J. Brandauer, N. Fujii, L.A. Witters, and L.J. Goodyear, *Skeletal muscle adaptation to exercise training: AMP-activated protein kinase mediates muscle fiber type shift.* Diabetes, 2007. **56**(8): p. 2062-2069.
5. Korhonen, M.T., A. Cristea, M. Alén, K. Häkkinen, S. Sipilä, A. Mero, J.T. Viitasalo, L. Larsson, and H. Suominen, *Aging, muscle fiber type, and contractile function in sprint-trained athletes.* Journal of Applied Physiology, 2006. **101**(3): p. 906-917.
6. Nilwik, R., T. Snijders, M. Leenders, B.B. Groen, J. van Kranenburg, L.B. Verdijk, and L.J. van Loon, *The decline in skeletal muscle mass with aging is mainly attributed to a reduction in type II muscle fiber size.* Experimental gerontology, 2013. **48**(5): p. 492-498.
7. Hansen, P.A., L.A. Nolte, M.M. Chen, and J.O. Holloszy, *Increased GLUT-4 translocation mediates enhanced insulin sensitivity of muscle glucose transport after exercise.* Journal of Applied Physiology, 1998. **85**(4): p. 1218-1222.
8. Lee, A.D., P.A. Hansen, and J.O. Holloszy, *Wortmannin inhibits insulin-stimulated but not contraction-stimulated glucose transport activity in skeletal muscle.* FEBS letters, 1995. **361**(1): p. 51-54.
9. Wallberg-Henriksson, H., S. Constable, D. Young, and J. Holloszy, *Glucose transport into rat skeletal muscle: interaction between exercise and insulin.* Journal of applied physiology, 1988. **65**(2): p. 909-913.
10. Wojtaszewski, J.F., Y. Higaki, M.F. Hirshman, M.D. Michael, S.D. Dufresne, C.R. Kahn, and L.J. Goodyear, *Exercise modulates postreceptor insulin signaling and glucose transport in muscle-specific insulin receptor knockout mice.* The Journal of clinical investigation, 1999. **104**(9): p. 1257-1264.
11. Funai, K. and G.D. Cartee, *Inhibition of contraction-stimulated AMP-activated protein kinase inhibits contraction-stimulated increases in PAS-TBC1D1 and glucose transport without altering PAS-AS160 in rat skeletal muscle.* Diabetes, 2009. **58**(5): p. 1096-104.
12. Wright, D.C., K.A. Hucker, J.O. Holloszy, and D.H. Han, *Ca2+ and AMPK both mediate stimulation of glucose transport by muscle contractions.* Diabetes, 2004. **53**(2): p. 330-5.
13. Mackrell, J.G. and G.D. Cartee, *A novel method to measure glucose uptake and myosin heavy chain isoform expression of single fibers from rat skeletal muscle.* Diabetes, 2012. **61**(5): p. 995-1003.
14. Deves, R. and R. Krupka, *Cytochalasin B and the kinetics of inhibition of biological transport. A case of asymmetric binding to the glucose carrier.* Biochimica et Biophysica Acta (BBA)-Biomembranes, 1978. **510**(2): p. 339-348.
15. Cartee, G.D., E.B. Arias, S.Y. Carmen, and M.W. Pataky, *Novel single skeletal muscle fiber analysis reveals a fiber type-selective effect of acute exercise on glucose uptake.*

American Journal of Physiology-Endocrinology and Metabolism, 2016. **311**(5): p. E818-E824.
16. Wang, H., E.B. Arias, C.S. Yu, A.R. Verkerke, and G.D. Cartee, *Effects of Calorie Restriction and Fiber Type on Glucose Uptake and Abundance of Electron Transport Chain and Oxidative Phosphorylation Proteins in Single Fibers from Old Rats.* Journals of Gerontology Series A: Biomedical Sciences and Medical Sciences, 2017. **72**(12): p. 1638-1646.
17. Pataky, M.W., H. Wang, C.S. Yu, E.B. Arias, R.J. Ploutz-Snyder, X. Zheng, and G.D. Cartee, *High-Fat Diet-Induced Insulin Resistance in Single Skeletal Muscle Fibers is Fiber Type Selective.* Sci Rep, 2017. **7**(1): p. 13642.
18. Castorena, C.M., E.B. Arias, N. Sharma, J.S. Bogan, and G.D. Cartee, *Fiber type effects on contraction-stimulated glucose uptake and GLUT4 abundance in single fibers from rat skeletal muscle.* American Journal of Physiology-Endocrinology and Metabolism, 2015. **308**(3): p. E223-E230.
19. Wallberg-Henriksson, H., *Glucose transport into skeletal muscle. Influence of contractile activity, insulin, catecholamines and diabetes mellitus.* Acta physiologica Scandinavica. Supplementum, 1987. **564**: p. 1-80.
20. Delp, M.D. and C. Duan, *Composition and size of type I, IIA, IID/X, and IIB fibers and citrate synthase activity of rat muscle.* Journal of applied physiology, 1996. **80**(1): p. 261-270.
21. Mackrell, J.G., E.B. Arias, and G.D. Cartee, *Fiber type-specific differences in glucose uptake by single fibers from skeletal muscles of 9- and 25-month-old rats.* J Gerontol A Biol Sci Med Sci, 2012. **67**(12): p. 1286-94.
22. Wang, H., E.B. Arias, C.S. Yu, A.R. Verkerke, and G.D. Cartee, *Effects of Calorie Restriction and Fiber Type on Glucose Uptake and Abundance of Electron Transport Chain and Oxidative Phosphorylation Proteins in Single Fibers from Old RatsCalorie restriction effects on single fiber glucose uptake.* The Journals of Gerontology: Series A, 2017.
23. Castorena, C.M., J.G. Mackrell, J.S. Bogan, M. Kanzaki, and G.D. Cartee, *Clustering of GLUT4, TUG, and RUVBL2 protein levels correlate with myosin heavy chain isoform pattern in skeletal muscles, but AS160 and TBC1D1 levels do not.* J Appl Physiol (1985), 2011. **111**(4): p. 1106-17.

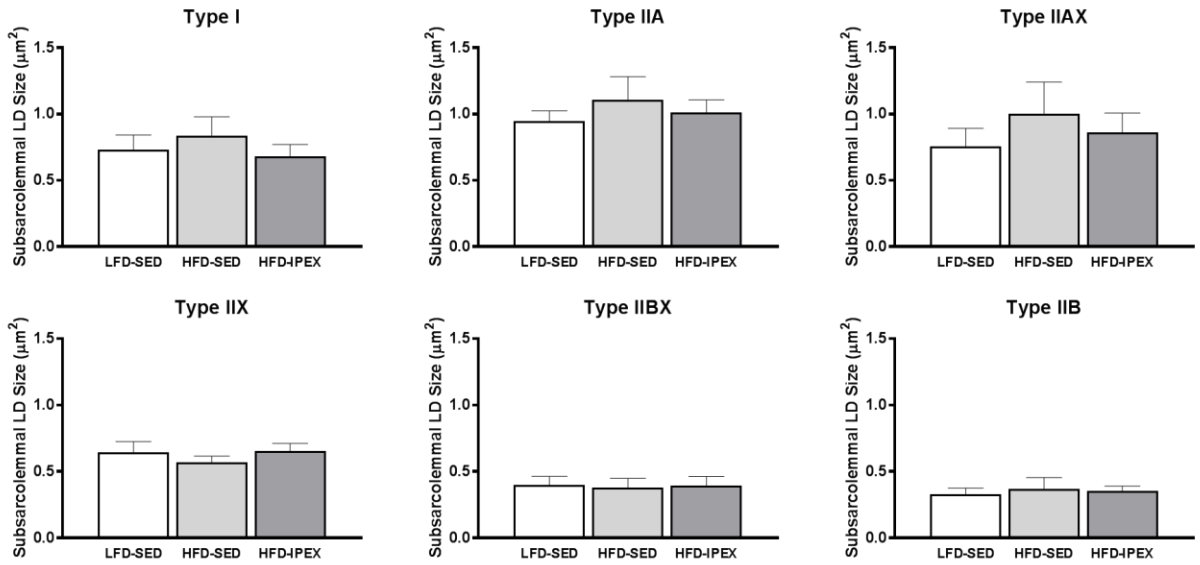

Appendix B

Figure B-1.1

Quantification of the size of lipid droplets located <1µm from the sarcolemma in single fibers of each fiber type. Bars represent the mean of all fibers within a given treatment group (LFD-SED, HFD-SED, or HFD-IPEX). Error bars are means ± 95% confidence interval. There were no significant differences among treatment groups for any fiber type. Subsarcolemmal lipid droplet size was quantified from the same images as lipid droplet density. Therefore, the rat numbers and fiber numbers are identical to those displayed in the figure 4.7 legend.

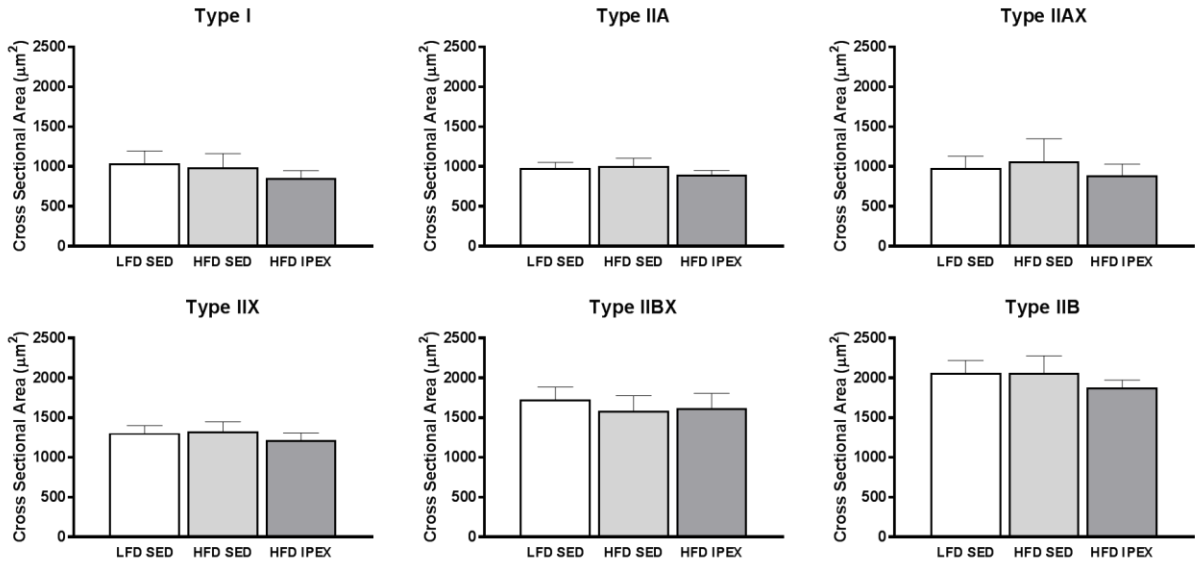

Appendix C

Figure C-1.1

Muscle fiber cross sectional area (CSA). Fiber CSA was not significantly altered by treatment group for any fiber type.). Error bars are means ± 95% confidence interval. CSA was calculated using the samples used for lipid analyses, therefore the number of rats and fibers of each fiber type used for CSA analysis from each treatment group are identical to those displayed in the figure 4.7 legend.